Dynamic and modal responses of the grouted multiple strands stay-cables of the Bill Emerson Memorial Bridge

by

Xiangwen Zuo

A thesis submitted to the Faculty of Graduate and Postdoctoral Studies in partial fulfilment of the requirements for the degree of

Master of Applied Science

In

Civil Engineering

Department of Civil Engineering

University of Ottawa

Ottawa, Canada

May. 2015

© Xiangwen Zuo, Ottawa, Canada, 2015

Acknowledgments

First and foremost, I would like to express my deepest appreciation and gratitude to my supervisor, Dr. Elena Dragomirescu, who has devoted much time and energy on this research project, for her support and invaluable guidance. It was an honor to know her and to work with her on my thesis. This study could never been done without her, and I will carry home my memories of working with her.

Secondly, I would like to thank all those who helped me during the course of my research program. To my fellow civil engineering students in Ottawa and China, especially Fan Feng, thank you for your kind advices which made my work easier. I would also like to thank Xi Chen and Songyu Cao, among other students, for their help and friendships over the past few years. Moreover, a sincere thank you to the other friends and family, although they were not able to be here with me, it's their encouragement and understanding that help me go through this process. Also, thanks to all the University of Ottawa engineering staff and faculty members who made my and graduate courses and other research possible.

Finally, I owe a debt of gratitude to my parents, for their unconditional love and support, enabling me to have an opportunity to study in Canada.

Abstract

Cable-stayed bridges are massive structures which rely on all their structural components for achieving the structural stability. Usually bridge stay-cables are the most flexible elements of the cable-stayed bridge structures, thus continuous efforts are made for improving their performance under different loadings. A new technology of constructing and installing the inclined bridge stay-cables, involves using internal strands grouted together in a cement paste or in a polymer gel material; such method has the advantage of allowing replacing of rusted strands individually, without affecting the functionality of the entire bridge stay-cable. However, recent studies have reported a change in natural vibrations of such inclined cables used for the construction of cable-stayed bridges. The current research aims at clarifying the dynamic properties of the internal strands in the cable, under the influence of the grout surrounding material and the interaction with the other inner strands under different wind loading scenarios. The effectiveness of the crossties in mitigating the wind-induced vibration has also been studied.

A finite element model was developed using the nonlinear analysis through the Abaqus commercial software. Some assumptions were made for modelling the stay-cables of the Bill Emerson Memorial Bridge, and to simulate the inner strands and the grout interaction. Both modal and time-history analyses were carried out on the stay-cables fan which connects the tower to the main span deck of the Bill Emerson Memorial Cable-stayed Bridge. The natural frequencies and the vibration mode shapes of a single cable, or group of cables respecting the arrangement of the inclined cables of the bridge has been determined, as well as the displacements under the field wind loads at different points in the stay-cables network. The results show how the behaviour of the cables differs from the previous research on the stay-cable which employed only a simplified beam element as one uniform property of the cable. Several comparisons haven been made between the results obtained in the current study and outcomes reported in the existing literature; the effectiveness of the crossties has been partly verified.

Also the results of the modal analysis were compared with the site measurements performed for the Bill Emerson Memorial Bridge and relatively good agreement was found for the natural frequencies and the mode shapes of the inclined stay cables.

Contents

List of Tables

List of Figures

List of notations

A	transverse area of the cable, m^2
a_{i1} , a_{i2}	displacements under the unit force of left side of two lumped mass, m
D	diameter of the cable, m
dl	selected arc length of the cable, m
ds_d	dynamic differential of arc length of the cable, m
ds_j	static differential of arc length of the cable, m
E	elasticity modulus, Pa
EA	axial tensile stiffness of stay cables, N
EI	bending stiffness, $N.m^2$
el	length of the cable elements, m
F	elastic force, N
F_C	cable tension, N
F_n	mode frequencies of the cable, Hz
f	sag at any point on the stay cable, m
f_w	vortex-shedding frequency, Hz
H	horizontal component of the cable force, N/m^2
k	spring stiffness, N/m
L_1	length of the cable 1, m
l	length of the cable, m
l_c	chord length of the stay cable, m
M	lumped mass of cable, kg
m	mass per unit length of cable, kg
m	lumped mass, kg
q	evenly distributed mass of the cable along the arc length, kg
R	radius of the cable, m
Re	reynolds number
S	horizontal tension increment of cable, N/m^2
S_0	chordwise tension of the cable, N/m^2
St	Strouhal number
T	string tension, N
T_A , T_B	tension of the stay cable at both ends, N
t	time, s
U	wind speed, m/s
x, y	local rectangular coordinates
y	young's modulus of the substance, Pa
α	wind angle, °
C'_L	derivative of lift coefficient

φ	slope of one cable element, °
η	vertical deflection of the cable, mm
ω	natural frequency of the cable, rad/sec
δ_n	correction factor
θ	oblique angle of the cable, °
ε_d	dynamic strain
β	attack angle of the wind load, °
μ	horizontal displacement of the element, m
v	vertical displacement of the element, m
θ	angle of rotation of the element, °
σ	stress on the substance, Pa
ε	strain on the substance
ΔL	absolute elongation of substance, m
λ^2	cable parameter to account both geometric and elastic effect, $\left(\frac{EA}{H}\right)\left(\frac{wl}{H}\right)^2$
σ_C	stress of the cable, Pa

Chapter 1 Introduction

1.1 Background of stay cables and cable-stayed bridge

As structures go across rivers, lakes and wide gullies, bridges show human's ability to overcome obstacles, while also promoting the development of human civilization. The cable-stayed bridges, as a kind of anchor structures, play an extremely important role in the field of structural engineering, considering their good structural performance and beautiful shapes, the strong seismic performance, and the magnificent construction methods providing superior spanning ability.

The cable-stayed bridges are sometimes preferred to the suspension bridges, especially when the main span is between 200 m and 800 m, given their aesthetics and challenging modelling, the convenient construction, the large spanning ability, the flexible span layout, and without the expensive anchorage compared to the suspension bridges. In 1956, the world’s first modern cable-stayed bridge, the Stromsund Bridge, with a main span of 183 m, was built in Sweden; then in 1957, the Theoder Heuss Bridge, with a main span of 260 m was constructed in Germany [1]. Since that point on, the cable-stayed bridges have been developing rapidly all over the world.

In the 1990s, with the emergence of the high-strength steel wire, the rapid development of the prestressed concrete technology and the advances of the manufacturing process of the orthotropic bridge panel, there was a significant improvement in the computational analysis and in the solutions to the technical problems associated with the construction of the cable-stayed bridges of longer spans, which thus have been widely used firstly in Germany, then in Europe, in North America, in Japan and in other regions spreading over the world. Currently, more than 300 cable-stayed bridges have been built around the world, among which the most significant to mention are the Normandy Bridge, with a main span of 856 m [2], built in France in 1995, and the Tatara Bridge, with main span of 890 m [3], built in 1999 in Japan. These are the new milestones in the history of the cable-stayed bridges

construction. The Sutong Yangtzw Bridge, built in 2008 in China (main span 1,088 m), and Hong Kong's Stonecutters Bridge (main span 1,104 m) made the span length of the cable-stayed bridges break the record of the 1,000 m. The Russky Island Bridge, which was built and has been used since 2012, has a main span of 1,104 m, and is currently the cable-stayed bridge with the longest main span in the entire world. Some researchers consider [4-5] that it is possible to build a cable-stayed bridge with a span of 1,500 m. Table 1-1 shows the top ten largest spans of cable-stayed bridges in the world [6-8].

Figure 1-1: Russky Island Bridge, main span of 1,104 m [1]

Figure 1-2: Tatara Bridge, main span of 890 m [3]

The stay cable is a tensioned and flexible component of high strength, used for large-span cable-stayed bridges. With the flexible configuration of the stay cables, their application in modern civil engineering has broadened.

1.2 Research Motivation

For a cable-stayed bridge, the inclined cables are a vital structural component, and special attention is

paid to wind-induced vibrations.

The research of the stay-cables has developed from the static to dynamic analyses, from linear theory to nonlinear theory, from the straight-line string to the string considering the effect of sag. The nonlinear effects mainly include the material nonlinearities, and the large deformations and geometric nonlinearities caused by the stay-cable sag. The main content of the dynamic structural integrity investigation of cable-stayed bridges includes the following aspects:

1) The dynamic response obtained through the time history analysis.
2) The in-plane vibration form, which contains main resonance, ultra-harmonic resonance and second-harmonic resonance.
3) The out-of-plane vibration form, including resonance between the modals of different dimensions, and resonance of modals between the same dimensions of different degrees.
4) The influences of cable geometry, physical parameters and damping parameters on the dynamic response.

The vibration characteristics and the control of the stay cables are obtained under the effect of complex loadings, such as wind and rain effects.

As the span of the cable bridge structure becomes larger, the problem of non-linear effects of stay cables is becoming increasingly obvious. Therefore, it is of strong theoretical significance to explore the dynamics and nonlinear dynamic characteristics of elastic stay cables.

Research nowadays is mainly focused on the dynamic response of single element cables, which is modelled as a uniform property cable. In reality, the stay cables are actually consisting of several individual wires that are assembled in spiral form and then are coated, thus forming the stay cable. What would make the multiple-strand model distinctive from the existing patents and published papers

is that it allows for the effect of the grout between the strands existing inside the cable and would allow modelling the interaction between the strands. Therefore in the current research each internal strand has been modelled individually, and the dynamic analysis herein shows the detail of each single strand and the combined reaction of the whole model. A novel aspect is the structural behaviour of the multiple-strand cable model which differs from the previous research performed for the cable modelled as a simplified beam element with one uniform property [9].

Moreover, with the increase in the span length of the cable-stayed bridges, the length of stay cables also increases, thus it becomes difficult to fulfill the mitigation requirements of stay cables using only damping devices installed at the cable ends. Crossties are smaller diagonal cables which connect the stay-cables between them, at different points, thus decreasing the vibrations and fulfilling the additional damping requirements for long-span cable-stayed bridges with longer stay cables. But due to a current lack of theoretical and experimental studies of the entire cable network system with crossties installed, the mechanism of cables vibrations has not been fully understood, thus there are no specific design guidelines for the multiple-stands stay cables with crossties. The practical engineering shows that the breakage of cable or connector and the damage of Poly Ethylene casing are prone to arise after the installation of poorly designed crossties. In addition, due to minimal detailed analysis on the internal force redistribution of the main cable, after the crossties installation, it might bring potential risks to the entire bridge structure. Therefore, the research of crossties as a mitigation measures for the vibrations of stay cables, is very necessary and urgent, both for the model of the uniform cable network and for the multiple-strand cable network.

Open to traffic on December 13, 2003, the Bill Emerson Memorial Bridge is a 1206-m long cable-stayed structure across the Mississippi River between Cape Girardeau, Missouri, and East Cape Girardeau, Illinois. The structure consists of 128 cables including a cable-stayed unit 636 m long with a 25 m wide roadway. The two towers are 106 m high; the four fans of the cables are symmetrical, each

with 32 stay cables ranging in length from 40 m to 157 m [10]. Four lines of crossties have been arranged for each fan of cables.

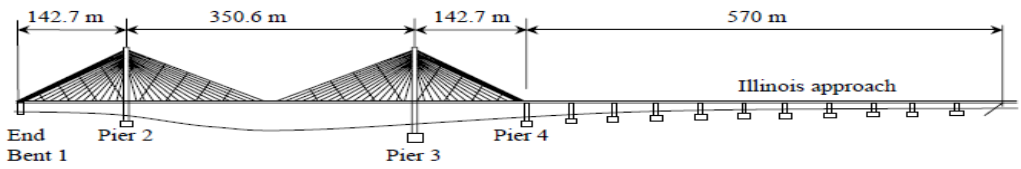

Figure 1-3: Schematic view of the Bill Emerson Memorial Cable-stayed Bridge [10]

1.3 Scope of the study

The main objective of this study is to determine the dynamic properties of the grouted multiple strands stay cables connected with crossties, of the Bill Emerson Memorial Bridge in Cape Girardeau, MO, U.S. This bridge has been selected because the monitoring data for the cable vibrations, before and after the grouting process, was extensively discussed in several papers available in the literature [9] [10] [11] [12] [13]. Prior to modelling the stay cables on the bridge, a series of investigations were performed on the model of a standard cable with uniform property and multiple strands and were compared with the experimental results provided by Hoftyzer (2008), in order to validate the modelling conditions proposed for the grouted cables. The material of the cable was selected, as per the references [9] [10] as the standard of the steel cable, with 0.1 m in diameter. The actual grout linking the inner strands was model as a series of springs connecting the strands and a study was carried out for determining the values of the spring elastic constant k for which the cable natural vibrations would be within the recommended range; the number of strands composing one cable has also been varied, increasing from a uniform property cable to a four-strand cable. The magnitude of the effect of the strands and the grout in one cable was confirmed. Once the standard multiple-strand grouted cable model was validated, its implementation for the study of the Bill Emerson Memorial Bridge stay cables vibrations was performed.

Another aspect that has been investigated was the behaviour of one single cable of the Bill Emerson Memorial Bridge. The longest cable has a length of 157 m and an angle of inclination between the tower and the cable of 28°. Forty inner strands have been modelled in one cable.

In modelling the stay-cables fan configuration, the real geometry and boundary conditions have been simulated in the finite element analysis. For the uniform property model, the modelling is similar to the model in reference [9]; a total of 16 structural elements have been modelled that represent each cable, respectively. For the multiple-strand grouted cable model, a total of 437 strands have been modelled, and each part has the same material properties and cross-section. Each cable was subjected to different pretensions and inclinations, as described in the construction details of the Bill Emerson Memorial Cable-stayed Bridge [10].

The 5-minute wind speed data at the site of the Bill Emerson Memorial Cable-stayed Bridge [9] were considered and the corresponding wind loads were derived from the field measurements around the bridge, which had a maximum wind speed of 30 m/s. Considering the difficulty of deriving the wind loading on the stay cables, some assumptions were made; the wind load has been simplified as the drag force only. Therefore, the approximate wind loads time history of 300 s was evaluated, which could be applied for the stay-cables fan. Different nodes in the cable network have been chosen to attain the dynamic response in terms of different numbers of crossties. Thus, the mitigation effect of crossties could be explored to some extent, along with the effect of using the uniform property or multiple-strand cables on the stay cables dynamic response.

1.4 Thesis outline

The current thesis is organized in five chapters and several Appendixes. The current chapter, Chapter 1, offers a brief introduction to this study, along with the motivation and the main objectives of this research.

In Chapter 2, the related literature in the field is reviewed; regarding the main objective of the study, types of vibrations, and the crossties, is summarized and the research status is introduced; the theoretical solution for cable vibrations as the fundamental of the finite element analysis, which has been demonstrated. Several experiments and numerical analyses conducted on the real bridge were also presented in this chapter.

In Chapter 3, modelling and verifying the standard stay cable is presented. After validating the modelling of a typical cable, several parameters could be identified, such as the choice of the element properties and the analysis steps. The effect of the grout is determined. Based on the results of the vibration behaviour of the typical cable, the stay-cables fan on the bridge is modelled, with different properties between the model of the uniform property cable and the multiple-strand cable. The wind load is modelled in the finite element analysis.

The results of both the modal and the time-history analyses are provided in Chapter 4. The results of the modal analysis of the uniform property model are compared with the results provided in the reference [9], which involved a similar finite element analysis on the Bill Emerson Memorial Bridge, but without multiple-strand cables. A brief comparison is made between vibration modes and natural frequencies of the multiple-strand model and the field measurements. The results of the displacements under the wind load have been widely discussed, with comparisons with the experimental and numerical results.

Finally, Chapters 5 contains the overall conclusions of the study, along with the recommendations for the future research.

Chapter 2 Literature Review

2.1 Overview – development of cable-stayed bridges

For a large-span cable-stayed bridge, the structure of the upper structure system is usually combined with the main girder, the cable system to maintain the cable and the tower to support the system of lasso. Closely linked in the design process, they produce different effects on the performance of the overall structure of the bridge. The following are basic mechanical characteristics:

-The cable under the tension lifts the girder through multiple connections, past the dead load of main girders and other loads like vehicles to the pillar, and then passes from the fountain of the pillar to the ground. The main girder with a large span works like a multipoint elastic support (lift) continuous beam, which makes the bending moment within the main girder greatly reduced. As the size of the girder decreases, so does the self-weight of the structure, improving the spanning capacity of the cable-stayed bridge.

-The pillar, cable and girder form a triangle structure, which increases the rigidity of the cable-stayed bridge, and improves the ability to resist the wind.

-The horizontal component of the axial force of stay cables produces preloading to the main girder, which can enhance the crack resistance of the main girder, saving the dosage of the pre-stressed steel girders.

2.2 Types of cables

The geometry of a cable and especially of a stranded cable could be very complicated. The commonality of all cables is that the individual wires are arranged in a spiral geometry. The wires are

made from high carbon steel and have a nominal tensile strength of up to 1,770 N/mm^2 [14].

In reality, there are three types of cables based on how the wires are arranged in terms of spiral geometry.

The most common cable is the spiral strand, which is simply made from round wires in several layers [14];

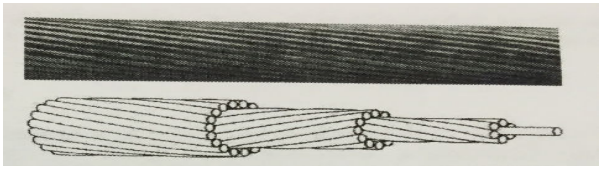

Figure 2-1: The spiral strand cross-section and side view [14]

Locked coil strands are assembled with one core of spirally spun round wires in several layers onto which covers of spirally spun full lock wires in several layers are added [14].

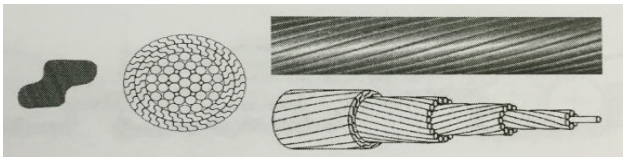

Figure 2-2: The full lock wire, locked coil strand cross-section and locked coil strand side view [14].

Stranded ropes, which are made from strands in a spiral arrangement.

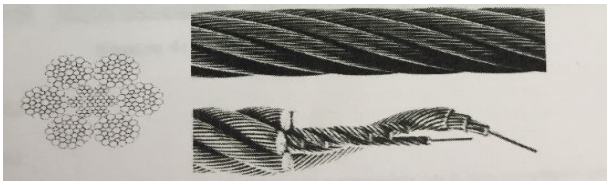

Figure 2-3: Strand rope cross-section and side view [14].

2.3 The vibration of cables and research status

With the continuous development of cable-stayed bridge construction, many challenging issues emerge for bridge workers, from which the vibration of the cable on the cable-stayed bridge and the control of the cable have become one of the key problems to be resolved. Cables are among the key components of the cable-stayed bridge, bearing and passing the majority of the load of the bridge. As the span of the cable-stayed bridge increases, there is a corresponding increase in the length of stay cable; for example, the Tatara Bridge cable reaches 460 m, while the Stonecutters Bridge's longest cable exceed 500 m. On the other hand, the diameter of the cable is basically stable at between 100 ~ 200 mm, so as the span of the cable-stayed bridge increases, so too does the cable flexibility; and while the damping decreases, the fundamental frequency is gradually reduced, cables are prone to substantial vibrations inspired by the wind, storms, earthquakes, bearing movements and other external loads [15-18]. The vibration of a cable will cause fatigue fracture, corrosion damage to the cable system, even failure of the cable; vibration relaxation of the cable also leads to deformation and redistribution of internal forces of the cable-stayed bridge, which destroys the mechanical performance of the bridge. Meanwhile, cable vibrations will cause discomfort to pedestrians and doubts about the safety of the bridge [19]. So far, as it has been observed in multiple countries, there are cables vibrate with large amplitudes on real bridges.

In 1974, a substantial vibration of the cable was observed on the Koehlbrand Bridge in Hamburg, Germany, with an amplitude up to l m [20]; in 1977, significant cable vibration was observed on the Brottonne Bridge in France, the amplitude of which was 0.6 m [21]. In 1986, rain-wind induced vibration of the cable was observed on the Meiko Nishi Bridge in Japan, and the amplitude peak reached 0.55 m [22]; in 1987, rain-wind induced vibration of the cable was observed on the Aratsu Bridge in Japan, and the amplitude peak reached 0.6 m [23]; in 1988, nine cables of the same side on Belgium's Ben-Ahin Bridge experienced first order vibration, the peak amplitude of which was up to l

m [24]; in 1993, a parametric resonance with large amplitude triggered by a lateral bending vibration of the main girder was observed in Japan on a pedestrian cable-stayed bridge, the frequency ratio of which was 2: 1 [25]; in 1996, the maximum amplitude of vibration of the cable up to 0.7 m under rain-wind weather was observed on the Erasmus Bridge in the Netherlands, the modes of which mainly were second-order vibration, while the amplitude of the deck was 2.5 cm [26]; in 1997, substantial rain-wind induced vibration occurred on the Yangpu Bridge Cable in China, with an amplitude up to l m [15]; in 2000, field measurements were conducted on the Fredhartman Bridge in the U.S.; it was found that despite the absence of rain, cable vibration occurred significantly [27]; in 2001, substantial rain-wind induced vibration occurred on the Dongtinghu Bridge Cable in China, with an amplitude up to 0.4 m [28].

In accordance with the induced factors of vibration, vibration of stay cables on cable-stayed bridges can be divided into two categories: the first kind is caused by the direct load on the cable, most typically, the wind-induced buffeting of stay-cables, vortex-induced resonance, wake galloping, wind and rain, vibration, etc.; the second category of vibration is induced by the vibration of the main girder and tower fixed at both ends of the cable. Furthermore, this kind of vibration can be divided again into the linear internal resonance between the structure "tower - line - beam" caused by excitation from the displacements of the tower top and the beam end and parametric vibration [29]. Cable vibration has been observed so far in real bridge and laboratory studies [29 - 40]:

(1) Karman vortex induced vibration;

(2) Ice galloping;

(3) Rain-wind induced vibration;

(4) Wake vibration;

(5) Resistance instability related to Reynolds number;

(6) Vortex-induced vibration;

(7) Dry galloping;

(8) Chattering;

(9) Parametric vibration.

At present, the types of cable vibration of concern in engineering are Vortex-induced vibration, rain-wind induced vibration and parametric vibration, which are briefly introduced as below.

2.3.1 Vortex-induced vibrations

Vortex-induced vibration is a kind of crosswind vibration, which is the vibration caused by the alternate shedding vortex (karman vortex), and appears in the wake of the cross-section when the wind blows over the cable. Vortex-induced resonance includes low wind speed and high wind speed vortex-induced resonance. According to the knowledge of structural wind engineering, the Karman vortex is related to the Reynolds number. The expression of the Reynolds number of the circular cross-section of the stay-cable is as follows:

$$Re = 690UD \qquad (2\text{-}3\text{-}1)$$

Where:

U = wind speed, m/s;

D = diameter of cable, m.

It can be seen from the expression above that the Reynolds number is related to the wind speed and the size of the cable diameter. According to the scope of the Reynolds number, the corresponding Strouhal Number, *St*, can be determined. Strouhal number is a dimensionless number describing oscillating flow mechanisms, which are often given as:

$$S_t = \frac{f_w D}{U} \qquad (2\text{-}3\text{-}2)$$

Where f_w is the frequency of vortex shedding, D is the characteristic length (for example hydraulic diameter, or chord length) and U is the flow velocity.

The relation of *St* of circular cross-section and Re is shown in the table below:

Table 2-1: Strouhal Number of circular cross-section [41]

Re	*St*
$[3\times10^2,\ 3\times10^5]$	0.2
$[3\times10^5,\ 3.5\times10^6]$	0.2-0.3
$[3.5\times10^6,\ +\infty]$	0.3

Therefore, vortex-shedding frequency is determined by the following formula:

$$f_w = \frac{S_t U}{D} \qquad (2\text{-}3\text{-}3)$$

When the vortex shedding frequency and the frequency of lateral vibration of stay cables are equal or close, cable-stayed resonance occurs. Due to the "lock-in" effect, vortex shedding frequency stays the same over a large range of wind speeds, locked by the frequency of cables, which means the stay cables will produce resonance under a modal frequency within a range of wind speeds, known as the wind speed resonant region.

Mature theoretical research [41] shows that when $\mathrm{Re} \le 3\times10^5$ or $\mathrm{Re} \ge 3\times10^6$, regular periodic vortex shedding happens, stay-cable resonance occurs. $\mathrm{Re} \le 3\times10^5$ region corresponds to low wind speed resonance, and the corresponding lasso vortex-induced resonance is known as low wind speed vortex-induced resonance; the $\mathrm{Re} \ge 3\times10^6$ resonance region corresponds to high wind speed and the corresponding cable vortex-induced resonance is known as high wind vortex-induced resonance. When $3\times10^5 \le \mathrm{Re} \le 3\times10^6$, vortex shedding occurs randomly, and the transverse random vibration of stay cables occurs.

2.3.2 Wake galloping

Galloping often occurs in lender structures like wires and cables, which is the large-amplitude vibration of pure bending vibration caused by the gas-solid coupled effect of the structure and the flow. The condition of instability of galloping is as follows:

$$C'_L < 0$$

C'_L means derivative of lift coefficient for the wind Angle α, because the α of circular cross-section of the stay cables is positive, therefore, no unstable galloping will occur.

Wake galloping refers to the phenomenon that when the stay cable is arranged along with the wind direction, the wake flow caused by the air flow passing through the cable in the upwind makes the cable in the downwind gallop in the direction of the crosswind, so that the downstream cable vibrates more strongly than the upstream cable. According to the wake galloping mechanism, when the downstream cable is located in an unstable galloping zone of the wake flow of upstream cable, its amplitude will increase continuously until it reaches a steady state vibration with the large amplitude [42-44]. When the distance between the two stay cables is large enough, cables in the downstream can avoid the unstable zone of cables in the upstream, and wake galloping won't happen. But as the span of

the cable-stayed bridge increases, the stay cables have developed from the rare cables with large distances to dense cables with short distances, so from this point, the stay cables are more and more prone to wake galloping. The wind speed when wake galloping occurs is called the critical wind speed, and research has shown that the critical wind speed is proportional to the modal frequency; therefore, improving the modal frequency of the cable can avoid wake galloping.

2.3.3 Rain-wind induced vibrations

Rain-wind induced vibration is the vibration of large amplitude of stay cables on the cable-stayed bridge under the combined load of wind and rain; it is the most dramatic form of vibration of cables known so far. Summarized from the observation of cable vibration on many cable-stayed bridges, the following are the characteristics of rain-wind induced vibration:

(1) Rain-wind induced vibration is most likely going to happen with stay cables of 100-200 mm in diameter, while diameters of most stay cables are in this range;

(2) Significant rain-wind induced vibration generally occurs for the wind speeds from 8 to 18 m/s; usually under small to moderate rain. When rainfall is too small, it is not enough to form a top and bottom water line; when the rain is too big, the waterline has easily been torn away;

(3) Rain-wind induced vibration is related to wind attack angles and wind direction, leeward plane, namely in the surface of the stay cable that dumps in the direction of the blowing wind, which is prone to rain-wind induced vibration, so the phenomenon that two planes with opposite direction, one vibrates while the other one does not occurs a lot;

(4) Rain-wind induced vibration is mainly low-order, single-mode vibration, usually two to three order modal; fourth order vibration may occur in stay-cables with a large slenderness ratio. The frequency range of rain-wind induced vibration is about 0.5 ~ 3.0 Hz;

(5) Although the amplitude of the rain-wind vibration is large, generally at least above two times the diameter of the cable, it is a limiting vibration that will not spread;

(6) Rain-wind induced vibrations are more likely to happen at stay cables of the cable-stayed bridge located in flat terrain; that is to say the lower the wind turbulence intensity, the higher the possibility of rain-wind induced vibration.

Requirements of wind speed are small for the rain-wind induced vibration of cables on the cable-stayed bridge cable; it is also likely to occur in light rain, and the vibration amplitude of which is large, which affects the driving comfort and the normal use of the bridge, so the research of rain-wind induced vibration of stay-cables has drawn the interest and attention of scholars.

In 1988, the Japanese scholars Hikami and Shiraishi [45] found the rain vibration phenomenon of cables on the Meiko Nishi Bridge in Japan, and had done the observation and statistics for five months of this phenomenon. In field measurements it was found that the peak amplitude of stay cables on the bridge is 0.55 m, which was higher than the frequency of the possible vortex vibration and lower than the wake galloping vibration, so they think this is a new form of vibration excitation, namely, rain-wind induced vibration. Based on the observation and statistics data, they made an original summary of excitation conditions of rain-wind induced vibration and characteristics of vibration, and their research conclusion is still widely quoted.

In 1992, Yoshimura [46] performed a systematic field observation of the rain-wind induced vibration phenomenon of cables in the process of constructing the Aratsu Bridge in Japan. It was found in field measurements that the peak amplitude of vibration of the stay cable was 0.6 m (about 3.5 times the cable diameter), and rain-wind induced vibration occured mainly under the condition of light rain. The main vibration mode of the stay cables was not fixed, and in some cases was the first order, while in other cases was the 2nd or 3rd order.

In 1998, Persoon et al.[47], have carried on the field measurement of rain-wind induced vibration on Erasmus Bridge in the Netherlands. It was found in field measurements that the maximum amplitude of stay-cables was about 0.5 ~ 0.7 m; in most cases it vibrates with the second order modal vibration. In addition, it was also found that the vibration of stay cables will cause the vibration of the bridge deck and the amplitude of the deck up to 25 mm.

In 1999, Main and Jones [48] had done a long-term and systematic observation of stay-cables on the Hartman Bridge in the U.S., and obtained a large amount of observation data. It was shown from the statistical analysis of these data that the vibration of the cables can be divided into three types: no rain vibration, rain vibration and heavy rain vibration, among which the amplitude of rain vibration is larger, while the large amplitude vibration might appear in heavy rain only when the wind speed is low.

In 2003, Matsumoto [49], etc., set up a 30 m long cable in the field of the Shionomisaki wind effect lab of Kyoto University, and observed the possible rain vibration phenomenon and obtained some research results.

Beginning in 2002, the Chinese scholar Zhenqing Cheng, et al, [50-54] had done a long-term observation of the rain vibration phenomenon of the cable on Dongtinghu Bridge. Statistical analysis of the measured data shows that:

1) The rain vibration of stay cables can reach large amplitudes in a very short period of time, and at the same time it can also decay quickly [51];

2) The rain-wind induced vibration occurs as well in windward cables, but the vibration of the leeward cable is more serious than that of the windward cable [52];

3) A relatively large range of the central area of the cable has nearly the same amplitude, which shows that the form of rain vibration of the cable has the characteristics of galloping [50];

4) Stable cable vibration with a large amplitude is the vibration with multiple modals, but is controlled by one order modal; in the initial and end stages of vibration of stay-cables, it is often accompanied by the main modal shift phenomenon, and the main modal of rain vibration of stay cables are mainly distributed in the third order modal [50];

5) Even if it is very close to the tower of stay-cables, its inclination reaches 70°; the rain vibration will obviously occur [50].

Field measurements, as described above, have deepen people's understanding of the rain vibration of stay cables; also, it has accumulated valuable information for carrying out the research associated with mechanisms of rain vibration and their control measures.

2.3.4 Parametric vibration

The parametric vibration of stay cables refers to coupled vibration between the cable and the tower. The anchor end of the stay cable is connected to the tower and the main girder. The vibration phenomenon of the girder and tower will occur under the wind or vehicle load. If the vibration frequency of the girder or the tower with the natural frequency of cables is in a two-fold relationship, a small vibration of the deck can cause changes in the tensile force of the cables, and induce lateral vibration with large amplitude transverse vibration of stay cables because the natural frequencies of the cables are related to their tensile force. The periodic characteristics of natural frequency will change as that in the tensile force change. Moreover, the frequency is an important parameter to the vibration of stay cables, thus we call this kind of vibration parametric vibration.

According to the form of excitations, the research methods of parametric vibration of the cable-stayed bridge can be divided into two categories: First, during the vibration, the response does not affect the amplitude and frequency of the excitation; rather, it changes according to some way. This kind of

excitation is called the ideal excitation system. Assume that the quality of the bridge deck is far greater than the quality of the stay cables, irrespective of the influence from the vibration of cables on the girder or deck. Second, the amplitude and frequency of excitation is changing constantly; it is regarded that the vibration of the deck and the vibration of the deck to cable is coupled and form a bridge coupling vibration system [55]. Kovacs is the first to explain the mechanism of the vibration of stay-cables explicating parametric [56]. Tagata conducted research on the first order parametric vibration, regardless of the cable sag effect, which meant he did not consider the weight of the cable, and derived the Mathieu equation [57]. Zhigang Wang [58] built the nonlinear mechanics model and illustrated the problem of parametric vibration of stay cables. Zhan Yun also did an analysis of the problem of parametric resonance of stay cables through a mathematical model with multiple degrees of freedom, and obtained the numerical results [39].

In addition to the above types of vibration, vibration forms such as chattering, ice freezing and galloping exist in stay cables. In the form of these vibrations, the rain-wind induced vibration has become one of the most intense vibrations, followed by the parametric vibration; the amplitude of the other kinds of vibration is small.

2.4 Introduction to the crossties

2.4.1 Mitigation measures on stay cables

Due to the characteristics of small quality, small damping and small stiffness, stay cables are prone to vibrate under the wind, rain, earthquakes and vehicle load. Sometimes multiple vibration mechanisms exist together, so the vibration control of cables has become important work. At present, there have been many effective measures used in the real bridge to control the vibration of cables. These measures are mainly divided into two categories: aerodynamic measures and mechanical measures.

（1） Aerodynamic measures

Aerodynamic measures refer to the spirals intertwined with the peripheral cables with circular cross-section or those made into a longitudinal rib. Aerodynamic measures are the most effective in reducing the vibration of rain-wind induced vibration. This is because forming an uneven surface of cables prevents the formation of an upper and lower water line, thus inhibiting the occurrence of rain-wind induced vibration. Aerodynamic measures have already been applied and achieved a promising vibration damping effect in many practical engineering situations. Both the Normandy Bridge in France and the Nanjing Yangtze River Bridge in China have applied the intertwine spiral method. The Higushi Kobe cable-stayed bridge in Japan adopted the cable with PE sheathed and longitudinal ribs.

（2） Mechanical measures

There are three types of mechanical measures: increasing the damping of the cable; increasing the natural frequency of the cable; and active control of the axial force of the cable.

1) Increasing the damping of the cable. Adding passive, semi-active dampers between the ends of the cable and deck improves the damping of the cable, thereby reducing its amplitude.

For passive dampers, there are rubber dampers, hydraulic dampers, viscous shear dampers and magnetic dampers. Installation of the passive damper is simple, the control of which is better, and has become the earliest and most widely used control method, among which the hydraulic damper is the most common. However, due to the restriction of height in the installation of the passive damper, the damper can only be installed in the vicinity of the cable end, and thus for long cables, the damper cannot provide sufficient damping to control cable vibration, as the effect of control is limited.

For semi-active dampers, there is ER (electrorheological) damper and MR (magnetorheological)

damper. The ER or MR damper is an intelligent device exploiting the rapid variable effects of electrorheological fluids or magnetorheological fluids under the load of electric or magnetic fields. They change the size of the damping force through the adjustment of intensity in electric or magnetic fields, thus altering the modal damping ratio of the cable, and reaching the optimal damping effect. Research shows that the MR damper has better control effects.

2) Increasing the natural frequency of the cable. By using crossties, the main cable will be connected to form a cable network, the effective length of the cable will be reduced and the natural frequency of the cable will be improved. The Faroe Bridge in Denmark, Normandy Bridge in France and Meiko Nishi Bridge in Japan adopted this approach.

3) Active control axial force of the cable. Applying active control force at the end of the cable to change the axial force of the cable changes the frequency, vibration mode and damping of the cable to achieve the purpose of controlling its vibration. Currently, this method is not yet mature; the application in engineering is still in research.

2.4.2 The crosstie system of stay cables and research status

The crosstie damping measure connects stay cables together laterally using a cable component called crossties to form a new cable network. Leonhard [59] first proposed the design idea for Italy's Messina Strait Bridge project to use crossties in the system of stay cables of a large span cable-stayed bridge. The main purpose is to increase the stiffness of the system of stay cables of the cable-stayed bridge, but this idea had not been put into practical use. The first time crossties were applied in engineering occurred on the Farø Bridge in Denmark. After the completion of the Farø Bridge, parts of long stay cables were easy to vibrate under the rain effect, but the amplitude was relatively small. Cowi Company established the solution of using crossties to connect long stay cables. Later on, crossties have been applied on the Iwakurojima Bridge and the Hitsuishijima

Bridge in Japan to avoid wake galloping between the ambient stay cables, and it turned out that the measurement of crossties was effective.

The most recent case of crossties is the Normandy Bridge in France. Because it has been found that the first-order frequency of vibration of stay cables and the low-order frequency of the cable-stayed bridge itself of the Normandy Bridge is in the same range due to theoretical analysis. The vibration of the deck may cause parametric vibration of stay cables and linear internal resonance, thus it is necessary to take crosstie measures to change the vibration frequency of stay cables to keep it away from the low-order frequency range of the cable-stayed bridge itself. Regarding the tension of crossties of the Farø Bridge in Denmark, the Iwakurojima Bridge and the Hitsuishijima Bridge in Japan, they had all been released completely during the process of vibrating with large amplitudes due to low initial tension, thus it resulted in impacting the fracture of crossties. Finally, crossties with higher pretension have been replaced on the bridges. The crossties of the Normandy Bridge were set with a larger initial tension to avoid the impact of crossties due to the low tension during the process of vibration with large amplitudes. For the differences between measures of crossties of Normandy Bridge and previous engineering instances, on the one hand it has been used as a solution to connect the crossties with the deck, so it was more conducive to increase the frequency of the cable network; on the other hand, it has been applied with high damping crossties, which suggests the damping of the cable network has improved to some extent.

Figure 2-4: Crossties on Normandy Bridge [2]

Figure 2-5: Detail of cable clip on Normandy Bridge [2]

From the application of the engineering of crossties, it shows that crossties can be used to reduce the vibration of various types of stay cables. Although the crosstie measures have achieved good results in practical engineering applications, the research of its damping mechanism is still in the exploratory phase.

Ehsan and Scanlan [60] in the U.S. firstly explored the damping mechanism of crossties from the perspective of energy redistribution. They preliminarily interpreted the damping mechanism of crossties from the perspective of energy redistribution, exploring the energy redistribution problem of cables caused by crossties and applying the method of sub-structure, but it did not include the discussion of dampers of the cable network. Their research certainly confirmed the effectiveness of measure of crossties in energy redistribution of cable network vibration in low-order modes. At the same time, their research also showed that dynamic analysis of the cable network was indispensable for designing crossties. Ehsan and Scanlan's research [60] could be considered as discussions in the damping mechanism of crossties from a frequency point of view, but they did not analyze the impact on damping ration of the cable network from the measure of crossties.

In order to study the impact of crossties on the damping of the cable network, Yamaguchi, etc., [61-64] in Japan used the finite element method, based on the energy theory, and has studied the damping effect of single cables and cable networks formed by stay cables and crossties. They make comparisons with the test results from the model cable network (2 horizontal main cable+2 vertical

crossties), indicating the feasibility of using the energy method to analyze damping, proposing that nonlinear dynamic strain is a fundamental of analysis on characteristics of damping of the cable network. They have analyzed the damping properties of the cable network using tension of crossties as parameters. The results showed the following:

1) With crossties, modal damping of stay cables-crosstie systems is larger than modal damping of a single cable;

2) The increase on modal damping of stay cables-flexible crossties system is more significant than that of stay cables-rigid crossties system.

Yamaguchi's research has further confirmed the necessity of dynamic property analysis of the cable network structure to design the crossties; meanwhile, it illustrates the effectiveness of the energy analysis. But for the real cable network structure, initial tension, tensioning method, rigidity and other factors of crossties will affect the initial non-linear equilibrium configuration of the cable network structure; therefore, determining the nonlinear dynamic strain of the cable network is on the premise of accurately determining the initial non-linear equilibrium configuration of the cable network composed by crossties and stay cables. Also it is the premise of using the energy analysis. At the same time due to the tiny structural damping of stay cables and crossties, the damping effect is limited for the damping of the cable network structure itself.

Caracoglia and Jones in the U.S. recently studied the in-plane modal frequencies and mode shapes of the cable network system consisting of two main cables and one crosstie using the semi-analytical method, and crossties of real bridges were analyzed using this method [65-66]. The method they used was generally the dynamic characteristics analysis method, but this method makes it difficult to consider the equilibrium position of geometric nonlinearity of the cable network structure composed by crossties and stay cables. Thus, it is difficult to accurately and quantitatively analyze the frequency

of the cable network structure.

Bosch and Park [67] in the U.S. have used the finite element method to calculate the damping effect with the joint action of crossties and dampers, and proposed the problem of the optimization of dampers considering the impact of crossties. But their analysis is mainly from the perspective of increasing the frequency of the cable network by measuring crossties and improving the damping of the cable network by dampers, regardless of the interaction between these two vibration damper measures, crossties and dampers.

Parametric analysis of crossties is also an important aspect of the crosstie design. Jiandong Wei, etc., in China have conducted an analysis on the impacts of internal forces of crossties, damping on the in-plane and out-of-plane mitigation effects [68]. Take the Nanjing Yangtze River Bridge as an example; Jiming Huang has analyzed the influence of the cable network layout and the number of crossties on the mitigation effects using the finite element method [69].

2.5 Theoretical solution of stay cables linear free vibration

2.5.1 Linear free vibration of stay cables ignoring the change of inner force of the cable

Generally for the stay cables which are relatively short, ignoring the change in cable force through vibration, it is consistent with the results of stay cables ignoring the sag effect, which will be explained later. Ignoring the sag effect is to ignore the influence of gravity. It is enough to use the following simplified natural frequency formula of horizontal standard string. Guohao Li has studied the natural vibration of standard string (wire) [16].

Figure 2-6 shows a horizontal tension string, cable length is l; the cable mass per unit length is m, when the cable is assumed that the string tension T from tiny lateral vibration remains unchanged.

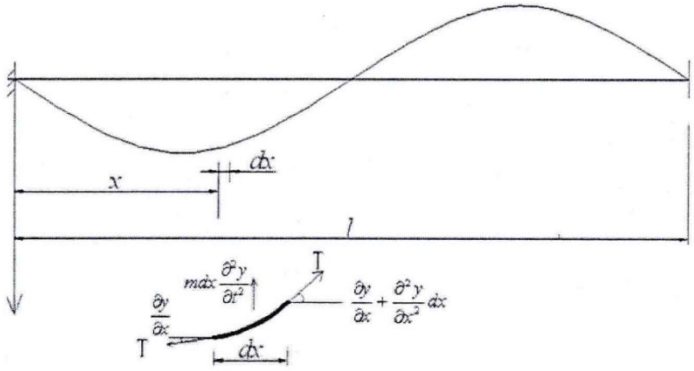

Figure 2-6: Lateral vibration of horizontal tension string [70]

Based on the principle of Hamilton, Yifan Song studied the natural vibration of the cable considering the influence of the bending stiffness [71]:

$$EI\frac{\partial^4 y}{\partial t^4}-T\frac{\partial^2 y}{\partial x^2}+m\frac{\partial^2 y}{\partial t^2}=0 \qquad (2\text{-}5\text{-}1)$$

EI is the bending stiffness of the cable. This is a constant-coefficient homogeneous linear partial differential equation, which can be solved by the method of separation variables:

Set $y(x,t)=\varphi(x)\cdot\eta(t)$, substituted into (2-5-1), obtained:

$$EI\frac{\varphi^{(4)}}{\varphi}-T\frac{\varphi''}{\varphi}=-m\frac{\eta''}{\eta}=c \qquad (2\text{-}5\text{-}2)$$

Because the first term of the above equation is the function only related to x, the second term of the above equation is the function only related to t, only for the case that every term equals to a constant, for arbitrary x and t, the above equation can be satisfied;

Set

$$\frac{EI\varphi^{(4)} - T\varphi''}{m\varphi} = -\frac{\eta''}{\eta} = \omega^2 \qquad (2\text{-}5\text{-}3)$$

Two individual equations can be derived:

$$\eta'' + \omega^2\eta = 0 \qquad (2\text{-}5\text{-}4)$$

$$EI\varphi^{(4)} - T\varphi'' + m\omega^2\varphi = 0 \qquad (2\text{-}5\text{-}5)$$

The general solution for（2-5-4）:

$$\eta(t) = A\sin\omega t + B\cos\omega t \qquad (2\text{-}5\text{-}6)$$

The general solution for（2-5-6）:

$$\varphi(x) = D_1\sin\alpha x + D_2\cos\alpha x + D_3\sinh\beta x + D_4\cosh\beta x \qquad (2\text{-}5\text{-}7)$$

$$\alpha = \sqrt{\sqrt{x^4 + y^4} - \lambda^2}$$

$$\beta = \sqrt{\sqrt{x^4 + y^4} + \lambda^2}$$

Where $\lambda^2 = \frac{T}{2EI}$， $\gamma^4 = \frac{m\omega^2}{EI}$

Four constant D_i (i = l, 2, 3, 4) in equation (2-5-7) are determined by the boundary conditions:

（1） For the hinged ends of the cable:

Equation of frequency:

$$\begin{vmatrix} \sin\alpha l & \text{sh}\,\beta l \\ \alpha^2 \sin\alpha l & -\beta^2 \,\text{sh}\,\beta l \end{vmatrix} = 0 \qquad (2\text{-}5\text{-}8)$$

$$(\alpha^2 + \beta^2)\sin\alpha l \,\text{sh}\,\beta l = 0 \qquad (2\text{-}5\text{-}9)$$

Due to $\alpha^2 + \beta^2 \neq 0$， $\text{sh}\,\beta l \neq 0$， thus $\sin\alpha l = 0$, $\alpha l = n\pi$

The equation of frequency becomes:

$$\omega_n = \frac{n\pi}{l}\sqrt{\frac{T}{m}(1+\delta_n)} \qquad (2\text{-}5\text{-}10)$$

Where $\delta_n = \frac{n^2\pi^2}{l^2}\frac{EI}{T}$ is the correction factor considering the influence of the stiffness of the cable.

（2） For the fixed ends of the cable:

Equation of frequency:

$$\begin{vmatrix} (\sin\alpha l - \frac{\alpha}{\beta})\,\text{sh}\,\beta l & \cos\alpha l - \text{ch}\,\beta l \\ \alpha(\text{ch}\,\beta l - \cos\alpha l) & \alpha\sin\alpha l + \beta\,\text{sh}\,\beta l \end{vmatrix} = 0 \qquad (2\text{-}5\text{-}11)$$

$$2\alpha\beta(1 - \cos\alpha l \cosh\beta l) + (\beta^2 - \alpha^2)\sin\alpha l \sinh\beta l = 0 \qquad (2\text{-}5\text{-}12)$$

Equation (2-5-12) is transcendental equation; the corresponding nature frequency can be obtained by

numerical methods.

2.5.1.1 The lumped mass method to solve the linear free vibration of cable

Put the distributed mass of the cable together in some proper positions, thus it is transformed into a number of lumped mass; lumped mass are connected with massless strings, the structure with infinite degree of freedoms are simplified to the structure with finite degree of freedoms, then the natural vibration analysis are conducted on the simplified structure.

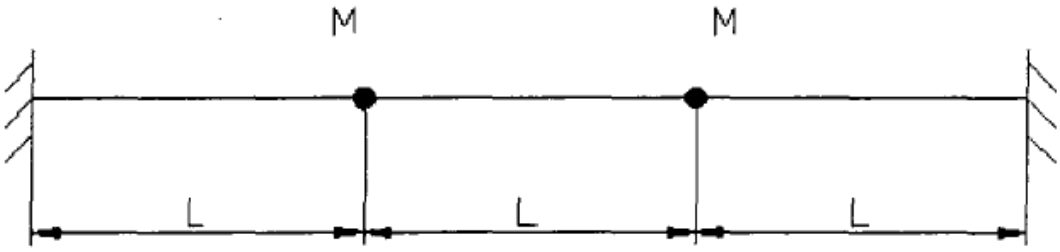

Figure 2-7: Lumped mass model for stay cables [70]

As the following figure shows, displacements under the unit force of left side of two lumped mass are a_{i1} and a_{i2} (flexibility coefficient)

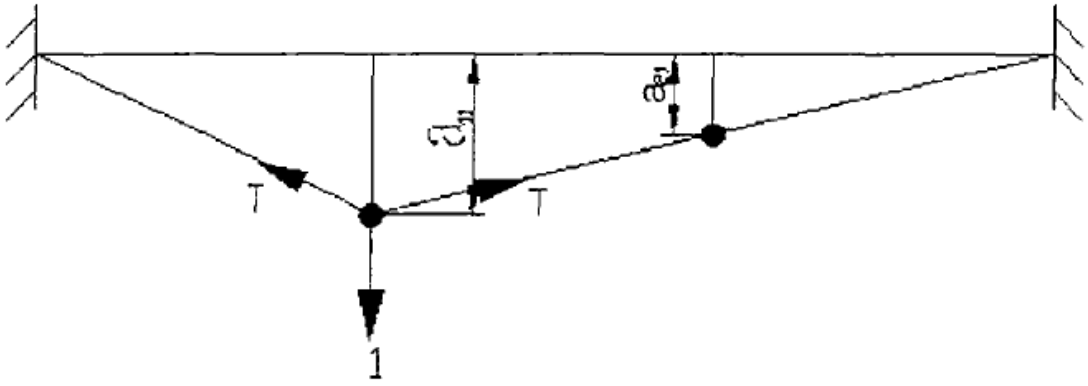

Figure 2-8: Stress analysis of the stay cable [70]

Obtained from the equilibrium relationship:

$$a_{11} = \frac{2L}{3T} \qquad (2\text{-}5\text{-}13)$$

By the employing of symmetry and reciprocal theorem, all the flexibility coefficients could be obtained:

$$a_{22} = a_{11} = \frac{2L}{3T} \qquad (2\text{-}5\text{-}14)$$

$$a_{12} = a_{21} = \frac{L}{3T} \qquad (2\text{-}5\text{-}15)$$

Equation of frequency:

$$\begin{vmatrix} a_{11}M - \frac{1}{\omega^2} & a_{12}M \\ a_{21}M & a_{22}M - \frac{1}{\omega^2} \end{vmatrix} = 0 \qquad (2\text{-}5\text{-}16)$$

Solution:

$$f_1 = \frac{\omega_1}{2\pi} = \frac{1}{2\pi}\sqrt{\frac{T}{LM}} \qquad (2\text{-}5\text{-}17)$$

$$f_1 = \frac{\omega_1}{2\pi} = \frac{1}{2\pi}\sqrt{\frac{T}{LM}} \qquad (2\text{-}5\text{-}18)$$

Assuming the distribution of mass of the cable is concentrated in three nodes, as the Figure 2-9 shows:

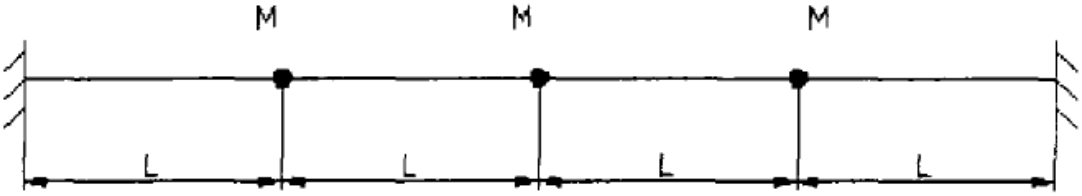

Figure 2-9: Three nodes of mass [70]

Similarly, the flexibility can be obtained as following:

$$a_{11}=\frac{3L}{4T} \qquad a_{12}=\frac{L}{2T} \qquad a_{13}=\frac{L}{4T}$$

$$a_{21}=\frac{L}{2T} \qquad a_{22}=\frac{L}{T} \qquad a_{23}=\frac{L}{2T} \qquad \text{(2-5-19)}$$

$$a_{31}=\frac{L}{4T} \qquad a_{32}=\frac{L}{2T} \qquad a_{33}=\frac{3L}{4T}$$

Equation of frequency:

$$\begin{vmatrix} a_{11}M-\frac{1}{\omega^2} & a_{12}M & a_{13}M \\ a_{21}M & a_{22}M-\frac{1}{\omega^2} & a_{23}M \\ a_{31}M & a_{32}M & a_{33}M-\frac{1}{\omega^2} \end{vmatrix}=0 \qquad \text{(2-5-20)}$$

The nature frequency can be derived by solving the equation.

2.5.2 Linear free vibration of stay cables considering the change of the cable force

A cable is a flexible structure; sag will occur under its own weight, moreover, geometric nonlinear effects caused by sag increase with the increase of cable length.

A calculation diagram of stay cables under gravity is shown in Figure 2-10, f is the sag at any point on the stay cable, l_c is the chord length of the stay cable, $l_c\cos\theta$, $l_c\sin\theta$ are the horizontal and vertical projection of cable length respectively, A、B are the upper and lower anchor end of the cable respectively, T is the tension in the tangential direction of the cable. The geometry of stay cables under self-weight is curve, sag will occur, and due to the oblique angle θ constituted by the tangential of the cable and horizontal line, the tension T_A and T_B of the stay cable at both ends will not be equal.

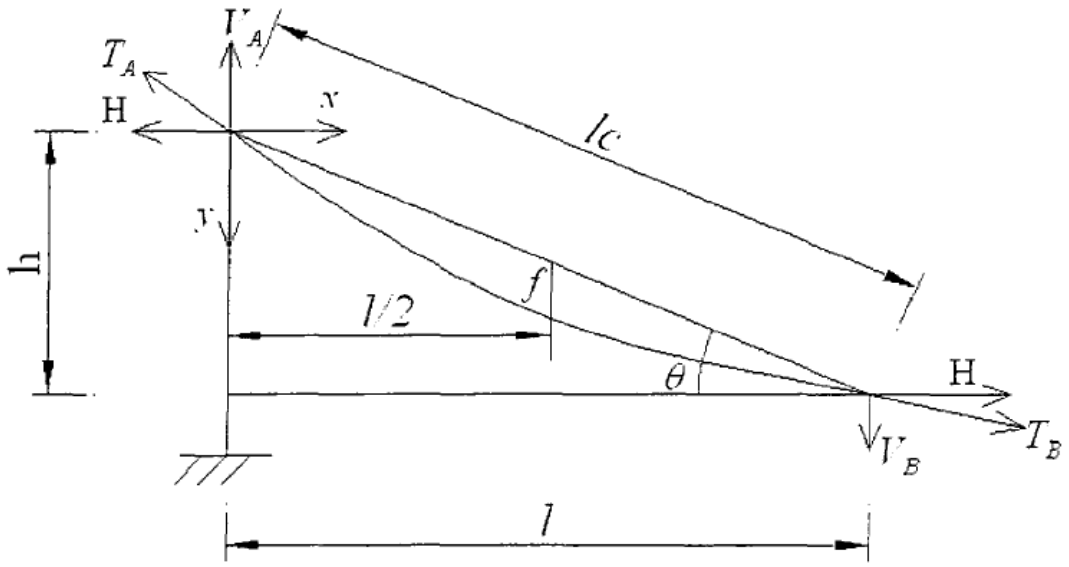

Figure 2-10: Calculation diagram of the cable under self-weight [70]

The self-weight of the cable is distributed evenly along the length of the cable, so the accurate static equilibrium equation can be written as:

$$H\frac{d^2y}{dx^2}+q\frac{dl}{dx}=0 \qquad (2\text{-}5\text{-}21)$$

H is the horizontal component of the cable fore, q is the evenly distributed mass of the cable along the arc length, dl is the selected arc length of the cable.

Actually the sag of the stay cable is not large; sometimes the self-weight could be ignored compared to the tension of the cable. When the horizontal component of cable force reached H from H_0 under the load, elastic tensile value of the tangential direction of stay cables can be expressed as:

$$\Delta = \frac{l_c^2}{EAl}\left(H - \frac{q^2 l^5 EA}{24 l_c^3 H^2} \right) - \frac{l_c^2}{EAl}\left(H_0 - \frac{q^2 l^5 EA}{24 l_c^3 H_0^{\ 2}} \right) \qquad (2\text{-}5\text{-}22)$$

In above equation EA is axial tensile stiffness of stay cables; l_c is the chord length of the stay cable， l the length of the horizontal projection of the chord. The second terms of the brackets in RHS of the above equation are the corrections of elongation of stay cables due to the effect of sags.

Introduce parameters:

$$\alpha = \frac{l_c^2}{EAl} \qquad (2\text{-}5\text{-}23)$$

$$\beta = \frac{q^2 l^5 EA}{24 l_c^3} \qquad (2\text{-}5\text{-}24)$$

Equation (2-5-22) could be rewritten as:

$$\Delta = \alpha\left(H - \frac{\beta^3}{H^2} \right) - \alpha\left(H_0 - \frac{\beta^3}{H_0^{\ 2}} \right) \qquad (2\text{-}5\text{-}25)$$

Set $H = k\beta$， $H_0 = k_0\beta$， thus:

$$\frac{\Delta}{\alpha\beta} + \left(k_0 - \frac{1}{k_0^2} \right) = k - \frac{1}{k^2} \qquad (2\text{-}5\text{-}26)$$

Above equation is the dimensionless equation, which could be used to imply the tight density of the stay cable: The change of k with $k-\frac{1}{k^2}$ is shown in Figure 2-11，it can be seen that when k>1.5, the cable could be considered as the tensioned cable.

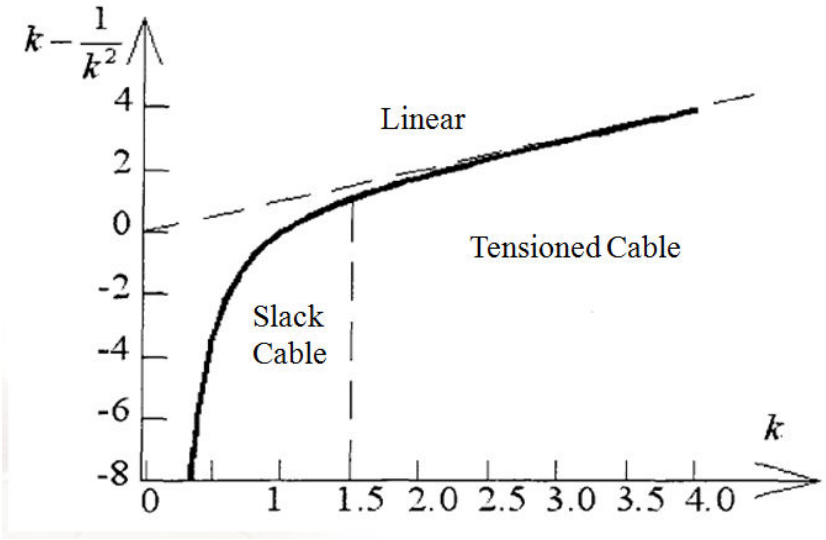

Figure 2-11: The degree of tension of the cable

2.5.2.1 Linear natural vibration of the horizontal cable

To explore the natural vibration of the stay cable better, discussion about the vibration of the horizontal cable as shown in Figure 2-12 comes first. The mass of the stay cable is evenly distributed, mass per unit length is m, and the static tension of the cable is S_0. When cable vibrates, horizontal tension increment of cable is S, ignoring the impact of the bending stiffness EI of the cable on vibration.

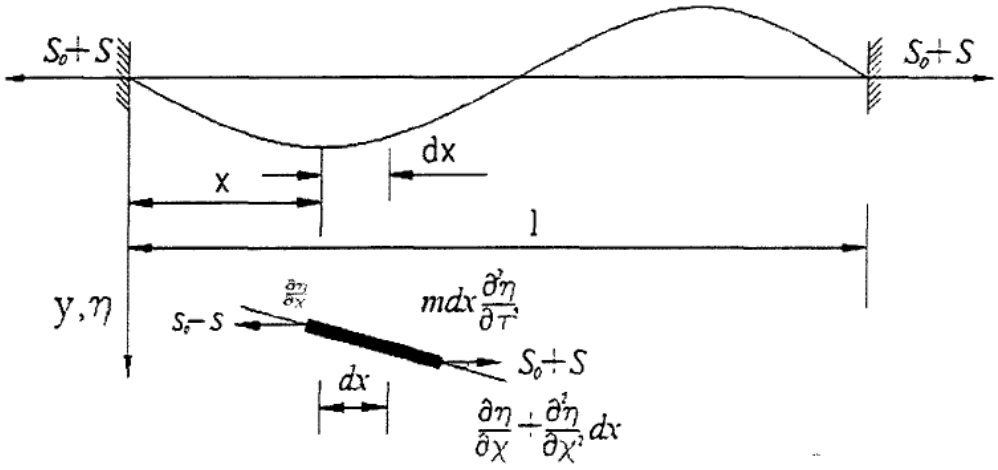

Figure 2-12: Calculation diagram of lateral vibration of horizontal cable [70]

Take a micro element of the cable, the vertical static equilibrium equation of the cable is:

$$S_0(\frac{\partial y}{\partial x}+\frac{\partial^2 y}{\partial x^2}dx)-S_0\frac{\partial y}{\partial x}+mgds=0 \qquad (2\text{-}5\text{-}27)$$

That is:

$$S_0\frac{\partial^2 y}{\partial x^2}d+mg\frac{ds}{dx}=0 \qquad (2\text{-}5\text{-}28)$$

In which y(x) is the static sag function of the cable, the catenary equation could be derived by solving the above differential equation. When the sag is far smaller than the span of the cable, equation 2-5-28 could be simplified; take the similar relationship $\frac{ds}{dx}\approx 1$

So:

$$S_0\frac{\partial^2 y}{\partial x^2}+mg=0 \qquad (2\text{-}5\text{-}30)$$

Solving the above equation could get that y(x) is the quadratic parabola:

$$y = \frac{mg}{S_0} x(\frac{l}{2} - \frac{x}{2}) \qquad (2\text{-}5\text{-}31)$$

The lateral vibration equilibrium equation of the cable is:

$$(S_0 + S)(\frac{\partial^2 y}{\partial x^2} + \frac{\partial^2 \eta}{\partial x^2}) + mg - m\frac{\partial^2 \eta}{\partial t^2} = 0 \qquad (2\text{-}5\text{-}32)$$

$\eta(x,t)$ is the displacement function of vibration of the horizontal cable.

So:

$$(S_0 + S)\frac{\partial^2 \eta}{\partial x^2} + S\frac{\partial^2 y}{\partial x^2} - m\frac{\partial^2 \eta}{\partial t^2} = 0 \qquad (2\text{-}5\text{-}33)$$

Equation（2-5-33）is the dynamic equilibrium differential equation of the horizontal cable.

2.5.2.2 Linear natural vibration of the stay cable

As shown in Figure 2-13 is an inclined cable, the coordinate system take *op* chordwise direction as the x axis, take the direction perpendicular to the chordwise as the y-axis and define the downward direction as positive, take the left supporting point O as the coordinate origin. θ and l represent the inclined angle and chord length of the stay cable respectively. The mass of the stay cable is uniformly distributed; mass per unit length is m, the static chordwise tension of the cable is S_0, $y(x)$ is the static sag function of the cable. When the cable vibrates, the value of its chordwise tension increment is *S*; $\eta(x,t)$ is lateral vibration displacement function of the cable, whose direction is along the y-axis

direction.

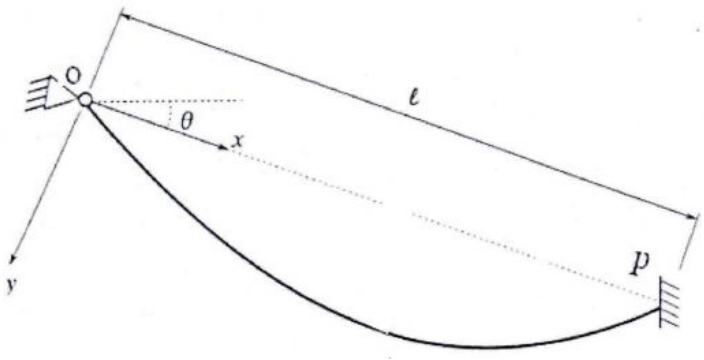

Figure 2-13: Diagram of the stay cable [70]

Assumptions through analysis:

(1) Considering only the vibration in xy plane of the cable; the vibration of the cable in the x direction is small, which is negligible.
(2) Gravity of the inclined cable is uniformly distributed along the chord length, whose direction is vertically downwards, the component in the x-direction is $mg\sin\theta$, the component in the y-direction is $mg\cos\theta$, the component of gravity in the x direction is very small compared to static chordwise tension of the cable, which can be ignored.
(3) Ignoring the impact of cable bending stiffness.
(4) The amplitude of the cable is relatively small.

The equilibrium equation in y direction could be derived as:

$$S_0\frac{\partial^2\eta}{\partial x^2}-AE\frac{(mg\cos\theta)^2}{S_0^2}(\frac{l}{2}-x)\frac{\partial\eta}{\partial x}=m\frac{\partial^2\eta}{\partial t^2} \qquad (2\text{-}5\text{-}34)$$

Following equation could be obtained by the graphing method [70]:

$$\eta(x,t) = q_n(t)\sin\frac{n\pi x}{l} \tag{2-5-35}$$

Applying the Galerkin method:

$$S_0[\int_0^l \varphi_n(x)\frac{d^2\varphi_n(x)}{dx^2}dx - \frac{\lambda^2}{l^3}(\int_0^l \varphi_n(x)dx)^2]q_n(t) = m\int_0^l \varphi_n^2(x)dx q_n(t) \tag{2-5-36}$$

Organized as:

$$\frac{d^2q_n(t)}{dt^2} + \omega_n q_n(t) = 0 \tag{2-5-37}$$

$$\omega_n = \frac{S_0}{m}\frac{\frac{\lambda^2}{l^3}(\int_0^l \varphi_n(x)dx)^2 - \int_0^l \varphi_n(x)\varphi_n''(x)dx}{\int_0^l \varphi_n^2(x)dx} \tag{2-5-38}$$

Substitute $\varphi(x) = \sin\frac{n\pi x}{l}$ into the above equation:

$$\omega_n = \frac{n\pi}{l}\sqrt{\frac{S_0}{m}(1+\mu_n)} \tag{2-5-39}$$

Where $\mu_n = \frac{2\lambda^2}{n^4\pi^4}[1+(-1)^{n+1}]^2$; it is the correction factor, n is the positive integer.

2.6 Experimental research of the dynamic behaviour of stay cables

The experimental analysis performed by Hoftyzer [72], for several different cases in terms of the angle of inclination and cable properties aimed at determining the frequency crossover of stay cables, thus multiple natural frequencies of stay cables has been obtained in different conditions.

A 1.59 mm diameter galvanized aircraft cable was used in the experiments, with approximate 1.187 mm^2 of metallic cross section. The mass per unit length of the cable was 9.39×10^{-6} kg/mm, derived from the density of 7850 kg/m^3. The modulus of elasticity of the cable was 93080 Mpa. The distance between the two fixed ends of the cable was 2.5 m.

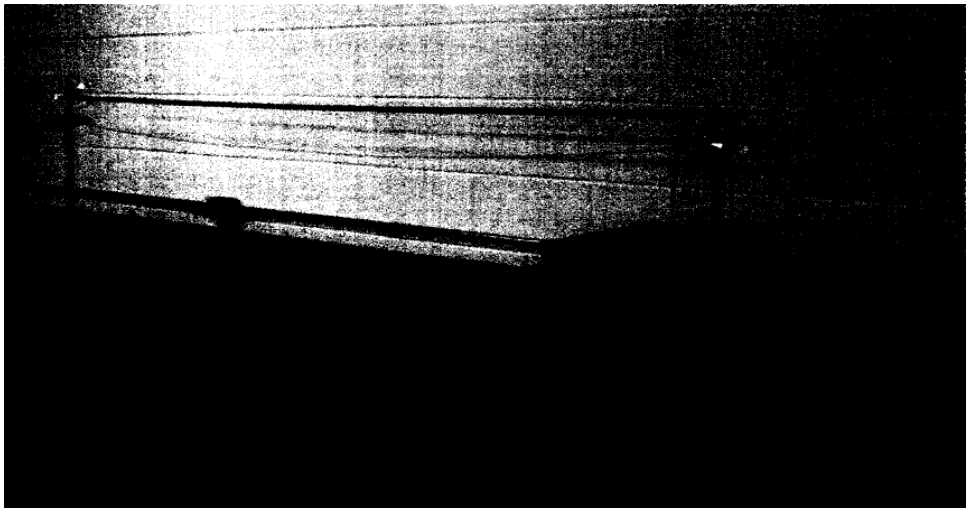

Figure 2-14: Experiment set-up [72]

Different angles of inclination were performed during the experiments. Following are the results:

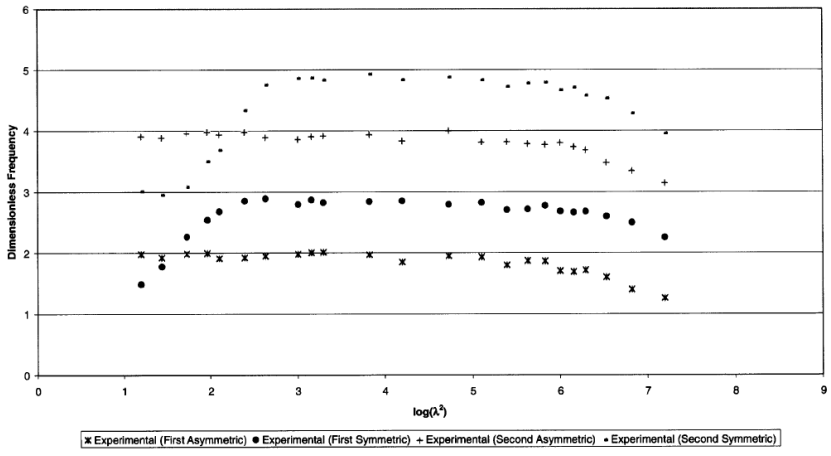

Figure 2-15: Results of horizontal cable [72]

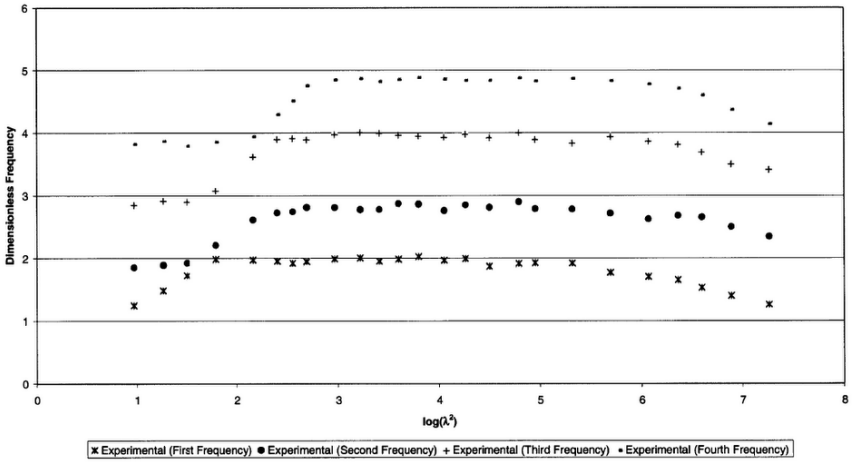

Figure 2-16: Results of 15 degrees [72]

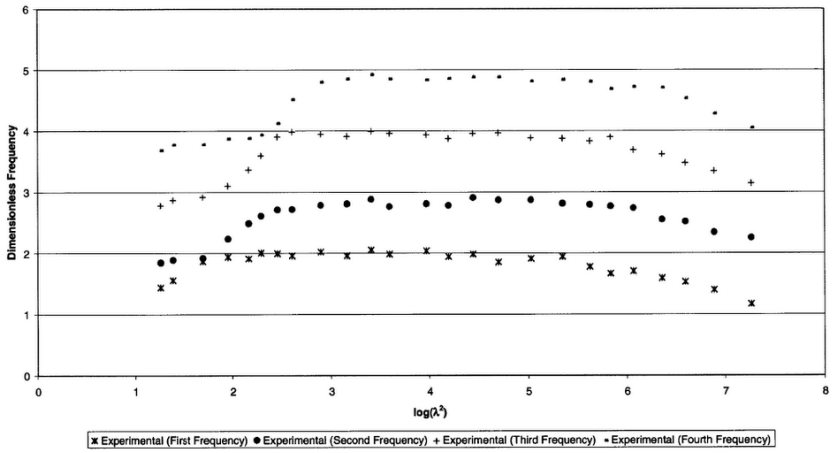

Figure 2-17: Results of 30 degrees [72]

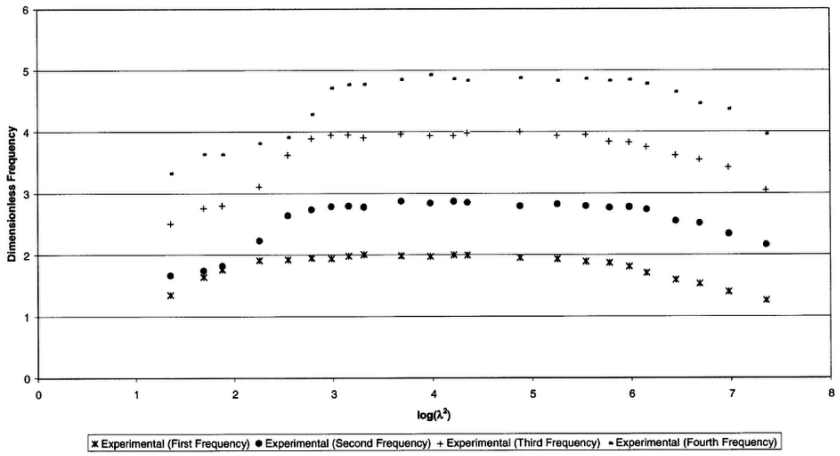

Figure 2-18: Results of 45 degrees [72]

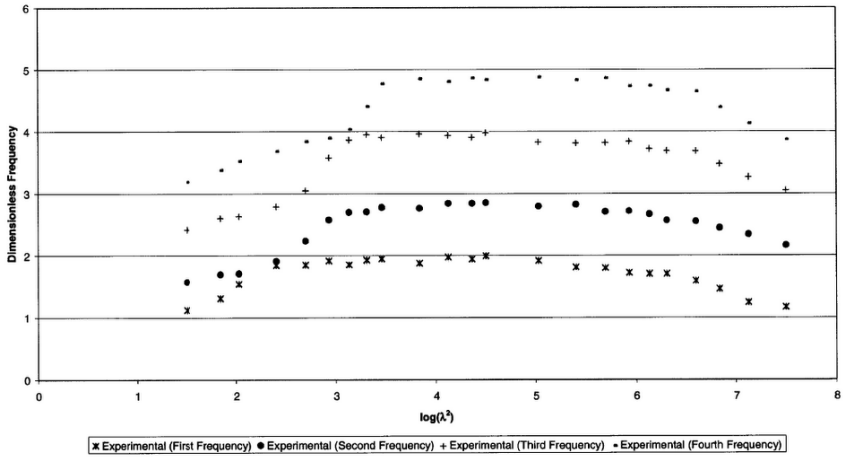

Figure 2-19: Results of 60 degrees [72]

Where λ^2 is a dimensionless parameter of the cable regarding both geometric and elastic effects, which equals to $(\frac{EA}{H})(\frac{wl}{H})^2$;

E is Young's modulus;

A is cross area;

w is unit weight of cable;

l is span length of cable;

H is horizontal component of cable tension.

2.7 Research results on the stay cables of existing bridges

2.7.1 Bill Emerson Memorial Bridge

The free-vibration and time-history analysis of the stay cable network equipped with crossties and the time-history analysis of stay cable systems with external dampers and external dampers combined with crossties had been discussed in Park and R. Bosch's study [9], in four different chapters, respectively.

Crossties are also known to reduce the cable sag variations among stay cables of various lengths. From a dynamics point of view, the presence of lateral constraints modifies the oscillation characteristics of the stay group. Also, the interconnection of individual stay cables results in a complex cable network [9].

As a result, a closed-form solution to a structural analysis problem of such network is elusive.

However, the dynamic behaviour of a stay cable system networked with crossties has not been fully understood yet; in fact, the mitigation effect of the crosstie in the cable network has not been well established.

The effectiveness of crossties in the mitigation of stay cable vibrations was numerically investigated.

Both modal analyses and time-history analyses were conducted on a set of stay cables from the completed Bill Emerson Memorial Bridge in Cape Girardeau, MO.

Numerical analysis was conducted using the general-purpose finite element code SAP 2000 [9].

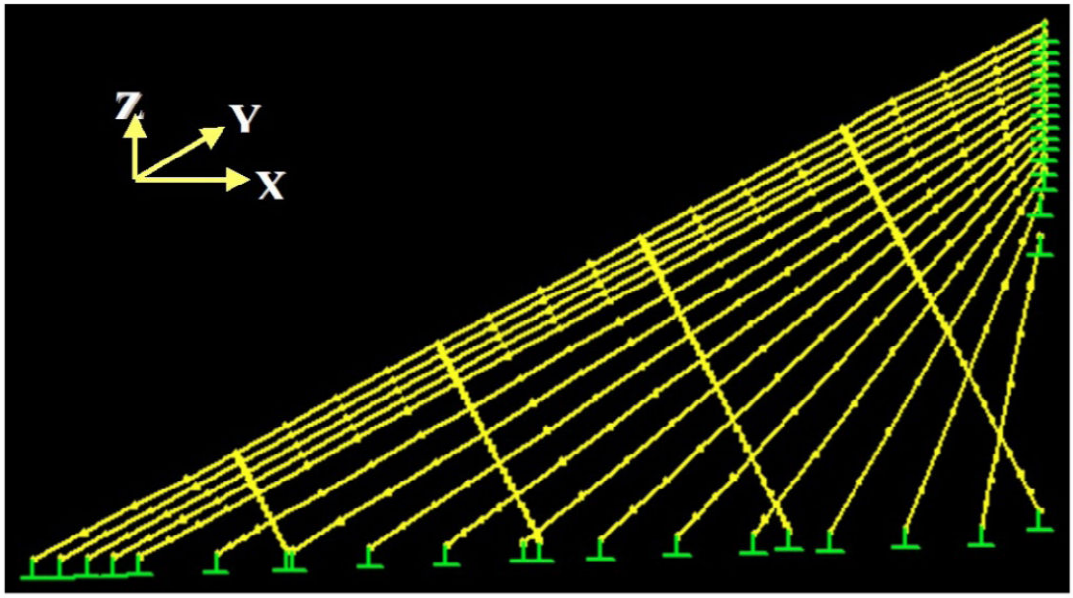

Figure 2-20: Finite element discretization of a cable system with four lines of crossties [9]

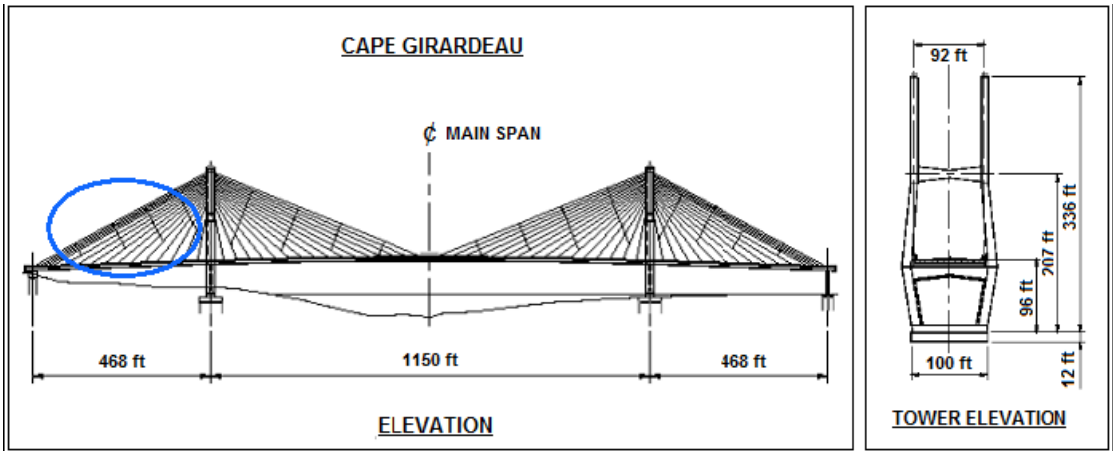

Figure 2-21: Bill Emerson Memorial Bridge in Cape Girardeau, MO [9]

An explicit time-history analysis of one of the four stay-cables fan under time-varying wind loads has been conducted to explore the behaviour of the network and derive the effectiveness of a mitigation measure, which has provided more explicit and detailed information about the system's dynamic structural performance.

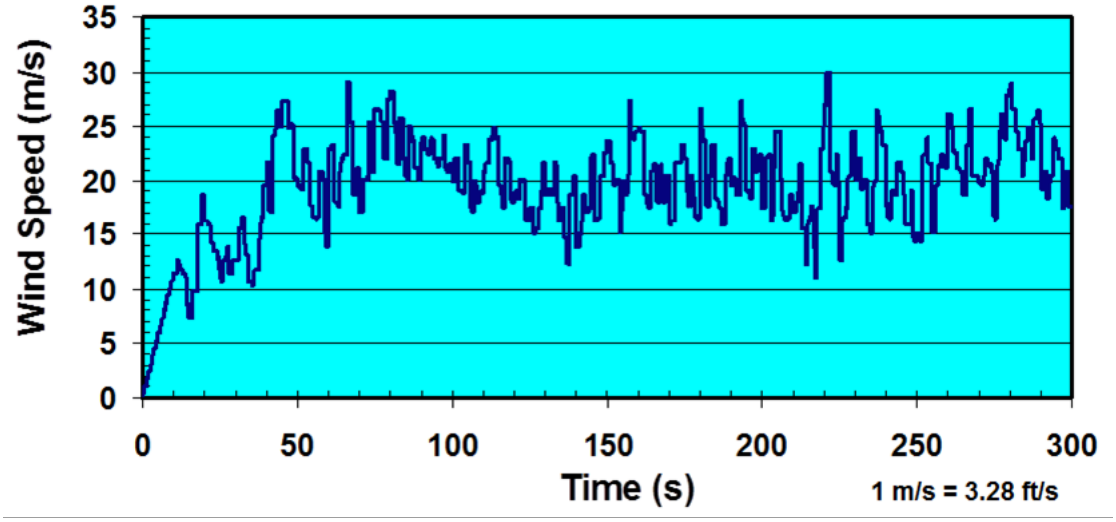

Figure 2-22: Reference wind speed profile [9]

2.7.2 Yibin Yangze River Bridge

From the paper "Study on rain-wind induced vibration of cables in cable-stayed bridges by wind tunnel test" [73], a series of wind tunnel tests were carried out to explore the effect of wind speed, inclined angle, yaw angle, rain precipitation and structural damping ratio on the rain-wind induced vibration of cables in cable-stayed bridges.

The experiment was conducted in the wind tunnel XNJD-2, of the Southwest Jiaotong University in China.

The following are the results of the vibration characteristics of different α, the angle between the stay cable and the horizontal plane, and β, the angle between the coming wind and the plane of the cable.

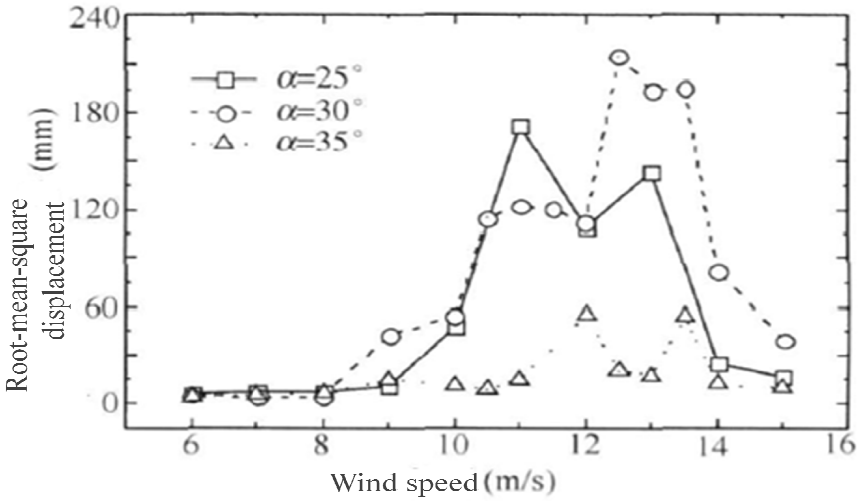

Figure 2-23: RMS of cables at the yaw angle β =25° [73]

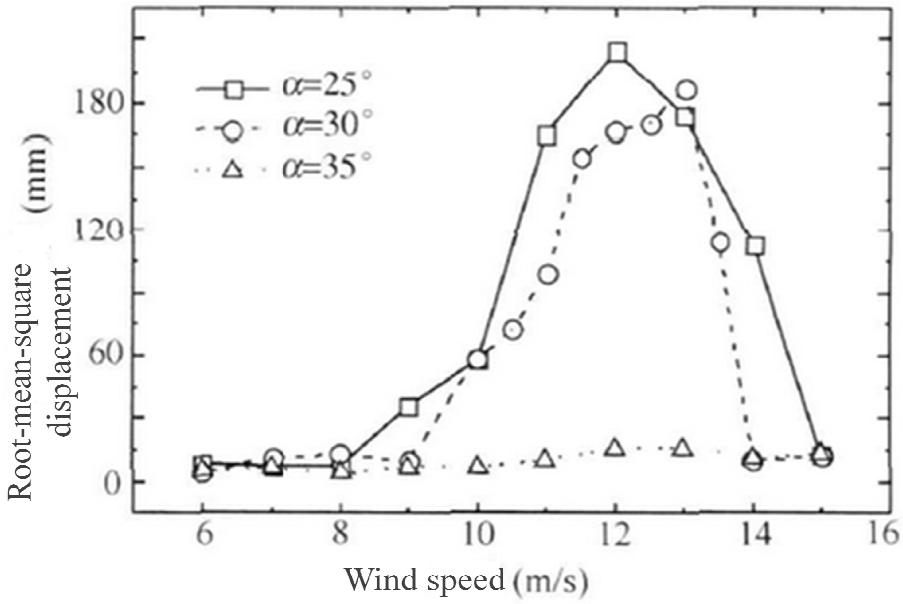

Figure 2-24: RMS of cables at the yaw angle β =30° [73]

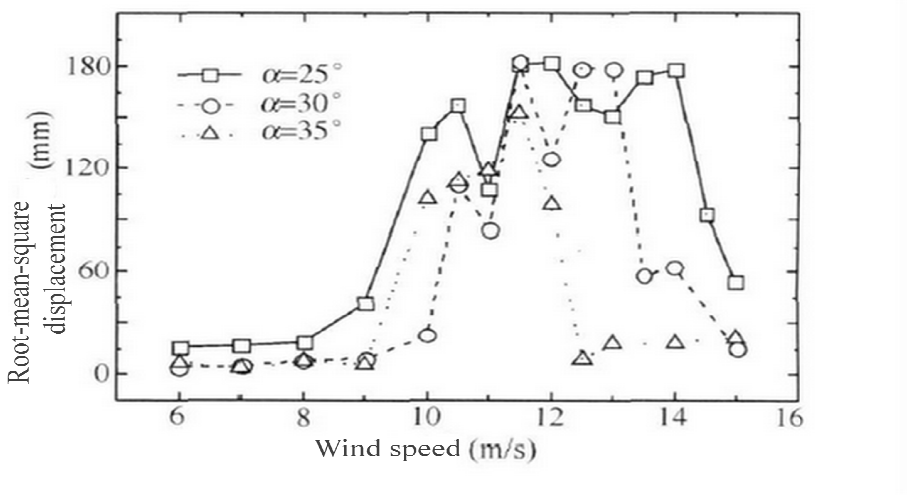

Figure 2-25: RMS of cables at the yaw angle β =35° [73]

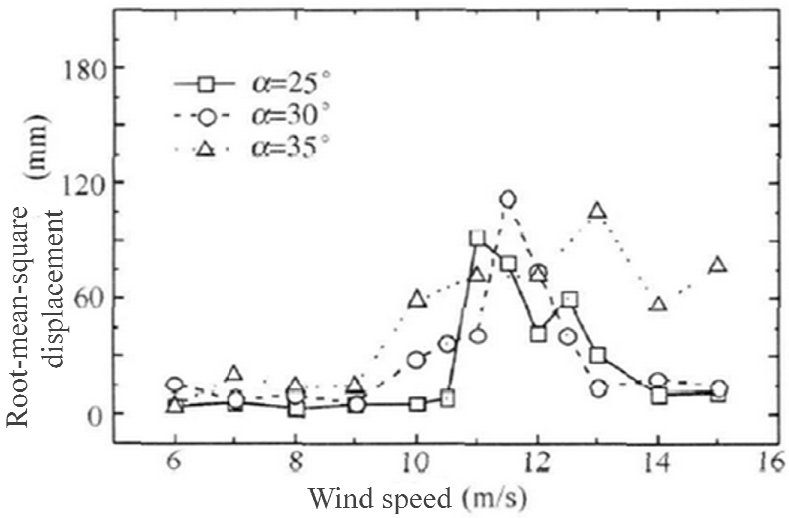

Figure 2-26: RMS of cables at the yaw angle β =40° [73]

2.7.3 Oshima Bridge

From the paper "Analysis of Local Vibrations in the Stay Cables of an Existing Cable-stayed Bridge under Wind Gusts" [74], the properties of local vibration in cables under wind loads are obtained by means of numerical analysis.

The response characteristics of the local vibrations in the stay cables under wind gusts are derived using the Oshima Bridge in Japan. The main span of this bridge is 350.0 m and the side spans are 160.0 m.

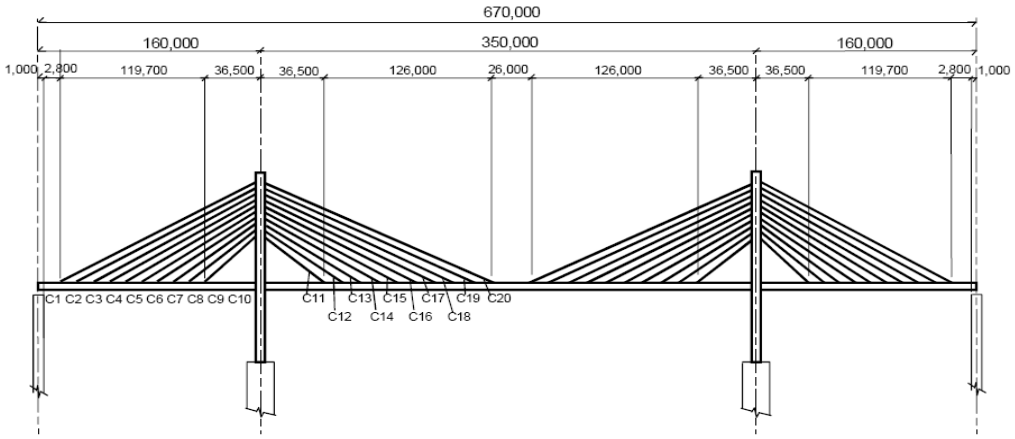

Figure 2-27: Bridge Configuration [74]

The results of the cable under a wind velocity of U=30 m/s are presented below for which the damping constants hc of the cables are assumed to be 0.001.

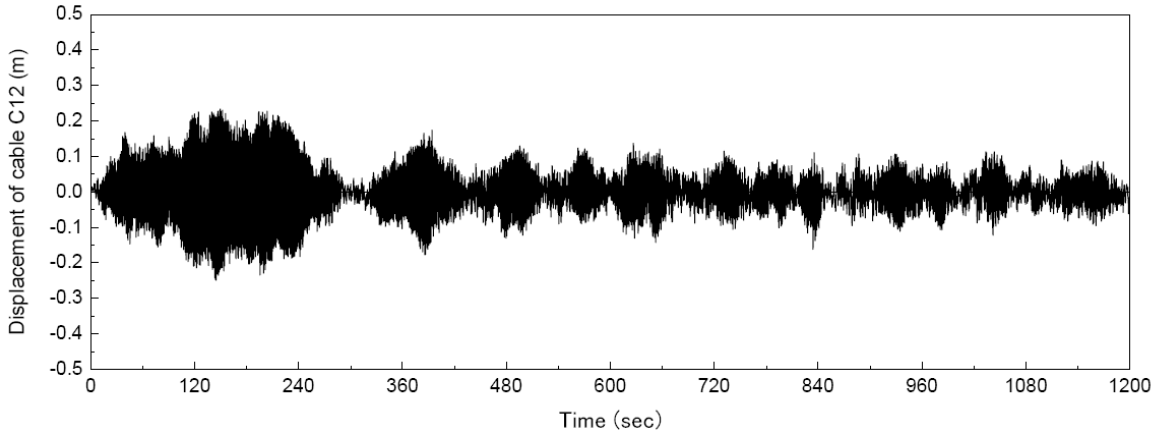

Figure 2-28: Displacement of Cable C12 [74]

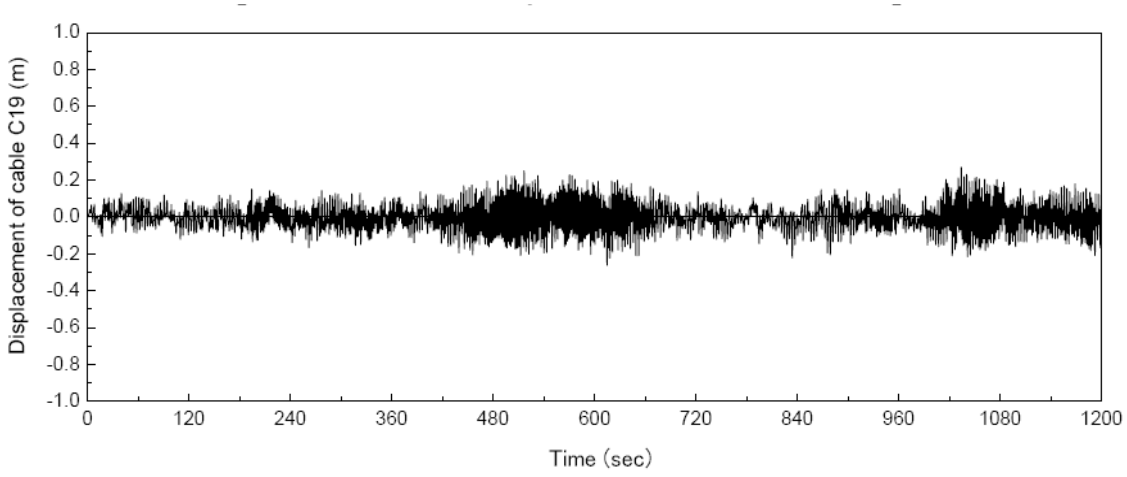

Figure 2-29: Displacement of Cable C19 [74]

2.8 Other Researches on the Bill Emerson Memorial Bridge

In 2014, comparative performance study among variable friction pendulum isolator (VFPI) and traditional friction pendulum system (FPS) isolators for seismic response of the bridge has been carried out by Purnachandra Saha [75]; For direct comparison among the different control strategies for a specific type of structure, benchmark problems were developed; Bill Emerson Memorial Bridge crossing the Mississippi River near Cape Girardeau, Missouri, designed by the HNTB Corporation, was the benchmark cable-stayed bridge used for the study.

In 2013, method for evaluating the economic efficiency of a semi-active Magneto-Rheological (MR) damper system for cable-stayed bridges under earthquake loadings has been described and its evaluation results were investigated by Daegi Hahm, Seung-Yong Ok [11], using the Bill Emerson Memorial Bridge;

In Dec, 2012, the results of system identification of cable-stayed bridge using the SSI method was presented by Dutta Atanu Kumar, J.M. Caicedo [12], which was applied to a real-life cable-stayed bridge, the Bill Emerson Memorial Bridge, Missouri, U.S.. The identification procedure uses 66

accelerometer data and 25 channel time histories.

In Nov, 2012, Mohammed Ismail, José Rodellar, etc. [76], presented the results of an extensive series of simulation tests to identify the mechanical characteristics of an innovative isolation device known as the Roll-N-Cage (RNC) isolator. Numerical assessment was used including finite element method; the Bill Emerson Memorial Bridge was chosen to be the bridge FE model.

In Sept, 2007, based on the seismic instrumentation data, the vibration characteristics of the Bill Emerson Memorial Cable-stayed Bridge were investigated and used to validate a three-dimensional Finite Element model of the bridge structure by G. Chen, D. Yan, etc. [10], which was successfully verified and validated by using the natural frequencies and mode shapes of the bridge extracted from the measured data. Both ambient and earthquake data measured from the Bill Emerson Memorial Bridge are reported and analyzed. In the FE model, the cables were simulated by Frame/Cable element, assuming the contribution of every internal wire inside the cable.

In June, 2007, a novel electromagnetic induction (EMI) system integrated in magnetorheological (MR) dampers was presented by Sang-Won Cho, Jeong-Hoi Koo, etc. [13]. In order to evaluate the performance and robustness of the MR-EMI sensor system with the MEDA control, the study performed an extensive simulation study using the first generation benchmark cable-stayed bridge, which was the Bill Emerson Memorial Bridge.

Chapter 3 Modelling set-up

3.1 Introduction

Several numerical analyses have been conducted for determining the stay-cables behaviour with uniform property and multiple-strand content, using Abaqus FEM software. Both modal analysis and time-history loading analysis were carried out on the 16 stay-cables connecting the tower to the main span deck of the Bill Emerson Memorial Cable-stayed Bridge. The bridge has a symmetric structural layout, therefore only one side of the stay-cables was analysed in detailed, and referred herewith as the stay-cables fan. The entire stay-cables fan network was modelled by employing the finite element discretization of the cables system, which reflects the final configuration of the bridge. The main contribution to the cable modelling consists in the procedure of simulating the inner strands of each stay-cable along with their interaction within the grout material installed between the inner strands of each stay-cable. To validate the FE modelling conditions and the grout-inner strands interaction, three cases were modelled: a) one single cable with one uniform property, simulating the stay cable of compact configuration without internal strands, as currently used in most of the bridge designs, b) one multiple-strand cable without the grout material linking the inner strands and c) one multiple-strand cable with the grout paste between the inner strands. The first two models were validated against the experimental results obtained by Hoftyzer (2008) for a single cable, under different loading conditions. Base on the validated one cable models, the stay-cables fan configuration of the Bill Emerson Memorial Cable-stayed Bridge was modelled and the natural frequencies and the response under wind loading were compared with the monitoring data obtained from the bridge construction site by Bosch et al (2013). Therefore, the overall goals of this FE modelling and the performed numerical study include the following:

- Determining the natural frequencies and the vibration mode shapes of a single cable model, with and

without the multiple strands and the grout material.

- Clarifying the dynamic properties of the internal strands in one single cable, which are under the influence of the grout material surrounding the inner strands, and the interaction between such strands, under wind loading scenarios. Furthermore, clarifying how the behaviour of the cables differs from the previous research on stay-cables that employed only a simplified beam element with one uniform property of the cable is sought.

- Determining the natural frequencies and the vibration mode shapes of the stay-cables fan, with the multiple-strand grouted configuration, used in the construction of the Bill Emerson Memorial Cable-stayed Bridge

- Investigating the effectiveness of the crossties installed on the Bill Emerson Memorial Cable-stayed Bridge, in the mitigation of stay-cable vibrations, through the modal analysis of the cable network with no crossties, with only one crosstie, with two crossties and with four crossties, respectively.

- Obtaining the system's dynamic structural performance under wind loading, to better understand the properties of the stay-cables system, and for acquiring the effectiveness of the mitigation measure with the added crossties. Although the modal and frequency investigations provide some important information regarding the dynamic characteristics of the stay cable network, the real behaviour of the structural system under different wind loads is difficult to estimate based only on such information. Therefore a time-history analysis under real wind forces, determined based on the wind data recorded at the Bill Emerson Memorial Cable-stayed Bridge site (Bosch et al, 2013) was conducted for more explicit and detailed response of the stay-cables under real wind conditions.

3.2 Finite element modelling of cables

The basic idea of the finite element method is to divide the solution domain of the structure, the cables

in this case, into a series of elements, thus the connections between the elements rely only on the nodes. Elements nodes of independent variables exploit the interpolation of the selected function to get dependent variable points inside the elements. Thus, because the element shape is simple, it is convenient to construct equations between the nodes by balancing the energy relationship, and then by adding the equations of the elements together, to form a set of overall algebraic equations to which boundary conditions are applied; these equations could be solved then. Generally, the more detailed the division of the elements, the more accurate the results can be achieved [77].

From the point of view of the selection of the dependent variable, the finite element methodology can be divided into three categories: the displacement method, the force method and the hybrid method. The displacement method consists in using the nodal displacements as unknowns to solve the problem; using the internal forces as unknowns to solve the problem is known as the force method. For the hybrid method part of the structure consists in using the node displacement as unknowns, and the other parts are using the internal forces as the unknowns to solve the problem, thus combining the two approaches. Because of its versatility and because of the processing capacity of the computer software, the displacement method, is simple and convenient, therefore, it is widely used [56]. The FE model in the current study is based on the displacement method.

The current cable modelling stages were performed according to the basic idea of the finite element displacement method; the first step is to discretize the area of solving the problem, which is to transform the continuous bodies with infinite number of degrees of freedom into structures of finite number of degrees of freedom. Secondly, the function expression representing the change of displacement at any point within the elements with positions was chosen, which estimated the displacement of any point within the elements based on the nodal displacements interpolation. Then, starting from the analysis of a single element, the energy variation equations are constructed. Finally, integration of all the elements displacement is performed, and is combined with the external load on

the node, to get a set of multiple linear equations, using the nodal displacements as unknowns, which could be solved by applying the boundary conditions. The basic steps of the finite element modelling and analysis performed for the cable element modelling can be summarized as follows:

1) Cable structural discretization.
2) Cable element analysis: Select the displacement mode; establish the element stiffness equations and the equivalent nodal force calculations.
3) Integration of the cable element displacement.
4) Solve the equations and derive the nodal displacements.
5) Calculate other values based on the nodal displacements.

Because the cable has no stiffness in bending, as a beam element would have, certain assumptions were developed for the modelling of the cable element, as follows:

1. Each cable is made of a finite number (n) of discrete structural rod elements (el) connected by pins.
2. The supporting points of each cable are considered fixed, which means there is no displacement at both ends of the cable. Thus, the lumped mass at both fixed ends (m_0, m_n) can be ignored, but it is considered at the middle of the element (Figure 3-1).

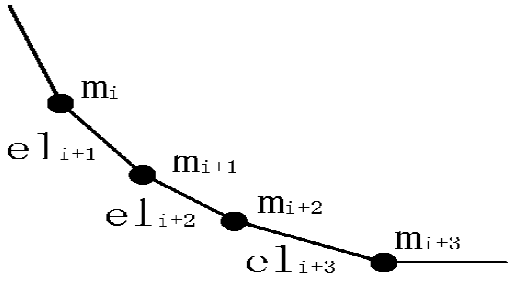

Figure 3-1: Derivation of the mass matrix

(m: Lumped mass el: length of the cable elements)

As Figure 3-1 shows, the mass of the cable is lumped at the nodes where the cable elements are linked; the nodes of the elements are allowed to have displacements both vertically and horizontally in plane and as rotation angle, as shown in Figure 3-3; For the cable elements the flexural stiffness is ignored, and the elements have only vertically and horizontally displacement, as the Figure 3-2 shows.

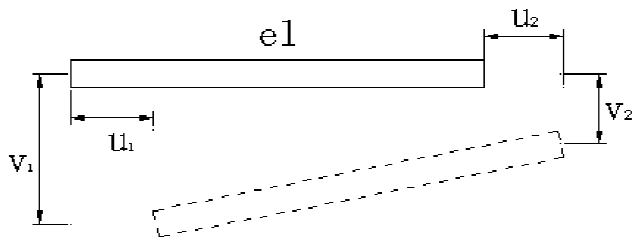

Figure 3-2: Derivation of the stiffness matrix of elements with no flexural stiffness

(u: Horizontal displacement v:Vertical displacement)

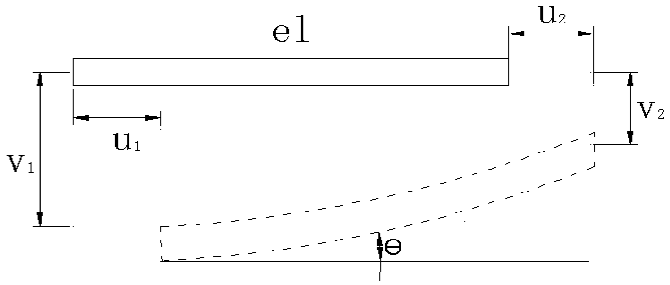

Figure 3-3: Derivation of the stiffness matrix of elements with flexural stiffness

(θ：Angle of rotation)

3.2.1 Uniform property cable modelling

The modal analysis is an effective tool for studying the structure dynamic characteristics. Modal procedure is the inherent vibration characteristics of the structure; each vibration mode has a specific natural frequency, damping ratio and modal vibration shape. The modal parameters can be obtained analytically or by experimental free-vibration analysis; such a calculation or experimental analysis process is known as the modal analysis. If the analysis process is achieved by the method of the finite element calculations, this is called an analytical modal analysis.

To clarify the vibration characteristics of the stay-cables, starting from the uniform property cable case, then by simulating the multiple strands, the modal analysis has been conducted on one stay-cable structure.

Abaqus is a set of powerful engineering finite element simulation software, the abilities to solve the problems range from relatively simple linear analysis to many complex nonlinear problems. Abaqus contains a rich library of elements which are able to simulate multiple shapes and geometries. Also it has various types of material model library; the structural performance of typical engineering materials can be easily simulated and investigated.

For a conventional linear problem, Abaqus can solve the structural element with very good accuracy, and it is desirable in terms of the model size limitations, computing processes and computing time. Meanwhile, the software has a very distinct advantage in solving nonlinear problems. The nonlinear problems cover aspects of the material nonlinearity, geometric nonlinearity and nonlinear states.

The current numerical analysis was conducted using the general purpose finite element modelling. The finite element discretization of a side section of a single cable comprises of 100 elements as it is shown in Figure 3-4.

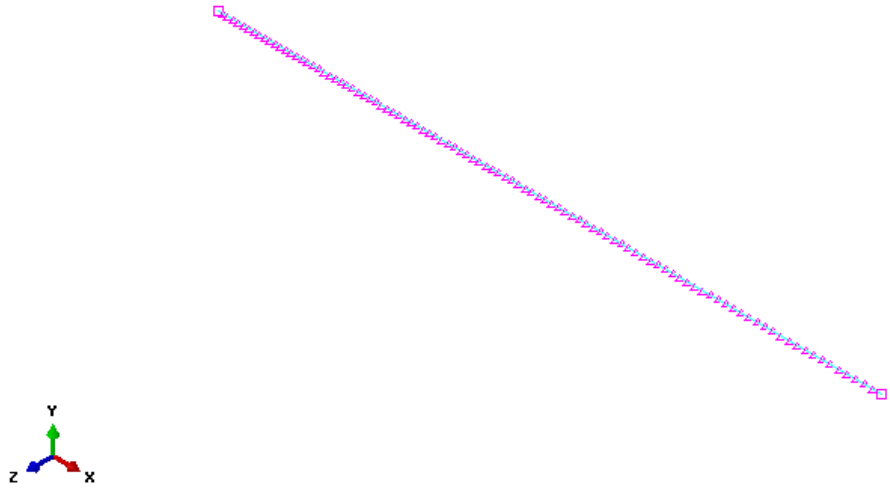

Figure 3-4: Configuration of a single cable (100 elements)

3.2.2 Selection of elements type

In linear analysis, the axial stiffness and the bending stiffness are considered to be uncoupled. Otherwise, when the deformations are large enough that cannot be ignored anymore, for the case of the stay-cables, these elements are loaded with an interaction between the axial force (tension or compression) and the bending moment. Based on the lateral deformation of a bending element, extra bending moment would be induced by a simultaneous axial force applied and the bending stiffness of the member would be converted. Consequently, the effective bending stiffness of the member will decrease for a compressive axial force and increase for a tensile axial force, furthermore, the bending moments will affect the axial stiffness of the member due to the shortening of the member that is caused by the bending deformations. These effects can be considered in the geometric stiffness matrix of the member modelling by choosing the non-linear geometry option in the analysis step.

For the cable element, supported at its ends and loaded under its own weight and under an externally applied axial force, like stayed-cables are, the cable sags into the shape of a catenarian cable. The axial

stiffness of the cable varies nonlinearly as a function of the cable tension force, thus it changes with the distance from the cable ends. For conventional truss elements, the sag due to self-weight can be ignored but for the cable elements this sag should be considered for an accurate analysis. The sagging cable problem needs an explicit stress stiffness matrix included in the mathematical formulation, to provide numerical stability. However, the cable sag effect can be considered by applying axial strains or stresses in the cables.

The truss elements can transmit only axial forces, which does not have any bending stiffness. Therefore, for stay-cables, solver and convergence problems would arise if the truss elements are used to simulate cables behaviour. Since the truss elements have no flexural stiffness in the transverse direction, however, the finite element method in software has abilities to consider the bending stiffness of pre-tensioned truss elements and therefore enable us to proceed with the frequency analysis from the deformed configuration due to self-weight.

Applying an initial stress in the truss element, can settle the calculation in the initial equilibrium state; however, if the initial stress is set to be too small, the calculation may not converge. Multiple trials should be conducted to reach a reasonable stress. Under normal circumstances, the initial value has little effect on the final value, which can be ignored.

In this section, after several attempts, the pretension in the stay-cable was finally confirmed as $5.61\times10^{8}\,Pa$. The rest of the material and geometrical properties used for the stay-cable model are shown in the Table 3-1:

Table 3-1: Properties of the uniform property stay-cable model

Material Properties			Physical Dimensions		Prestresses
Mass Density	Young's Modulus	Poisson's Ratio	Total cable length	Diameter	Pretension
7,700 kg/m	1.999×10^{11} Pa	0.3	80 m	0.1 m	5.61×10^{8} Pa

The natural frequencies of the single stay-cable with flexural stiffness, (the beam elements are used in the cable modelling) and those of single stay cable without flexural stiffness (the truss elements are used in the cable modelling) are shown in Figure 3-5. It can be seen that the natural frequencies of the truss elements are generally higher when compared with the frequencies of the same cable modelled as beam element. The significance of the flexural stiffness is insignificant for lower-order vibration modes but increases with the mode number.

Table 3-2: Natural frequencies and eigenvalues of beam and truss elements

Mode Number	Truss element		Beam element		Differences of frequencies
	Eigen Value	Frequency (cycles/time)	Eigen Value	Frequency (cycles/time)	
1	112.54	1.6884	112.58	1.6885	0.01%
2	112.92	1.6912	113.06	1.6923	0.07%
3	450.03	3.3763	450.63	3.3786	0.07%
4	450.04	3.3763	450.64	3.3786	0.07%
5	1012.2	5.0635	1013.6	5.0669	0.07%
6	1012.2	5.0636	1013.6	5.067	0.07%
7	1798.4	6.7493	1801	6.7542	0.07%
8	1798.4	6.7493	1801	6.7542	0.07%
9	2807.9	8.4335	2812.1	8.4399	0.08%
10	2807.9	8.4336	2812.1	8.4399	0.07%
11	4039.7	10.116	4046.2	10.124	0.08%
12	4039.7	10.116	4046.2	10.124	0.08%
13	5492.6	11.795	5502.1	11.805	0.08%
14	5492.6	11.795	5502.1	11.805	0.08%
15	7165.1	13.472	7178.4	13.484	0.09%

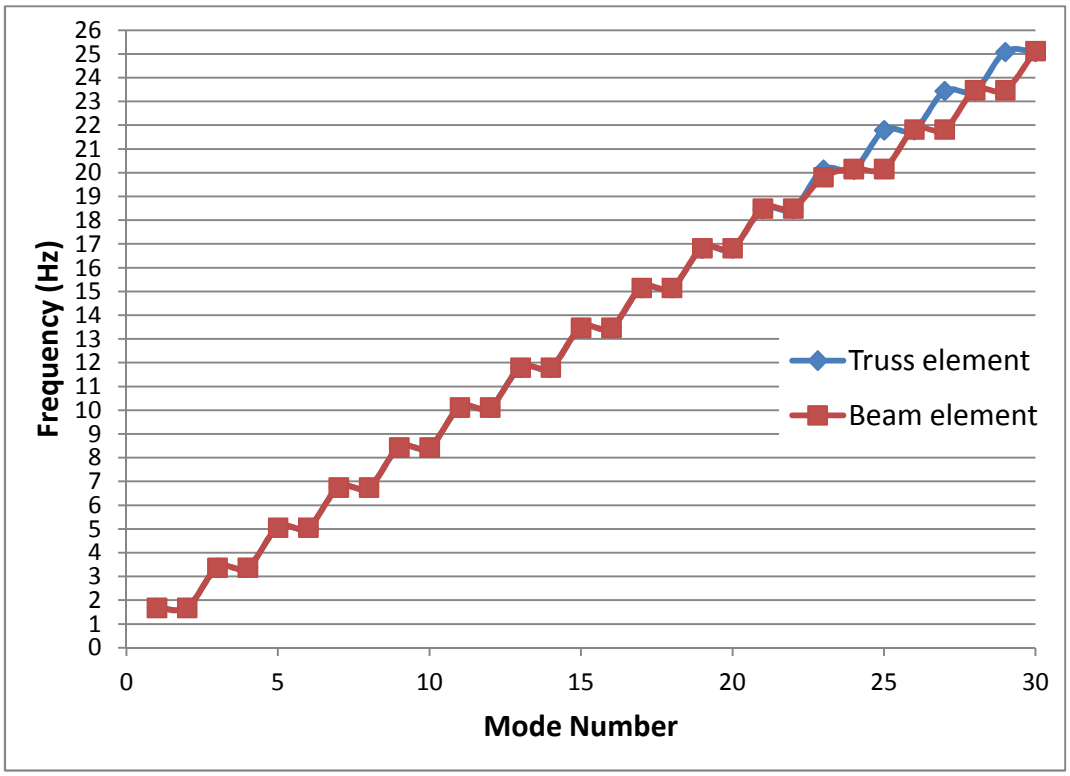

Figure 3-5: Frequencies of beam and truss elements.

To avoid the problem of no convergence given by the software solver and also for achieving a higher accuracy of the analysis, the beam element has been chosen. Many other researchers have also adopted for using the beam element type for simulating the model the properties of the cables [78] [9] [10].

3.3 Modelling of the uniform property and multiple strands stay-cables

Initially, numerical analysis has been done for investigating the natural frequencies and the corresponding mode shapes of one single cable as a uniform property cable and as a multiple strands stay-cable. In order to identify the factors that affect the characteristics of the interactive behaviour between the inner strands within the stay-cable, the numbers of strands chosen to be modelled were varied.

Also considering the basic modelling of one single stay-cable used for the validation in the initial part of this study, all the mode shapes investigated in this chapter are the in-plane modes.

Table 3-3 shows the material and the geometrical properties of the Billings Memorial Bridge stay-cable number 1, which was used for the current modelling.

Table 3-3: Material and geometrical Properties of the stay-cable 1 [10]

Material Properties			Physical Dimensions	
Mass Density	Young's Modulus	Poisson's Ratio	Total cable length	Diameter
7,700 kg/m	1.999×10^{11} Pa	0.3	158 m	0.1 m

3.3.1 Typical uniform property cable

At first, a uniform property stay-cable model, which corresponds to one compact steel cable, without strands and grout material inside, as it is currently used in most bridge designs and FE investigations, has been analyzed. Figure 3-6 and Figure 3-7 show the mode shapes of the dominant vibration modes, which are the 3rd, the 19th, the 20th and the 29th modes respectively.

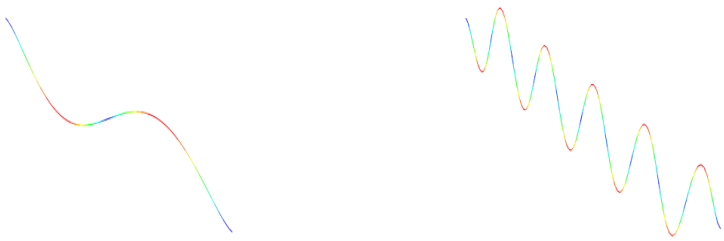

Figure 3-6: 3rd, 19th mode shape of uniform property cable

Figure 3-7: 20^{th}, 29^{th} mode shape of uniform property stay-cable

It can be seen that the vibration modes of the uniform property stay-cable becomes more complex with the increase of the mode number, generally. The first 10 natural frequencies and vibration modes are presented in Table 3-4 along with the generalized mass contributing for each mode shape.

Table 3-4: First 10 natural frequencies of the uniform property cable

Mode Numbers	Eigenvalue	Frequency(Hz)	Generalized Mass
1	14.108	0.59779	9003.3
2	39.023	0.99421	8595.8
3	58.527	1.2176	9083.7
4	58.57	1.218	9071.8
5	139.77	1.8816	9139
6	139.87	1.8823	9012.7
7	268.19	2.6064	9191.6
8	268.21	2.6065	9183.2
9	458.32	3.4073	9177.2
10	459.9	3.4131	9079.4

3.3.2 Modelling of multiple strands stay-cable

Considering the complexity of the real stay-cable modelling, it was assumed that the inner strands in cable are arranged inside the cable as shown in Figure 3-8 and Figure 3-9 [79]:

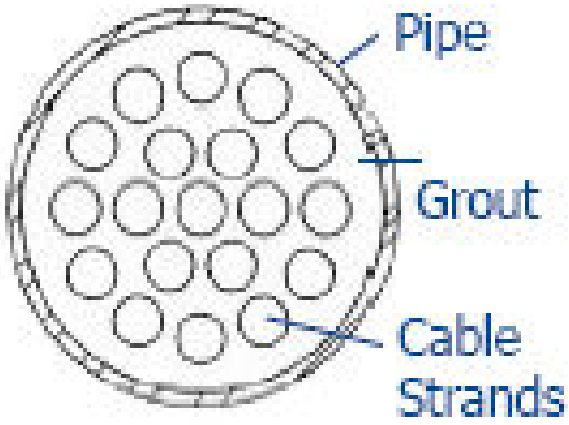

Figure 3-8: Cross section of the multiple strands stay-cable [79]

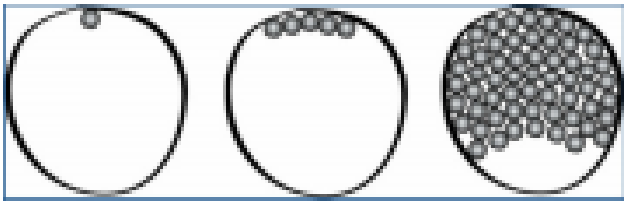

Figure 3-9: Cross-sections of multiple strands stay-cable manufacturing stages[79]

All the strands inside the stay-cable are parallel and very close to each other, and as a result, the strands motion would affect each other. In the current modelling, it was assumed that all of the stay-cables are fixed, meaning that every single strand is fixed on both ends. The grout paste is the material applied inside the stay-cable to fill the voids between the tension elements (strands) and the outer covering membrane of the stay-cables. This is an integral part of the corrosion protection system. Examples of the grout paste in use nowadays for the bridge stay-cables are cement epoxy grouts, greases and waxes [80].

To model the effect of the grout covering the inner strands, springs links have been added between each two or three strands. It can easily be concluded that the more springs are modelled in, that is, the more spring elements are spread along the strands, which means that more quantity of the grout is simulated around the strands, the closer to the real situation, thus more accurate results are expected.

Between each two strands 63 springs along the length of the strands have been added, as Figure 3-10 shows; As a result, each vibrating strand would affect the adjacent strands.

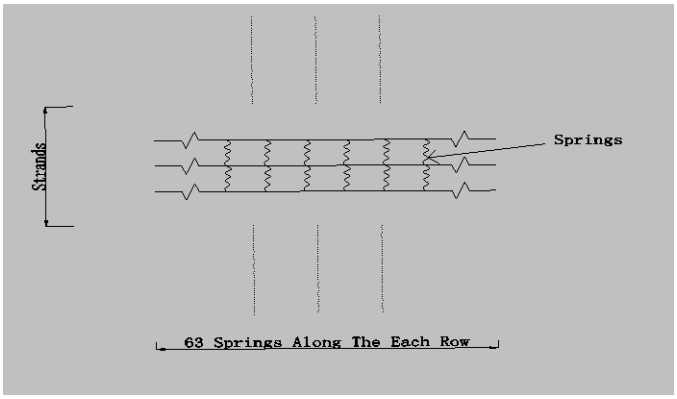

Figure 3-10: Springs along the strands

As reported [10] the stay-cables of the Bill Emerson Memorial Bridge have different number of inner strands; therefore in the current modelling, for different number of strands, the stay-cables are modelled with various space positions of strands inside. Figure 3-11 show the example of stay-cables cross-sections with four-strand, nine-strand, and twelve-strand:

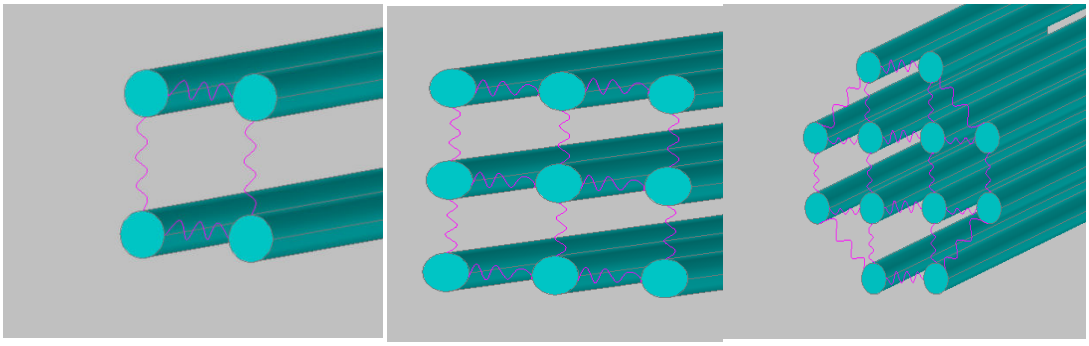

Figure 3-11: Cross section of Multiple-strand cable model

Moreover, the stiffness k of the springs is a key factor that may affect the vibration results. In the modelling of the one single stay-cable, the modelling of the grout is based on the polymer gel material. However, the grout within the stay-cables of the Bill Emerson Memorial Bridge is Portland

cement [9]. In the Sunwoo Park and Harold R. Bosch's study [9], the cable was modelled as one uniform property stay-cable, and the cement grout inside the cable was not taken into consideration. Actually none of the bridge studies are currently considering the grout material, nor the multiple strands, in the modelling of the stay-cable. The cement is a brittle material, which has the capability of stabilizing the strands, preventing them from relative motion; moreover, it adds considerable mass inside the cable. As a result, the cable with the grout is modelled as uniform property cable, with properties derived from those of the cable steel and the cement. In this study, both the uniform property cable, which is grouted with cement, and the multiple-strand cable with or without the polymer gel grout have been modelled.

Stay-cables which use Portland cement grout as a blocking agent have many of the characteristics of an external tendon of a post-tensioned box girder that has been removed from the box girder and was placed outside in the environment [80].

The grout mainly has two applications in the external post-tensioning tendons [80]. One is to provide bonding between the tendon and the bridge at the deviators. The other major purpose is to cover the strands with an alkaline environment to prevent corrosion and to become a barrier for the entrance and transport of deleterious substances into and through the duct of the stay-cable. Therefore, in both stay-cables and in external post-tensioning tendons, the grout is injected mainly to serve as a physical barrier and also an alkaline environment.

In the cable-stayed Bridges of Honshu and Shikoku design guide in Japan, is specified that due to the fact that the deflection of the cable is too large, the cement grout may crack [81]. As a matter of fact, people have developed a method using polyurethane and polymer gel as the flexible grout material. Because the polyurethane is a waterproof material, whose elongation is as large as 235%, there is no risk of cracking. Polyurethane costs more than the polymer cement, but it has better flexibility.

The range of the Young's modulus of the polyurethane is from 10 MPa to 1,000 MPa [82]. Normally, for the polyurethane, the lower the value of the Young's modulus, the better the ability to prevent cracking. To compare the cement grout and the polyurethane grout in the cables of Bill Emerson Memorial Bridge, the case of polyurethane grout applied in the cable has been modelled. To confirm the equivalent stiffness of the polyurethane grout, the following conversion has been made:

Introducing the Hook's law:

$$F = -kx \tag{3-1}$$

Under normal conditions, Hook's law could be represented as: within the elastic limit, the stress of the substance is proportional to the strain of the substance, that is:

$$\sigma = y\varepsilon \tag{3-2}$$

In which y is the Young's modulus of the material. Considering the stress σ as the elastic force on the unit area, shown as $\sigma = F / S$, as a component in the normal direction of the cross-section of the inner force, which shows the level of the inner force caused by the strain in the elastomer. The strain ε means the value of the change of the cable length of the unit length, which could be written as: $\varepsilon = \Delta L / L_0$ (L_0 is the original length, $\Delta L = L - L_0$ is the absolute elongation. Therefore, Hook's law could also be expressed as:

$$\frac{F}{S} = \frac{y\Delta L}{L_0} \tag{3-3}$$

The meaning of x in equation（3-1）is the same with ΔL in equation （3-3）, thus it can be concluded from comparing equations （3-1） and （3-3） that:

$$k = \frac{yS}{L_0} \tag{3-4}$$

For the stay-cable 1 of the Bill Emerson Memorial Bridge for example, the length of the cable equals to 158 m, the cross-section area of the cable is 0.008m^2, which could be obtained from Table 3-15 [10].

Assuming that the percentage of the grout is 20%, the area of the grout becomes:

$$0.008 \times 20\% = 0.0016 m^2 \tag{3-5}$$

Substituting the parameters of the stay-cable into equation 3-4; the range of the equivalent stiffness can be obtained as follows:

$$100.63 N/m = \frac{10^7\ pa \times 0.008 m^2}{159 m} < k < \frac{10^8\ pa \times 0.008 m^2}{159 m} = 1006.3 N/m \tag{3-6}$$

To explore the role of the spring stiffness in the modal properties of the stay-cables, two different spring stiffness are chosen at first: k=100 N/m, k=500 N/m

First of all, the analysis of the cable that did not account for the effects of the grout has been conducted, and parallel multiple strands without springs and with k equals to zero were modelled.

3.3.2.1 Two-strand cable without grout (no springs)

To compare with the uniform property cable, the same stay-cable modes has been chosen , as shown in Figure 3-12 and Figure 3-13

Figure 3-12: 3rd, 19th mode of two-strand cable without grout

Figure 3-13: 20th, 29th mode of two-strand cable without grout

Basically, the mode shapes did not change; the difference when compared with the uniform property cable is that while one strand of the two vibrates the same way as the uniform property cable does, the other strand has no vibration. The frequencies of the uniform property cable and of two-strand cable are the same as well, except that two-strand cable contains the frequencies of two individual strands.

Table 3-5: Mode frequencies 1-10 of two-strand cable without grout

Mode Numbers	Eigenvalue	Frequency(Hz)	Generalized Mass
1	14.108	0.59779	9003.3
2	14.108	0.59779	9003.3
3	39.023	0.99421	8595.8
4	39.023	0.99421	8595.8
5	58.527	1.2176	9083.7
6	58.527	1.2176	9083.7
7	58.57	1.218	9071.8
8	58.57	1.218	9071.8
9	139.77	1.8816	9139.1
10	139.77	1.8816	9139.1

3.3.2.2 Four-strand cable without grout

To verify the impact of the number of the strands on the natural frequencies, more strands have been modelled; the following figures are the vibrations of the four-strand cable:

Figure 3-14: 3rd, 19th mode of four-strand cable without grout

Figure 3-15: 20th, 29th mode of four-strand cable without grout

It can be seen that for the four-strand cable, the mode frequencies include the vibrations of every individual strand; the mode shapes of each strand did not change. Therefore the number of strands has no impact on the frequencies and on the mode shapes of the overall stay-cable.

Table 3-6: Mode frequencies 1-10 of Four-strand cable without grout

Mode Numbers	Eigenvalue	Frequency(Hz)	Generalized Mass
1	14.108	0.59779	14511
2	14.108	0.59779	14511
3	14.108	0.59779	13625
4	14.108	0.59779	13625
5	39.023	0.99421	11449
6	39.023	0.99421	11449
7	39.023	0.99421	14057
8	39.023	0.99421	14057
9	58.527	1.2176	11960
10	58.527	1.2176	11960

3.3.2.3 Two-strand cable with springs k=100 N/m

The effects of grout have been considered in the following results. Figure 3-16 and Figure 3-17 show the mode shapes of two-strand cable modelled with an equivalent stiffness k equal to 100 N/m.

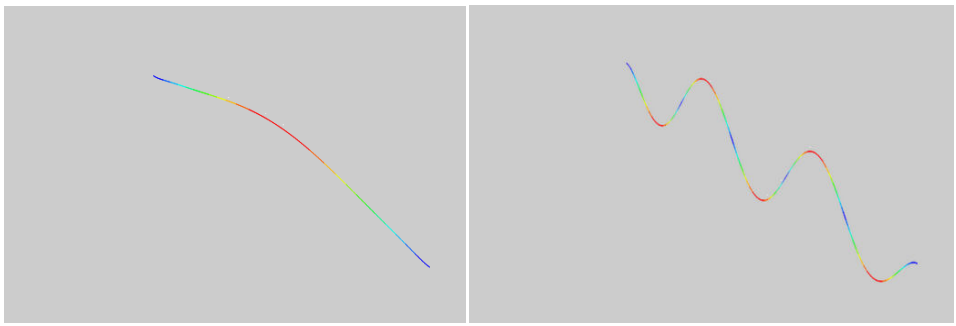

Figure 3-16: 3rd, 19th mode of two-strand cable with springs k=100 N/m

Comparing Figure 3-12 and Figure 3-16, it can be seen that the existence of the grout has changed

the 3rd mode shape which now consists of the vibration of the two strands together.

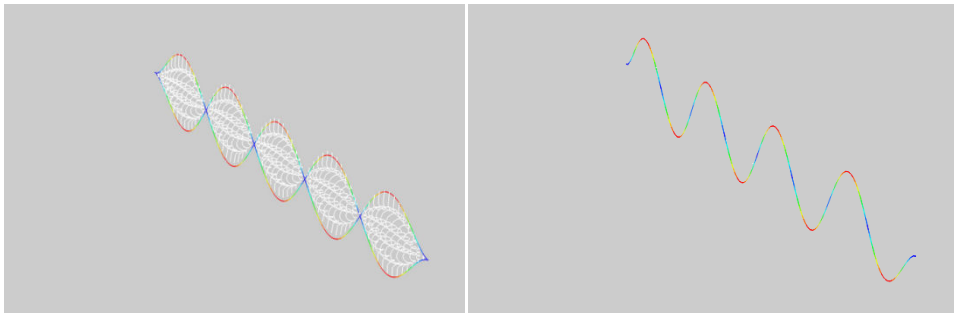

Figure 3-17: 20th, 29th mode of two-strand cable with springs k=100 N/m

Comparing Figure 3-12 with Figure 3-16, Figure 3-13 with Figure 3-17, it can be found that the mode shapes of the above four valuable modes all differ from those of the two-strand cable without grout; slight differences in the natural frequencies have also been observed, as the Table 3-7 shows:

Table 3-7: Mode frequencies 1-10 of two-strand cable with springs k=100 N/m

Mode Numbers	Eigenvalue	Frequency(Hz)	Generalized Mass
1	14.11	0.59783	9002.8
2	14.11	0.59783	9002.8
3	39.032	0.99432	17189
4	39.693	1.0027	17189
5	58.54	1.2177	18162
6	58.583	1.2182	9069.3
7	58.583	1.2182	9069.3
8	59.2	1.2246	18162
9	139.82	1.882	9135.8
10	139.82	1.882	9135.8

3.3.2.4 Four-strand cable with springs k=100 N/m

For the same value of stiffness k, more strands inside the cable have been modelled as well; Figure 3-18 and Figure 3-19 show the results of vibration of mode shapes:

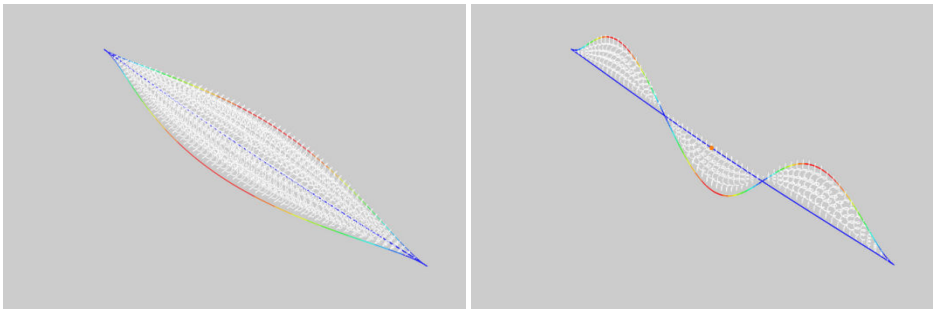

Figure 3-18: 3rd, 19th mode of four-strand cable with springs k=100 N/m

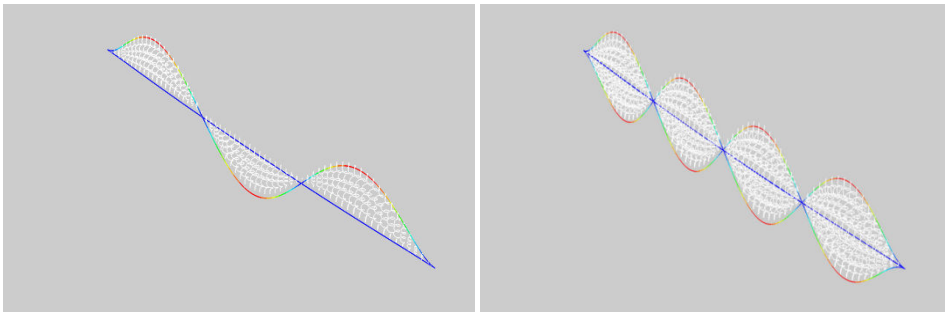

Figure 3-19: 20th, 29th mode of four-strand cable with springs k=100 N/m

Clearly, when comparing Figure 3-14 to Figure 3-18, it can be seen that the mode shapes of the four-strand cable changes as well by adding the springs, so do the natural frequencies, which are shown in Table 3-8:

Table 3-8: Mode frequencies 1-10 of four-strand cable with springs k=100 N/m

Mode Numbers	Eigenvalue	Frequency(Hz)	Generalized Mass
1	14.11	0.59783	18006
2	14.11	0.59783	18006
3	14.771	0.61168	18006
4	14.771	0.61168	18006
5	39.032	0.99432	17189
6	39.032	0.99432	17189
7	39.693	1.0027	17189
8	39.693	1.0027	17189
9	58.54	1.2177	18162
10	58.54	1.2177	18162

3.3.2.5 Two-strand cable with springs k=500 N/m

Figure 3-20 and Figure 3-21 show the results of the two-strand cable with higher value of stiffness k, which equals to 500 N/m:

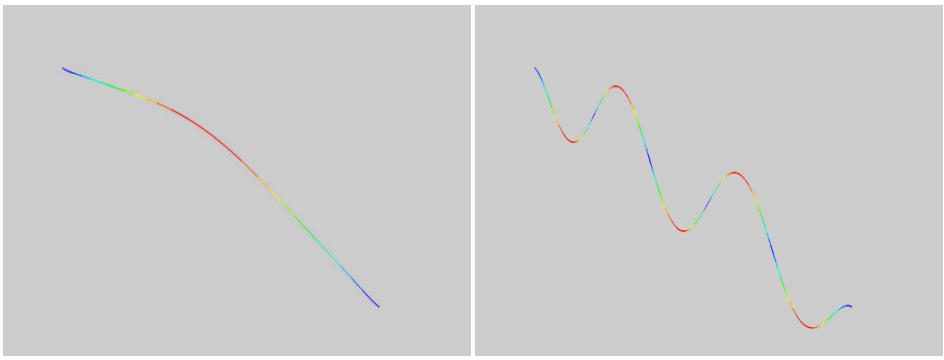

Figure 3-20: 3rd, 19th mode of two-strand cable with springs k=500 N/m

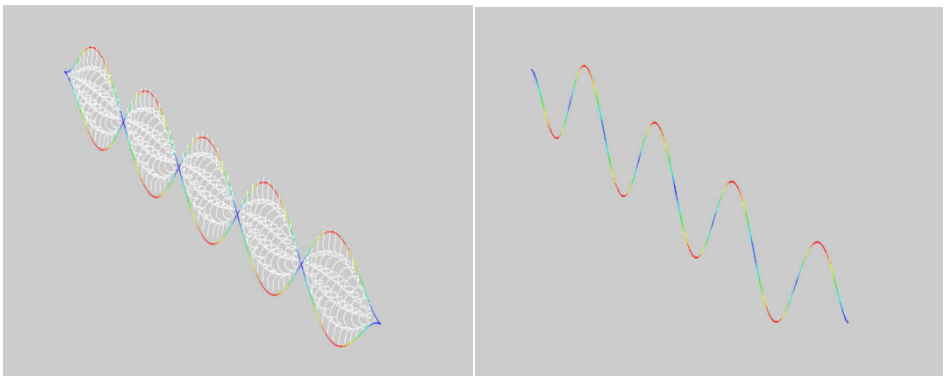

Figure 3-21: 20th, 29th mode of two-strand cable with springs k=500 N/m

No differences in the mode shapes have been observed with the lower stiffness k= 100 N/m, while there are some increase in the natural frequencies, as the figure Table 3-9 shows:

Table 3-9: Mode frequencies 1-10 of two-strand cable with springs k=500 N/m

Mode Numbers	Eigenvalue	Frequency(Hz)	Generalized Mass
1	14.11	0.59783	9036.7
2	14.11	0.59783	9036.7
3	39.032	0.99432	17189
4	42.338	1.0356	17189
5	58.54	1.2177	18162
6	58.583	1.2182	9069.2
7	58.583	1.2182	9069.2
8	61.842	1.2516	18162
9	139.82	1.882	9135.9
10	139.82	1.882	9135.9

3.3.2.6 Four-strand cable with springs k=500 N/m

Figure 3-22 and Figure 3-23 show the vibrations of the four-strand cable with higher value of stiffness k, which equals to 500 N/m:

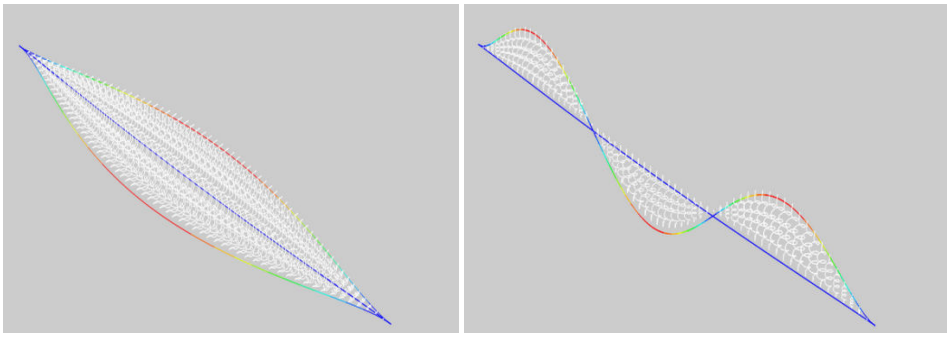

Figure 3-22: 3rd, 19th mode of four-strand cable with springs k=500 N/m

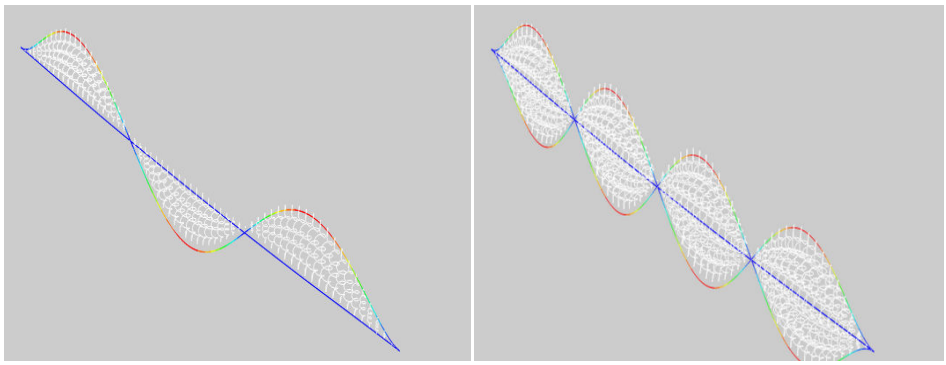

Figure 3-23: 20th, 29th mode of four-strand cable with springs k=500 N/m

Similar to the case of the two-strand cable, differences only arise in the natural frequencies, as the Table 3-10 shows:

Table 3-10: Mode frequencies 1-10 of Four-strand cable with springs k=500 N/m

Mode Numbers	Eigenvalue	Frequency(Hz)	Generalized Mass
1	14.11	0.59783	18006
2	14.11	0.59783	18006
3	17.417	0.66421	18006
4	17.417	0.66421	18006
5	39.032	0.99432	17189
6	39.032	0.99432	17189
7	42.338	1.0356	17189
8	42.338	1.0356	17189
9	58.54	1.2177	18162
10	58.54	1.2177	18162

3.3.3 Summary of one single stay-cable results

As the Figure 3-24 shows, the number of the strands does not have a major impact on the natural frequency of the stay-cable, when the grout material is not considered. The multiple-strand cables have the frequencies consist of the individual frequencies of each strand.

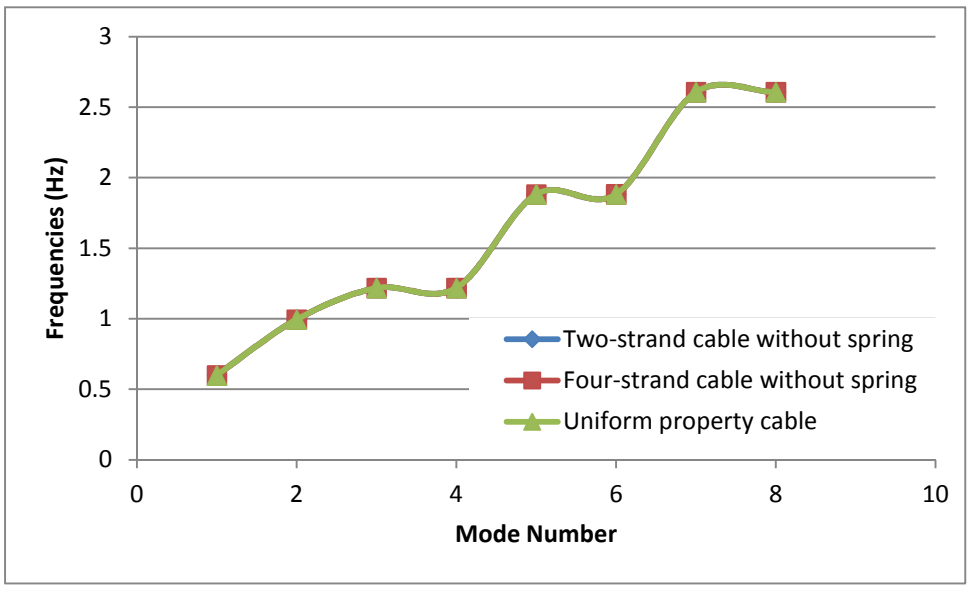

Figure 3-24: Frequencies of cables with different number of strands

The vibration mode shapes of the strands and of the stay-cable alter completely after adding springs between the strands for modelling the grout material.

The spring stiffness has significant influence on the frequencies of vibrations, as well as on the mode shapes. As the spring stiffness increases, the frequencies become gradually larger, as expected ; as the number of the strands increased, the frequency differences between the cable without springs and the cable with springs also increased, as Figure 3-25 and Figure 3-26 show:

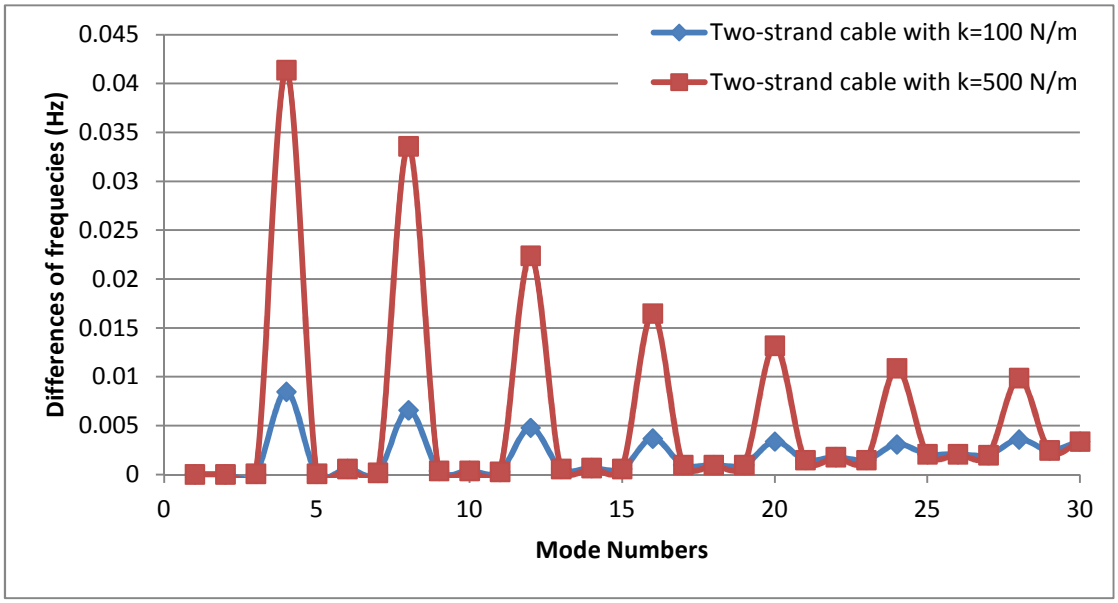

Figure 3-25: Differences of two-strand cable with springs of various k

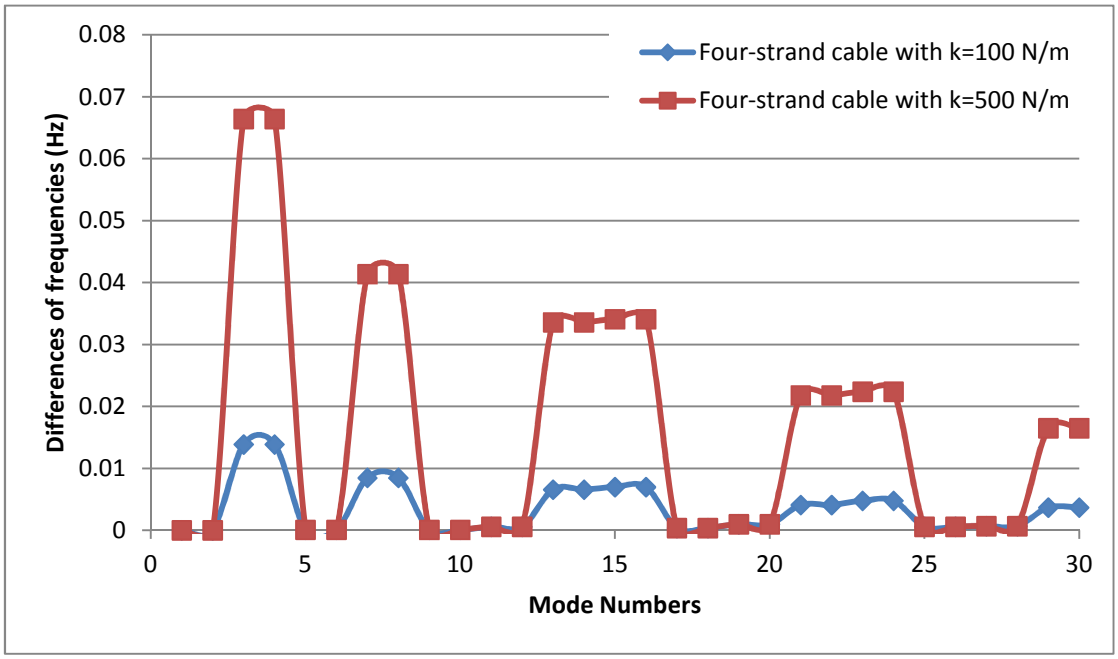

Figure 3-26: Differences of four-strand cable with springs of various k

Table 3-11: Differences of frequencies with different value of k in two-strand cable

Mode Numbers	No Spring	K=100 N/m		K=500 N/m	
	Frequency (Hz)	Frequency (Hz)	Percentage of Difference	Frequency (Hz)	Percentage of Difference
1	0.59779	0.59783	0.0067%	0.59783	0.0067%
2	0.59779	0.59783	0.0067%	0.59783	0.0067%
3	0.99421	0.99432	0.0111%	0.99432	0.0111%
4	0.99421	1.0027	0.8539%	1.0356	4.1631%
5	1.2176	1.2177	0.0082%	1.2177	0.0082%
6	1.2176	1.2182	0.0493%	1.2182	0.0493%
7	1.218	1.2182	0.0164%	1.2182	0.0164%
8	1.218	1.2246	0.5419%	1.2516	2.7586%
9	1.8816	1.882	0.0213%	1.882	0.0213%
10	1.8816	1.882	0.0213%	1.882	0.0213%

Table 3-12: Differences of frequencies with different value of k in Four-strand cable

Mode Numbers	No Spring	K=100 N/m		K=500 N/m	
	Frequency (Hz)	Frequency (Hz)	Percentage of Difference	Frequency (Hz)	Percentage of Difference
1	0.59779	0.59783	0.0067%	0.59783	0.0067%
2	0.59779	0.59783	0.0067%	0.59783	0.0067%
3	0.59779	0.61168	2.3236%	0.66421	11.1109%
4	0.59779	0.61168	2.3236%	0.66421	11.1109%
5	0.99421	0.99432	0.0111%	0.99432	0.0111%
6	0.99421	0.99432	0.0111%	0.99432	0.0111%
7	0.99421	1.0027	0.8539%	1.0356	4.1631%
8	0.99421	1.0027	0.8539%	1.0356	4.1631%
9	1.2176	1.2177	0.0082%	1.2177	0.0082%
10	1.2176	1.2177	0.0082%	1.2177	0.0082%

3.3.3.1 Comparison with experimental results [72]

In reference [72], as presented in detail in Chapter 2, the cable model of 1.59 mm diameter has been tested by performing a free-vibration experiment based on different parameters, such as angle of inclination, cable length, while they share the same property of material. Moreover, each cable in the

experiment has been subjected to a certain value of pretension, however in the current analysis, the finite element analysis of the one stay-cable model, did not include pretensions. A comparison of the frequencies for the one single stay-cable FE model and the experimental results reported in reference [72] has been considered.

As the stay-cable used in the finite element analysis has no inclination, only the results of the flat cable case [72] have been included into the comparison; also, because the two strands and the four strands cables showed very good agreement, only the case of four strands cable stayed are presented here. Considering the case of $\log \lambda^2 = 7.2$:

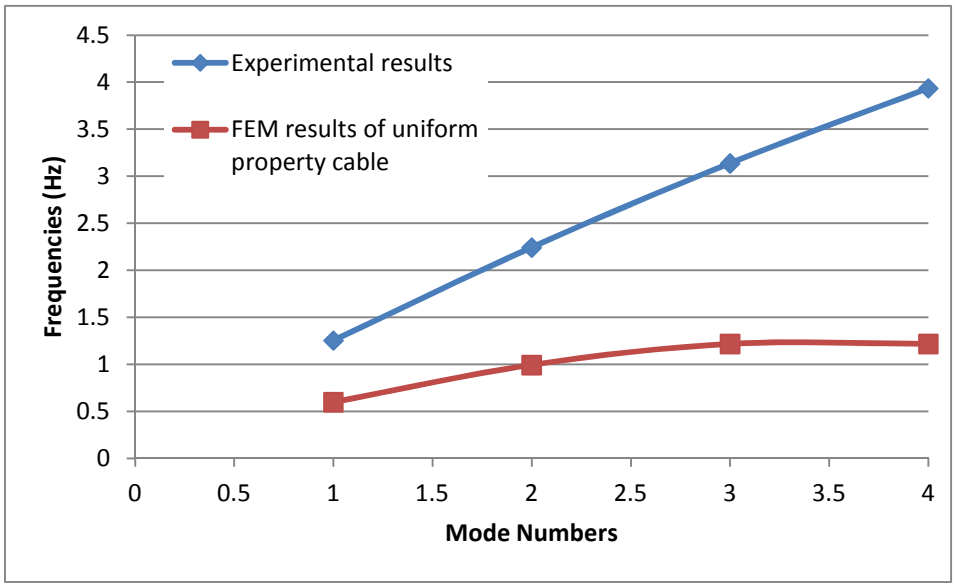

Figure 3-27: Uniform property cable

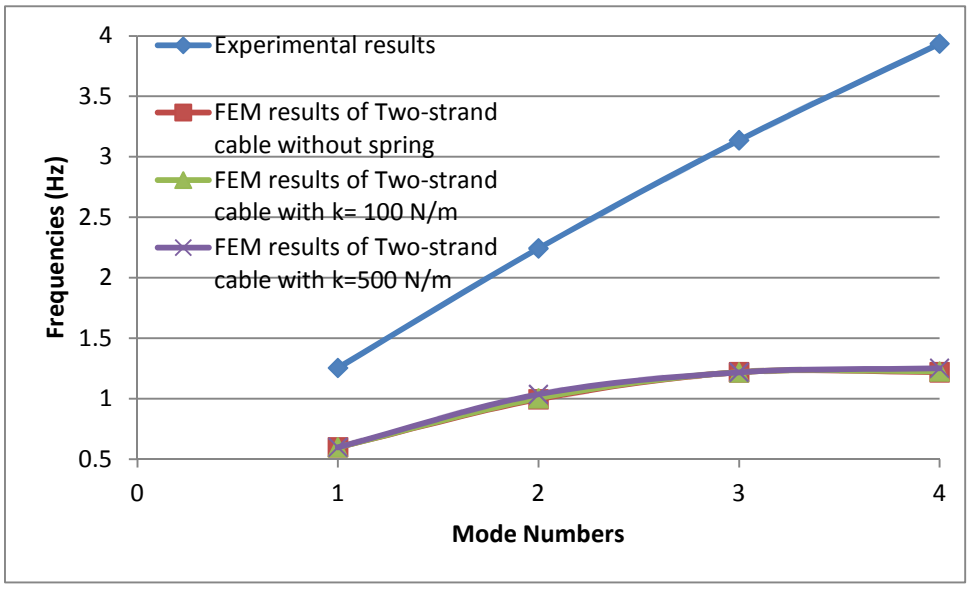

Figure 3-28: Two-strand cable

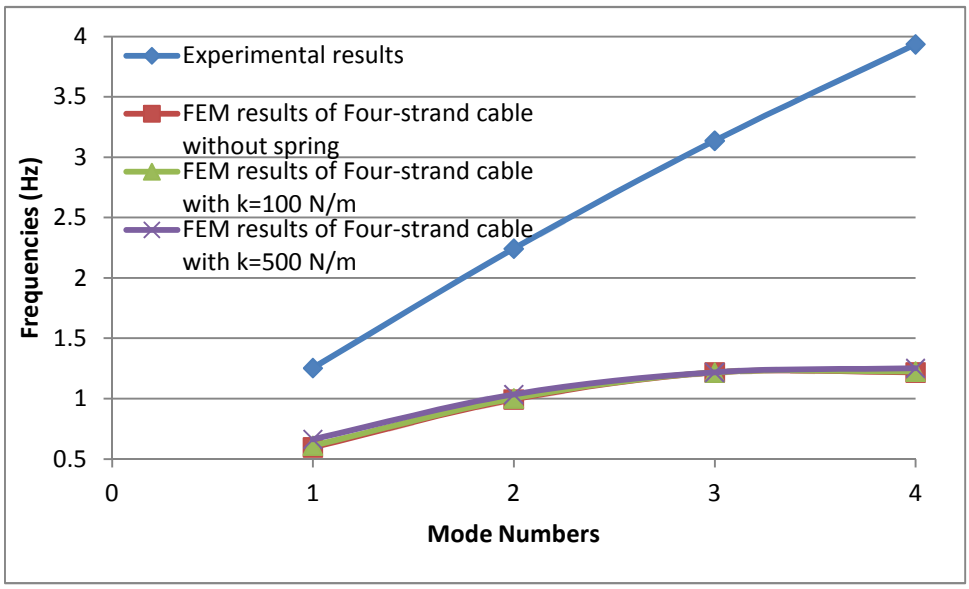

Figure 3-29: Four-strand cable

From Figure 3-27 to Figure 3-29, it could be seen that the experimental results showed much larger frequencies then the uniform property cable and the four strands cables, with and without grout. Moreover, the existence of the pretension in the experimentally tested cable has increased the

differences between the adjacent modes of vibration. For one cable alone, there is not much difference between the different values of k compared to the differences caused by the pretension.

3.4 Modelling of the stay-cables fan on Bill Emerson Memorial Bridge

Before modelling the cable under the effect of grout and the inner strands composition, a finite element analysis considering each cable as a uniform property cable has been performed.

The material property and the distance of each cable were derived from the U.S Federal Highway Administration (FHWA) report.

According to the stress equation:

$$\sigma=\frac{F}{S} \qquad (3\text{-}7)$$

Where $S=\pi R^2$ is the cross-section area, and R and F are the radius and the tension force derived from reference [9] Therefore, pretension of each cable could be obtained from the above equation.

3.4.1 Modelling of the one uniformed property stay-cables fan of the Bill Emerson Memorial Bridge

The properties of the cables are shown in Table 3-13, where the Young's modulus, mass density and radius are employed from the FHWA reference [9]:

Table 3-13：Cable properties from FHWA [9]

Cable Number	Young's Modulus(Pa)	Mass Density(Kg/m^3)	Radius(m)	Pretension(Pa)
1	15578290000	2593.6	0.137	77484701
2	15578290000	2593.6	0.137	81269262
3	15020200000	2544	0.137	77484701
4	19071520000	2763.2	0.109	115781003
5	18058690000	2728	0.109	110568731
6	17383470000	2688	0.109	106526560
7	16708250000	2688	0.109	101113361
8	16708250000	2688	0.109	97792162
9	24555960000	2889.6	0.090	127381876
10	23729160000	2832	0.090	116485208
11	22902360000	2774.4	0.090	110248642
12	22075560000	2716.8	0.090	102418285
13	19216210000	2750.4	0.084	112822362
14	17004520000	2683.2	0.084	93083976
15	15895230000	2616	0.084	82249974
16	15344030000	2616	0.084	76420919

Table 3-14: Coordinates of cable ends from FHWA [9]

Cable Number	Distance from the origin of Tower-End(m)	Distance from the origin of Deck End(m)
1	74.23	140.39
2	72.76	136.73
3	71.23	133.08
4	69.71	129.45
5	68.15	125.91
6	66.66	115.33
7	65.17	104.79
8	63.64	94.24
9	62.15	83.76
10	60.65	73.24
11	59.16	62.73
12	57.55	52.21
13	55.72	41.79
14	53.67	31.30
15	50.05	20.85
16	44.77	10.39

The cable ends are assumed to be fixed to the deck and to the tower. The stay-cables and the crossties

are modelled using the beam elements with flexural stiffness.

For the Bill Emerson Memorial Bridge, four lines of cross ties were planned for each side of each quadrant as well as HDPE (High Density Polyethylene) pipe line with a helical fillet was used [78]. The lines of the crossties are arranged normal to the stay cables and are equally spaced at 32 m along the top cable in each fan as shown in Figure 3-30. Each crosstie line is anchored to the deck, as Figure 3-31 to Figure 3-34 show:

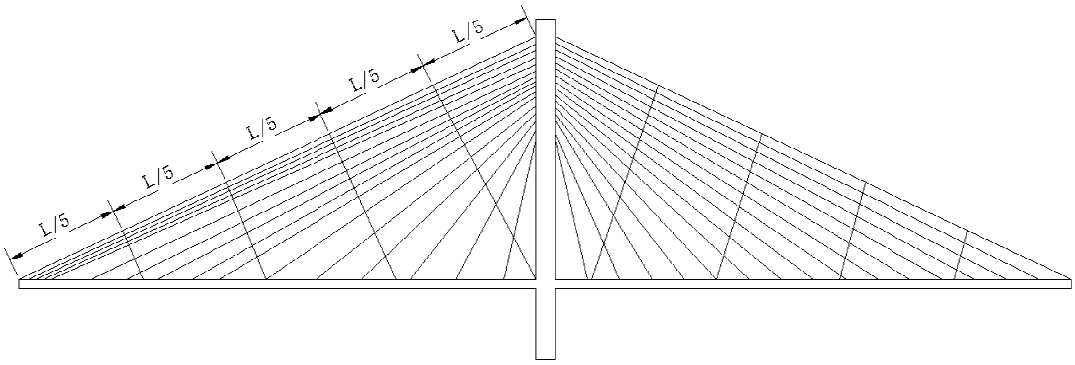

Figure 3-30: Placements of crossties (L: Length of the cable 1)

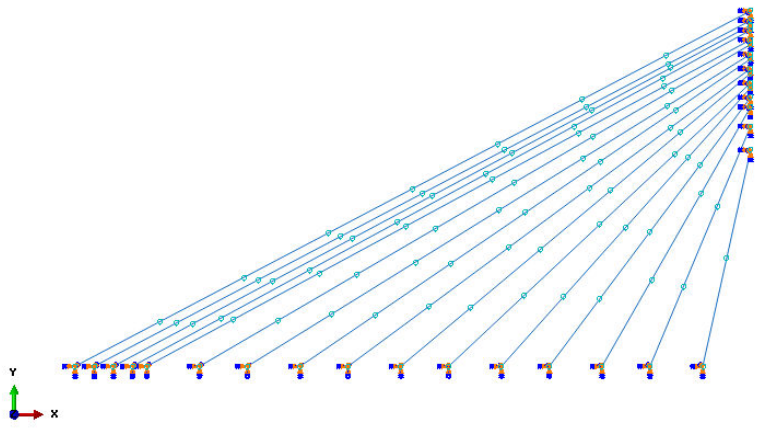

Figure 3-31: Configuration of the stay-cables fan without crossties

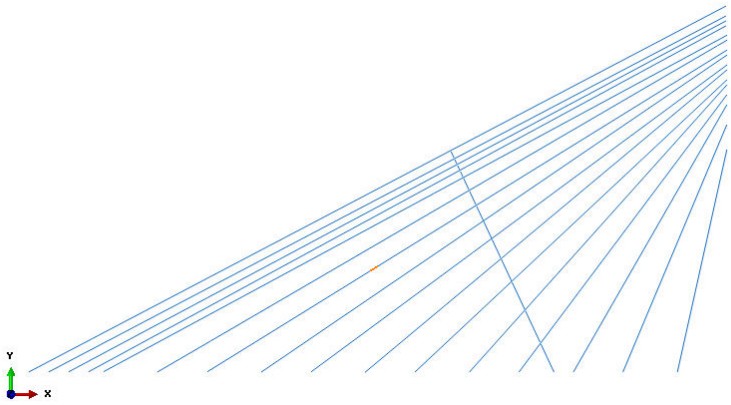

Figure 3-32: Configuration of the stay-cables fan with 1 crosstie

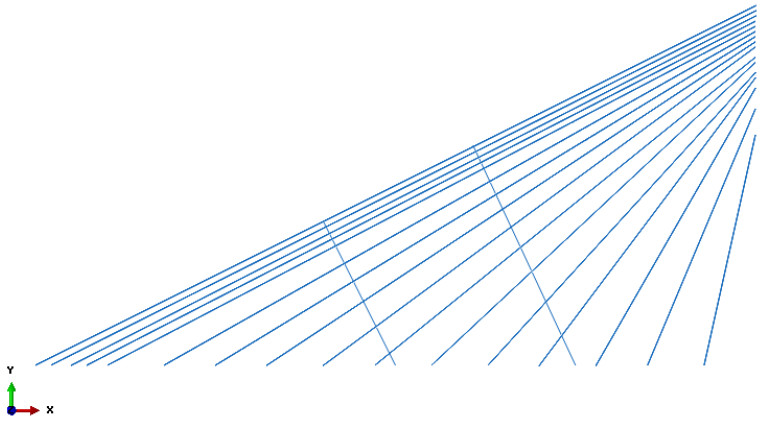

Figure 3-33: Configuration of the stay-cables fan with 2 crossties

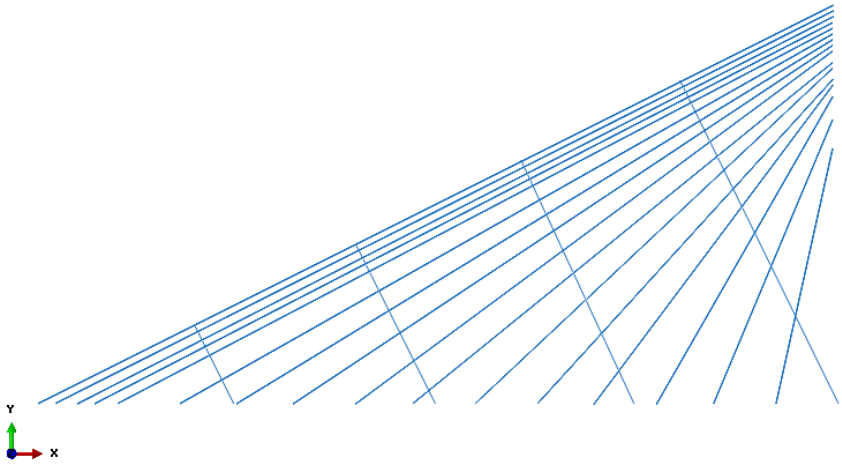

Figure 3-34: Configuration of the stay-cables fan with 4 crossties

In reality the crossties are tied to the stay-cables at the joint points as shown in Figures 3-35:

Figure 3-35: Joint points of Crossties of Bill Emersion Memorial Bridge [10]

3.4.2 Modelling of the stay-cables fan with grouted inner strands of the Bill Emerson Memorial Bridge

To determine the number of the strands used for each stay-cable, the total area of the inside strands was determined and was divided by the cross-section area of each stay cable, information which was obtained from the relevant publication. [10]

Table 3-15: Net area of strands within each cable 1-16 [10]

Cable Number	Diameter(m)	Area(m^2)
1	0.1014	0.00808
2	0.1014	0.00808
3	0.0976	0.00748
4	0.0926	0.00673
5	0.0905	0.00643
6	0.0884	0.00614
7	0.084	0.00554
8	0.084	0.00554
9	0.0817	0.00524
10	0.0769	0.00464
11	0.0769	0.00464
12	0.0756	0.00449
13	0.0717	0.00404
14	0.0662	0.00344
15	0.0632	0.00314
16	0.0602	0.00285

The diameter of each strand equals to 0.0157 m [10], therefore, the area of each strand equals to $0.0001936m^2$. Dividing the value of each strand by the net area of strands of each cable, the number of strands of individual cable could be obtained for each case.

As the total diameter of cable contains the strands, grout and the outer membrane, the strands only take a part of the whole area of a cable. Moreover, each cable has tens of strands, and it is acceptable that several numbers of strands would vary from the real condition. As a result, the approximate number of

strands for each cable has been taken as the following Table 3-16 shows:

Table 3-16: Number of strands within each cable

Cable Number	Max Number Of Strands	Number Of Strand In Model
1	41.71	40
2	41.71	40
3	38.64	36
4	34.79	35
5	33.23	33
6	31.70	30
7	28.62	30
8	28.62	30
9	27.08	26
10	23.99	24
11	23.99	24
12	23.19	22
13	20.86	20
14	17.78	17
15	16.20	16
16	14.70	14

Also to model the geometrical configuration of the strands within each cable, basically, the outline of all the strands arranged together within each cable is closer to a circle, the more accurate the results, However in the FE modelling the circle configuration of the cable cross-section could not be always followed due to the software limitations; based on the number of strands used for each stay-cable, and considering that a symmetric arrangement of the inner strands must be developed, the cross-sections closest to a circle which could be achieved for several stay-cables of the entire fan, which include 1 to 16 strands, are presented in Figures 3-36 to Figure 3-38.

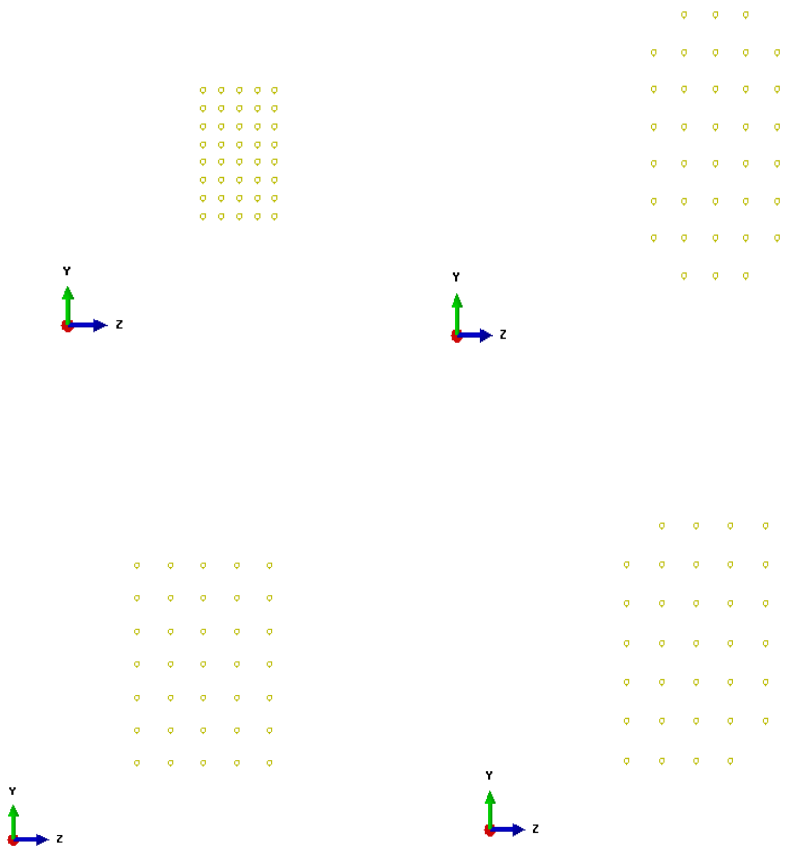

Figure 3-36: Arrangement of strands from cable 1-5

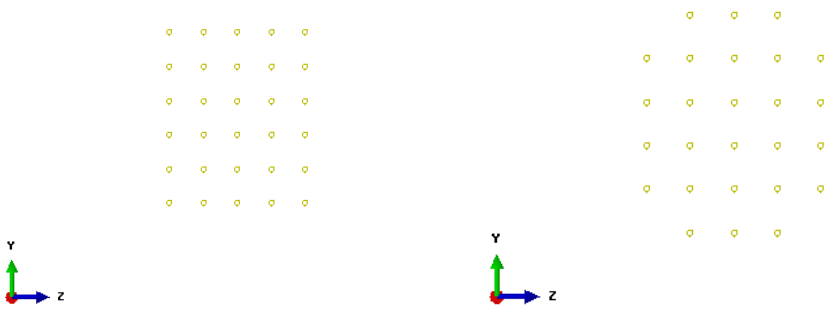

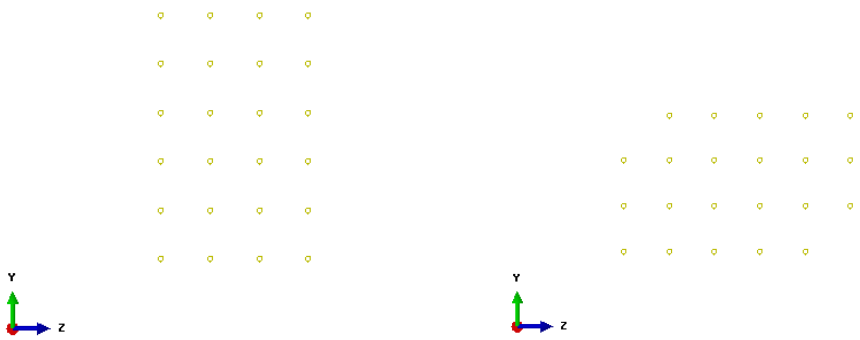

Figure 3-37: Arrangement of strands from cable 6-12

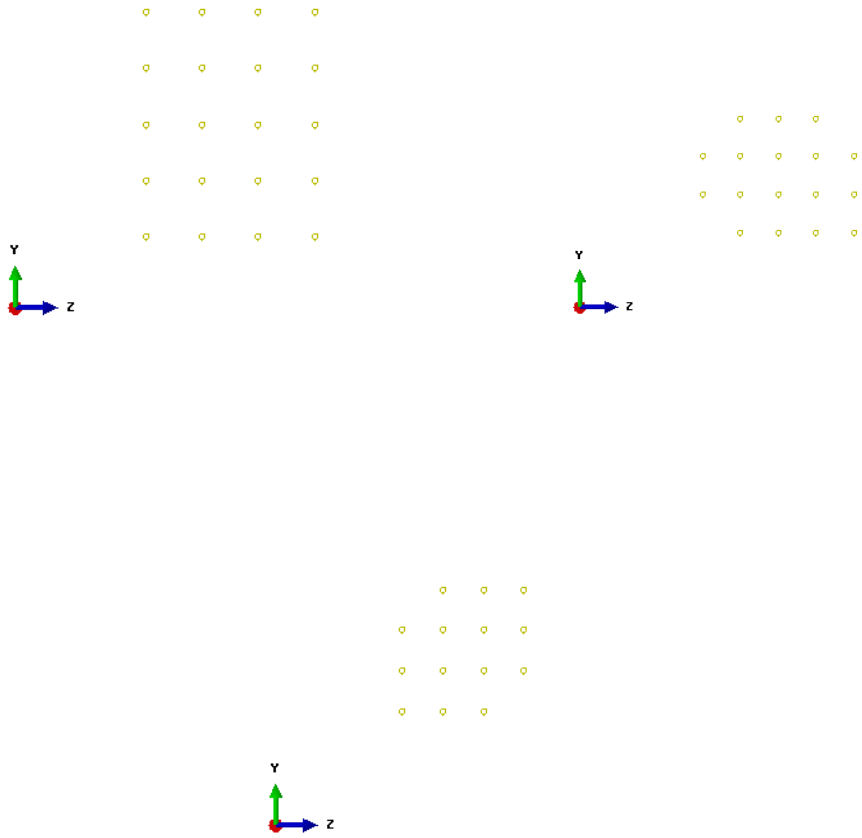

Figure 3-38: Arrangement of strands of cable 13-16

3.4.3 Modelling of the grout material for the stay-cables fan

It can be seen from the Table 3-14 and Table 3-15 that the ratio of the cross-section area to the length of the cable is basically unchanged, which means that the value of the equivalent stiffness stays approximately the same in the cables. From the above discussion, it could be concluded that the stiffness k simulating the grout, has little impact on the higher modes of vibration; for the cables of the Bill Emerson Memorial Bridge, the analysis of the frequency is beyond the 100^{th} mode, where the value of the k does not have much effect . Consequently, a uniform value of stiffness k = 500 N/m has been considered.

3.4.4 Modelling of the crossties for the stay-cables fan

Similar to the case of the uniform property cable the finite element analysis of the entire stay-cables fan with 1 crosstie, 2 crossties and 4 crossties has been performed**.** Each joint of strands and crossties are tied together by the "tie" constrain in modelling. Figure 3-39 show the joint configuration in FE model.

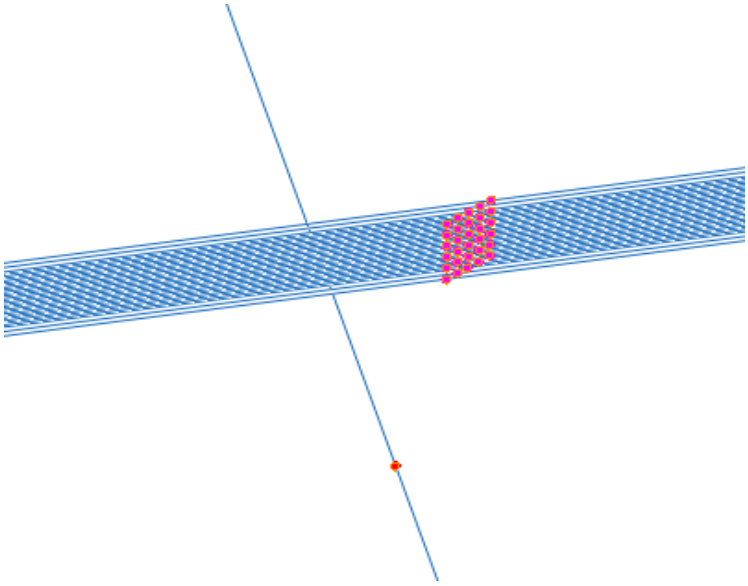

Figure 3-39: Joint model of the crosstie and strands

3.4.5 Modelling of the wind dynamic loading

To determine the dynamic properties of the stay-cable with grouted inner strands, as well as the effects of the crossties through the performance of the displacements, a time-history analysis under a realistic wind loading has been conducted for the developed model, which provided more explicit and detailed information about the entire stay-cables fan.

The wind speed data comes from the anemometer device installed at the Bill Emerson Memorial Bridge site in Cape Girardeau, MO [9], which has been converted to simulate the relevant wind loading condition. The following wind data contains the wind speed of 5-min retrieved from the Bill Emerson Memorial Bridge site, besides, the speed has been scaled up so that the peak 3-s speed reaches 30 m/s. For preventing an incorrect oscillation because of the abrupt load at the beginning of the analysis, an artificial transition has been supplemented between the initial time interval and 10 s. The originally wind speed was fully recovered at t = 10 s.

Only wind-induced drag force was taken into consideration for transforming the velocity of the wind into the force. Due to the complexity of the wind pressure, it is not practical to calculate the distributed wind pressure on the stay–cables. The wind force (per unit length) profile was applied in the direction of the bridge longitudinal axis, inducing the in-plane vibration of the stay-cable fan [9]. Figure 3-40 show the approximate wind load in 300s.

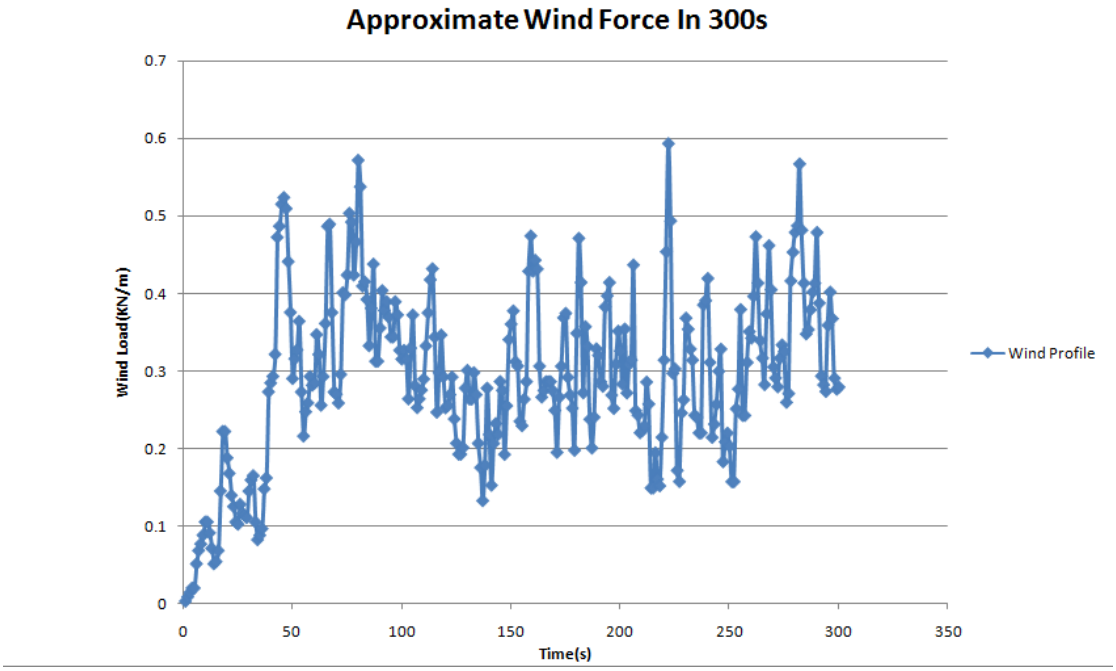

Figure 3-40: Derived wind load in 300s [9]

To simulate the wind force in finite element analysis, a line load with the amplitude to satisfy the time interval of 300 s has been appended. A line load is a concentrated load which appears as a point load in the 2D view, but actually represents a linear load when considering the out-of-plane dimension of the model. Hence the units of a line load are force / length (N/m) where the length dimension is measured along the slope surface perpendicular to the 2D cross-section.

Line loads can be added anywhere along the slope face or upper slope, at any angle. For an entire stay-cables fan, the wind force is assumed evenly distributed along each stay-cable, which could be regarded as a line load. Moreover, it was assumed that each stay-cable of the fan is under the same loading condition, which is the wind load has the same direction on each cable and each crosstie, and there will be no variation or increase of the wind load at the different locations of the cable fan (Figures 3-41 and 3-42).

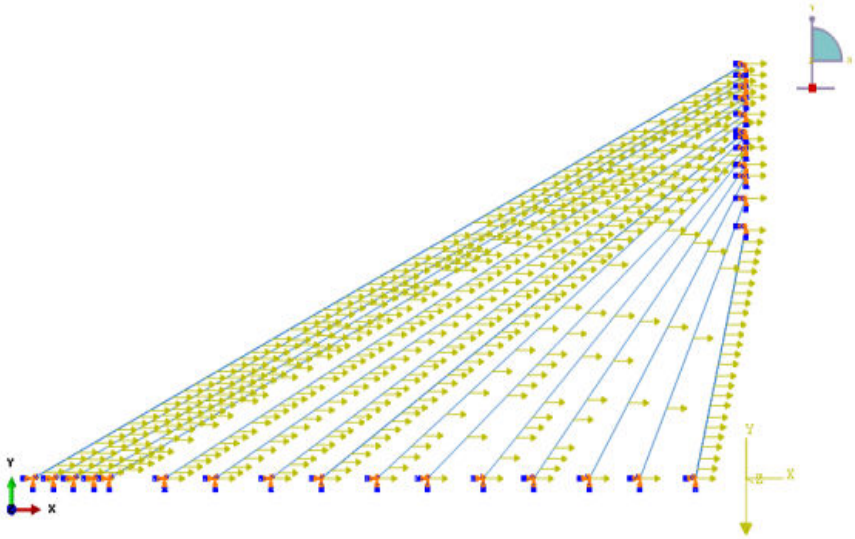

Figure 3-41: Modelling of the wind loads without crossties

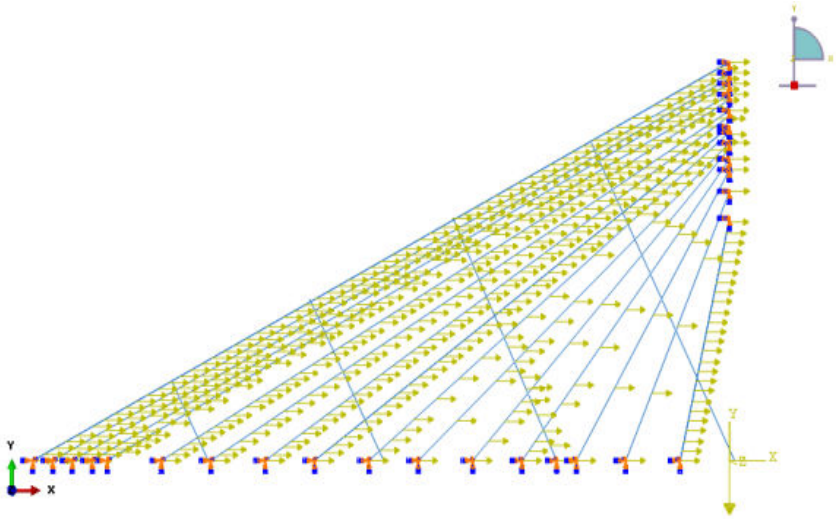

Figure 3-42: Modelling of the wind loads with crossties

Chapter 4 Results and Discussions

In order to develop the model and the dynamic analysis of the grouted cables with inner strands, in a fan arrangement connected by four cross ties, as it is currently in use for the Bill Emerson Memorial Bridge, several cases for one cable model were created and were compared with the experimental results available in the literature. Also the grout properties were extracted based on the analysis presented in section 3.4 and were integrated for the multiple-strand models of one cable and multiple-strand cable to verify the effect the grout material would have on the natural vibrations of individual inner strands and on the dynamic properties of the entire cable. The results and analysis conducted in the current chapter aim at establishing the FE model of the grouted cables which would simulate the real stay-cables construction techniques used for the Bill Emerson Memorial Bridge and thus would clarifying the dynamic response of the grouted stay-cables under the wind load.

4.1 Modal analysis of one cable

Prior to the analysis of the entire stay-cables fan, one single stay-cable, with and without inner strands has been analyzed to verify the accuracy of the developed FE model and to lay a foundation for further simulations.

4.1.1 Cable of uniform property (no strands)

As concluded from Table 3-14, each stay-cable has a different inclination angle when it is installed between the tower and the deck; the first cable of the fan configuration was selected in the current section, which has an inclination angle of approximately 28^0; no inner strands were initially considered, thus stay-cable 1 was modelled as a compact beam element, with uniform properties with no bending rigidity; the modelling assumptions and other factors characterizing cable 1 in the finite element analysis can be found in Table 3-13.

A modal analysis was carried out for determining the natural frequencies of cable 1, with no inner strands. Table 4-1 shows the results of the mode frequencies 1-10.

Table 4-1: Frequencies from 1-10 of cable 1 modelled as uniform property beam

Mode Numbers	Eigenvalue	Frequency (Hz)	Generalized Mass
1	41.697	1.0277	12030
2	41.729	1.0281	15342
3	166.79	2.0555	15244
4	166.8	2.0555	12020
5	375.33	3.0834	12020
6	375.33	3.0834	15247
7	667.34	4.1114	15254
8	667.35	4.1115	12035
9	1042.9	5.1398	15246
10	1042.9	5.1398	12024

For the first two vibration modes, it was noticed that stay-cable 1 has almost the same natural frequencies, though considering the mass contribution which is higher for the second mode, these two modes might have different mode shapes; for example, in-plane and out-of-plane modes will share the same frequencies. For the sake of simplicity, the vibration modes with the same frequencies are taken as one mode, which is applicable to the rest of the frequencies and the results of the cable with grouted inner strands.

4.1.2 Cable with grouted inner strands

The same cable 1 was modelled as a cable with 40 inner strands grouted inside the stay-cable, as shown in Table 3-16; the inside strands were considered as truss elements of uniform material properties shown in Table 3-13; the grout material in which the strands are embedded, was simulated

by a total of 4288 springs linking the strands along their total length and allowing for their individual motion. Thus the natural frequencies of cable 1 were obtained as shown in Table 4-2:

Table 4-2: Natural frequencies for cable 1 with grouted inner strands

Mode Numbers	Eigenvalue	Frequency (Hz)	Generalized Mass
1 to 8	14.984	0.61608	1053.3 to 1088.7
9 to 14	16.152	0.63963	144.95 to 1159.7
15 to 18	32.847	0.91215	603.4 to 603.43
19	37.867	0.97938	534.42
20 to 30	59.917	1.232	143.26 to 902.25

For grouted cable 1 with 40 inner strands, it was noticed that the same eigenvalue and the same natural frequency were reported for several consecutive vibration modes, thus it would be more depictive to group the modes as 1 to 8, 9 to 14, 15 to 18, 19 and 20 to 30. Some of the reported frequencies have the same value, but they might belong to different shapes of vibration modes. However the aim of the one cable FE analysis is to verify if the natural frequencies of the modelled stay-cable is within the range reported by the experimental work performed on similar stay-cables, available in the literature.

4.1.3 One cable frequencies comparison with experimental results

As the angle of inclination of cable 1 is close to 30^0, the experimental results with the same inclination angle were used as presented in reference [72] for the comparison, as inferred from Table 3-14. The experiments performed by Hoftyzer [72], however used a uniform property cable, thus simulating better the first case performed in the current research, for the cable without inner strands. It should be mentioned however that the laboratory experiments for grouted singular cables with inner strands are not currently available, because this requires a full-scale (real) stay-cable and scaled models were not yet developed, due to technical challenges.

From Figure 4.1 [72], various sets of frequencies have been demonstrated allowing for the value of λ; λ^2 is a dimensionless parameter of the cable regarding both geometric and elastic effects, which equals to $(\frac{EA}{H})(\frac{wl}{H})^2$.

From Figure 2-17, it can be seen that when $\log\lambda^2$ approximately equals 7.25, the frequencies are the closest to that of cable 1:

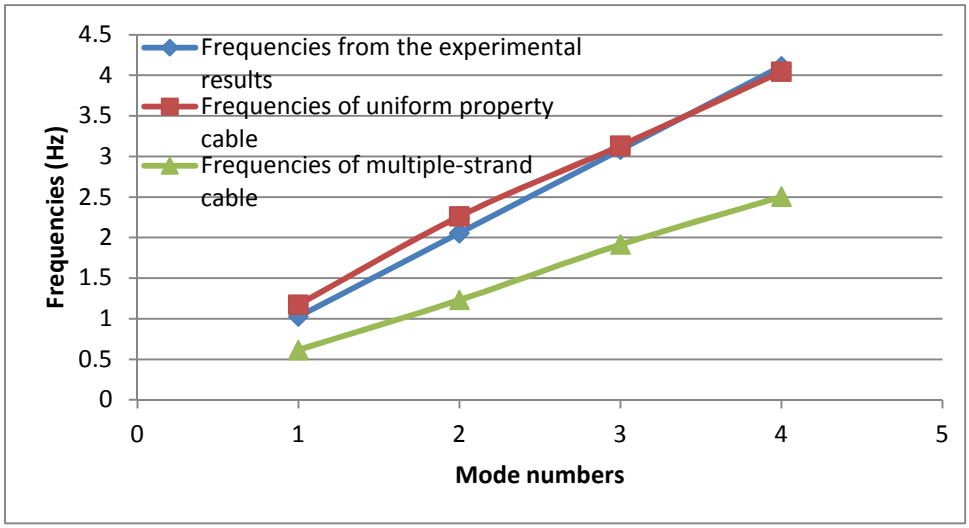

Figure 4-1: Natural frequencies comparison for one cable

4.2 Modal analysis of the stay-cables fan of uniform property stay-cables (without strands)

In this section, a total of 16 stay-cables were modelled in a fan configuration respecting the stay-cable arrangement used for the Bill Emerson Memorial Bridge [78]. In order to determine the effect of losing the connection between the stay-cables, different numbers of crossties have been investigated for the entire stay-cables fan on the bridge, modelled initially as single element cables (uniform property). Because of the symmetrical geometry of the stay-cables layout employed for the Bill Emerson Memorial Bridge, only one stay-cables fan was considered in the current research.

4.2.1 Stay-cables fan without crossties

The FE model assumptions and the boundary conditions were applied as explained in detail in section 3.4 and the modal analysis was performed for determining the natural frequency and vibration mode shapes for the cables in the fan.

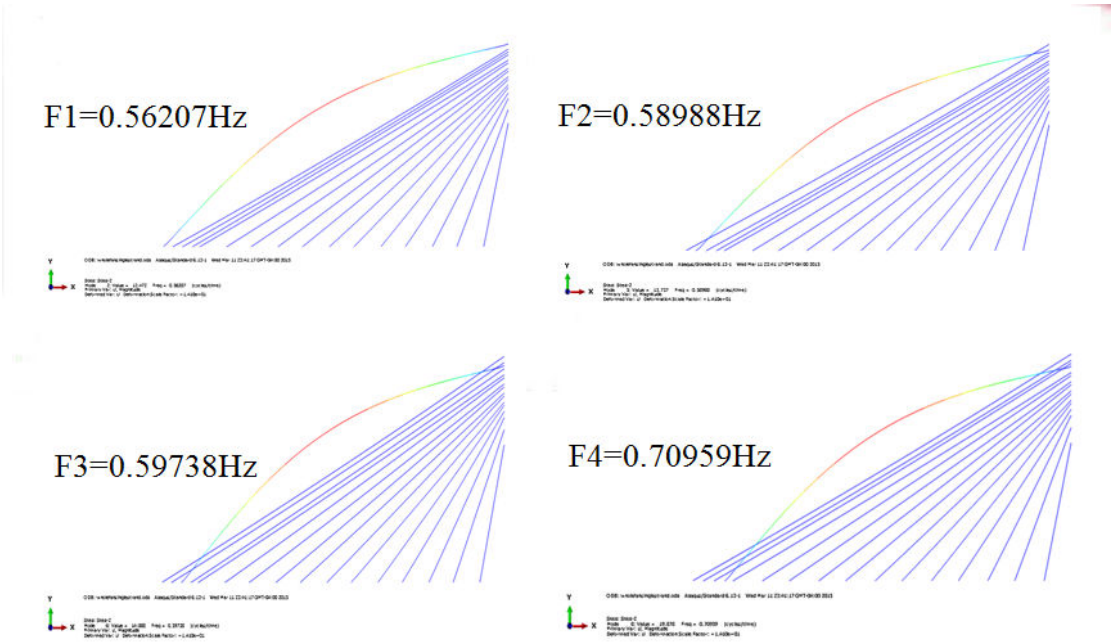

Figure 4-2: First four in-plane vibration mode shapes (no crosstie)

It was noticed that for the no strands stay cables fan without crossties, the cables would respond in consecutive order, starting with cable one. The natural frequencies are in the same range as the one cable model presented in section 4.1 The in-plane modes start from the second mode of vibration, thus the first four in-plane modes correspond to the 2nd, 5th, 6th and 8th modes, respectively, as it can be noticed in Figure 4-2.

All the modes within the first 30th modes of vibration are local cable modes of the stay-cables. It can be concluded that all the vibration modes reported for the entire stay-cables fan of cables without strands and without crossties are the nature modes of the individual cables. For the higher modes, some

coupled vibration mode shapes, corresponding to high modes of long cables mixed with the low modes of short cables were identified. More details can be found in Appendix B and Appendix C.

4.2.2 Stay-cables fan with one crosstie

The installation of one diagonal crosstie connecting all the stay-cables in the fan, changed the natural frequencies and the vibration modes for the entire fan. Thus it was noticed that first the lower part of the stay-cables respond in a consecutive order, as it can be seen in Figure 4-3.

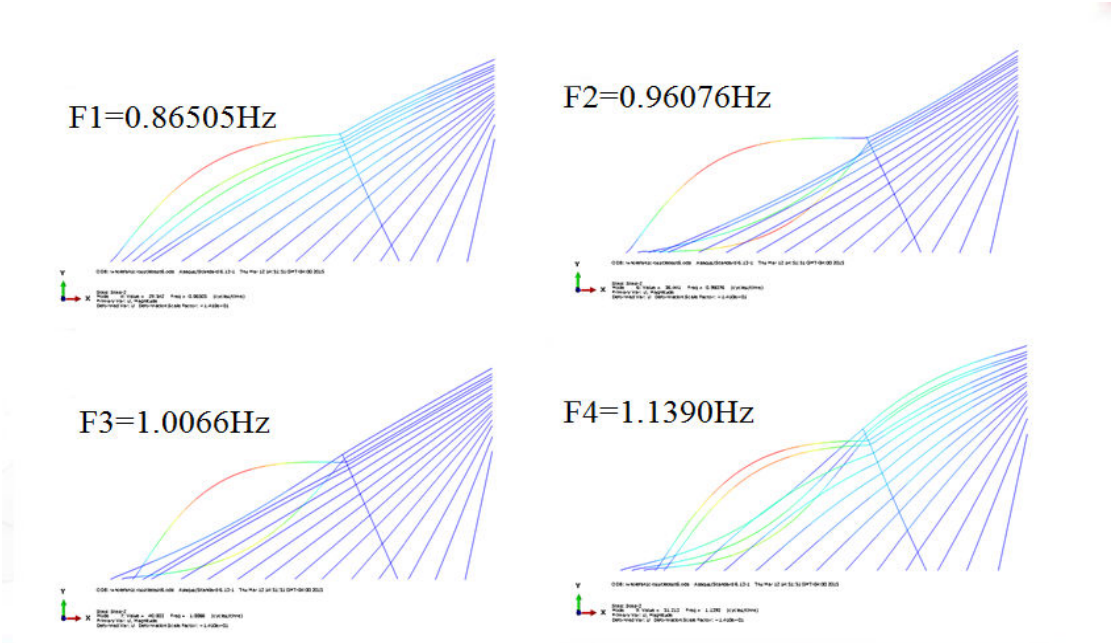

Figure 4-3: The first four in-plane mode shapes (1 crosstie)

The in-plane modes started from the 4th mode of vibration. The first four in-plane modes correspond to the 4th, 6th, 7^{th,} 9th modes, respectively. Figure 4-3 shows the frequencies and mode shapes. Also the first four in-plane modes 1-4 are the local modes of the lower part of the cables, which remain the same in a set of following modes. Global modes however start to be observed for higher frequencies, as presented in detail in Appendix C. Therefore, the modes of cables with crossties are a mixture of local and global modes. Moreover, the frequencies of the dominant modes increase significantly, when

compared with the fan without the crossties.

4.2.3 Stay-cables fan with two crossties

When two crossties, which divide the stay cables in equal segments, are used, the values of the natural frequencies almost doubled and in the same time it was noticed that the lower and the upper stay-cables segments would react, while the middle segment would respond only for higher frequency modes. The first crosstie is also affected by the vibration modes of the stay-cables.

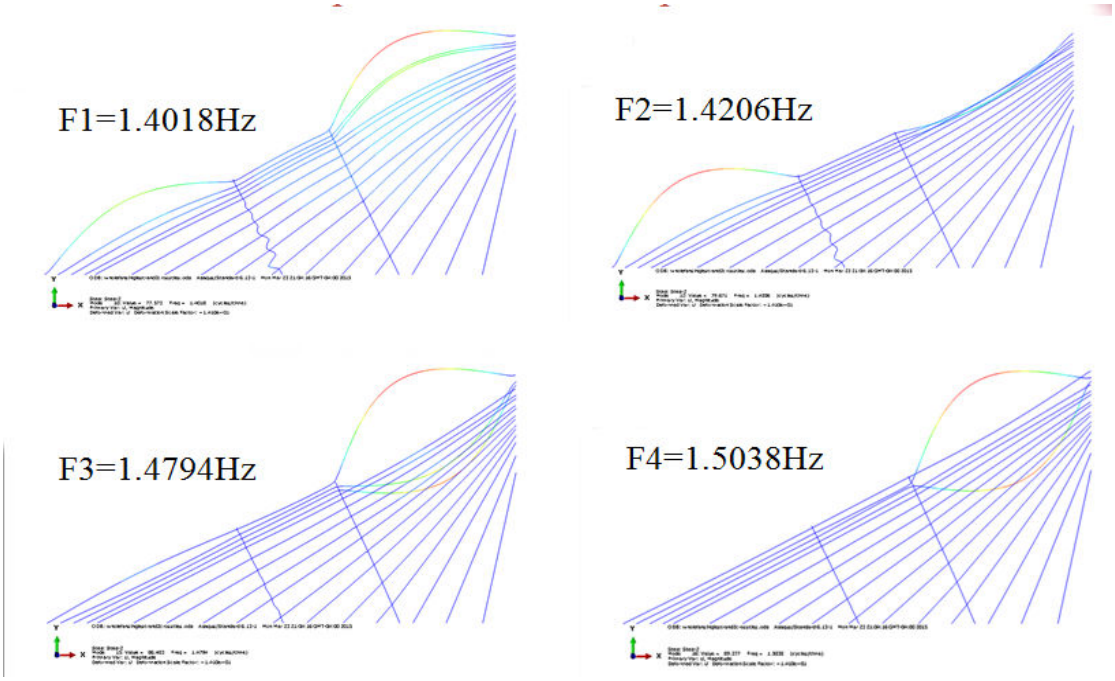

Figure 4-4: The first four in-plane mode shapes (2 crossties)

The in-plane modes start from the 10th mode of vibration, thus the first in-plane modes correspond to the 10th, 12th, 15^{th,} 16th global modes, respectively, as presented in Figure 4-4.

The 1st in-plane mode is the global mode of the stay-cable, after which three local modes are noticed. It can be said that the transition from the global to the local vibration modes becomes more evident as

the number of the crossties increases. Meanwhile, the nature frequencies obtained keep increasing when compared to the single or no crosstie configurations reported above.

4.2.4 Stay-cables fan results comparison with FHWA model

As part of a project of U.S. national research, FHWA (Federal Highway Administration), finite element analysis simulations have been conducted to verify the effectiveness of the crossties in the mitigation of the wind-induced vibrations for the Bill Emerson Memorial Cable-stayed Bridge [9]. The stay-cables and the crossties were modelled using beam elements, similar to the current study.

Figure 4-5 to Figure 4-7 show the natural frequency and the first in-plane vibration modes, reported by the FHWA model [9] for the stay-cables fan without crosstie, with one crosstie and with two crossties, respectively.

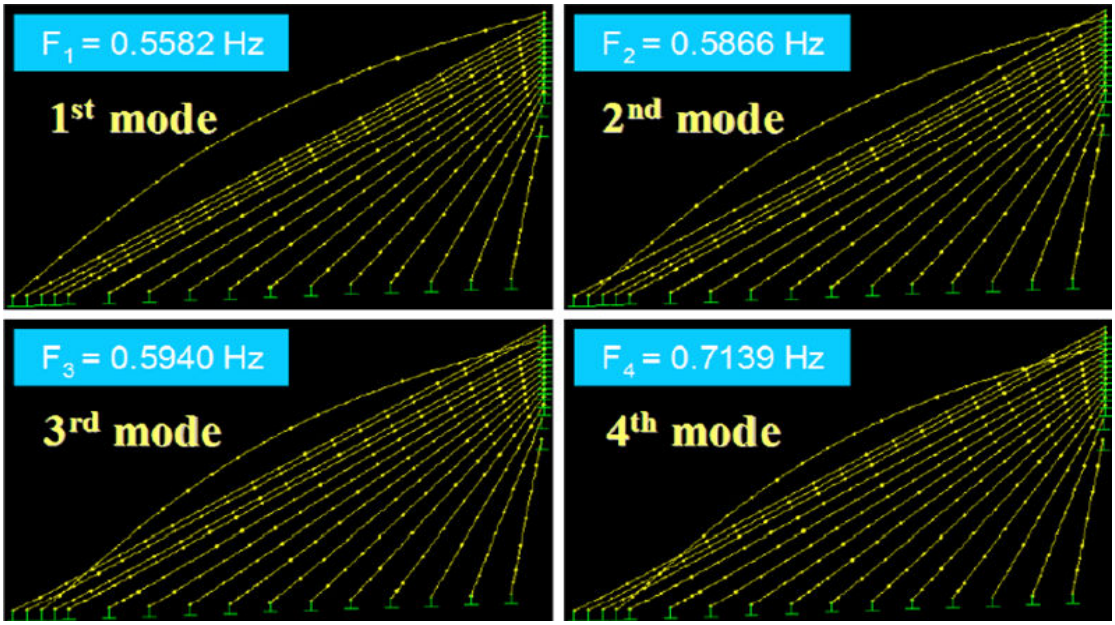

Figure 4-5: The first in-plane mode shapes (no crosstie) from FHWA report [9]

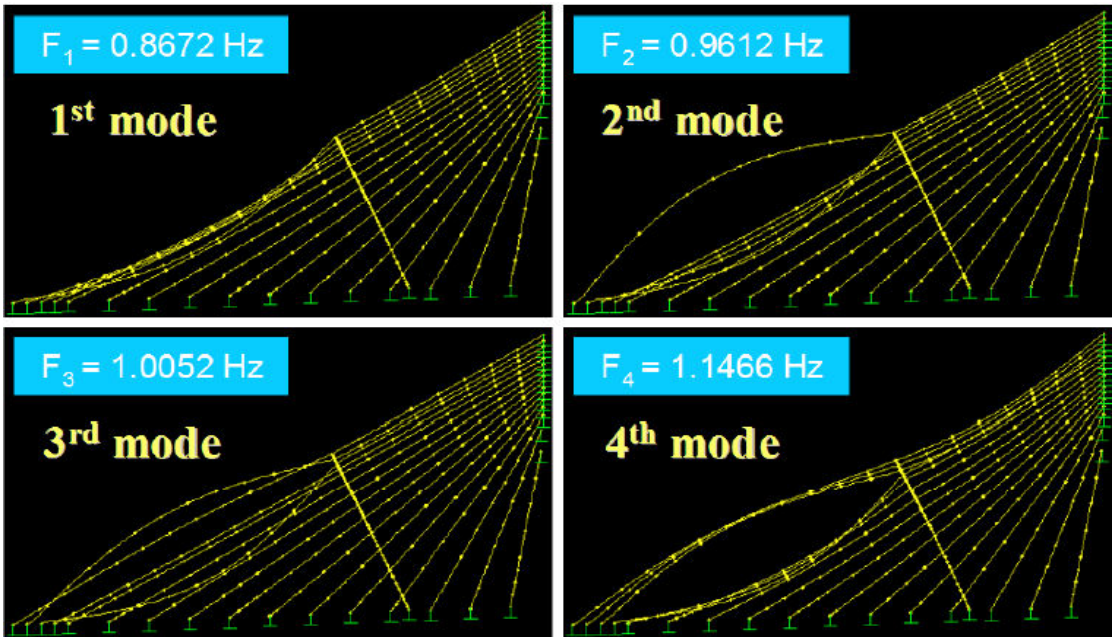

Figure 4-6: The first in-plane mode shapes (1 crosstie) from FHWA report [9]

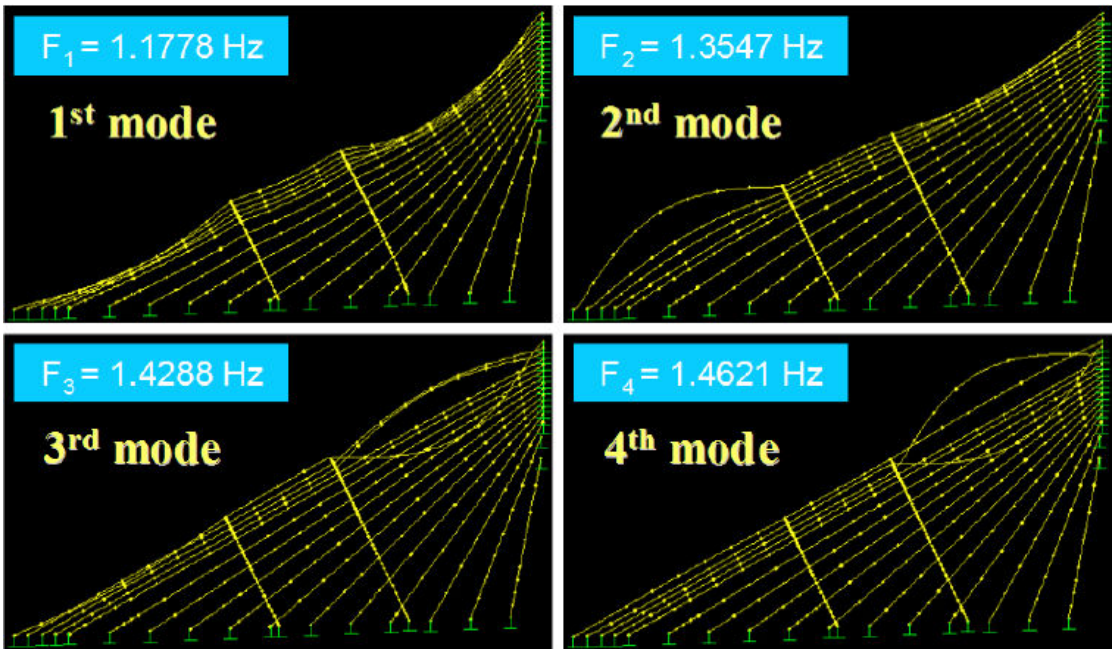

Figure 4-7: The first in-plane mode shapes (2 crossties) from FHWA report [9]

Table 4-3: Comparison of frequencies with FHWA of the uniform property cable

No crosstie

Mode Number	Frequencies (Hz)		
	Current Study	FHWA	Differences
1	0.56207	0.5582	0.69%
2	0.58988	0.5866	0.56%
3	0.59738	0.594	0.57%
4	0.70959	0.7139	0.60%

1 crosstie

Mode Number	Frequencies (Hz)		
	Current Study	FHWA	Differences
1	0.86505	0.8672	0.25%
2	0.96076	0.9612	0.05%
3	1.0066	1.0052	0.14%
4	1.139	1.1466	0.66%

2 crossties

Mode Number	Frequencies (Hz)		
	Current Study	FHWA	Differences
1	1.4018	1.1778	19.02%
2	1.4206	1.3547	4.86%
3	1.4794	1.4288	3.54%
4	1.5038	1.4621	2.85%

By comparing the information provided in the FHWA model of the same stay-cables fan configuration developed for the Bill Emerson Memorial Cable-stayed Bridge, as the Table 4-3 shows, with the natural frequency results obtained from the FE model developed in the current research, for the same fan configuration it could be concluded that:

1) For the stay-cables fan with no crossties, the natural frequencies were almost the same as the results reported from the FHWA model, but the first three frequencies of the current study are slightly higher (0.69%, 0.56%, 0.57%) and the 4^{th} mode frequency is slightly smaller. The

in-plane vibration mode shapes of the two models are consistent with each other, presenting the same evolution.

2) For the cable fan with one crosstie, the results of the mode frequencies remain in a close range when the two studies are compared. However, the 3rd natural frequency of the current study is larger than that of FHWA model, which is contrary for the other three modes. The vibration mode shapes are the same as well; differences arise only in the directions of the vibration in the graphs of the deformed shapes.
3) For the cable network with two crossties, similar to the former cases, the results match well between the two studies, except that the differences between the 1st mode frequency is relatively larger than the case with fewer crossties.
4) The differences between the natural frequencies and the vibration mode shapes reported by the FHWA study and by the current research, for the stay-cables fan configuration of the Bill Emerson Memorial Cable-stayed Bridge, were found to be under the acceptable error percentage of 10%, thus the developed FE model is considered to be appropriate for performing the further analysis for the grouted stay-cables with inner strands. Moreover the slight discrepancies between the two studies might be due to different boundary conditions between the tower and the stay-cables, the stay-cables and the deck and the crossties and the stay-cables.

4.3 Modal analysis of the multiple strands stay-cables fan

For the stay-cables with multiple parallel inner strands inside, a grout material is used, usually a polymer gel or cement paste, for allowing the replacement of individual strands in case a local damage of the respective strand is detected. As described in chapter 3, models of two types of multiple-strand cables have been developed: one with the multiple strands, but without the grout material inside and the other with the polymer gel grouted inner strands.

4.3.1 Multiple strands stay-cables fan without grout inside

The effectiveness of the crossties for cables of uniform properties (no strands) and their effect on the modal properties of the stay-cables has been presented in sections 4.1 and 4.2 above, when the results of the cable fan with no crossties, one crosstie and two crossties were discussed. The same configurations of no crosstie, one crosstie, two crossties, and also four crossties are investigated for the multiple strands stay-cables fan, with and without grout, in the following sections. For all the cases a number of 19 to 40 strands were used for the stay-cables, as detailed in Table 3-16 which describes the construction conditions for the real Bill Emerson Memorial Cable-stayed Bridge.

4.3.1.1 Multiple strands stay-cables fan without crossties

The modal analysis was conducted initially for the multiple strands cables fan without crossties and according to the frequency results, there are no in-plane modes within the first 300 modes of vibration; all these modes are the out-of-plane deformation of each cable, as it can be noticed in Figure 4-8. It can also be concluded that the natural frequency increased very slow, thus the first four out-of-plane modes reported in Figure 4-8 being recorded for the same frequency of 0.41741 Hz. The same value of the frequency is evident for several sequential vibration modes, which is then followed by a set of other vibration modes with larger value of the frequency. The range of the mode frequencies within 300 modes is 0.41741Hz~0.4474Hz.

To clearly demonstrate the mode shapes of the out-of-plane modes, two different views (general view and top view and) have been captured for the first case, as shown in Figures 4-8 and Figure 4-9 below.

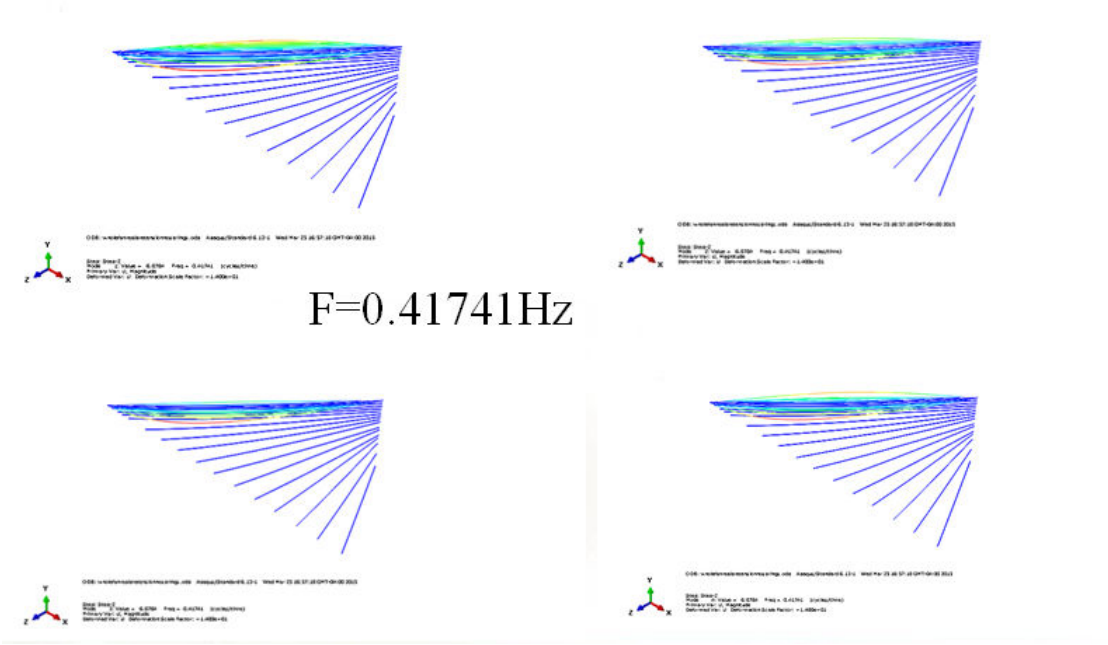

Figure 4-8: General views of the first four out-of-plane mode shapes for the multi strands stay-cables fan (no crossties)

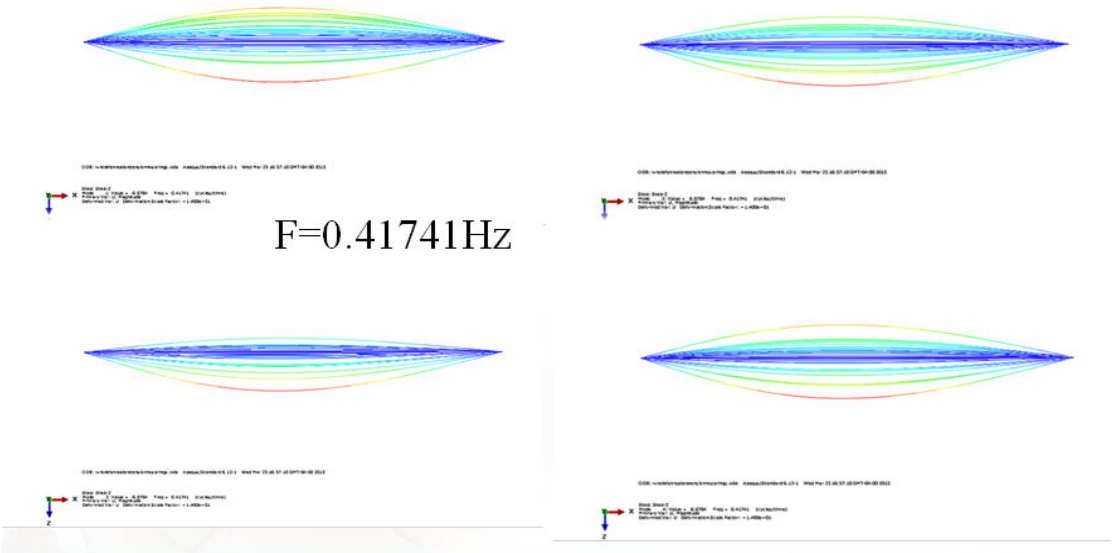

Figure 4-9: Top views of out-of-plane mode shapes 1-4 (no crosstie)

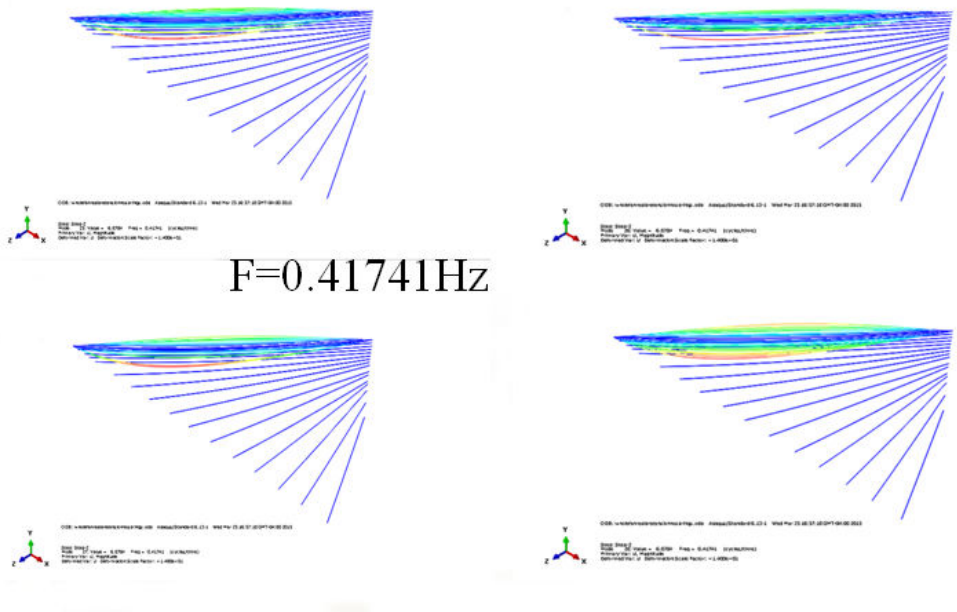

Figure 4-10: Out-of-plane mode shapes 25-28 (no crosstie)

As one can see in Figure 4-8 and Figure 4-10, the frequencies from 1-28 remain the same namely 0.41741Hz and together with the mode shape identification shown in the same figures, it proves that the first 28 vibration modes belong to the inner strands of stay-cable 1.

Also, it can be seen that the vibration modes of the entire stay-cables fan without crossties consists of local modes of individual strands, and each mode appears sequentially from cable 1 to cable 16. Also it was noticed that the frequencies of the mode shapes within one stay-cable stay the same.

4.3.1.2 Multiple strands stay-cables fan with one crosstie

For the case of multiple strands stay-cables fan, with one crosstie installed, it can be noticed that all the in-plane vibration mode shapes are dominated by the local stay-cable modes of the lower segment, as shown in Figure 4-11 and Figure 4-12.

Each vibration mode presented in Figures 4-11 and 4-12, is the local mode of the stay-cable which actually comprises of different mode shapes of inner strands. The in-plane modes start from the vibration of the lower segment of the cable one; increments of the frequencies have been observed between the lower modes (1-4) and higher modes (10-13).

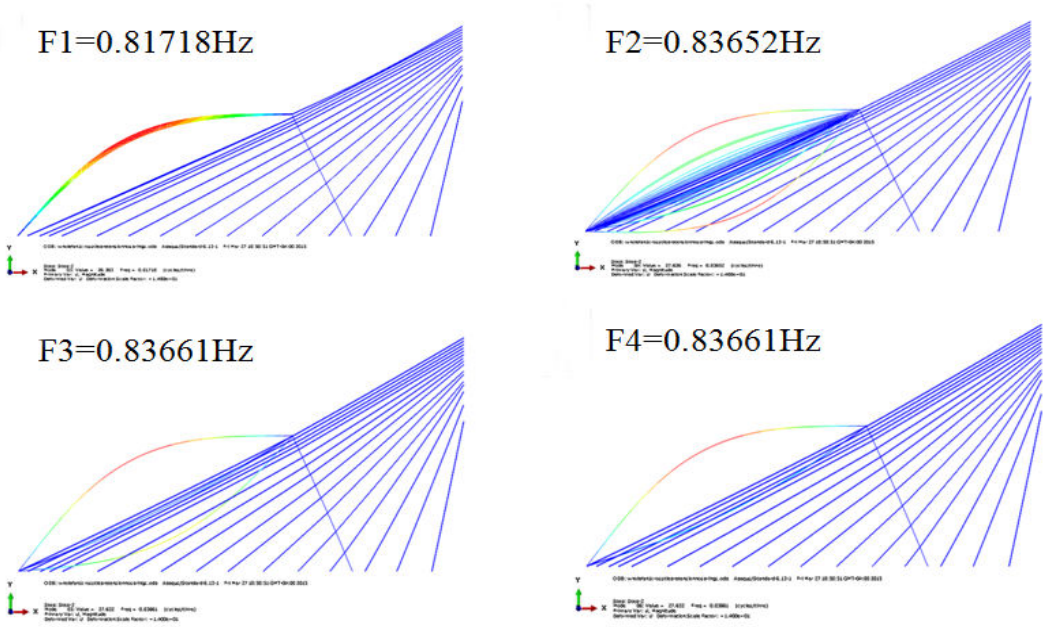

Figure 4-11: The first four in-plane mode shapes (1 crosstie)

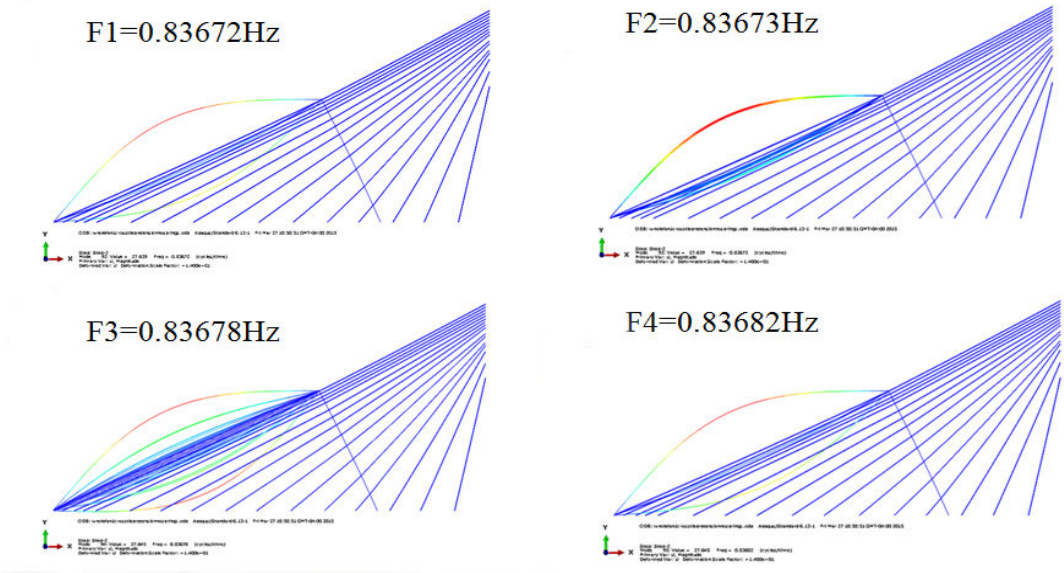

Figure 4-12: The in-plane mode shapes 10 to 13 (1 crosstie)

It can be seen that the in-plane modes start with the vibration of cable 1, from the vibration of the cable in the left side of the crosstie. Each in-plane mode as shown above consists of different deformed shapes of strands inside cable one.

As shown in Figure 4-13, the 1st and 2nd out-of-plane modes are the global modes:

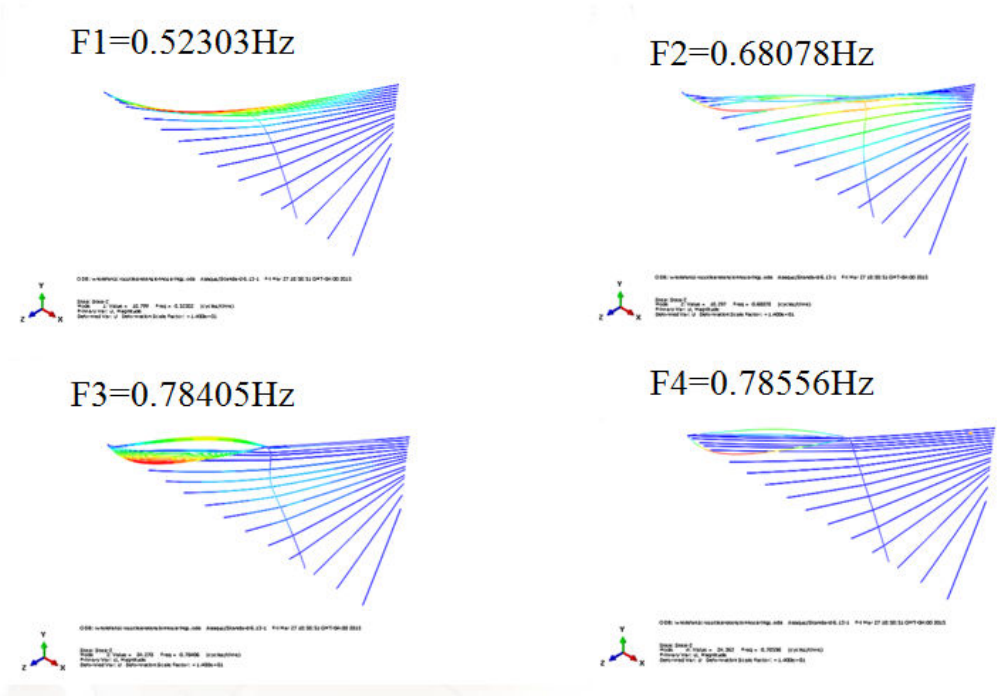

Figure 4-13: The first four out-of-plane mode shapes (1 crosstie)

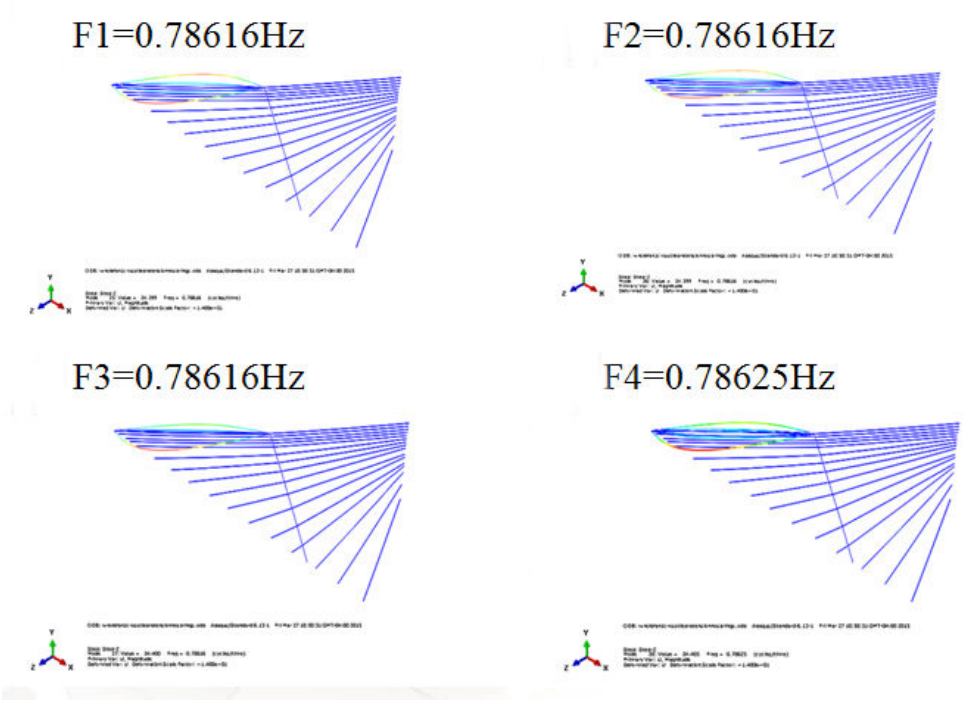

Figure 4-14: The out-of-plane mode shapes 25-28 (1 crosstie)

From Figure 4-13 and Figure 4-14, it can be seen that the out-of-plane modes become a mixture of global and local modes of the stay-cables for the low frequencies. The out-of-plane local vibration modes start from the vibration of the lower segment of the fan as well.

4.3.1.3 Multiple strands stay-cable fan with 2 crossties

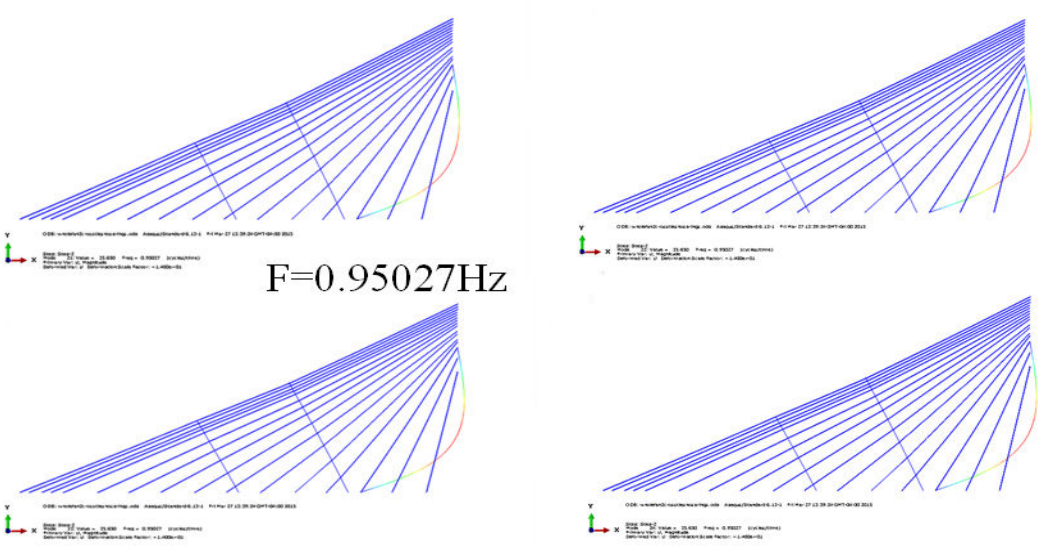

Figure 4-15: The first four in-plane mode shapes (2 crossties)

The first four frequencies for the in-plane modes registered the same value of 0.95027Hz, followed by a second group of vibration modes of 10 to 13, with the same frequency, as Figure 4-15 and Figure 4-16 show:

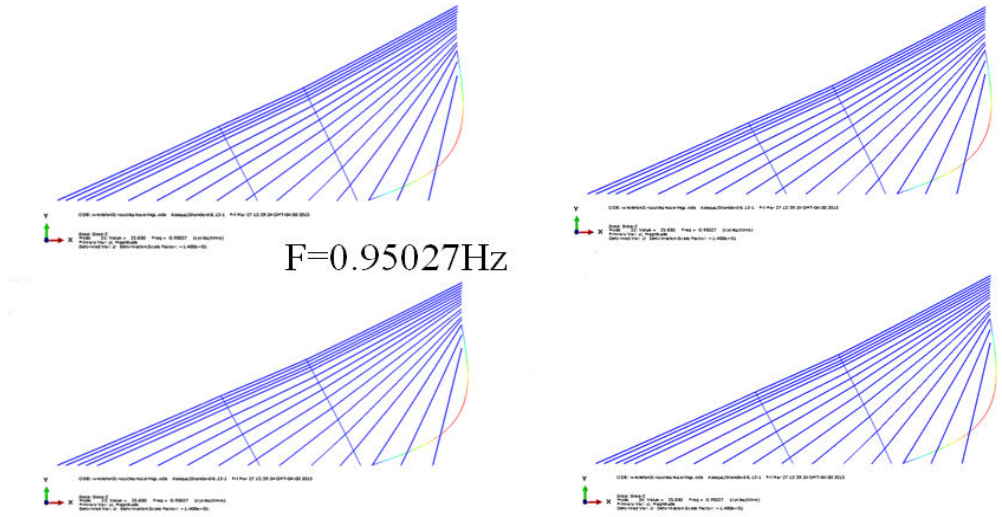

Figure 4-16: The in-plane mode shapes 10-13 (2 crossties)

More significant is the fact that the order of the responding stay-cables changed, the cables near the tower reacting first. All the in-plane modes spanning from modes1 to 13 are the local modes of the cable 14. Each mode detailed in Figure 4-16 represents a different vibration of the inner strands belonging to cable 14.

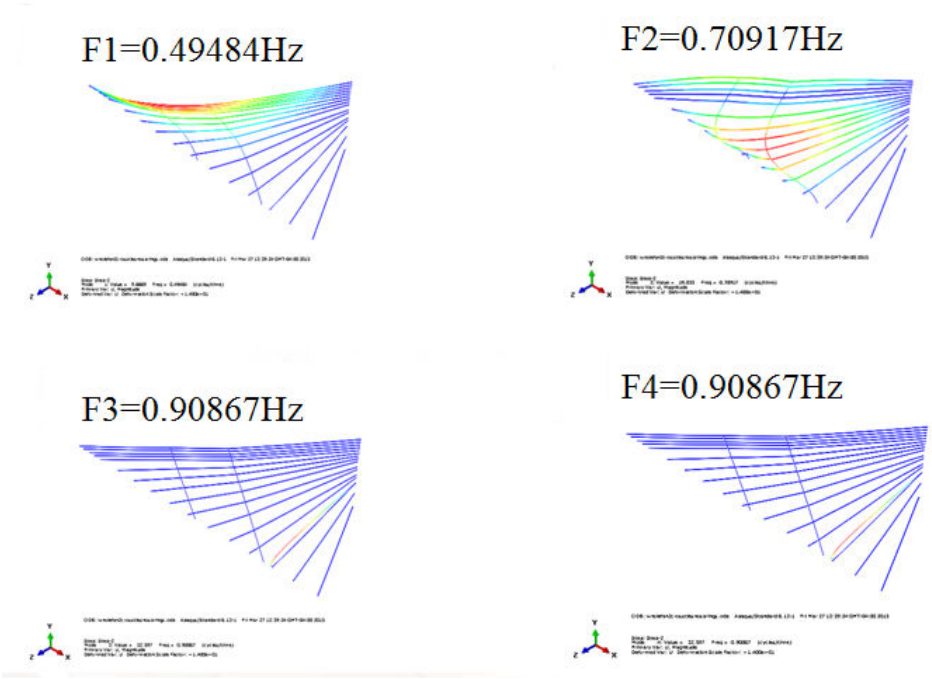

Figure 4-17: Out-of-plane mode shapes 1-4 (2 crossties)

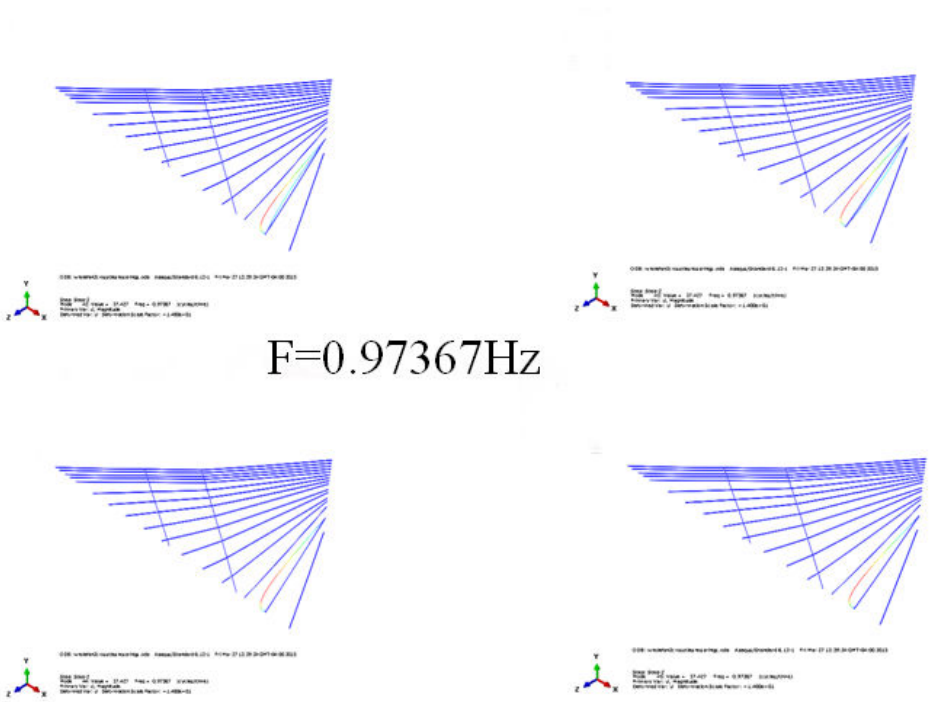

Figure 4-18: Out-of-plane mode shapes 25-28 (2 crossties)

Local out-of-plane modes start with the vibration of cable 14 as well, as Figure 4-17 and Figure 4-18 show.

4.3.1.4 Multiple strands stay-cables fan with 4 crossties

From the results of the analysis performed on the multiple strands stay cables fan, contacted by four diagonal crossties, it can be summarized that all the in-plane vibration modes occurring within the total number of 300 modes extracted, are the local stay-cables modes. Figure 4-19 and Figure 4-20 show the in-plane vibration modes identified for lower frequencies, where the dynamic effect of the wind loading is expected to dominate the structural response of the stay-cables. The inner strands of the stay-cables located near the tower started vibrating first, on the lower segment of the fan, but more important is the fact that they registered asymmetric vibration modes, which is much different than all the previous cases of fans without crossties and fans with one or two crossties.

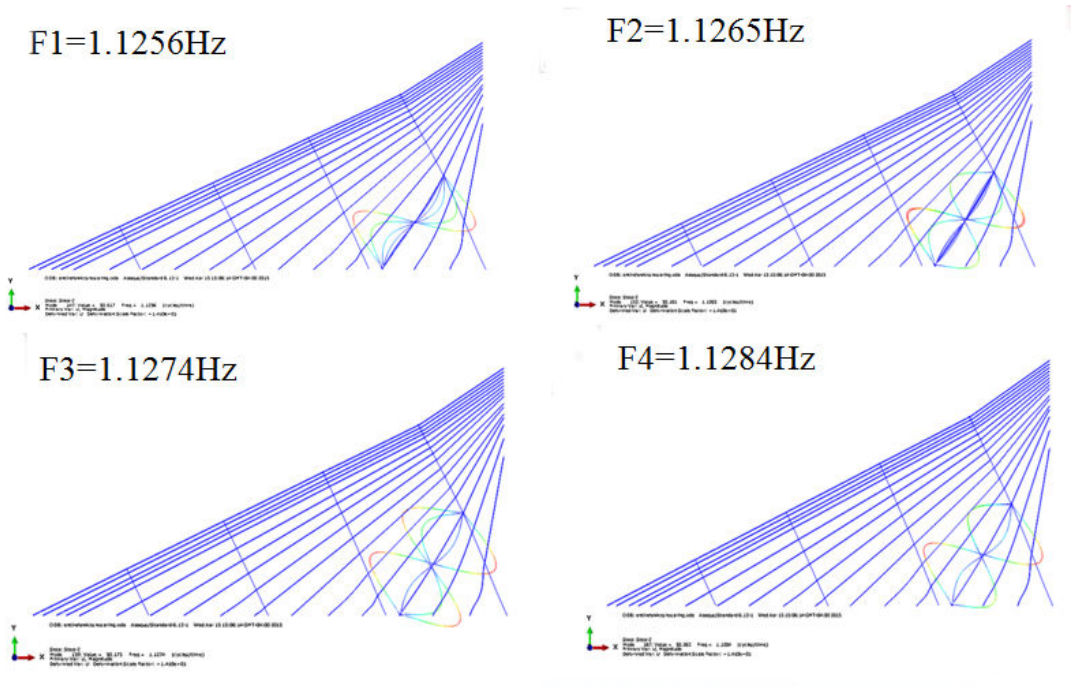

Figure 4-19: In-plane mode shapes 1-4 (4 crossties)

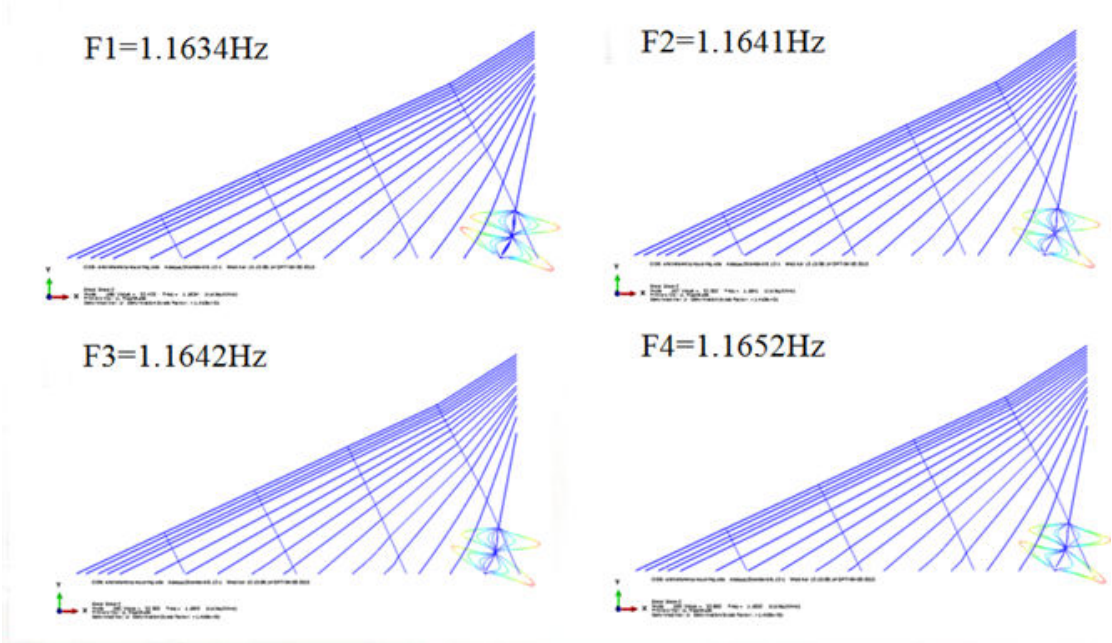

Figure 4-20: In-plane mode shapes 10-13 (4 crossties)

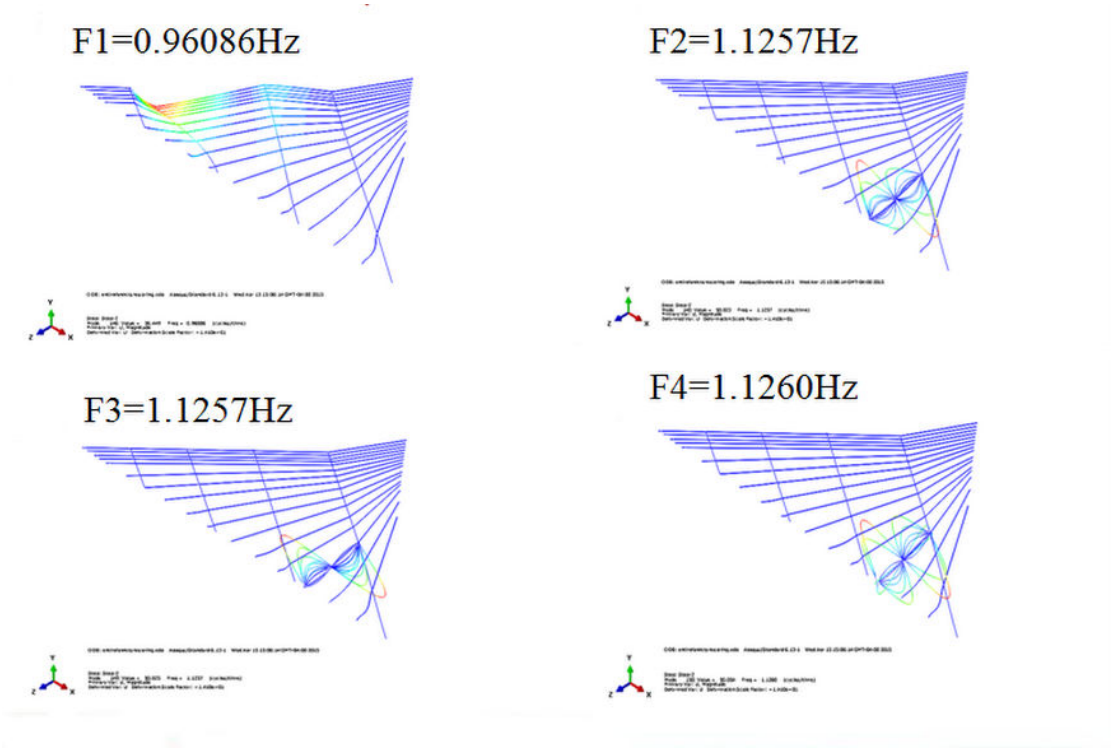

Figure 4-21: Out-of-plane mode shapes 1-4 (4 crossties)

From Figure 4-21, it can be noticed that only the first out-of-plane vibration mode is the global mode of the stay-cables, while the rest of the recorded out-of-plane vibration modes are strands modes of the stay-cables situated near the tower, stay-cable 14 here.

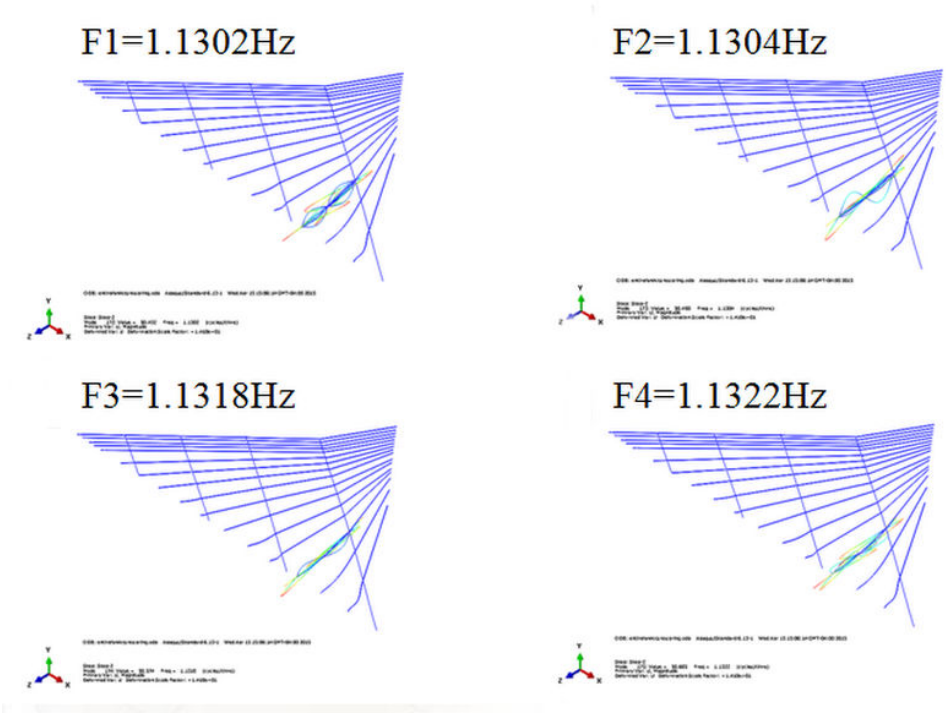

Figure 4-22: Out-of-plane mode shapes 25-28 (4 crossties)

Similar to the case of 2 crossties, the in-plane modes and local out-of-plane modes start with the global vibration of the stay-cable 14, followed by a series of modes of the inner strands of the same stay-cable registered at very close frequency. However, as a general pattern, the stay-cable in the lower side of the fan, under the crossties vibrates first; such behaviour is not reported for the case of the stay-cables fan with two crossties.

Also, it can be seen that the vibration of the stay-cable fan suddenly becomes stronger, and has a more complicated and larger curvature of the deformed shape of the cable (Figure 4-22).

4.3.1.5 Summary

In order to categorize the vibration modes for all the multiple strands stay-cables fans investigated, summarizing Table 4-4, Table 4-5, Table 4-6, Table 4-7 show the representative modes of different number of crossties respectively:

Table 4-4: Main frequencies and mode shapes without crosstie (no grout)

Mode Number	Frequencies (Hz)	Mode Shape description
1	0.41741	1st out-of-plane, local, asymmetric
2	0.41741	2nd out-of-plane, local, asymmetric
3	0.41741	3rd out-of-plane, local, asymmetric
4	0.41741	4th out-of-plane, local, asymmetric
25	0.41741	25th out-of-plane, local, asymmetric
26	0.41741	26th out-of-plane, local, asymmetric
27	0.41741	27th out-of-plane, local, asymmetric
28	0.41741	28th out-of-plane, local, asymmetric

Table 4-5: Main frequencies and mode shapes with 1 crosstie (no grout)

Mode Number	Frequencies (Hz)	Mode Shape description
1	0.52303	1st out-of-plane, global, asymmetric
2	0.68078	2nd out-of-plane, global, asymmetric
3	0.78406	3rd out-of-plane, local, asymmetric
4	0.78556	4th out-of-plane, local, asymmetric
25	0.78616	25th out-of-plane, local, asymmetric
26	0.78616	26th out-of-plane, local, asymmetric
27	0.78616	27th out-of-plane, local, asymmetric
28	0.78625	28th out-of-plane, local, asymmetric
83	0.81718	1st in-plane, local, asymmetric
84	0.83652	2nd in-plane, local, asymmetric
85	0.83661	3rd in-plane, local, asymmetric
86	0.83661	4th in-plane, local, asymmetric
92	0.83672	10th in-plane, local, asymmetric
93	0.83673	11th in-plane, local, asymmetric
94	0.83678	12th in-plane, local, asymmetric
95	0.83682	13th in-plane, local, asymmetric

Table 4-6: Main frequencies and mode shapes with 2 crossties (no grout)

Mode Number	Frequencies (Hz)	Mode Shape description
1	0.49484	1st out-of-plane, global, asymmetric
2	0.70917	2nd out-of-plane, global, asymmetric
3	0.90867	3rd out-of-plane, local, asymmetric
4	0.90867	4th out-of-plane, local, asymmetric
21	0.95027	1st in-plane, local, asymmetric
22	0.95027	2nd in-plane, local, asymmetric
23	0.95027	3rd in-plane, local, asymmetric
24	0.95027	4th in-plane, local, asymmetric
30	0.95027	25th out-of-plane, local, asymmetric
31	0.95027	26th out-of-plane, local, asymmetric
32	0.95027	27th out-of-plane, local, asymmetric
33	0.95027	28th out-of-plane, local, asymmetric
42	0.97367	10th in-plane, local, asymmetric
43	0.97367	11th in-plane, local, asymmetric
44	0.97367	12th in-plane, local, asymmetric
45	0.97367	13th in-plane, local, asymmetric

Table 4-7: Main frequencies and mode shapes with 4 crossties (no grout)

Mode Number	Frequencies (Hz)	Mode Shape description
1	0.96086	1st out-of-plane, global, asymmetric
2	1.1256	1st in-plane, local, symmetric
3	1.1257	2nd out-of-plane, local, symmetric
4	1.1257	3rd out-of-plane, local, symmetric
5	1.126	4th out-of-plane, local, symmetric
8	1.1265	2nd in-plane, local, symmetric
14	1.1274	3rd in-plane, local, symmetric
22	1.1284	4th in-plane, local, symmetric
27	1.1302	25th out-of-plane, local, symmetric
28	1.1304	26th out-of-plane, local, symmetric
29	1.1318	27th out-of-plane, local, symmetric
30	1.1322	28th out-of-plane, local, symmetric
41	1.1634	10th in-plane, local, asymmetric
42	1.1641	11st in-plane, local, asymmetric
43	1.1642	12nd in-plane, local, asymmetric
44	1.1652	13rd in-plane, local, asymmetric

4.3.2 Multiple strands stay-cables fan with grout

Depending on the properties, grouting material can be stiffer (if concrete) or could be very flexible (polymer gel). The stiffer grouting materials would influence the global vibration of the stay-cable, because this would not allow the inner strands to move or vibrate, and thus the overall stay-cable frequencies will approach the cables of uniform properties (without strands). However the more flexible grouting material (the polymer gel) would allow the inside strands to move and vibrate, thus developing local strands vibration modes as illustrated in Figures 4-23 and 4-24, for example; such polymer material however might not affect directly the local vibration modes of the strands, because of the low elastic constant (k = 500 N/m) as determined in section 3.4.

In order to determine the effect of the polymer grouting material on the local vibrations of the strands and on the global vibration of the multiple strands stay-cables fan, the modal analysis for the FE model considering the grout inside each stay-cable, between the strands, was carried out. The grout-strand interaction was simulated by placing a total of 45360 spring links placed along the length of each strands. The details about the FE modelling for the grouted cables can be found in section 3.4. Similar to the cable without the grout inside, presented above, the results of the multiple strands stay-cables fan with no crosstie, one crosstie, two crossties and four crossties are presented.

4.3.2.1 Multiple strands grouted stay-cables fan without crossties

The grouted stay-cables with multiple inner strands developed in-plane vibration modes starting with the 47th mode and frequencies of 0.533 Hz; when the grouted model was not used, no in-plane local or global vibrations occurred in the first 300 modes, as described in section 4.3.1.

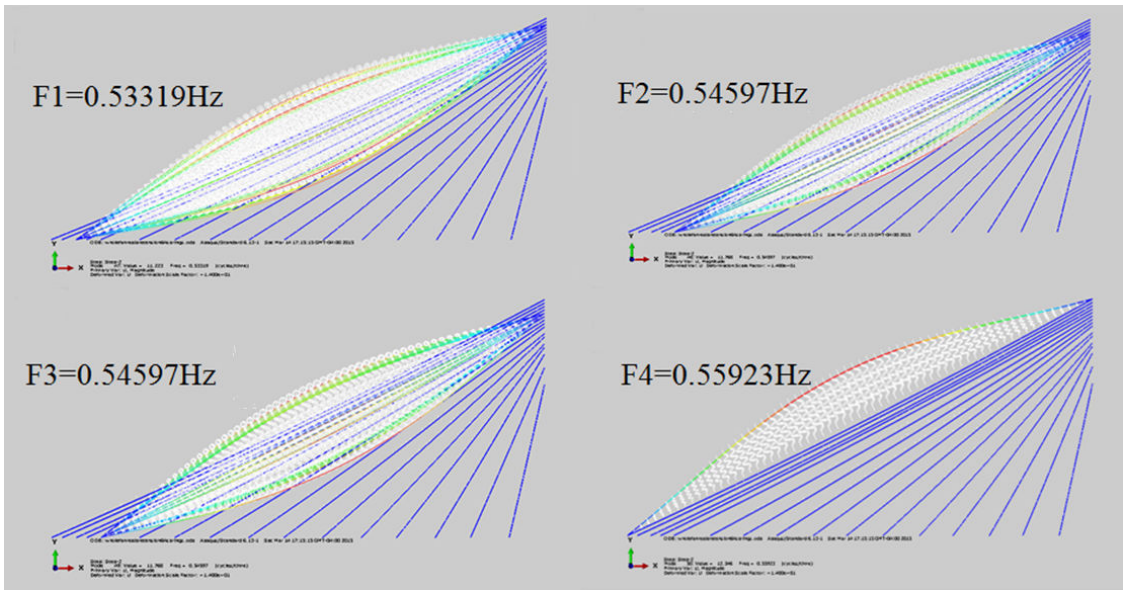

Figure 4-23: In-plane mode shapes 1-4 (no crosstie)

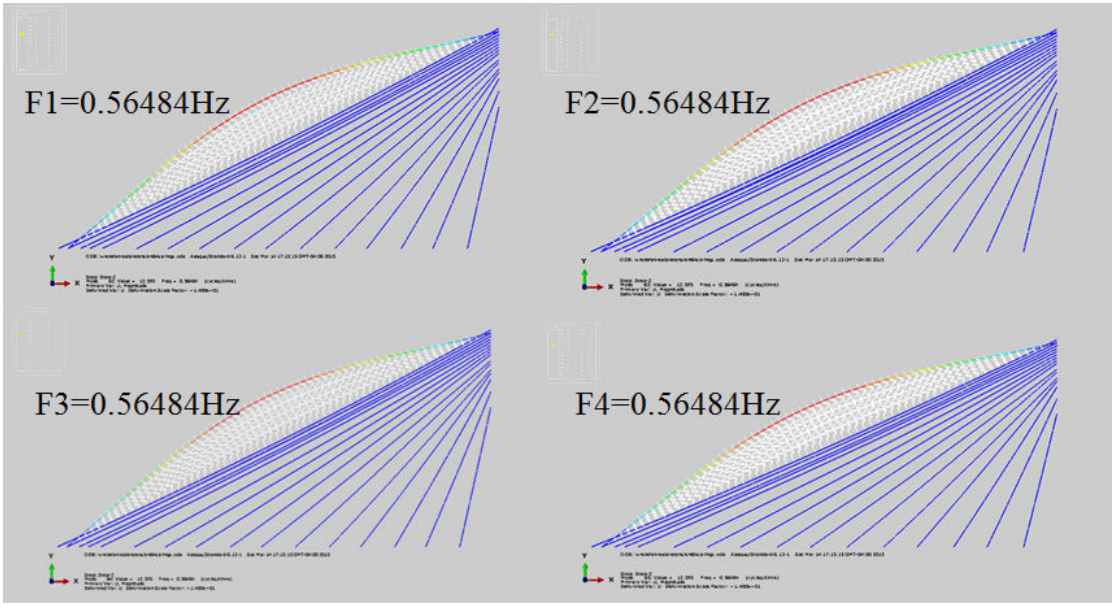

Figure 4-24: In-plane mode shapes 10-13 (no crosstie)

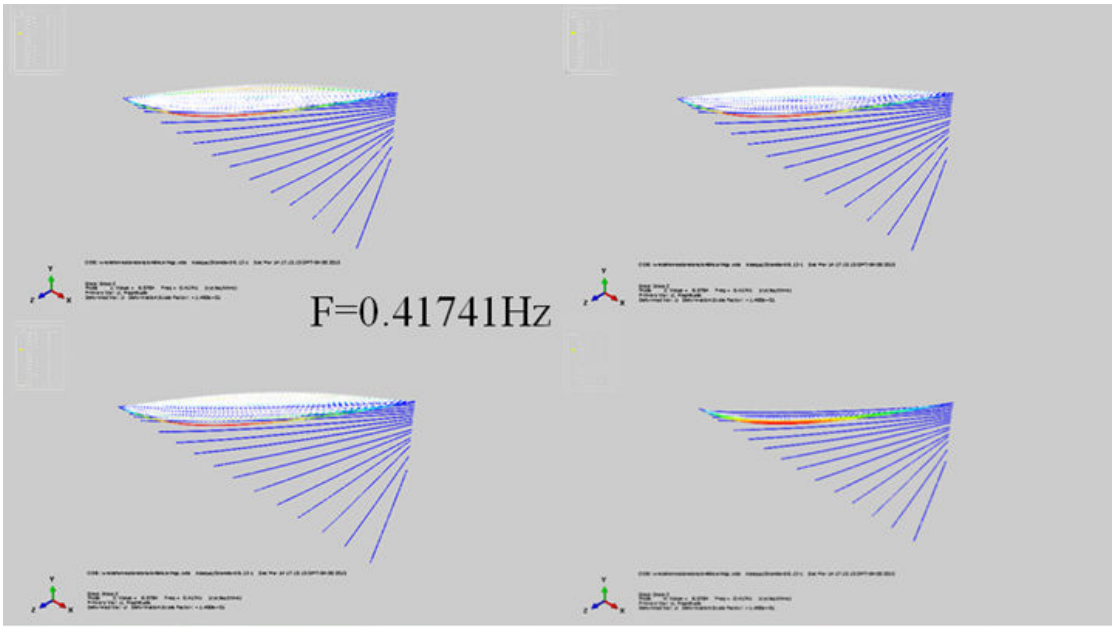

Figure 4-25: Out-of-plane mode shapes 1-4 (no crosstie)

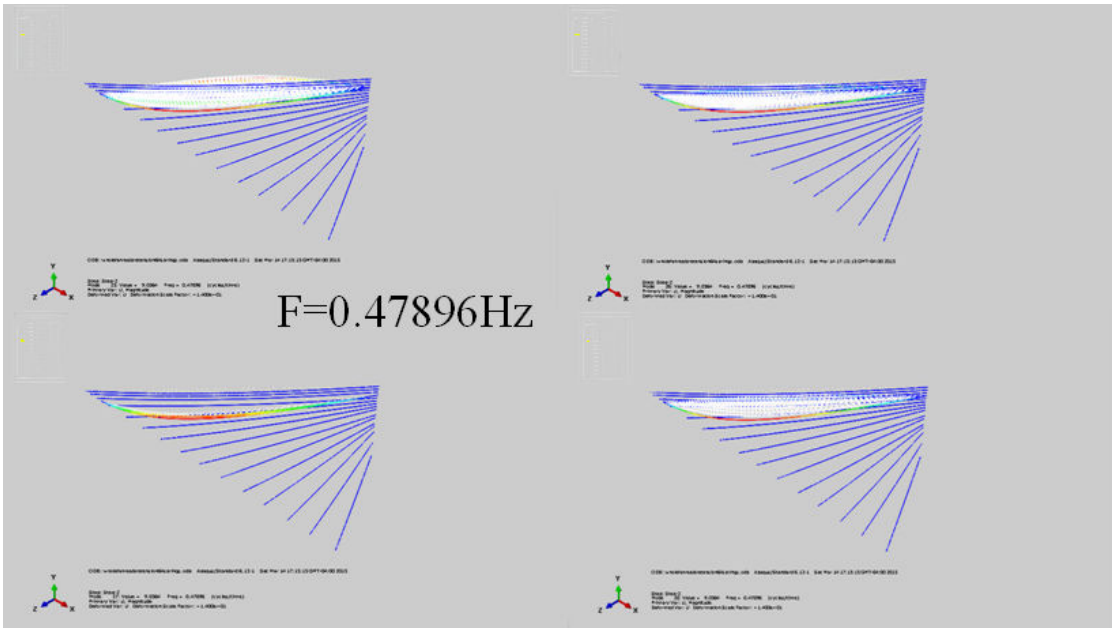

Figure 4-26: Out-of-plane mode shapes 25-28 (no crosstie)

The frequencies of the first four out-of-plane vibration modes are registered as 0.41741Hz, exactly the same as for the cases when the grouted material was not integrated in the model; also the same stay cables responded for these type of out-of-plane vibration as for the case with no grouting material. The out-of-plane vibrations, modes 25 to 28 are also the same as for the case of the stay-cables without the grouted material.

It can be concluded that the grouting polymer material did not have influence on the out-of-plane vibration modes which started with the first mode, and registered different mode shapes for the first four modes, but shared the same frequency, and are all the modes of stay-cable 1, as shown in Figure 4-25 and Figure 4-26. The exact same response was found for the model of the multiple strands stay-cable fan without grouting material.

The difference was found however for the in-plane modes. They started from modes 47 and above, which occurred in a non-consecutive order for the in-plane modes 1 to 20, while for the no grouting case these did not occur in the first 300 modes of vibration.

Identical evolution was found for the stay-cables fan with one and two crossties, for the case when the grouting material was modelled inside the stay-cables and for the case when no grouting material was used. The details of the modal analysis and the figures of the vibration modes identified for the grouted stay-cables fan were detailed in Appendix E.

4.3.2.2 Multiple strands grouted stay-cables fan with 4 crossties

For the case of four crossties used for connecting the grouted multiple-strand stay-cables of the fan, all the in-plane vibration modes were encountered within the 300 modes extracted and these were local modes; this is similar to the case without the grout inside; Figure 4-27 and Figure 4-28 show the mode shapes of the in-plane vibration modes registered at low frequency range.

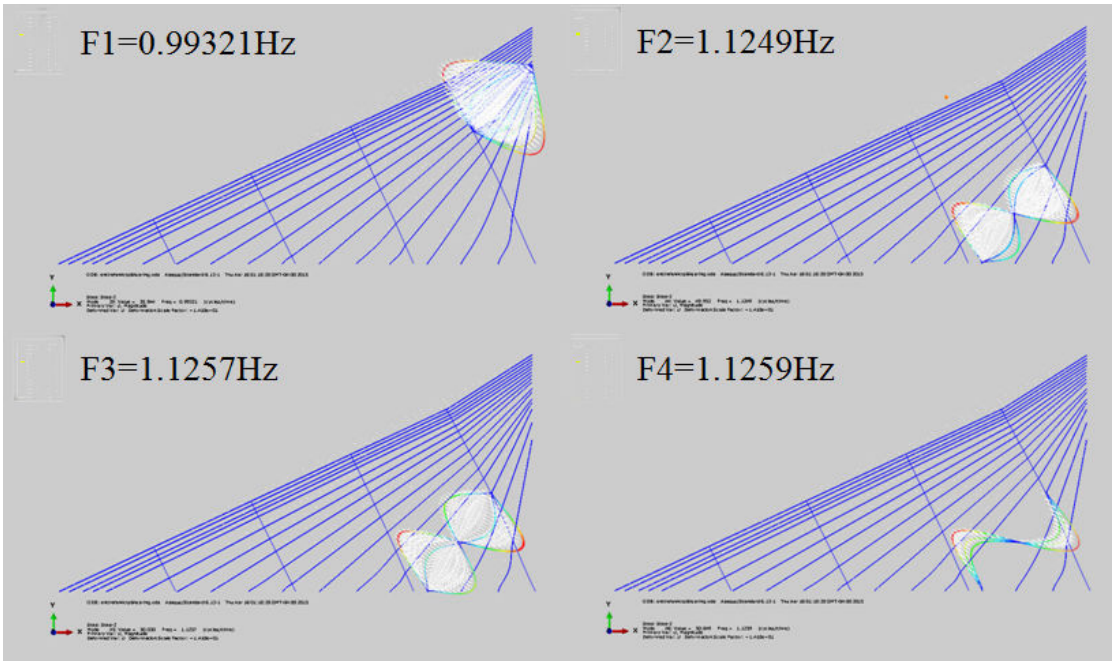

Figure 4-27: In-plane mode shapes 1-4 (4 crossties)

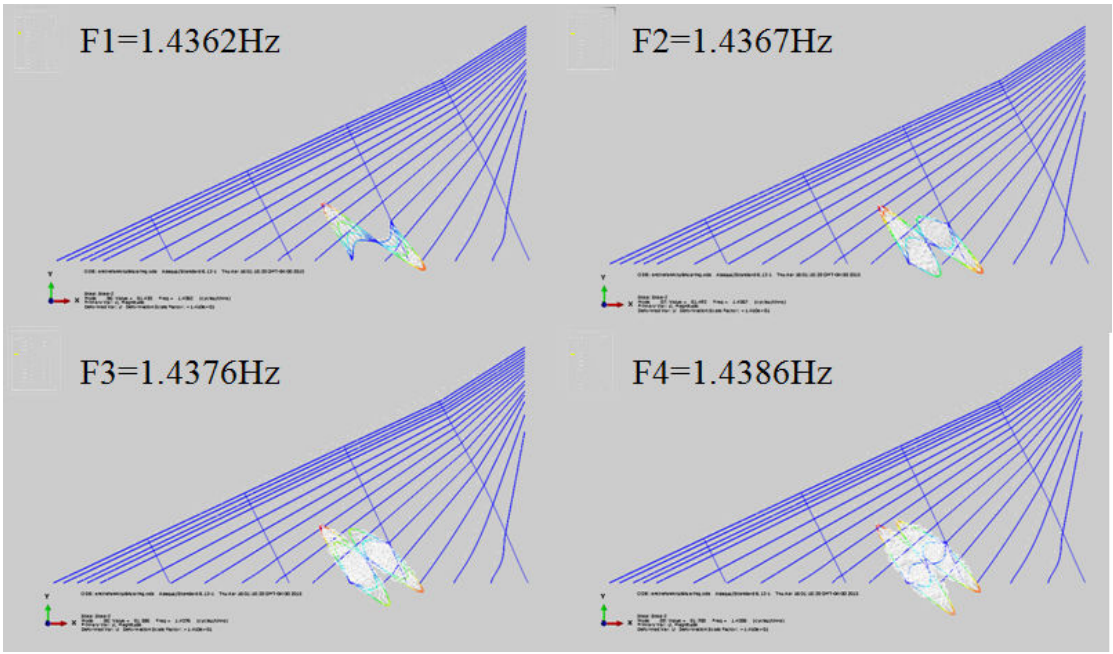

Figure 4-28: In-plane mode shapes 10-13 (4 crossties)

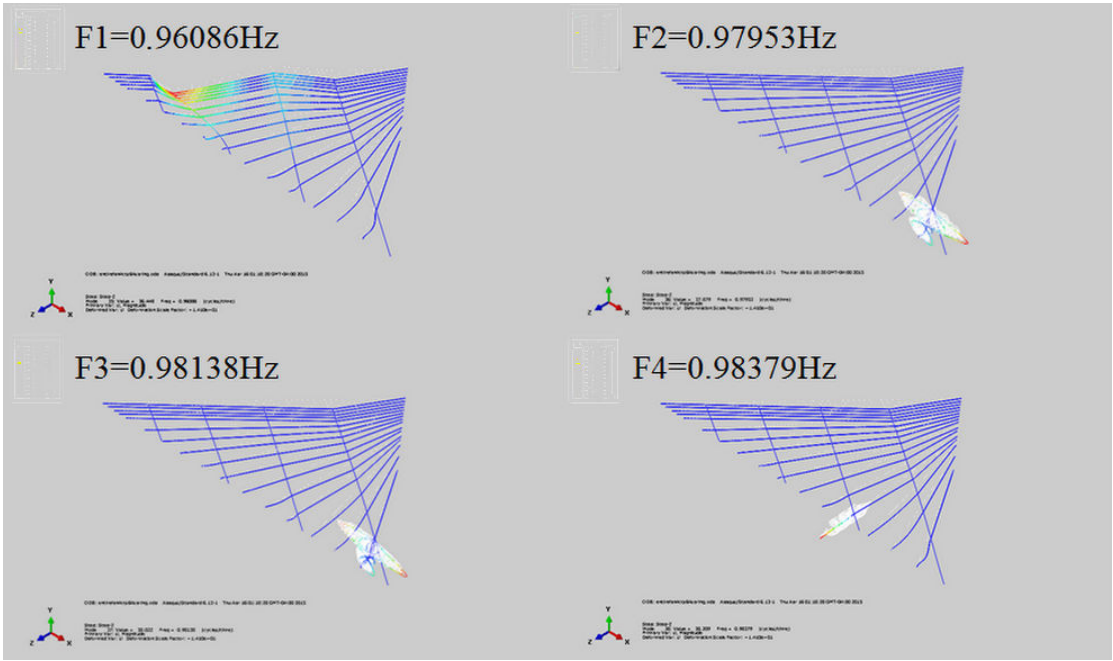

Figure 4-29: Out-of-plane mode shapes 1-4 (4 crossties)

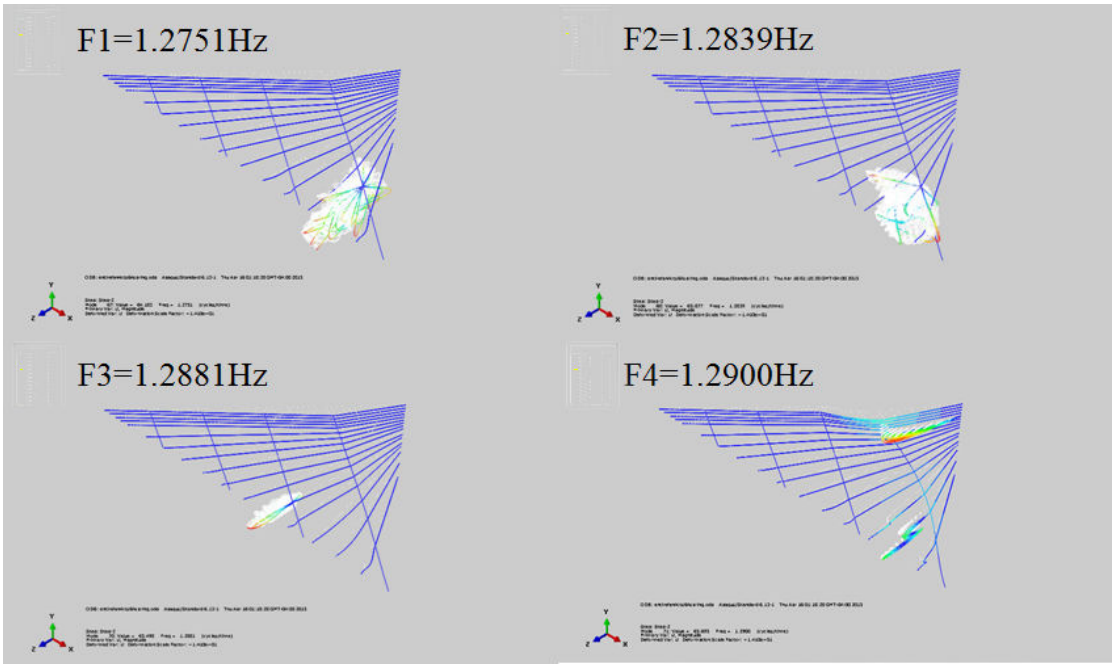

Figure 4-30: Out-of-plane mode shapes 25-28 (4 crossties)

As Figure 4-29 and Figure 4-30 show, the 1st and the 28th out-of-plane vibration modes are the global stay-cable modes, the rest however are local models registered by the inner strands of the same cables.

4.3.2.3 Summary

Table 4-8 and Table 4-9 show the representative vibration modes of different number of crossties respectively:

In general, adding the crossties increased the natural frequencies of the multiple strands stay-cables. Moreover, as the number of the crossties increased, more in-plane modes tend to occur within the first 100 vibration modes. It is also noticeable that symmetric modes have appeared for the stay-cables fan with four crossties, for both in in-plane and out plane mode shapes.

Table 4-8: Main frequencies and mode shapes without crosstie (with grout)

Mode Number	Frequencies (Hz)	Mode Shape description
1	0.41741	1st out-of-plane, local, asymmetric
2	0.41741	2nd out-of-plane, local, asymmetric
3	0.41741	3rd out-of-plane, local, asymmetric
4	0.41741	4th out-of-plane, local, asymmetric
25	0.47896	25th out-of-plane, local, asymmetric
26	0.47896	26th out-of-plane, local, asymmetric
27	0.47896	27th out-of-plane, local, asymmetric
28	0.47896	28th out-of-plane, local, asymmetric
47	1.1302	1st in-plane, local, asymmetric
48	1.1304	2nd in-plane, local, asymmetric
49	1.1318	3rd in-plane, local, asymmetric
50	1.1322	4th in-plane, local, asymmetric
62	1.1634	10th in-plane, local, asymmetric
63	1.1641	11th in-plane, local, asymmetric
64	1.1642	12th in-plane, local, asymmetric
65	1.1652	13th in-plane, local, asymmetric

Table 4-9: Main frequencies and mode shapes with 4 crossties (with grout)

Mode Number	Frequencies (Hz)	Mode Shape description
1	0.96086	1st out-of-plane, global, asymmetric
2	0.97953	2nd out-of-plane, local, asymmetric
3	0.98138	3rd out-of-plane, local, asymmetric
4	0.98379	4th out-of-plane, local, asymmetric
5	0.99321	1st in-plane, local, asymmetric
10	1.1249	2nd in-plane, local, symmetric
11	1.1257	3rd in-plane, local, symmetric
12	1.1259	4th in-plane, local, symmetric
33	1.2751	25th out-of-plane, local, asymmetric
34	1.2839	26th out-of-plane, local, asymmetric
36	1.2881	27th out-of-plane, local, asymmetric
37	1.29	28th out-of-plane, global, asymmetric
51	1.4362	10th in-plane, local, symmetric
52	1.4367	11st in-plane, local, symmetric
53	1.4376	12nd in-plane, local, symmetric
54	1.4386	13rd in-plane, local, symmetric

4.3.3 Discussion

The following conclusions can be summarized from the modal analysis performed for the multiple strands stay-cables fan, with and without grout, without crossties, and with one, two and four crossties:

1) The mitigation effectiveness of the crossties has been confirmed with respect to the mode frequency. The natural frequencies increased significantly in the presence of the crossties, which mean that the cables are more difficult to excite, thus they have less displacements under the external loads. Moreover, an increase in natural frequencies has been observed, when compared with the stay-cable fan with fewer crossties.
2) After the polymer grouting was modelled, the natural frequency increased compared to the multiple-strand cable without the grout, especially for the four crossties stay-cables fan, which echoes previous studies of the impact of the spring stiffness.
3) The out-of-plane vibration modes always would occur first; the in-plane vibration mode shows up after a certain number of out-of-plane modes.
4) The global in-plane modes have not been observed in the relatively low frequency range, which would appear in the higher modes. For the out-of-plane modes a mixture of global modes and local modes in the relatively lower frequency range, was noticed.
5) For the cable network with four crossties, the mode shapes of the natural vibration frequency became unsteady, which means this has an irregular shape. The curvature of the mode shape increased as well. This may be explained by the complexity of the boundary conditions imposed by the stay-cable fan due to the crosstie; this might have reached a certain limit beyond which the vibration of the cable fan would develop coupled vibrations.
6) For the cable network have fewer than four crossties, no symmetric mode shapes have been observed, while a series of symmetric modes exist in the stay-cables fan with four crossties, both in in-plane and out-plane modes.

4.3.4 Comparison with field measurements

Prior to completion of the construction of the Bill Emerson Memorial Bridge, the U.S. Federal Highway Administration (FHWA) had conducted a series of experimental tests, by installing accelerometers on each stay-cable of one fan of the bridge and thus their natural frequencies and damping ratios could be measured, both before and after the installation of the grout material and before and after the installation of crossties. Data from accelerometers was recorded using a portable data acquisition system [78], as the Figure 4-31 shows:

Figure 4-31: The data acquisition system (left) and mounting accelerometers on a stay cable (right) [78]

Dynamic testing was performed in three phases. The first phase took place during the later stages of the stay-cables construction, to establish the cable characteristics just prior to the installation of the grout. The second phase was conducted about one month after the installation of the grout was completed. The final phase was initiated after one line of cross ties had been installed in several cable fans [78].

Data from the first phase of measurements was fully described in the literature [78] and was used for comparing with the results obtained from the current research. Multiple-strand cable one without the grout inside was compared with the field measurements, as Table 4-10 presents:

Table 4-10: Phase I stay-cables mode frequencies for cables 1 [78]

Mode Number	Mode Peaks (Frequency, Hz)		
	Field measurements	FE results	Differences
1	0.745	0.63963	14.14%
2	1.48	1.217	17.77%
3	2.22	1.872	15.68%
4	2.98	2.486	16.58%

4.4 Wind loading time-history analysis

For acquiring more comprehensive results of the stay-cables fan displacements under dynamic loading, and for judging the effectiveness of the crossties considering a wind loading action, four main points along the stay-cables of the fan have been chosen to be investigated, two of them in the middle and on the lower half of stay-cable 1 (points A and B) and another two on stay-cable 9 in the middle of the fan (point C) and on stay-cable 16 (point D), the last cable in the fan , as Figure 4-32 shows. The wind speed recorded at the site of Bill Emerson Memorial Bridge was used [9] for determining the wind loading based on the quasi-steady formulations [9] as presented on section 3.4.5 the wind loading was applied uniformly on each stay cable and crossties as shown in Figure 3-41 and Figure 3-42.

Apparently, the behaviour depends on the location where displacements were retrieved. Also, the obtained displacements are in the horizontal direction, which is parallel to the bridge longitudinal axis.

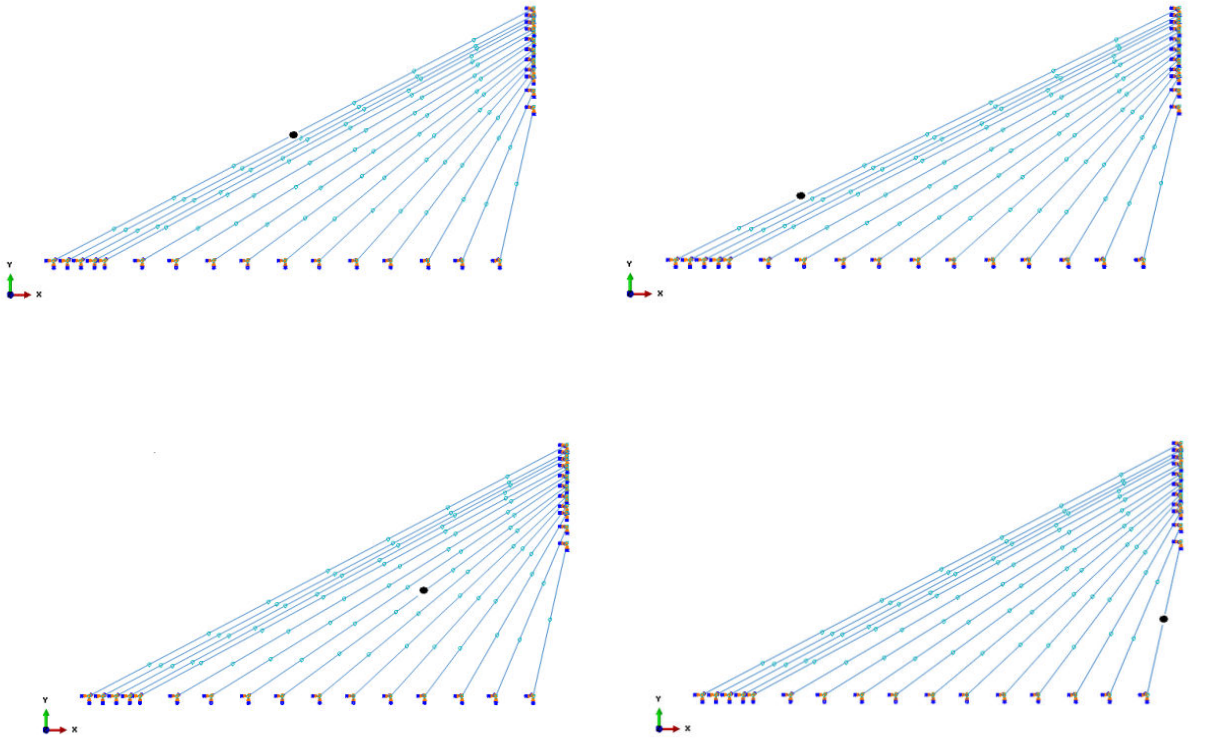

Figure 4-32: Locations of the midpoint of cable 1, a quarter of cable 1, cable 9 at fan centre and midpoint of cable 16

4.4.1 Results of the uniform property stay-cable fan under the time-history wind loading

For each selected node in the cable network, results of the displacements with different numbers of crossties are presented. The evolutions of the displacement are similar for all the cases investigated, because these are obtained under the same wind loading; only the stay-cable fan properties and configuration of the crossties were varied.

4.4.1.1 Displacements at the middle of stay-cable 1 (point A)

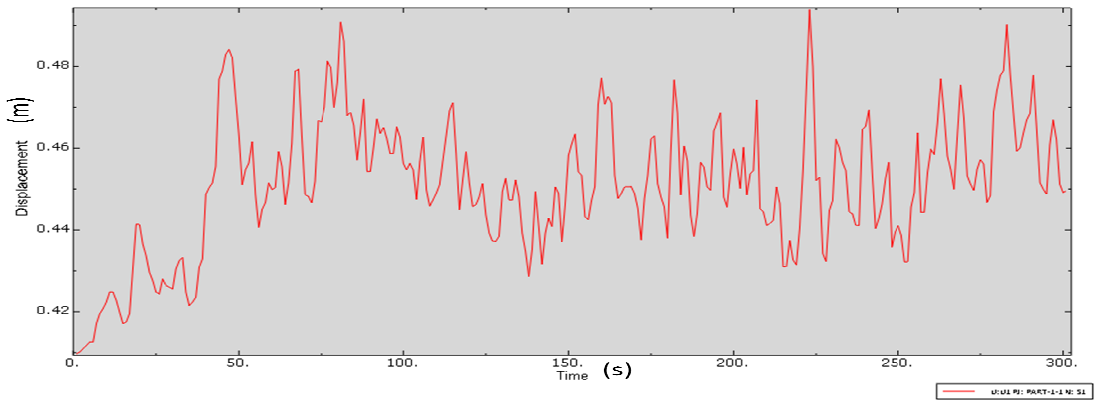

Figure 4-33: Displacements of point A with no crosstie (uniform property cable)

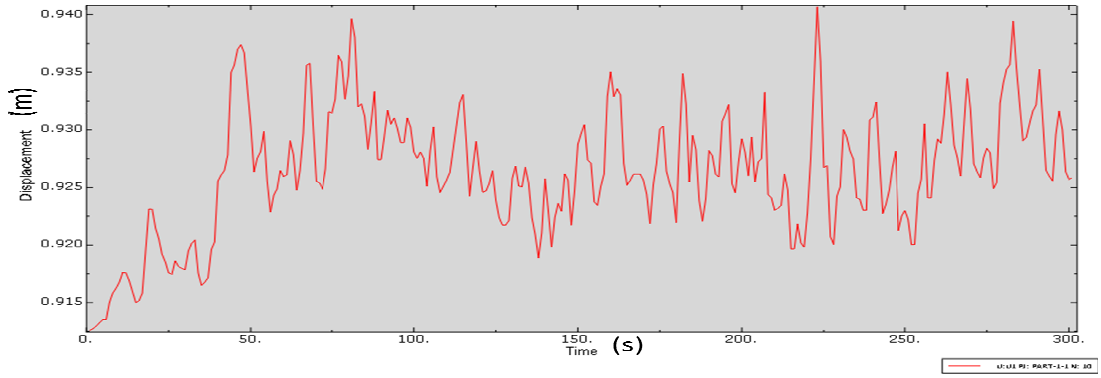

Figure 4-34: Displacements of point A with 1 crosstie (uniform property cable)

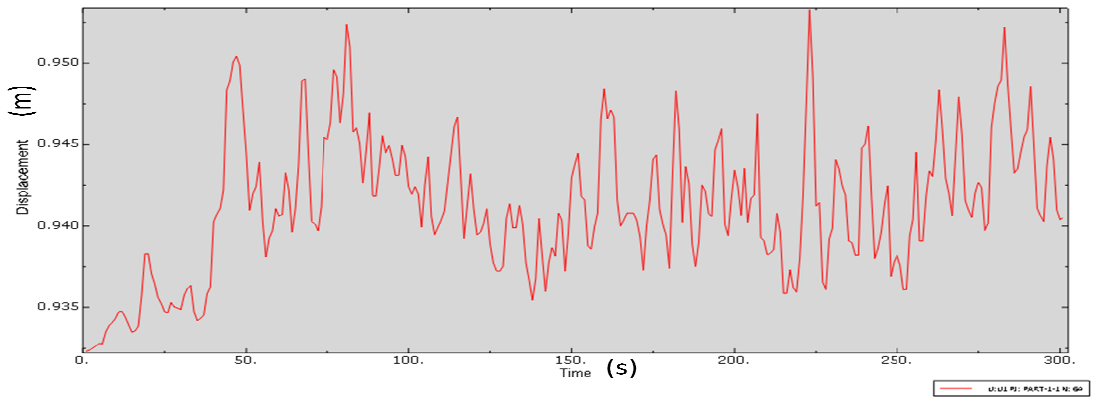

Figure 4-35: Displacements of point A with 2 crossties (uniform property cable)

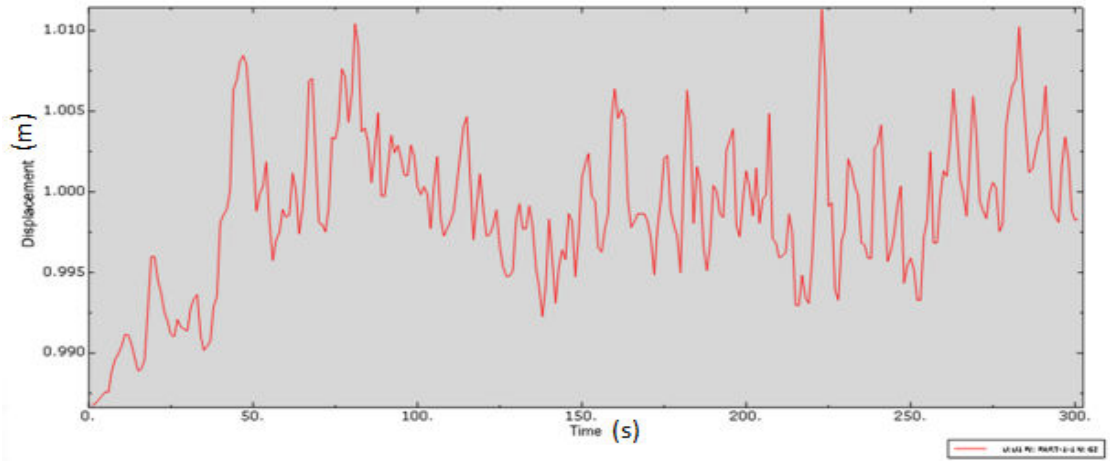

Figure 4-36: Displacements of point A with 4 crossties (uniform property cable)

Among the cases of the cable with one uniform property, as shown in Figures 4-33 to Figure 4-36, it can been noticed that the displacements of the point A at the middle of stay-cable 1 have not been reduced in the presence of the crossties; the displacements have been observed to increase as the number of the crossties increases.

The maximum displacement of the case without crossties is 0.49 m, while the maximum displacement of the case with four crossties is 1.01 m.

Despite the fact that the magnitude of the displacements increased with the crossties, the rate of change in the response has been slowed down by the crossties constraints. The biggest difference between the displacements under the 300 sec wind loading of the point A on stay-cable 1 without crosstie is 0.08 m, while the biggest difference of the displacement of the case with four crossties under the same load is 0.02 m.

4.4.1.2 Displacements at the quarter of stay-cable 1 (point B)

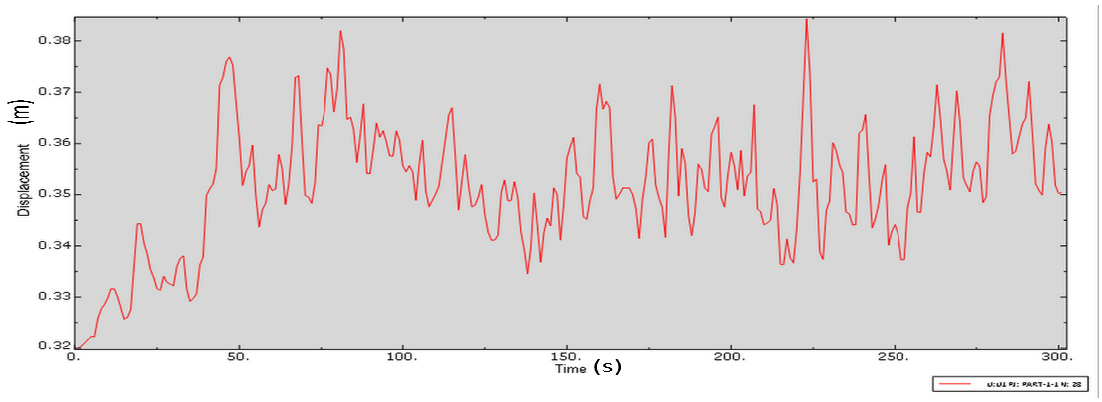

Figure 4-37: Displacements of point B with no crosstie (uniform property cable)

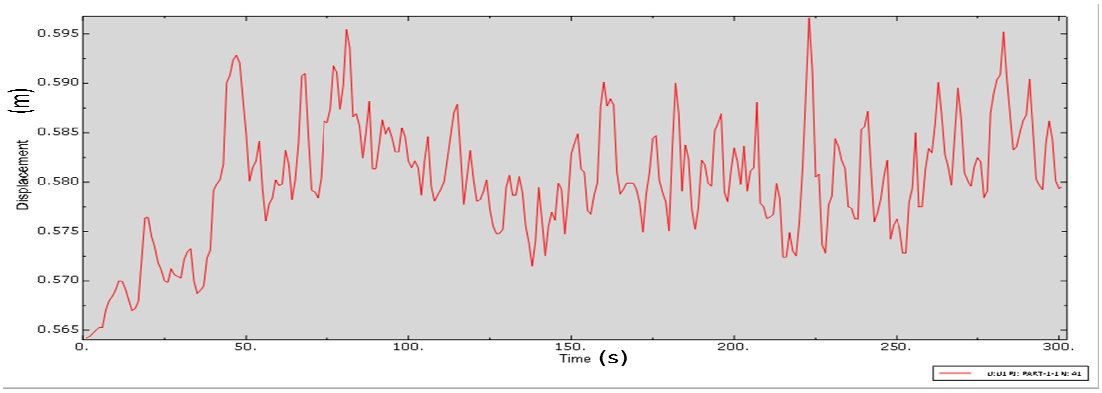

Figure 4-38: Displacements of point B with 1 crosstie (uniform property cable)

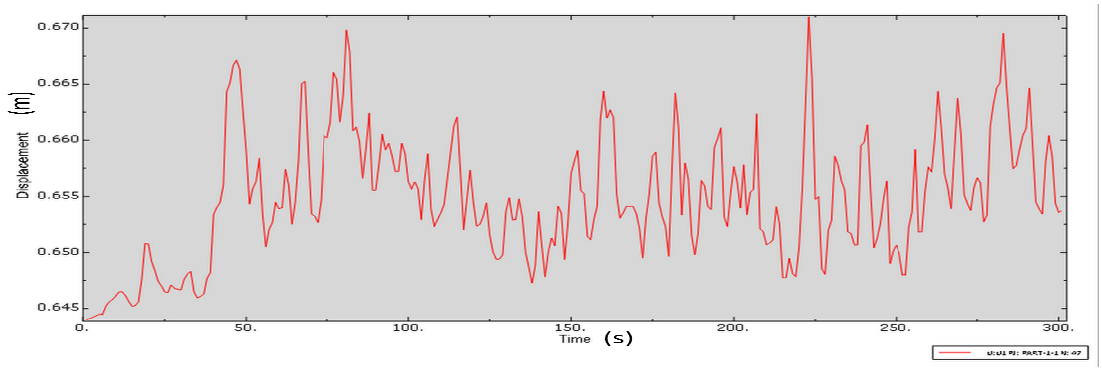

Figure 4-39: Displacements of point B with 2 crossties (uniform property cable)

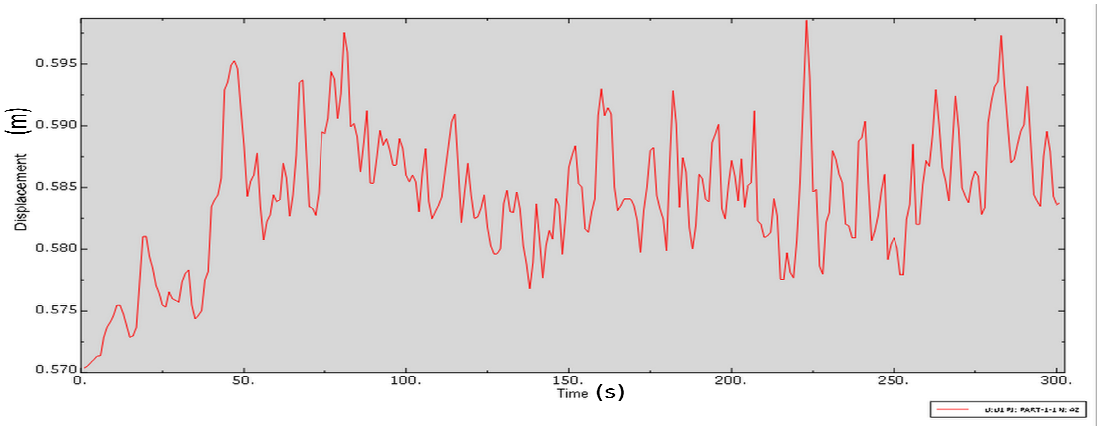

Figure 4-40: Displacements of point B with 4 crossties (uniform property cable)

As shown in Figure 4-37 to Figure 4-40, it can be noticed that the overall displacements are smaller than those registered for point A, at the midpoint of stay-cable 1. Similar to the point A results, the installation of the crossties increased the magnitude of the displacements, and the case of 2 crossties had the maximum displacement of 0.67 m among the four cases.

The displacement variation within the 300 sec wind loading interval was more stable when the additional crossties were considered.

4.4.1.3 Displacements at the middle of the fan on stay-cable 9 (point C)

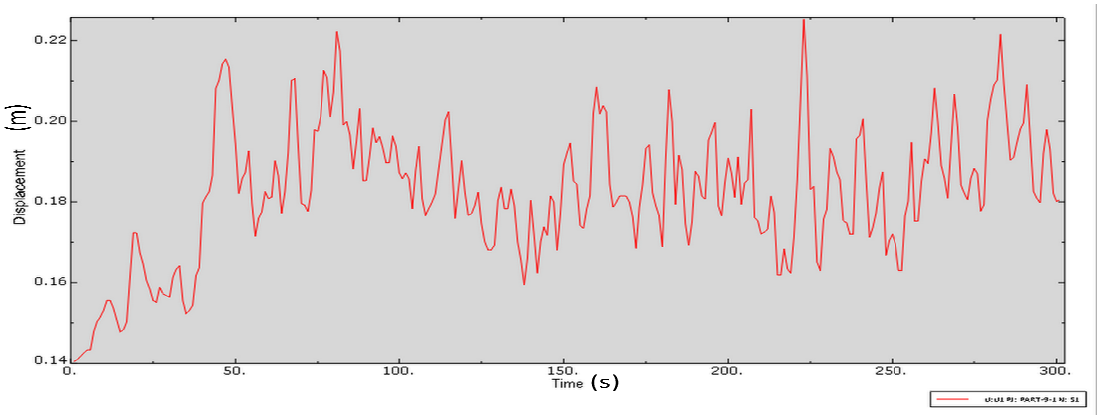

Figure 4-41: Displacements of point C with no crosstie (uniform property cable)

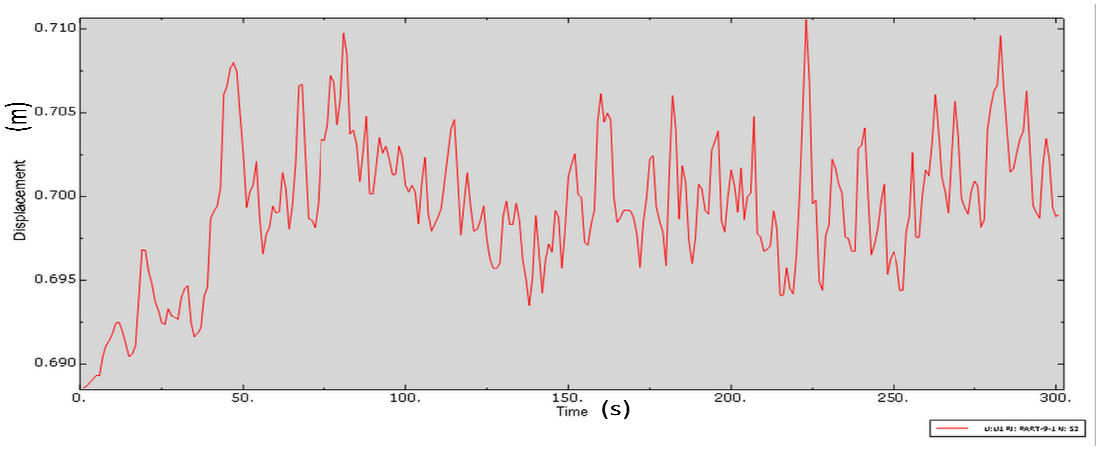

Figure 4-42: Displacements of point C with 1 crosstie (uniform property cable)

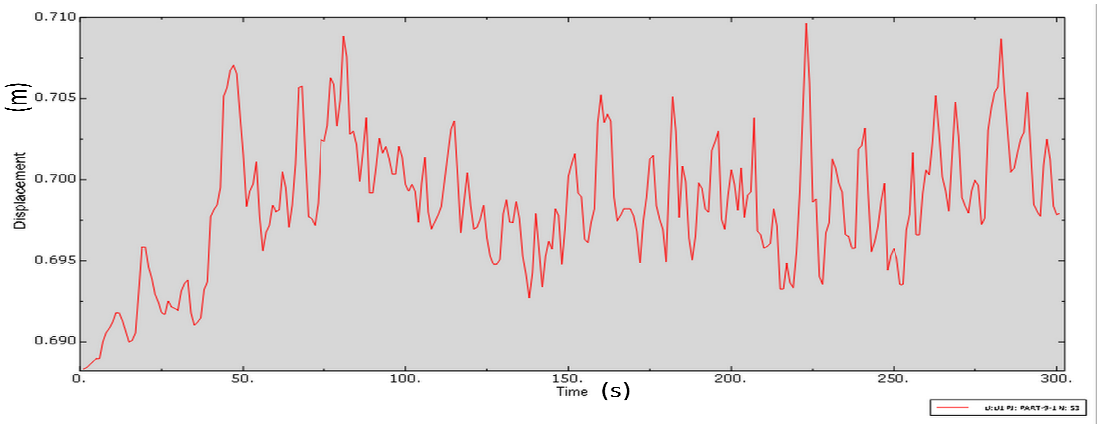

Figure 4-43: Displacements of point C with 2 crossties (uniform property cable)

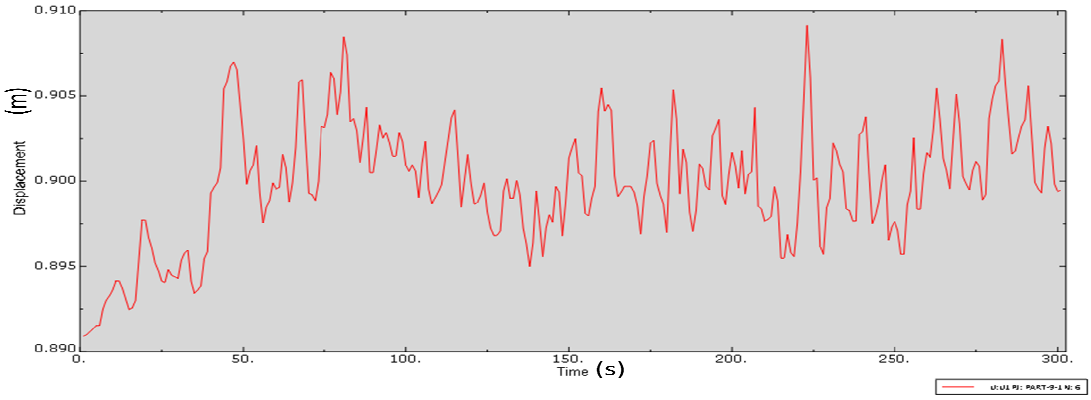

Figure 4-44: Displacements of point C with 4 crossties (uniform property cable)

As shown in Figure 4-41 to Figure 4-44, the displacements registered for the stay-cable 9, (point C)

located in the center of the fan, have a sharp growth after the addition of the crossties. The maximum displacement of the cable without crossties is 0.22 m, while the maximum displacement of the cable with four crossties is much higher, 0.91 m.

4.4.1.4 Displacements at the middle of stay-cable 16 (point D)

For the shortest cable of the stay-cables fan (cable 16), only one of the four crossties has effect on the cable displacement, since the other three crossties have no common points with the stay-cable 16; as a result, only two cases have been considered for analysis: without the crosstie and with four crossties (but actually only one on the stay-cable16 itself), as Figure 4-45 and Figure 4-46 show.

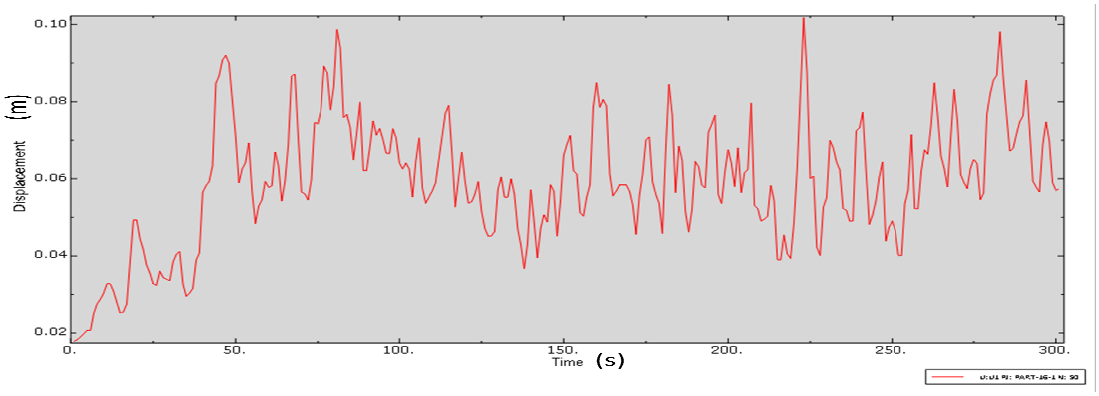

Figure 4-45: Displacements of point D with no crosstie (uniform property cable)

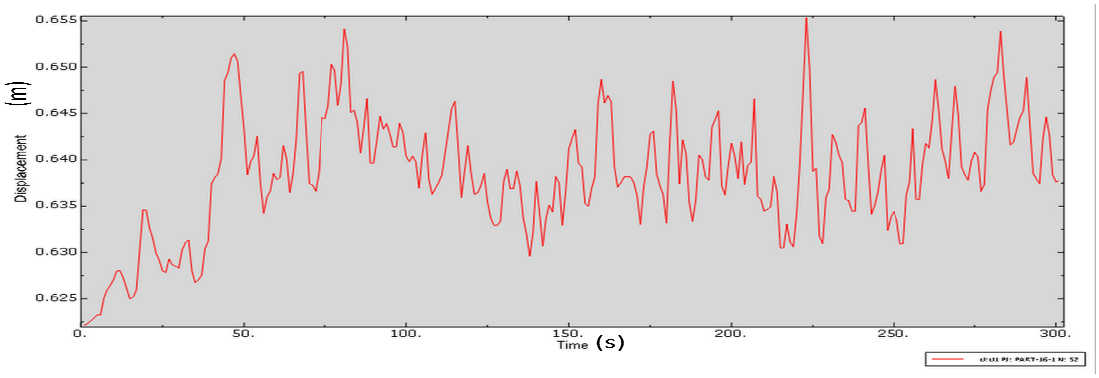

Figure 4-46: Displacements of point D with 4 crossties (uniform property cable)

Clearly, the results show that the case without crossties had smaller displacements of 0.1 m, when

compared with 0.655 m registered for the last case of four crossties.

Also, there is a decrease in the variation of the displacement with the installation of the additional crossties.

4.4.2 Results of the multiple-strand stay-cables fan with polymer grout

For the stay-cables fan with the grouted inner strands, it can be estimated that each strand within will have a different reaction during the 300 sec wind loading interval, due to the different conditions of the arrangements and the area surrounding grout, which is a very complicated parameter to measure and simulate.

To make a comparison of the displacement of the different strands inside the cable, two of the most extreme cases have been analyzed: one is on the middle strand, in the centre of the stay-cable (N1 Points = A1, B1, C1 and D1) and the other is on the strand located on the edge of the stay-cable (N2 Points = A2, B2, C2 and D2), as schematically shown in Figure 4-47.

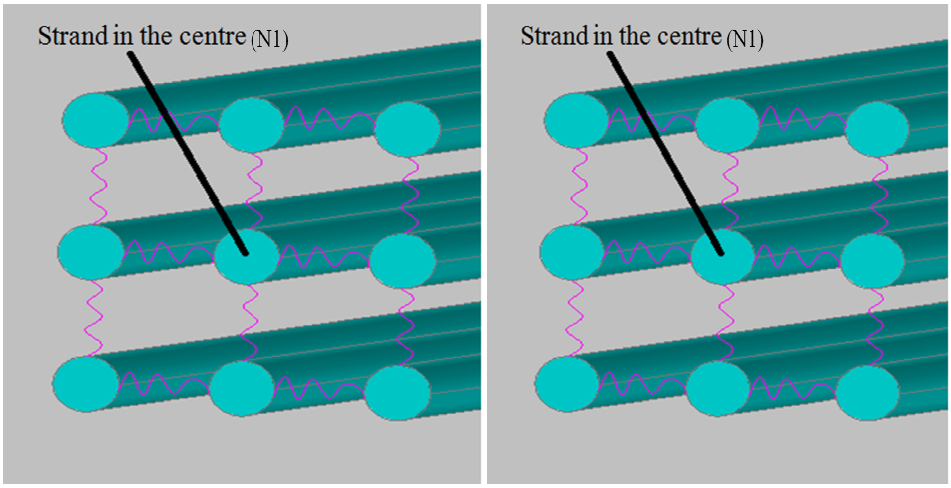

Figure 4-47: Selected inner strands of the stay-cables

Similar evolution was found for the stay-cables fan with one and two crossties; the figures of the wind loading response and of different points in stay-cables fan were detailed in Appendix F.

4.4.2.1 Displacements at the middle of stay-cable 1 (points A1 and A2)

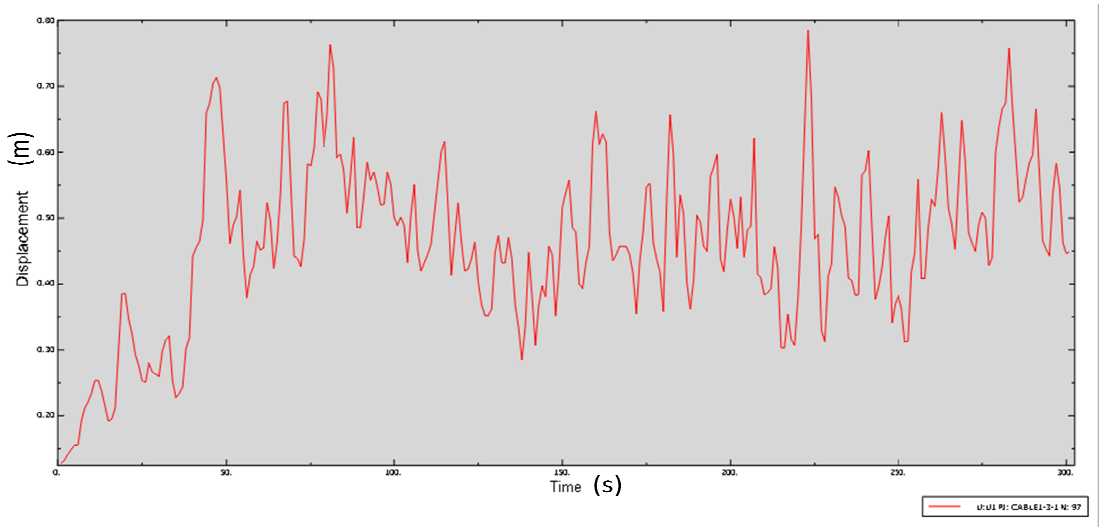

Figure 4-48: Displacements of centre strand without crosstie (point A1)

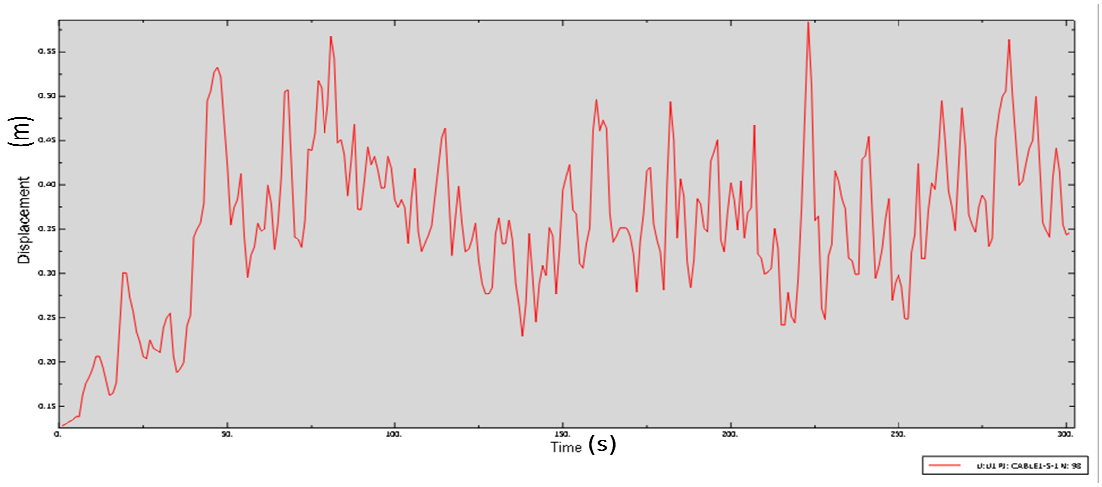

Figure 4-49: Displacements of side strand without crosstie (point A2)

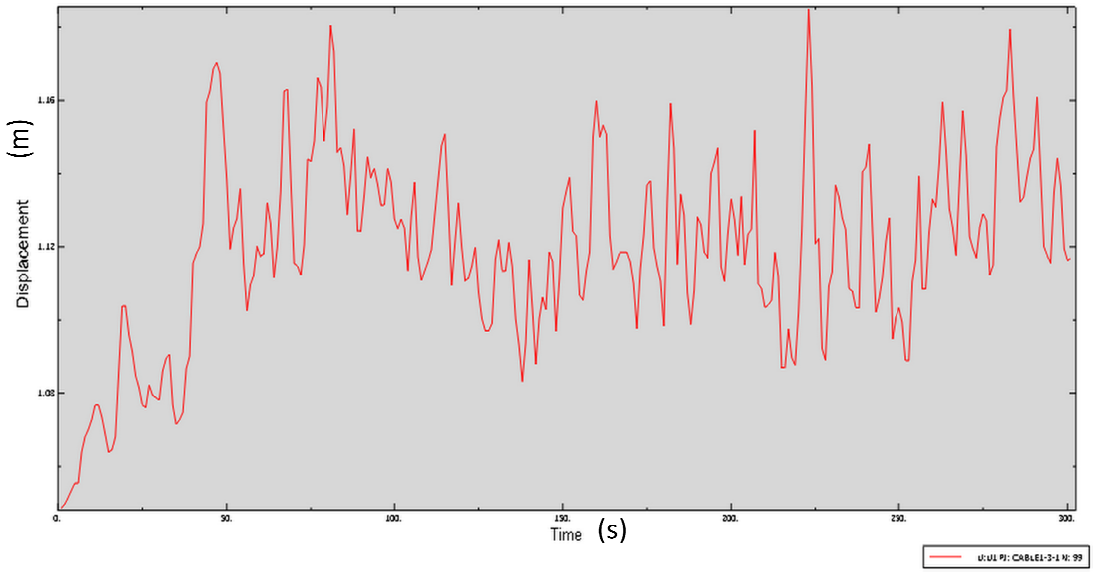

Figure 4-50: Displacements of centre strand with four crossties (point A1)

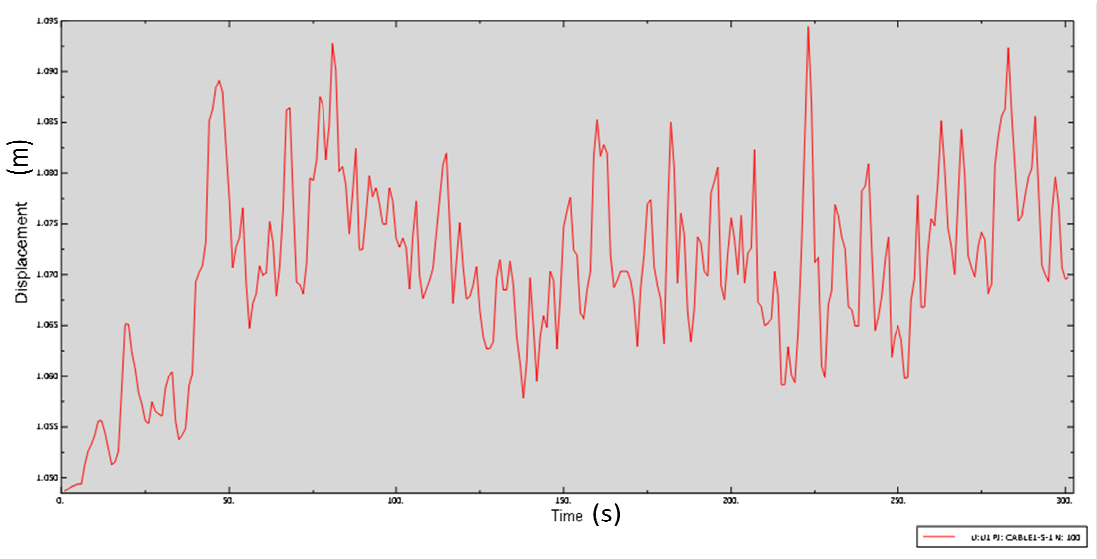

Figure 4-51: Displacements of side strand with four crossties (point A2)

Comparing Figure 4-48, Figure 4-49 with Figure 4-50, Figure 4-51, generally, it was noticed that the strand in the centre (point A1) has larger displacements than the strands on the edge (point A2). The recorded displacements showed an irregular variation with a different number of strands. It can be seen that the maximum displacement of the centre strand without crosstie is 0.8 m, while the maximum displacements of the centre strand with one, two and four crossties are 1.43 m, 1.15 m,

1.19 m, respectively. For the side strand, the maximum displacement without crosstie is 0.575 m, while the maximum displacements of the side strand with one, two and four crossties are 1.3 m, 1.06 m, 1.095 m, respectively.

4.4.2.2 Displacements at a quarter of cable 1 (points B1 and B2)

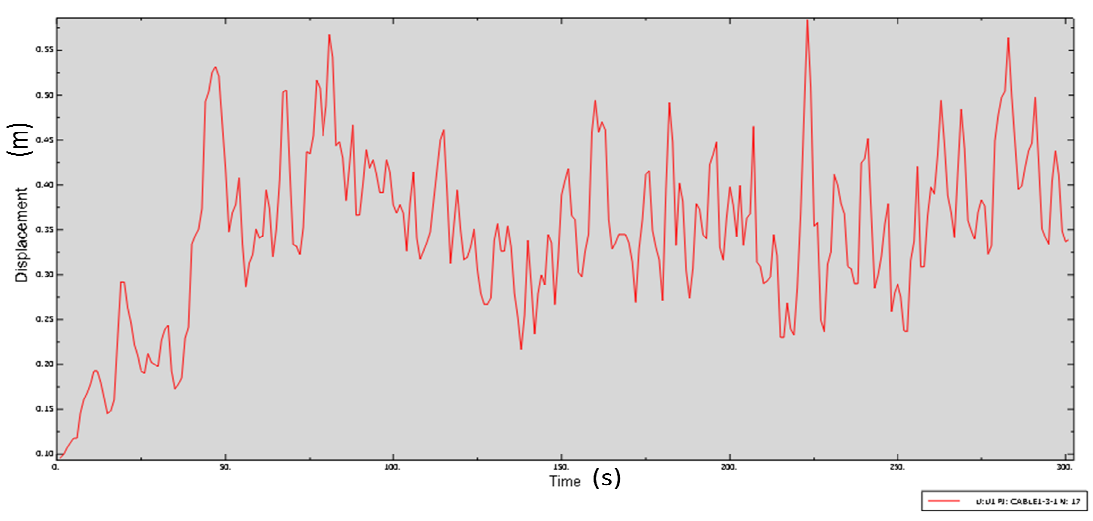

Figure 4-52: Displacements of centre strand without crosstie (B1)

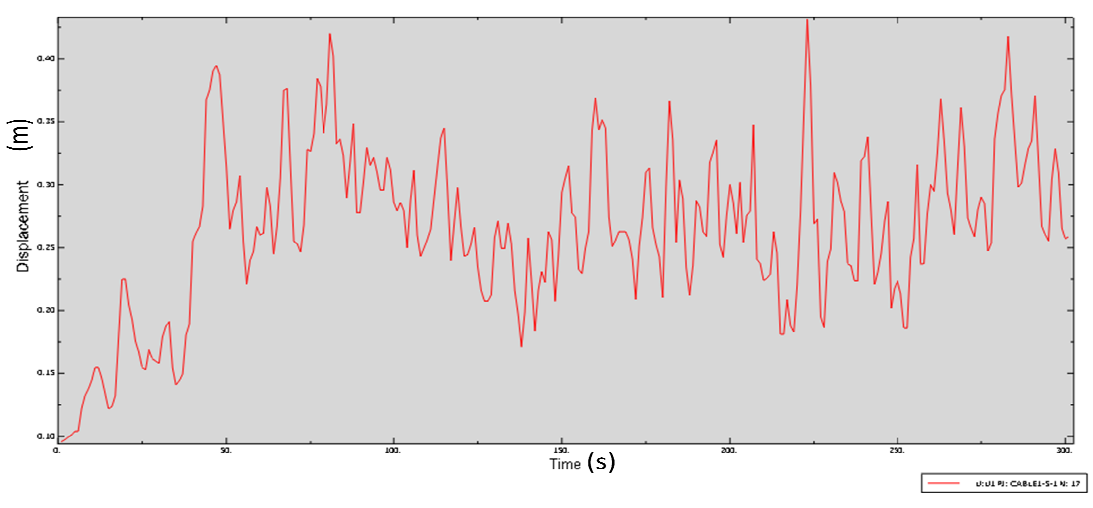

Figure 4-53: Displacements of side strand without crosstie (B2)

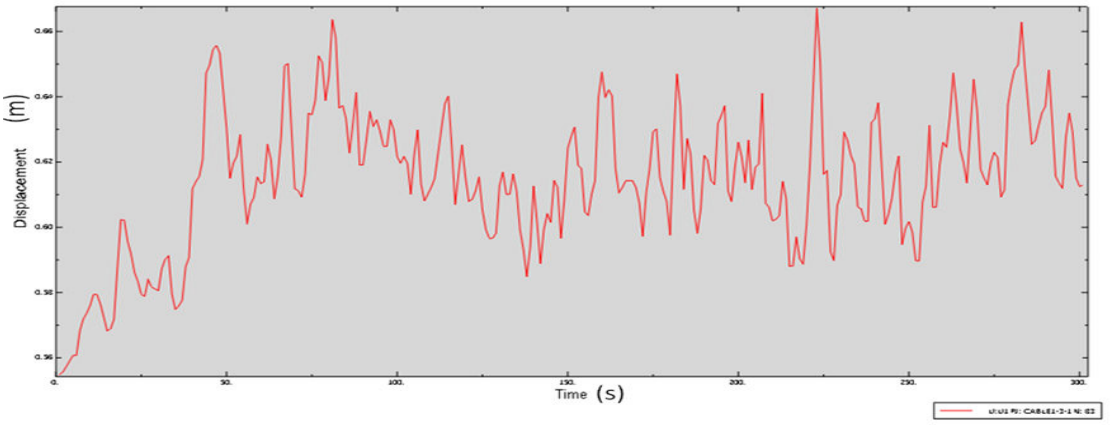

Figure 4-54: Displacements of centre strand with four crossties (B1)

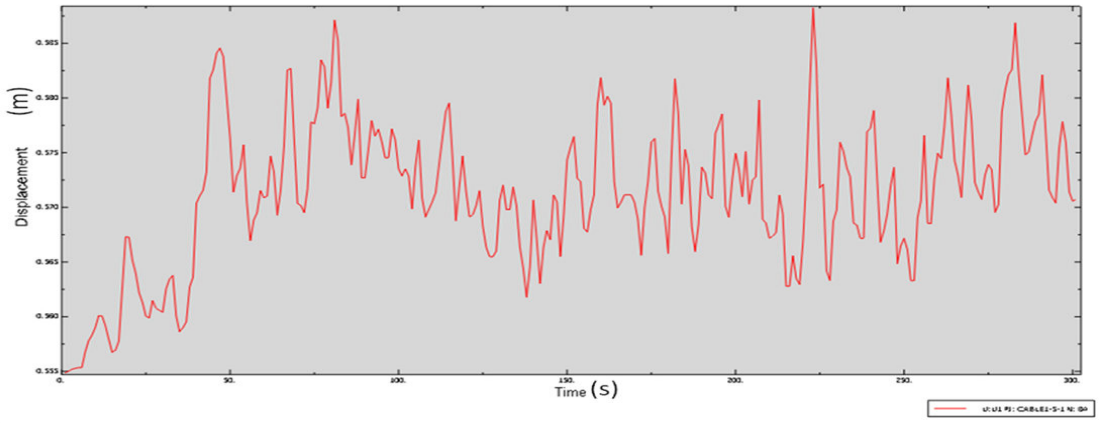

Figure 4-55: Displacements of side strand with four crossties (B2)

From Figure 4-52 to Figure 4-55, it can be seen that the displacements also show an irregular variation with the increase of the number of strands. The maximum displacement of the centre strand without the crosstie is 0.58 m, while the maximum displacements of the centre strand with one, two and four crossties are 1.15 m, 0.88 m, 0.67 m, respectively. For the edge strand, the maximum displacement without crosstie is 0.43 m, while the maximum displacements of the edge strand with one, two and four crossties is 1.025 m, 0.88 m, 0.5875 m, respectively.

4.4.2.3 Displacements at the middle of cable 9 (points C1 and C2))

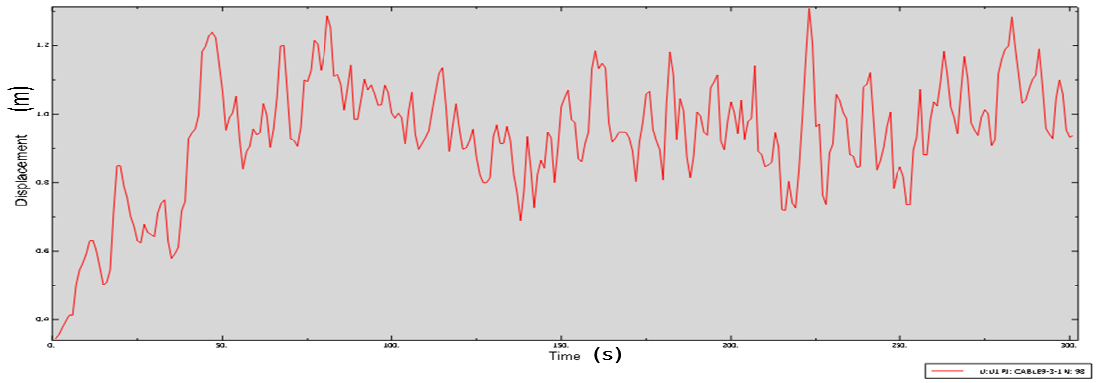

Figure 4-56: Displacements of centre strand without crosstie (C1)

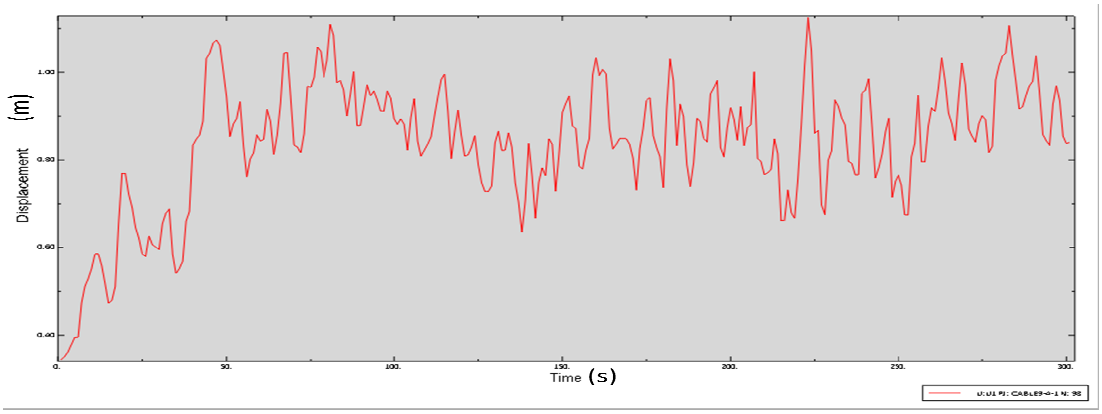

Figure 4-57: Displacements of side strand without crosstie (C2)

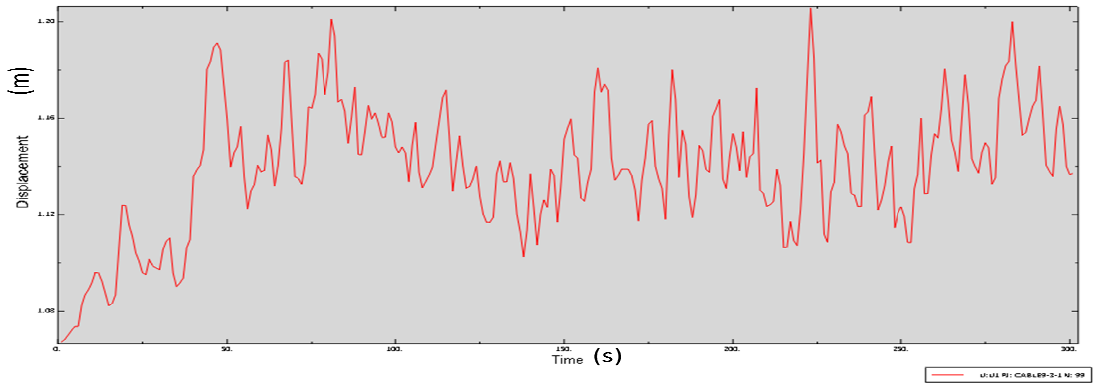

Figure 4-58: Displacements of centre strand with four crossties (C1)

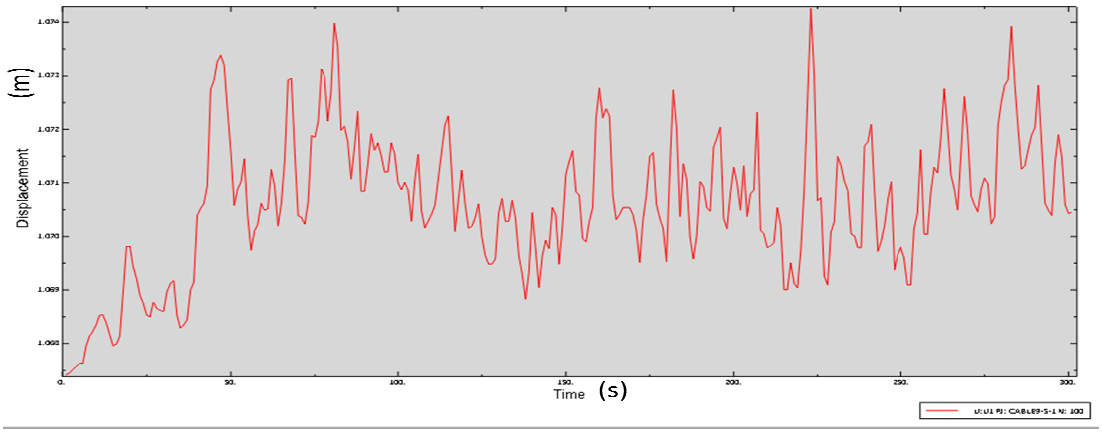

Figure 4-59: Displacements of side strand with four crossties (C2)

From Figure 4-56 to Figure 4-59, it can be seen that there is mitigation in the displacements after adding the crossties. The maximum displacement of the centre strand without crosstie is 1.3 m, while the maximum displacements of the centre strand with one, two and four crossties are 1.0 m, 1.01 m, 1.2 m, respectively. For the edge strand, the maximum displacement without the crosstie is 1.1 m, while the maximum displacements of the side strand with one, two and four crossties is 0.818 m, 0.92 m, 1.074 m, respectively. The case with 1 crosstie has the least displacement.

4.4.2.4 Displacements at the middle of cable 16 (points D1 and D2)

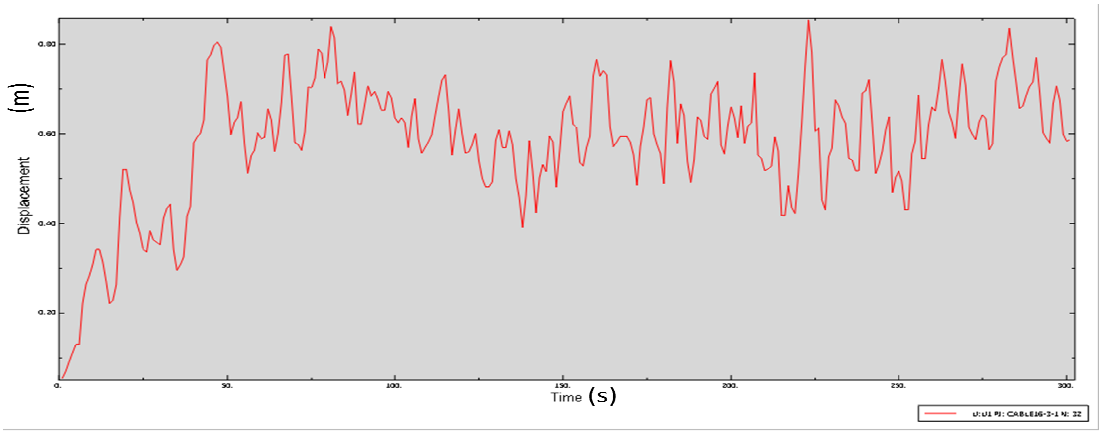

Figure 4-60: Displacements of centre strand without crosstie (D1)

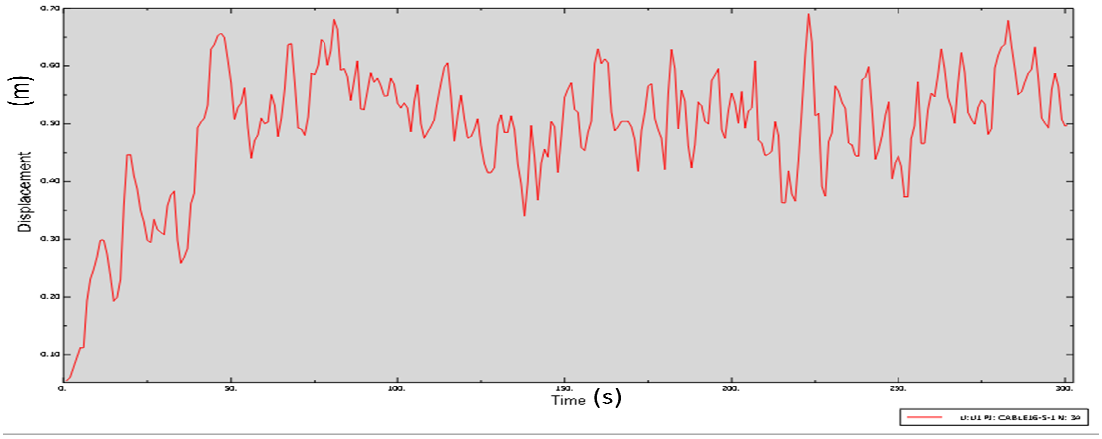

Figure 4-61: Displacements of side strand without crosstie (D2)

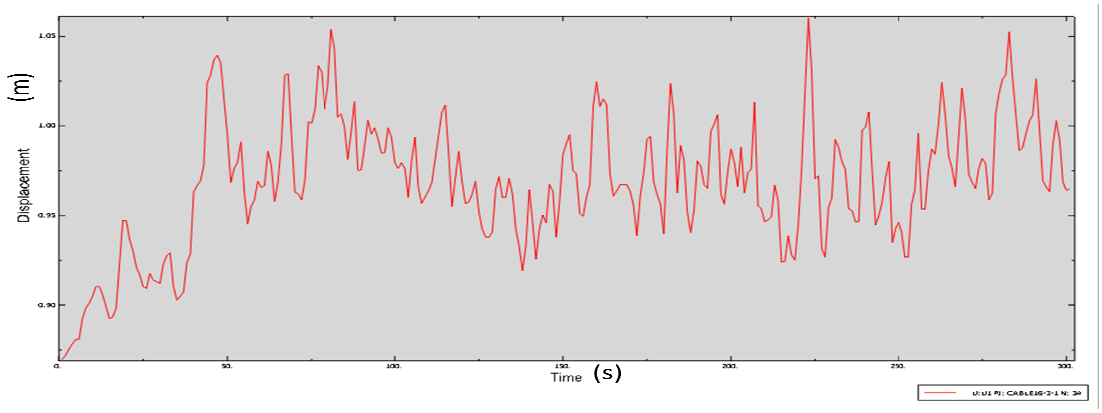

Figure 4-62: Displacements of centre strand with one crosstie (D1)

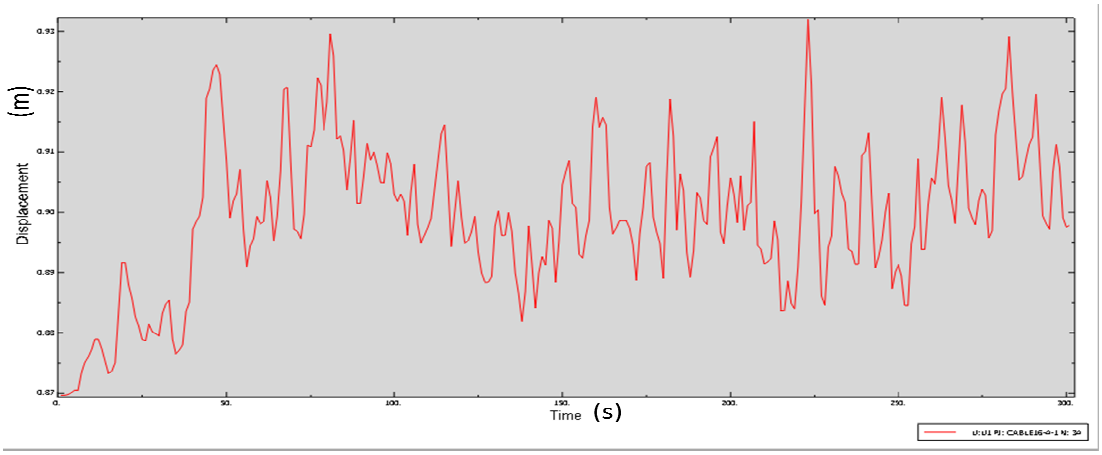

Figure 4-63: Displacements of side strand with one crosstie (D2)

From Figure 4-60 to Figure 4-63, it can be noticed that the displacements with the crossties are larger

than the displacements without the crossties. The maximum displacement of the centre strand without crossties is 0.85 m, while the maximum displacement of the centre strand with one crosstie is 1.06 m. For the edge strand, the maximum displacement without crosstie is 0.7 m, while the maximum displacement of the edge strand with one crosstie is 0.93 m.

For the stay-cables fan without grout, the wind loading response of the each strand inside the cable was the same. Identical evolution was also found for the case when the grouting material was modelled inside the stay-cables and for the case when no grouting material was used. The results of wind loading time-history analysis were detailed in Appendix F.

4.4.3 Results interpretation and discussions

The effectiveness of using one, two or four crossties for the grouted stay-cables fans of cabled stayed bridges, for mitigating the wind-induced displacements, has been partly verified in this chapter. To describe the effect of the crossties more directly, the displacement responses of the wind speed has been considered for all the investigated cases and the wind-induced of the inner strands and of the stay-cables have been compared.

For the middle of the stay-cables fan, on cable 9 (point C) the response with several crossties were considered under the wind speed ranging from 0 m/s to 30 m/s, which has been applied on the stay-cables fan for an interval of time of 300 sec. Each wind speed corresponds to a specific displacement during this time interval, which has been reorganized in terms of the ascending order of the wind speed.

Figure 4-64 to Figure 4-66 show the displacement responses at points C, C1 and C2 for the cases of no crosstie, one, two and four crossties obtained from the three different stay-cables models: no strands stay-cables (uniform property), multiple strands stay-cable without grout and multiple strands

stay-cables with grout.

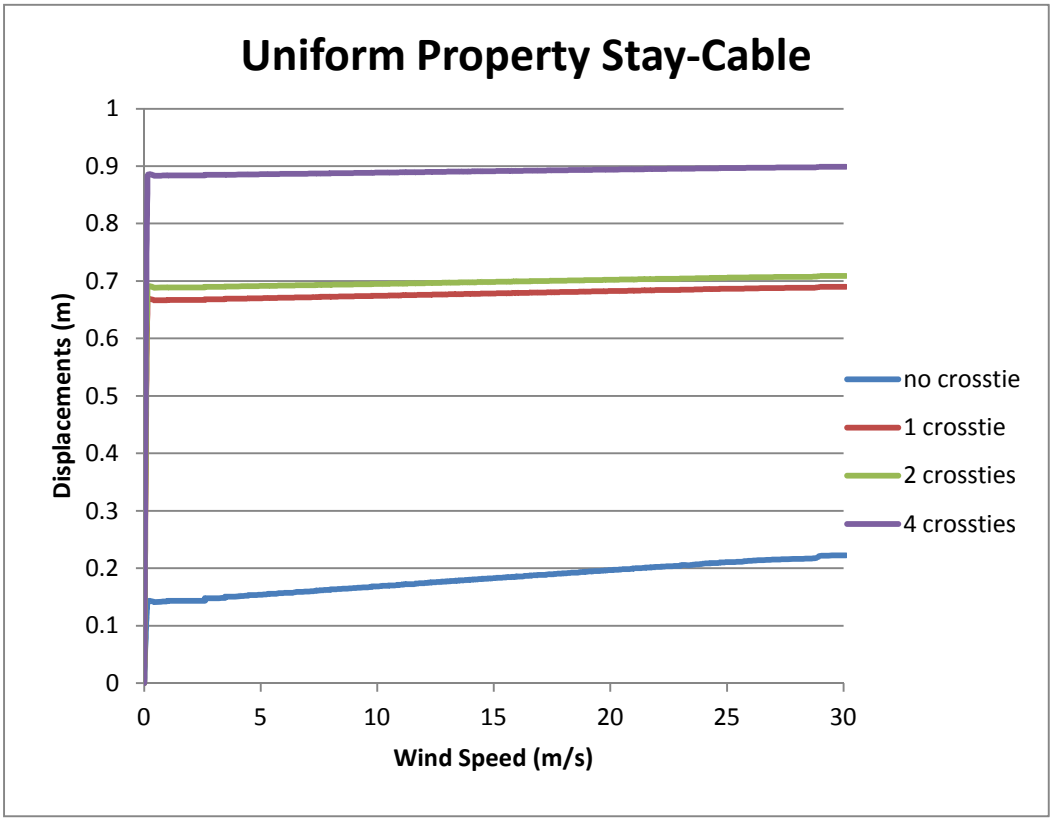

Figure 4-64: Displacements of uniform property cable 9 (point C)

When the stay-cables are modelled as a beam element, with uniform properties and ignoring the internal grout-strand composition, the wind-induced displacements do not increase very much with the increase of the wind speed, for the point C situated in the middle of the stay-cables fan on cable 9. Also, was noticed that the no-crossties stay-cables fan registered the smallest displacement of 0.15 m to 0.22 m for wind speeds of 5 m/s to 30 m/s, while for the four crossties the displacements were much higher in the range of 0.88 m to 0.91 m for the same wind speeds. This result is unexpected because the installation of crossties is supposed to mitigate the stay-cables vibrations and to limit displacements they register under the wind action.

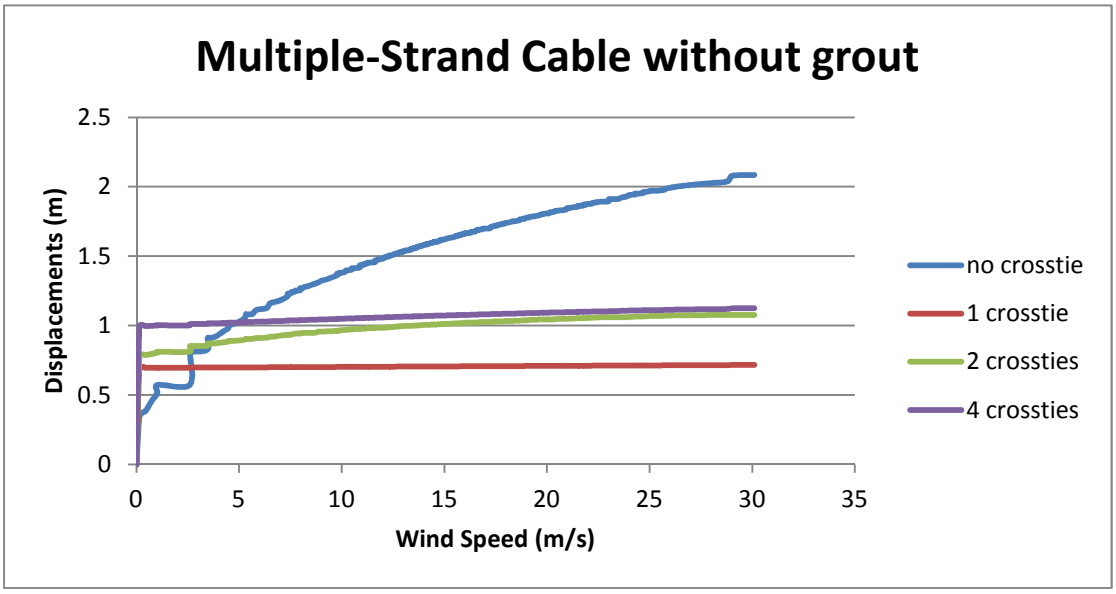

Figure 4-65: Displacements of multiple strands stay-cable 9 without grout

When the multiple strands model of the stay-cable 9 was employed (Figure 4-65) the displacements for the no-crossties fan were slightly higher, of about 0.5 m, for the small wind speeds, but increased drastically for the higher wind speeds reaching a maximum value of 2.15 m at 30 m/s. for the one and two crossties fan, the displacement was between 0.7 m and 0.8 m increasing more for the two crossties fan for 30 m/s registering 1.15 m displacement. The most constant, but slow increase was noticed for the displacements of the point C in the middle of the fan, for the four crossties, from 0.97 m at low wind speeds until 1.2 m at 30 m/s.

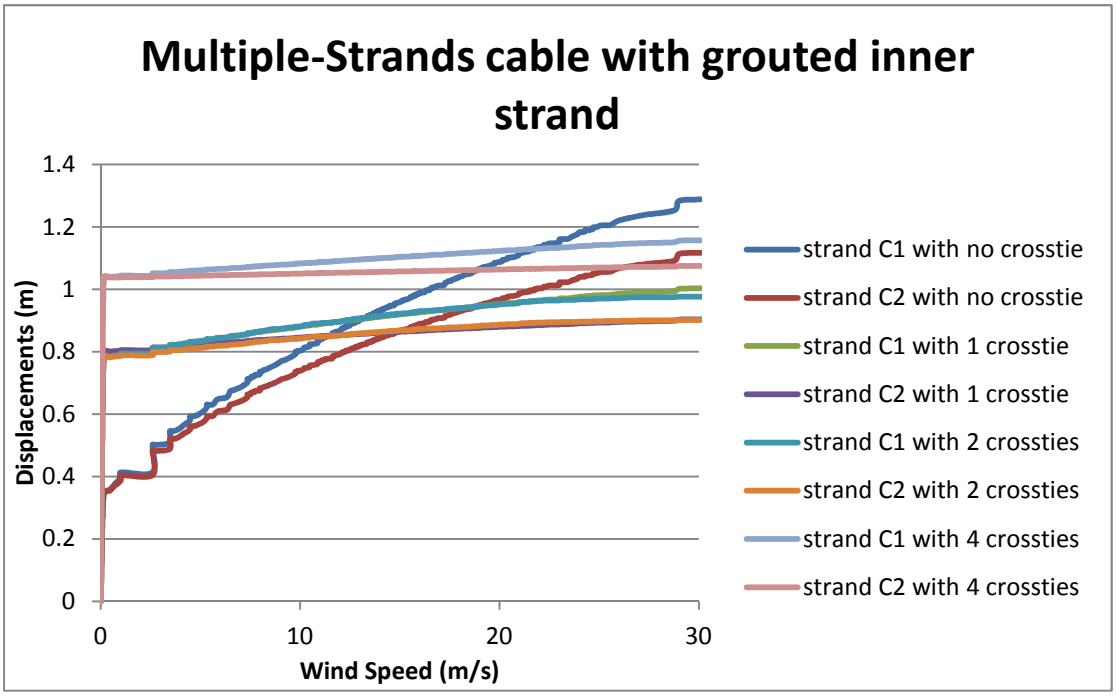

Figure 4-66: Displacement of multiple strands stay-cable 9 with grout inside

When multiple strands and the grout material were modelled for the inside of the stay-cables, it was observed that there are significant differences between the displacements of the inner strands situated in the center and at the edge of the stay-cable (Figure 4-66). The general trend of a sudden increase of the displacement for the no-crossties stay-cables fan with multiple strands with grouted inner strands was similar to the case of the no-crossties stay-cables fan with multiple strands without grout; however the displacements were slightly smaller, for the high wind speeds, 1.3 m for 30 m/s wind speed. For the fan with the four crossties, figures 4-65 and 4-66 showed the same trend of slow increase of displacements with the increase of the wind speed, the displacements of the two cases are close, 1.1 m for 30 m/s wind speed.

Therefore from the above structural response of the stay-cables fan of different composition and different crossties arrangement, it can be concluded that:

a) Generally, the crossties always has the mitigation effect on the wind-induced displacement, and this is clearly seen for the case of the multiple strands stay-cable fan with and without the grout material inside; the magnitudes of the displacement were more stable after adding the crossties, which is applicable for other investigated locations (points A, B and D) in the stay-cable fan.

b) Despite the magnitude of the maximum displacement, the crossties always had the effect of stabilizing the variation of the displacements under the wind loading. As the number of crossties increases, the rate of change of the displacements becomes gradually smaller.

c) Among the three different types of models investigated, the no-strand (uniform property) stay-cable had the lowest displacements, while the multiple-strand cable without the grout inside had the largest displacements for wind speeds up to 30 m/s.

d) For the multiple strands stay-cables with grout inside, the centre inner strand always has larger displacement than the side strand, under the wind loading. Only for the midpoint of the stay-cable 9 (point C), the crosstie has the mitigation effect on the magnitude of the displacements, where the case of one crosstie fan has the smallest displacements.

e) For the multiple strands stay-cables without grout inside, the cases of two, four and one crossties, have the smallest displacements for the midpoint of cable 1 (point A), the quarter of cable 1 (point B), the centre of the fan on cable 9 (point C) and the midpoint of the cable 16 (point D), respectively.

f) For the no-strand (uniform property) cable, adding the crossties always increased the displacements under the wind load, for all the investigated location along the stay-cables of the fan.

4.4.4 Comparison of the FE stay-cable model of Bill Emerson Memorial Bridge with FHWA

in the study performed by Park and Bosch [9], finite element simulations were carried out on the stay

cable systems of Bill Emerson Memorial cable-stayed bridge under realistic wind forces in order to develop technical recommendations that may be incorporated into design guidelines. The project mainly focused on the effectiveness of cable crossties, external dampers, and the combined use of crossties and dampers.

The amplitude of 300sec wind load applied on the bridge was the same as the current study. The middle point of the cable 9 (point C) has been used for comparison. Figure 4-67 show the displacements of point C from the FE model of FHWA [9]:

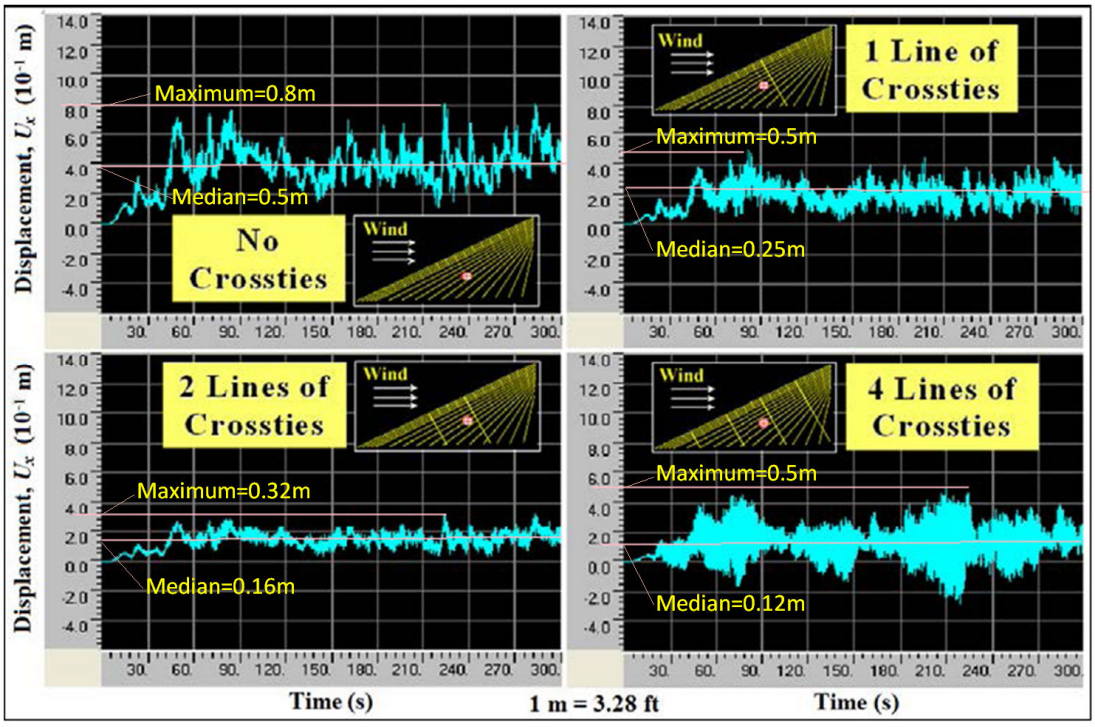

Figure 4-67: Displacements at point C from FHWA [9]

It can be seen that the evolution of the displacement under the 300s wind load is similar to the FE results of the current study. The median displacement of the point C was 0.4 m, 0.25 m, 0.16 m, 0.12 m for the no-crosstie, one-crosstie, two-crossties, four-crossties stay-cables fan respectively. Referred from Figure 4-41 to Figure 4-44, Figure 4-56, Figure-4-58 and Appendix F, the median

displacements of point c with no crosstie, one crosstie, two crossties, four crossties could be obtained respectively.

Table 4-11 Show a comparison of the results from FHWA and the uniform property cable, multiple-strand cable without grout, multiple-strand cable with grout in the current study:

Table 4-11: Comparison of displacement at the middle of the cable 9 (point C)

Number of crossties	Median displacement in 300sec (m)			
	FE Results from FHWA	Uniform Property cable	Multiple-strand cable without grout	Multiple-strand cable with grout (centre strand)
No crosstie	0.4	0.11	1.055	0.65
1 crosstie	0.25	0.345	0.51	0.5
2 crossties	0.16	0.355	0.545	0.5
4 crossties	0.12	0.45	0.565	0.58

It could be seen that FE results from FHWA has verified the effectiveness of the crosstie, where the displacements decreases as the increasing number of crossties added. For the uniform property cable, adding the crosstie has enhanced displacements of the cable; such differences may arise from the influences of dampers and different models of wind loading in the modelling. For the multiple-strand cable, the mitigation effect has been partly verified. Among the above comparison multiple-strand cable without grout has the largest displacements.

4.4.5 Comparison of the FE stay-cable model with other existing bridge

Based on the Oshima Bridge in Japan, the response characteristics of the local vibrations in the stay cables under wind gusts are described using a numerical analysis [74].

The maximum displacement of cable C12 is approximately 0.25 m, while that of cable C19 is approximately 0.3 m.

Considering the incline of cable C12 and C19, the results of cable 1 and cable 9 of Bill Emerson Memorial Bridge have been chosen, which have the most similar inclines as the above cables. The results are shown in Figure 4-104 and Figure 105:

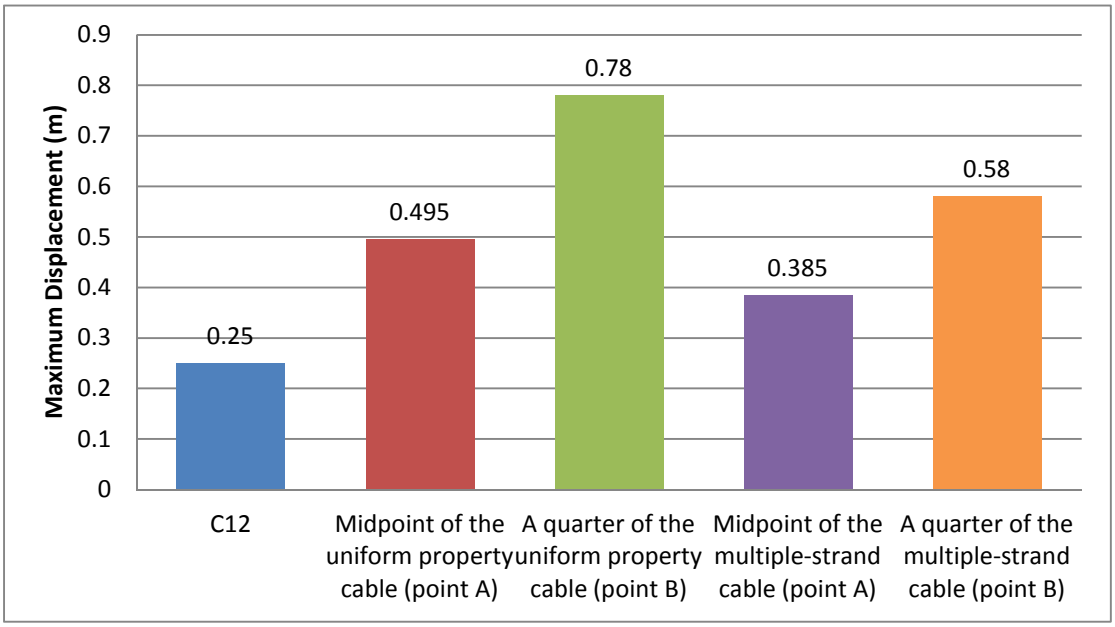

Figure 4-68: Comparison of the maximum displacement of cable 1

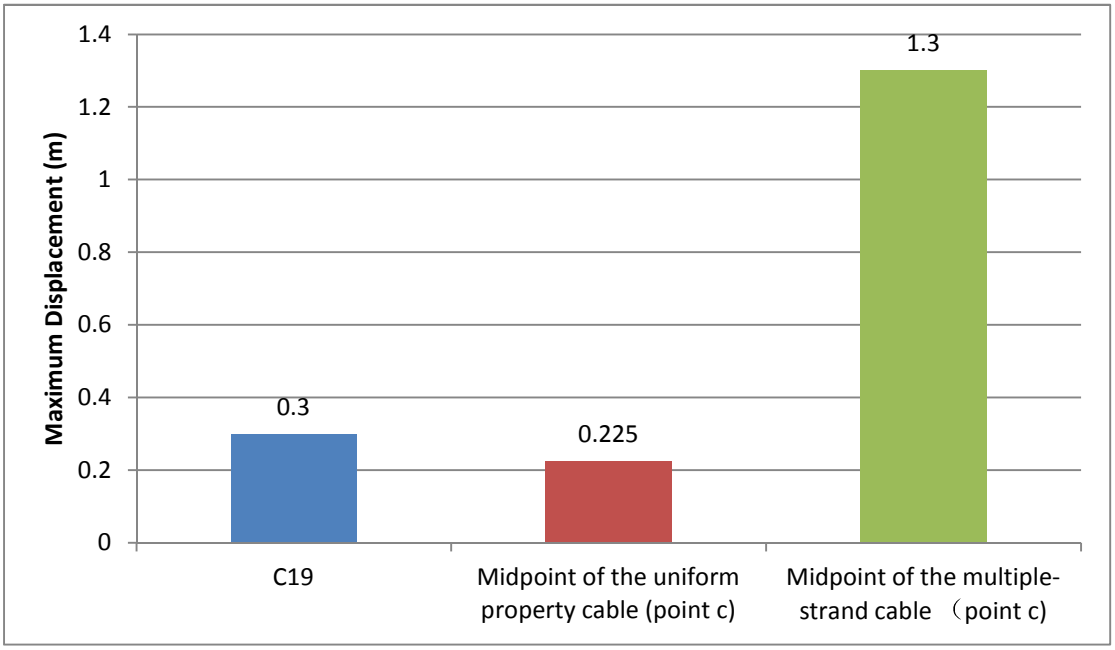

Figure 4-69: Comparison of the maximum displacement of cable 9

However, the results of the finite element analysis do not agree well with the numerical results of the above paper.

The existence of cable damping and dampers might be among the reasons, which has been ignored in this analysis. Cable damping is mainly associated with energy dissipation caused by material strain. Normally, damping increases with vibration amplitude [83].

Chapter 5 Conclusions

The existing literature on stay cables is mainly focused on the dynamic characteristics of a single cable modelled as one uniform property. In the current study, a multiple-strand cable has been modelled, which also contains the effect of the grout. In reality, the geometry of a cable, especially a stranded cable, is complicated; therefore, it was determined to build up the cable similar to the initial configuration of the cable in the manufacturing process. Each strand is placed in an approximate position, which is parallel in the same direction and has the same length. Major differences of the dynamic response between the uniform property cable and multiple-strand cable are caused by the interaction of each strand and the grout inside.

The analysis of the cable was completed using the finite element method; the cable has been modelled in three types: uniform property cable, multiple-strand cable without the grout and multiple-strand cable with the grouted inner strands. Both modal analysis and wind load time-history analysis have been conducted to obtain a comprehensive behaviour analysis of the stay cables on Bill Emerson Memorial Bridge. The mitigation effectiveness of the crosstie has also been investigated through the current study.

According to modal analysis, it can be concluded that:

1) The number of strands has no impact on the magnitude of the frequencies of the cable. For more strands inside the cable, natural frequencies of each strand remain the same; the mode frequencies of the multiple-strand cable without the grout consist of the frequencies of individual strands alone.

2) The equivalent stiffness k of the grout increases the natural frequencies of the cable. As the number of strands increases, the influence becomes larger and larger. Also, the natural frequencies

increase with the magnitude of k. For higher modes, the influence of k tends to reduce.

3) The natural frequencies increase significantly in the presence of the crossties, which mean that the cables are more difficult to excite, thus have less displacements under external loads. The more crossties added in the cable network, the higher the natural frequencies.

4) The frequency of the single element cable that is modelled as one uniform property (cement grout cable) has the largest natural frequencies, while the multiple-strand cable without the grout has the smallest frequencies.

5) For the multiple-strand cable, global in-plane modes have not been observed in relatively low modes, which might appear in the higher modes. For out-of-plane modes it shows a mixture of global modes and local modes in the relatively lower modes. Overall, there are more out-of-plane modes than in-plane modes.

6) As more numbers of crossties are added in, the mode shapes of the cable network become complicated and unstable.

In terms of the time-history displacements under the real wind load, the behaviour of the cable network could be further concluded as follows:

1) Among the three different types of models, the uniform property cable has the least displacements, while the multiple-strand cable without the grout inside has the results of largest displacements.

2) The crosstie always has the mitigation effect on the case of the multiple-strand without grout inside, in accordance with the magnitude of the displacements; for the multiple-strand cable with the grout inside, only in the midpoint of cable 9, the crosstie has the mitigation effect on the displacements; for the uniform property cable, adding the crossties always increases the

displacements under the wind load.

3) The crosstie always has the effect of slowing down the rate of change in the displacements under the wind load. As the number of crossties increases, the rate of change in displacements becomes smaller and smaller.

Future work

While the current study has demonstrated the dynamic properties of the multiple strands stay-cables, there are several lines of research arising from this work that could be pursued:

1) The simulation of the strands within the stay-cable is simplified from the inner configuration of the stay cable. For the most commonly used stay-cables, they are made of circular strands arranged in several layers; as a result, the modelling of the multiple-strand cable is very complicated, which includes the complex positions of the strands and the connections between them. In this study, all the strands were assumed to be parallel, and no constraint has been modelled between the strands, in this regard. Besides, sheathing membrane covering the cable exists for the practical engineering technology of the stay-cables, which is the outer enclosure for the strands to provide rigidity and/or confinement for the corrosion protection system, such as steel pipe and high-density polyethylene (PE) pipe [14]. Differences will arise in the vibrations of the stay cables after the installation of the protecting membrane, whose mode shapes might be more uniform, unlike the multiple-strand cable without the sheathing in this study whose mode shapes of the cable could be various large deformations in different directions of different strands. Generally, more accurate simulation in the strands could be explored in the future, thus the cable model is closer to the real configuration from the manufactured stay-cables.

2) The increase of the frequency has been observed in this study after adding the grout material,

mainly due to the constraints of the motion of the inner strands, while the modelling of the grout is massless. More physical properties of the grout could be considered, like the density of the grout, which could have a considerable impact on the frequency of the stay-cable. Moreover, additional kinds of grout could be simulated to have a comprehensive evaluation of the behaviour of the stay-cables at present.

3) In terms of the wind loading, more detailed information of the structural and aerodynamic conditions of the stay-cables and the wind could be taken into account, as chapter 3.4.5 explains. In addition to the drag force, pressure from other sources should also be factored into the wind load. Different attack angles of the wind load should be implemented for future exploration of the dynamic response of the multiple strands stay- cable.

4) Although the results presented here have partly demonstrated the effectiveness of the crosstie as the mitigation measure for high displacements induced by wind loading, some problems may arise in the meantime. Decreasing the displacements of the stay-cables is always observed only in the multiple strands cables without the grout; possible reasons are due to the relatively inaccurate modelling of the cables and crossties connections and boundary conditions. Perhaps by simulating more pretension scenarios and other conditions of the material property, more accurate results can be obtained. Furthermore, mitigation effectiveness of more numbers of crossties in the cable network could be investigated in future research.

5) As the anchor end of the stay cable is connected to the tower and the main girder, the coupled vibration between the cable and the tower will occur under the external load, known as parametric vibration. In current study, only the cable has been modelled,, while in reality the dynamic properties of the stay-cables should be related to the deck and the tower. Thus, complete bridge structures including the stay-cables and other supporting structural components could be modelled for more accurate research.

References

[1]Yuanpei Lin, Cable-stayed Bridge [M]. Beijing: *China communication press*, 1997.
[2] Zenghong Jin, Introduction to Normandy Bridge in France [J].*Highway overseas*, 1996, 14(4).
[3] Zenghong Jin, Introduction to Tatara Bridge in Japan [J], *Highway overseas*, 1999, 17(4): 8-13.
[4] Haifan Xiang, Research on the wind engineering of bridge in 21st century, The 10th national conference on structural wind engineering[C], 2001.11.5-10，Guilin, China.
[5] Haifan Xiang, Cable system and its vibration control on cable-stayed bridge [J].*OVM communication*.2001, (2).3-8.
[6]S.L Liu, Z.T Liang, J.L Hou, F.C Meng, Cable-stayed Bridge [M], *China communication press*, 2002.
[7] Haifan Xiang, Developing prospect on cable-stayed bridge in china[J].*Traffic engineering science and technology*, 1999.2: 35-39.
[8] Yanshu Ren, *Research on the parametric vibration of stayed cables* [D].Shanghai, Tongji University, 2007.
[9] Sunwoo Park and Harold R. Bosch, Mitigation of Wind-Induced Vibration of Stay Cables: Numerical Simulations and Evaluations, FHWA-HRT-14-049, 2014.
[10] G. Chen, D. Yan, W. Wang, M. Zheng, L. Ge, and F. Liu, *Assessment of the Bill Emerson Memorial Cable-stayed Bridge Based on Seismic Instrumental Data*, Report of University of Missouri-Rolla, OR08-003, Sep 2012.
[11] Daegi Hahm, Seung-Yong Ok, Wonsuk Park, Hyun-Moo Koh, Kwan-Soon Park, Cost-Effectiveness Evaluation of an MR Damper System based on a Life-Cycle Cost Concept, *KSCE Journal of Civil Engineering*, Vol 17(1), 145-154, 2013.
[12] Dutta Atanu Kumar, J.M. Caicedo, Zarate Boris, System Identification of Cable-Stayed Bridge: A Case Study, Proceedings of the International Symposium on Engineering under Uncertainty: Safety Assessment and Management (ISEUSAM - 2012), pp 777-786, 2013.
[13] Sang-Won Cho, Jeong-Hoi Koo, Ji-Seong Jo, In-Won Lee, Vibration Control of a Cable-Stayed Bridge Using Electromagnetic Induction Based Sensor Integrated MR Dampers, *Journal of Mechanical Science and Technology*, Vol 21 (6), pp 875-880, 2007.
[14] M. Bechtold, Modelling of Steel Ropes, 2009, SIMULIA Customer Conference.
[15] Ming Gu, C.J Liu, G.Q Luo, etc. Rain-wind induced vibration and control of stay cables on cable-stayed bridge [J].*Shanghai mechanism*, 1998, 19(4): 281-288.
[16]Guohao Li, Stability and vibration of bridge structure [M].Beijing: *China Railway Publishing House*, 1992.
[17] Virlogeux，M, Cable vibrations in cable-stayed bridges [J]. *Bridge Aerodynamics*，Larsen and Esdahl(eds)，1998 Balkeman，Rotterdam.
[18] Yamaguchi, H. and Fujino, Y., Stay cable dynamies and its vibration control [J]. *Bridge Aerodynamics*，Larsen and Esdahl(eds), 1998, Balkema: Rotterdam, pp235-253.

[19]Shuisheng Chen, *The vibration and passive, semi-active control of the stay cables of large-span cable-stayed bridge* [D]. Hangzhou: Doctoral Dissertation of Zhejiang University, 2002.
[20] Ruscheweyh H.P., The mechanism of rain-wind- induced vibration[C].*Bridge Aerodynamics*, Balkema, Rotterdam, 1999, 1041-1047.
[21] Sena Kumarasena, Nicholas P. Jones, Peter lrwin, Wind induced vibration of stay cables[R]. Report to HNTB Corporation and FHWA, 2005.2.
[22] Y. Hikam, N. Shiraishi, Rain-wind induced vibrations of cables in cable-stayed bridge [J]. *Journal of Wind Engineering and Industrial Aerodynamics*, 1988, 29:409-418.
[23] Takashi Yoshimura, A Sato Inoue, Ken- ich Kaji, Aerodynamic stability of the Aratsu Bridge, Recent advanced in wind engineering[C]. Proceedings of the 2nd Asia-Pacific Symposium on Wind Engineering, Beijing China, 1989:637-644.
[24] Linlien J L, Pinto da Costa A P, Vibration amplitude caused by parametric excitation of cable stayed structures [J]. *Journal of Sound and Vibration*，1994，171(1): 69-90.
[25] Benito, Pacheco M., Fujino Yozo, Keeping cable calm [J]. *Civil Engineering*, 1993, 8:56-58.
[26] Persoon A.J. Noorlander K, Full-scale measurements on the Erasmus Bridge after rain-wind induced cable vibrations[C]. *Wind Engineering into the 21th century*, Baikema, Rotterdam, 1999, 1019-1026.
[27] Joseph A. Main, Nicholas P. Jones, A comparison of full-scale measurement of stay cable vibration[C]. Structures Congress 2000- Advanced Technology in Structural Engineering, Section 2, Chapter2: l-8.
[28] X.Y Wang, Z.Q Chen, Y.Q N, Observation and control on the rain-wind induced vibration of stay cables [J]. *China Civil Engineering Journal*, 2003, 36(6):53-59.
[29] Shuisheng Chen, Bing Nan, Numerical research on the nonlinear first order coupled-vibration of stay cables [J]. *China Civil Engineering Journal*, 2003, 36(4):70-75.
[30] Hover Franz S., Miller Scott N. Triantafyllou. Miehael S, 1997, Vortex-induced oscillations in inclined cables [J]. *Wind Engineering and Industrial Aerodynamics* Vol. 69-71, July10, 203-211.
[31] Guy L. Larose, Leif Wagner Smitt.1999.Raill/Wind Induced Vibrations of the Stay Cables of the Oresund High Bridge[C]. Proc. of IABSE Conference on Cable-stayed bridge-Past, Present and future.Malmo.301- 311.
[32] M. Matsumoto, M. Yamagishi, J. Aoki, N.Shirashi.1995.Various Mechanism of Inclined Cable Aerodynamics[C]. Wind Engineering Retrospect and Prospect Papers for the 9th International Conference. New Delphi.759-770.
[33] M.Matsumoto.1998.Observed Behaviour of Prototype Cable Vibration and Its Generation Mechanism [J]. *Bridge Aerodynamics.*
[34] Masara Matsumoto, Tomomi Yagi, Mitsutaka Goto, Seiichiro Sakai.2003. Rain-Wind-induced vibration of inclined cables at limited high reduced wind velocity region [J], *Journal of wind Engineering and Industrial Aerodynamics*. Vol.91.1-12
[35]Shouying Li, Ming Gu. 2004. *Numerical simulation on the cable flow with fixed artificial rivulet* [J], Tongji University Journal, 32(10). 1334-1338

[36] P. Warnitchai, Y Fujino, B. M. Pacheco, R. Agret. 1993. An experimental study on active tendon control of cable-stayed bridges [J]. *Earthquake Engineering and Structural Dynamics,*Vol.22. 93-111.
[37] P. Warnitchai. 1990. *Nonlinear Vibration and Active Control of Cable-stayed Bridges* [M]. Doctoral dissertation, Department of Civil Engineering, University of Tokyo.
[38] A. Pinto da. Costa, J. A. C. Martins, F. Branco, J. L. Lilien, 1996, Oseillations of Bridge Stay Cables Induced by Periodic Motions of Deck and/or Towers [J]. J*ournal of Engineering Mechanics*, ASCE. 122.7.613-622.
[39] Zhan Kang, Wan Sai, Numerical research on the parametric resonance of cable-stayed bridge [J]. *China Civil Engineering Journal*, 1998, Vol.31. 4: 14-22.
[40] Y. Hikami, N. Shiraish.1988.Rain-wind induced vibration of cables in cable stayed bridges [J]. *Journal of Wind Engineering and Industrial Aerodynamics*, VOI.29.409-418.
[41]Xiangting Zhang, Structural wind engineering [M]. *China Building Industry Press*, Beijing.2006.
[42] Min Ling, *Exploration on the durability of stay cable system* [D]. Beijing: Dissertation of Beijing Jiaotong University, 2010.
[43] Xiuyong Wang, *Research on the new control technology on the vibration of stay cables of cable-stayed bridge* [D]. Changsha: Dissertation of Central South University, 2002.
[44] Zhi Fu, *Research on the parametric vibration of stay cables of cable-stayed bridge* [D]. Tianjin, Dissertation of Tianjin University, 2009.
[45] Y. Hikami, N. Shiraishi. Rain-wind-induced vibration of cables in cable stayed bridges [J], *Journal of wind Engineering and Industrial Aerodynamics*.1988, 29:409-418.
[46] T. Yoshimura. Aerodynamic stability of four medium span bridges in Kyushu District [J], *Journal of wind Engineering and Industrial Aerodynamics*.1992, 41:203-213.
[47] A. J. Persoon, K. Noorlander. Full-scale measurements on the Erasmus Bridge after rain/wind induced cable vibrations[C], *Wind engineering into 21th century*, 1999:1019-1026.
[48] J. A. Main，N. P. Jones，Full-seale measurements of stay cable vibration[C], *Wind engineering into 21th century*, 1999:963-970.
[49] M. Matsumoto, H. Shirato, T. Yagi, et al. Field observation of the fu1-seale wind-induced cable vibration [J], *Journal of wind Engineering and Industrial Aerodynamics.*2003, 91:13-26.
[50]Zhengqing Chen, Field observation on the rain-wind induced vibration and vibration control [J]. *Journal of construction science and engineering*, 2005, 22(4):5-10.
[51] X.Y Wang, Z.Q Chen, Y.Q Ni, Field observation on the rain-wind induced vibration and vibration control [J]. *China Civil Engineering Journal*, 2003, 36(6):53-59.
[52] J.D Yu, Z.Q Chen, X.Y Wang, *Research on the rain-wind induced vibration characteristics of stay cables based on field observation* [J], Journal of hunan science and technology university, 2006, 2l(2):22-24.
[53] J.H Hu, X.Y Wang, Z.Q Chen, Y.Q Ni, Z.M Gao, Rain-wind induced vibration response characteristics of stay cables [J]. *China Journal of Highway and Transport* 2006, 19(3):41-48.
[54] Z.Q Chen, C.Y Liu, Y.Q Ni, X.Y Wang, X.N Fu, Wind Field Parameters of rain-wind induced

vibration of stay cables on Dongting Lake Bridge [J]. *Journal of railway science and engineering*, 2004,1(1):52-57.
[55]Shuisheng Chen, *Vibration of stay cables on large-span cable-stayed bridge and passive, semi-active control* [D], Hangzhou, Zhejiang University, 2002.
[56] Jongseok Oh, *Dynamic characteristics of inclined cable*, Master's Thesis, University of Ottawa, 2004.
[57]G. Tagata. Harmonically Forced, Finite Amplitude Vibration of a String[J], *Journal of Sound and Vibration*, 1977, 51(4), 483-492.
[58] Zhigang Wang, Large amplitude vibration of stay cables caused by parametric vibration of cable-stayed bridge [J], *Engineering mechanics*, 2001.2.Vol.18 No1.
[59] Virlogeux, M. Recent evolution of cable-stayed bridges[J]. *Engineering Structures*, 1999. 21(8): 737- 755.
[60] Ehsan，F., R. H. Seanlan. Damping stay cables with ties[C]. In 5th US-Japan Bridge Workshop. 1990.
[61] Yamaguchi, H., L. Jayawardena. Analytical Estimation of Structural Damping in Cable Structures[J]. *Journal of Wind Engineering and Industrial Aerodynamics*, 1992.43(l-3): 1961-1972.
[62] Yamaguchi, H., H. D. Nagahawatta. Damping Effects of Cable Cross Ties in Cable-Stayed Bridges [J]. *Journal of Wind Engineering and Industrial Aerodynamics*, 1995.54:35-43.
[63] Yamaguchi，H.，R. Adhikari. Energy-Based Evaluation of Modal Damping in Structural Cables with and without Damping Treatment. *Journal of sound and Vibration*, 1995. 181(l): 71-83.
[64] Yamaguchi，H.， R. Adhikari. Loss Factors of Damping Treated Structural Cables [J]. *Journal of Sound and Vibration*, 1994.176(4): 487-495.
[65] Caracoglia, L., N. P. Jones. In-Plane dynamic behaviour of cable networks. Part 1: formulation and basic solutions [J]. *Journal of Sound and Vibration*, 2005.279(3-5): 969-991.
[66] Caracoglia, L., N. P. Jones. In-Plane dynamic behaviour of cable networks. Part 2: Prototype Prediction and validation [J]. *Journal of Sound and Vibration,* 2005.279(3-5): 993-1014.
[67] Bosch，H.R., S. W. Park. Effectiveness of External Dampers and Crossties in Mitigation of Stay Cable Vibrations [C]. 6th International Symposium on Cable Dynamics, 2005.
[68]Jiandong Wei, Youfa Yang, Finite element analysis on mitigation effectiveness of crosstie [J].*China journal of highway and transport*, 2000(4):66-69.
[69] Jiming Huang, *Research on the mitigation of vibration of crossties of large-span cable-stayed bridge* [D].Master's thesis, Shanghai, Tongji University, 2001.
[70] Congsen Yuan, STUDY ON THE CABLE VIBRATION [D], Master's Thesis, Chengdu, Southwest Jiaotong University, 2012.
[71]Yifan Song, Dynamics of highway bridge [M], Beijing: *China Communication Press*, 2000.
[72] Michael Hoftyzer, *Experimental Investigation of the Dynamic Behaviour of Inclined Sagged Cables*, Master's Thesis, University of Ottawa, 2006.
[73] Y.L Li, Wei Lu, Q. Y Tao, W.B Xiaong, Study on rain-wind induced vibration of cables in cable-stayed bridges by wind tunnel test, *Journal of Experiments in Fluid Mechanics*, Vol. 21. No. 4,

2007.
[74] Qingxiong WU, Kazuo TAKAHASHI, Shozo NAKAMURA, *Analysis of Local Vibrations in the Stay Cables of an Existing Cable-stayed Bridge under Wind Gusts*, Research report from department of engineering, Nagasaki university, Vol. 35, 65, 2005.
[75] Purnachandra Saha, Sesmic Control of Benchmark Cable-Stayed Bridges Using Variable Friction Pendulum Isolator, *Advances in Structural Engineering*, pp 1271-1282, 2015.
[76] Mohammed Ismail, José Rodellar, Gennaro Carusone, Marco Domaneschi, Luca Martinelli, Characterization, modelling and assessment of Roll-N-Cage isolator using the cable-stayed bridge benchmark, Acta Mechanica, Vol 224 (3), pp 525-547, 2013.
[77] Ayman Sabri, FINITE ELEMENT MODELLING OF THE STONECUTTERS CABLE-STAYED BRIDGE, *a report submitted to the University of Ottawa*, 2013.
[78] Harold R.Bosch, James R. Pagenkopf, Dynamic Properties of Stay Cables on the Bill Emerson Bridge, The 12th Americas Conferences on Wind Engineering, Seattle, Washington, USA, June 16-20, 2013.
[79] Guy Larose, Wind-induced vibration of bridge cables, FHWA Aerodynamics Webinar Series, Session 4, 2014.
[80] H. R. Hamilton III, J. E. Breen and K. H. Frank, Investigation of Corrosion Protection Systems for Bridge Stay Cables, No. 1264-3F, Texas Department of Transportation, 1995.
[81] Fatigue strength of stay cables with large diameters on cable-stayed bridge, Bridge Overseas, Phase 1, 1994.
[82] Polyurethane chemistry and technology, http://kecheng.baidu.com/view/8203eb39e518964bce847c53.html, ASCE, consulted on May 2015.
[83] Xu Xie, Xiaozhang Li, Yonggang Shen, Static and Dynamic Characteristics of a Long-Span Cable-Stayed Bridge with CFRP Cables, *Materials*, 4854-4877, 2014.7

Appendix A

Table of additional mode frequencies of the typical cables

Table A-1: Mode frequencies 20- 30 of uniform property cable

Mode Numbers	Eigenvalue	Frequency(Hz)	Generalized Mass
20	3105	8.8685	9049.7
21	4180	10.29	8911.9
22	4187.8	10.299	8892.5
23	5520.2	11.825	9041.3
24	5523.1	11.828	9017.8
25	7178.6	13.485	8906.8
26	7186.6	13.492	8886.1
27	9188.9	15.256	8840.7
28	9194.7	15.261	8808.8
29	11623	17.159	9077.9
30	11631	17.164	9044.1

Table A-2: Mode frequencies 20-30 of two-strand cable without grout

Mode Numbers	Eigenvalue	Frequency(Hz)	Generalized Mass
20	459.9	3.4131	9080.2
21	728.29	4.2951	9205.9
22	728.29	4.2951	9205.9
23	728.39	4.2954	9201.2
24	728.39	4.2954	9201.2
25	1100.4	5.2796	9102.7
26	1100.4	5.2796	9102.7
27	1104.9	5.2903	9172.1
28	1104.9	5.2903	9172.1
29	1599.8	6.3659	9058.8
30	1599.8	6.3659	9058.8

Table A-3: Mode frequencies 20-30 of Four-strand cable without grout

Mode Numbers	Eigenvalue	Frequency(Hz)	Generalized Mass
20	139.77	1.8816	14044
21	139.87	1.8823	15537
22	139.87	1.8823	15537
23	139.87	1.8823	10574
24	139.87	1.8823	10574
25	268.19	2.6064	9295.9
26	268.19	2.6064	9295.9
27	268.19	2.6064	11621
28	268.19	2.6064	11621
29	268.21	2.6065	9247.3
30	268.21	2.6065	9247.2

Table A-4: Mode frequencies 20-30 of two-strand cable with springs k=100 N/m

Mode Numbers	Eigenvalue	Frequency(Hz)	Generalized Mass
20	460.82	3.4165	18151
21	728.79	4.2966	18337
22	728.89	4.2969	9163.8
23	728.89	4.2969	9163.8
24	729.45	4.2985	18337
25	1101.3	5.2817	9125.6
26	1101.3	5.2817	9125.6
27	1105.7	5.2923	18364
28	1106.4	5.2939	18364
29	1601.1	6.3684	18205
30	1601.6	6.3693	9099.6

Table A-5: Mode frequencies 20-30 of four-strand cable with springs k=100 N/m

Mode Numbers	Eigenvalue	Frequency(Hz)	Generalized Mass
20	139.92	1.8826	18020
21	140.48	1.8864	18272
22	140.48	1.8864	18272
23	140.58	1.8871	18020
24	140.58	1.8871	18020
25	268.32	2.607	18364
26	268.32	2.607	18364
27	268.34	2.6071	18346
28	268.34	2.6071	18346
29	268.98	2.6102	18363
30	268.98	2.6102	18363

Table A-6: Mode frequencies 20-30 of two-strand cable with springs k=500 N/m

Mode Numbers	Eigenvalue	Frequency(Hz)	Generalized Mass
20	463.47	3.4263	18151
21	728.79	4.2966	18337
22	728.89	4.2969	9163.8
23	728.89	4.2969	9163.8
24	732.09	4.3063	18337
25	1101.3	5.2817	9125.5
26	1101.3	5.2817	9125.5
27	1105.7	5.2923	18364
28	1109	5.3002	18364
29	1601.1	6.3684	18205
30	1601.6	6.3693	9097.8

Table A-7: Mode frequencies 20-30 of Four-strand cable with springs k=500 N/m

Mode Numbers	Eigenvalue	Frequency(Hz)	Generalized Mass
20	139.92	1.8826	18020
21	143.13	1.9041	18272
22	143.13	1.9041	18272
23	143.23	1.9047	18020
24	143.23	1.9047	18020
25	268.32	2.607	18364
26	268.32	2.607	18364
27	268.34	2.6071	18348
28	268.34	2.6071	18348
29	271.62	2.623	18363
30	271.62	2.623	18363

Appendix B

Table of mode frequencies of stay-cables fan modelled with one uniform property

Table B-1: Frequencies from mode 1-30 of the whole fan without crossties

Mode Numbers	Eigenvalue	Frequency(Hz)	Generalized Mass
1	12.092	0.55344	11957
2	12.472	0.56207	15219
3	13.39	0.58238	11621
4	13.73	0.58974	11097
5	13.737	0.58988	14804
6	14.088	0.59738	14235
7	19.652	0.70555	7568.6
8	19.878	0.70959	9789.4
9	19.985	0.7115	7287.9
10	20.216	0.7156	9403
11	22.633	0.75717	6670.1
12	22.861	0.76097	8927.8
13	24.993	0.79567	6183
14	25.228	0.7994	8546.9
15	28.563	0.85059	5686.6
16	28.799	0.8541	8317.9
17	40.947	1.0184	3831.2
18	41.157	1.021	5916.3
19	46.159	1.0813	3415.9
20	46.374	1.0838	5799.1
21	48.395	1.1072	14926
22	48.407	1.1073	11924
23	53.591	1.1651	14536
24	53.602	1.1652	11591
25	54.327	1.1731	3031.3
26	54.532	1.1753	5688.4
27	54.958	1.1799	13974
28	54.969	1.18	11069
29	63.516	1.2684	2673.6
30	63.702	1.2703	4821.9

Table B-2: Frequencies from mode 1-30 of the whole fan with 1 crosstie

Mode Numbers	Eigenvalue	Frequency(Hz)	Generalized Mass
1	14.574	0.60759	17571
2	19.964	0.71112	35162
3	29.067	0.85807	20991
4	29.542	0.86505	19436
5	34.24	0.9313	16223
6	36.441	0.96076	19441
7	40.003	1.0066	12896
8	41.778	1.0287	27169
9	51.213	1.139	23386
10	51.687	1.1442	16978
11	52.215	1.1501	14749
12	56.189	1.193	15164
13	60.389	1.2368	12778
14	60.488	1.2378	10784
15	66.046	1.2934	15934
16	67.067	1.3034	18542
17	71.491	1.3457	8934.8
18	73.85	1.3677	14936
19	78.584	1.4109	6245.6
20	82.634	1.4468	4250.7
21	83.486	1.4542	10371
22	86.756	1.4824	11719
23	87.964	1.4927	8693
24	91.4	1.5216	8576.4
25	91.625	1.5234	1816.9
26	91.72	1.5242	2415.6
27	94.135	1.5442	2153.2
28	97.253	1.5695	4720.3
29	97.879	1.5746	10103
30	98.663	1.5809	5863.6

Table B-3: Frequencies from mode 1-30 of the whole fan with 2 crossties

Mode Numbers	Eigenvalue	Frequency(Hz)	Generalized Mass
1	15.661	0.62983	21285
2	24.327	0.78499	20019
3	34.81	0.93902	30138
4	44.656	1.0636	23266
5	52.078	1.1485	12498
6	54.681	1.1769	11210
7	61.975	1.2529	8889
8	65.058	1.2837	16061
9	72.396	1.3542	15698
10	77.573	1.4018	15680
11	78.434	1.4095	13574
12	79.671	1.4206	7509.3
13	82.309	1.4439	8714.7
14	83.653	1.4557	8394
15	86.403	1.4794	14106
16	89.277	1.5038	11088
17	90.658	1.5154	6172.3
18	91.483	1.5223	1818.2
19	91.578	1.5231	2417.2
20	92.96	1.5345	6228.4
21	93.796	1.5414	8514.5
22	97.572	1.5721	2242.8
23	101.54	1.6038	4458.3
24	103.04	1.6155	10329
25	103.67	1.6205	6789.1
26	104.91	1.6301	10856
27	105.74	1.6366	3301
28	106.04	1.6389	3272.1
29	106.28	1.6408	7725.6
30	110	1.6693	1539

Table B-4: Frequencies from mode 1-50 of the whole fan with 4 crossties

Mode Numbers	Eigenvalue	Frequency(Hz)	Generalized Mass
1	17.209	0.66024	21152.
2	28.666	0.85213	24992.
3	41.208	1.0217	14370.
4	57.683	1.2088	15579.
5	68.904	1.3211	21405.
6	78.237	1.4078	11236.
7	98.181	1.5770	14399.
8	110.63	1.6740	30448.
9	121.32	1.7530	10020.
10	146.65	1.9273	16887.
11	147.21	1.9310	17427.
12	154.96	1.9812	18905.
13	162.00	2.0257	17276.
14	189.63	2.1916	6855.8
15	193.00	2.2111	16395.
16	213.65	2.3263	5623.3
17	220.05	2.3609	30480.
18	240.61	2.4687	14333.
19	251.89	2.5260	10640.
20	273.64	2.6327	2589.7
21	280.56	2.6658	13004.
22	290.42	2.7123	13723.
23	298.46	2.7496	15344.
24	317.04	2.8339	5889.7
25	326.21	2.8746	11759.
26	332.70	2.9030	17950.
27	338.39	2.9277	13017.
28	341.99	2.9433	11608.
29	357.39	3.0088	4794.8
30	360.67	3.0226	1955.0

Appendix C

Additional in-plane modes of stay-cables fan modelled with one uniform property

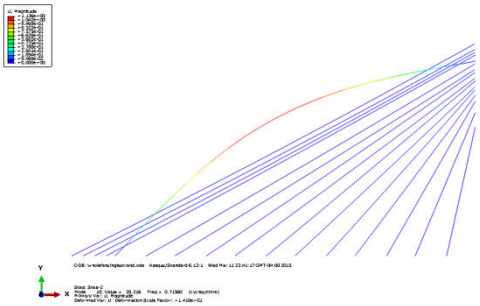

Mode 5 (f=0.7198Hz)

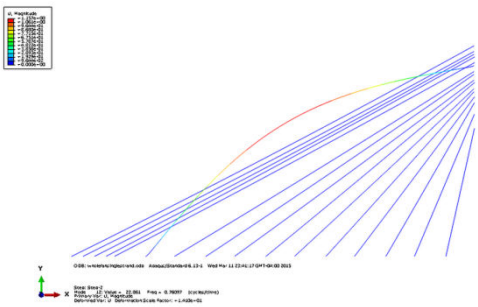

Mode 6 (f=0.79097Hz)

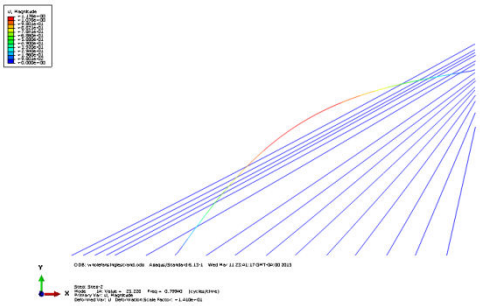

Mode 7 (f=0.7994Hz)

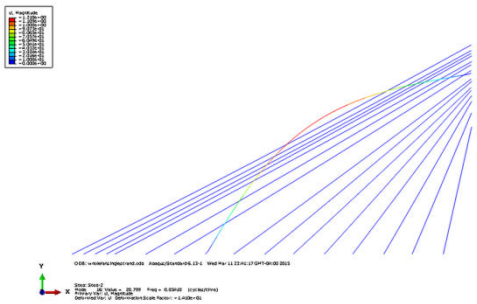

Mode 8 (f=0.8541Hz)

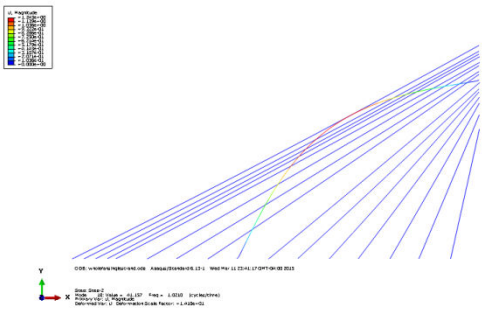

Mode 9 (f=1.021Hz)

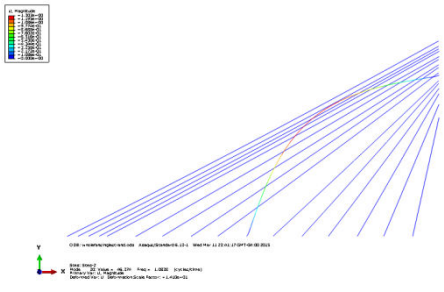

Mode 10 (f=1.0838Hz)

Figure C.1: Modes 5-10 for cable network with no crosstie

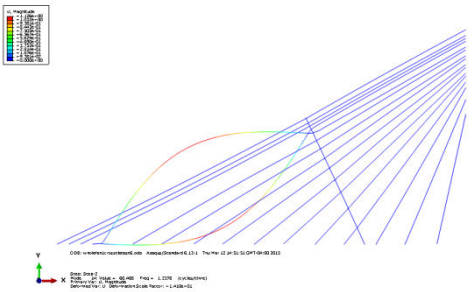

Mode 5 (f=0.1.2378Hz)

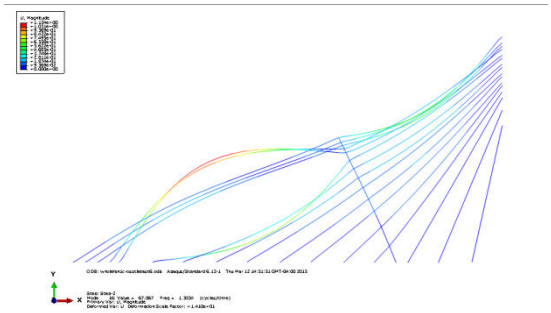

Mode 6 (f=1.3034Hz)

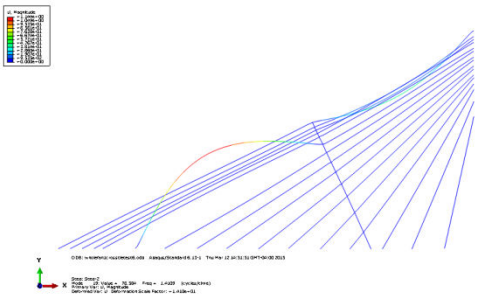

Mode 7 (f=1.4109Hz)

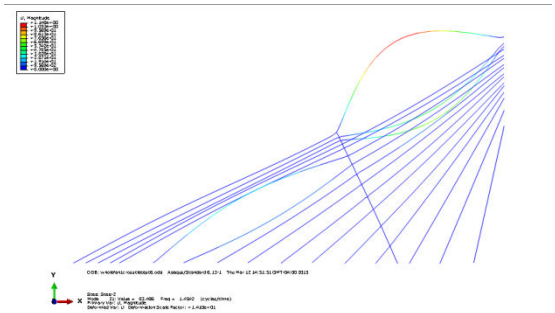

Mode 8 (f=1.4542Hz)

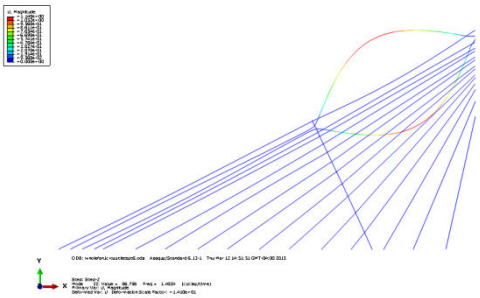

Mode 9 (f=1.4824Hz)

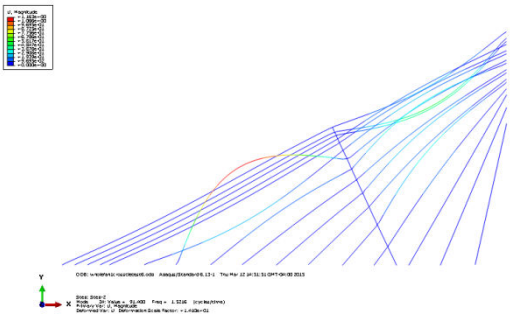

Mode 10 (f=1.5216Hz)

Figure C.2: Modes 5-10 for cable network with 1 crosstie

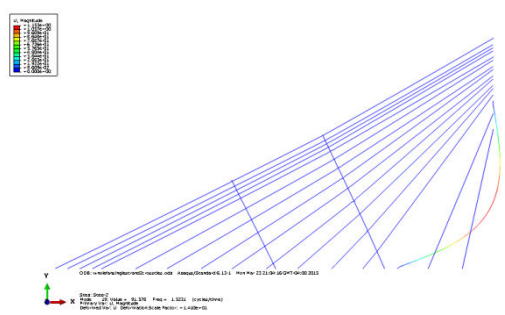

Mode 5 (f=1.5231Hz)

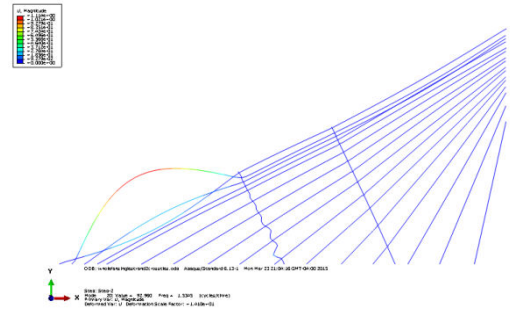

Mode 6 (f=1.5345Hz)

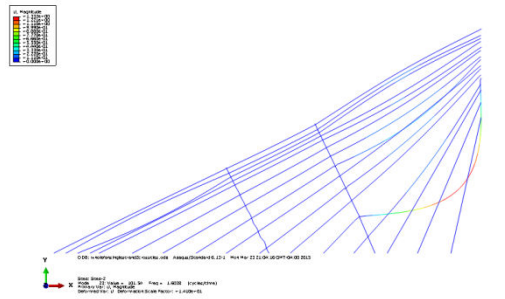

Mode 7 (f=1.6038Hz)

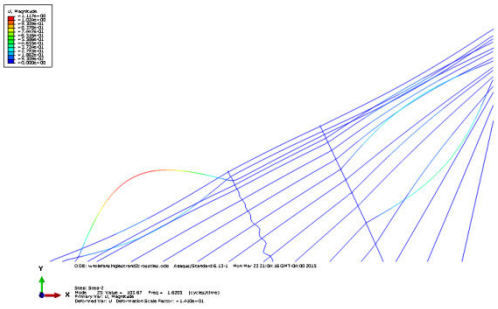

Mode 8 (f=1.6205Hz)

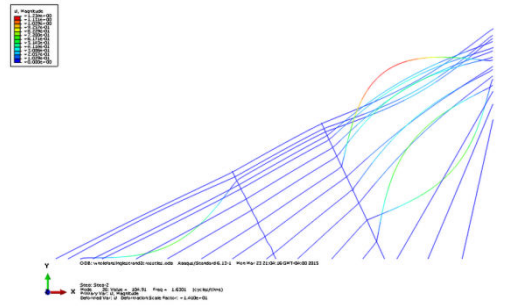

Mode 9 (f=1.6301Hz)

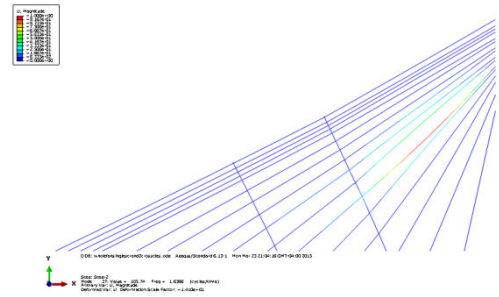

Mode 10 (f=1.6366Hz)

Figure C.3: Modes 5-10 for cable network with 2 crossties

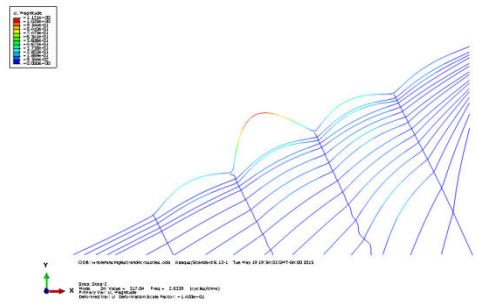

Mode 1 (f=2.8339Hz)

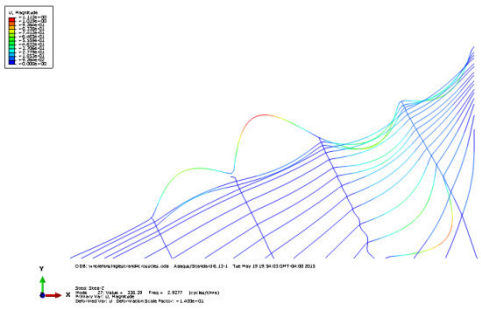

Mode 2 (f=2.9277Hz)

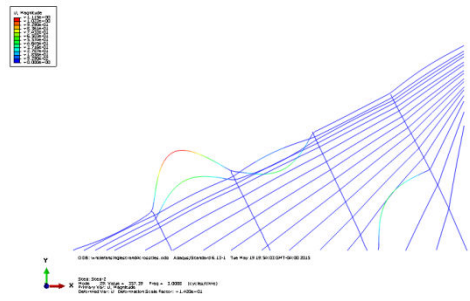

Mode 3 (f=2.9277Hz)

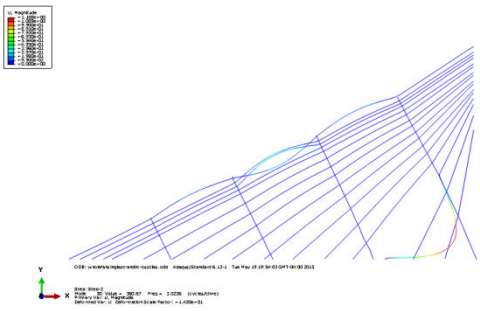

Mode 4 (f=3.0226Hz)

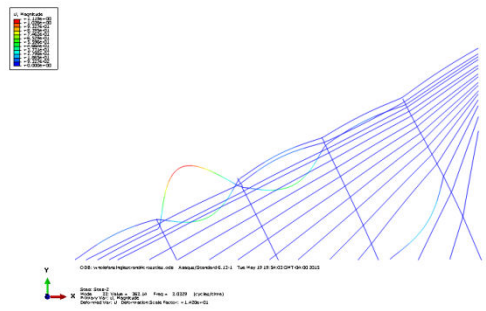

Mode 5 (f=3.0329Hz)

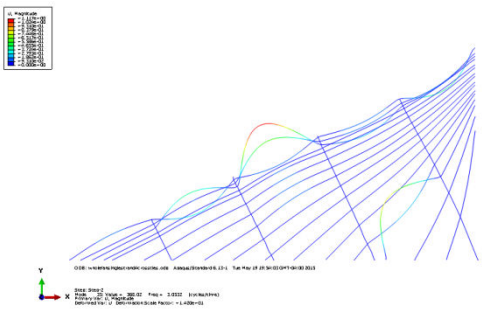

Mode 6 (f=3.0523Hz)

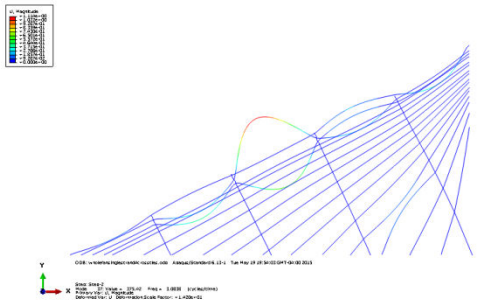

Mode 7 (f=3.0938Hz)

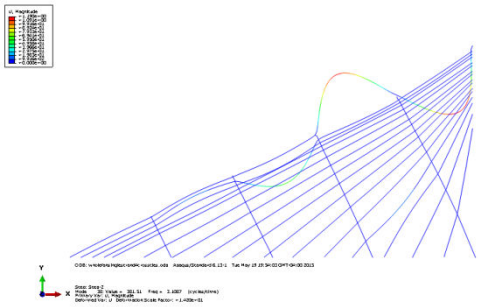

Mode 8 (f=3.1087Hz)

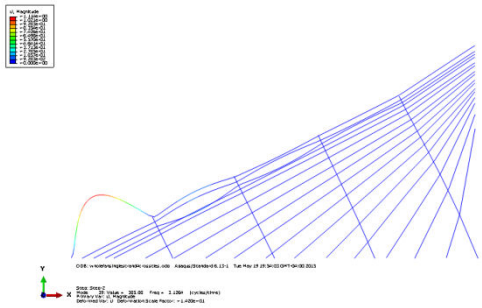

Mode 9 (f=3.1264Hz)

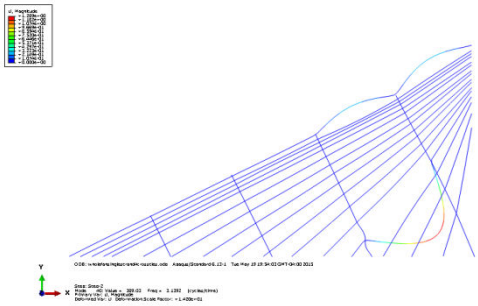

Mode 6 (f=3.1392Hz)

Figure C.4: Modes 1-10 for cable network with 4 crossties

Appendix D

Additional modes of stay-cables fan modelled as multiple-strand without grout

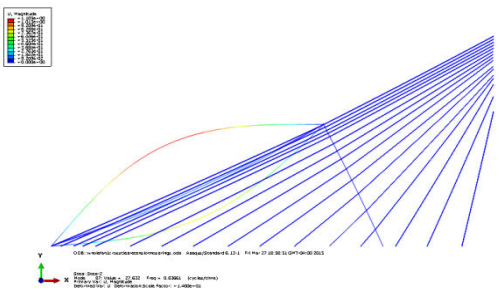

Mode 5 (f=0.83661Hz)

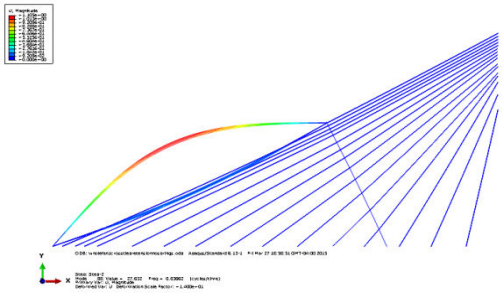

Mode 6 (f=0.83662Hz)

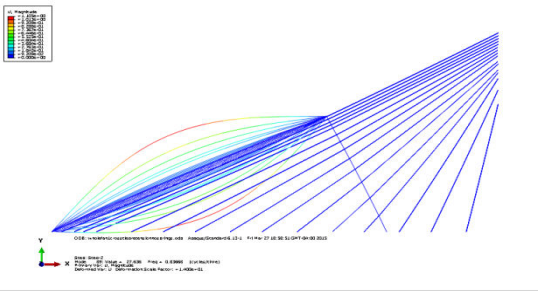

Mode 7 (f=0.83668Hz)

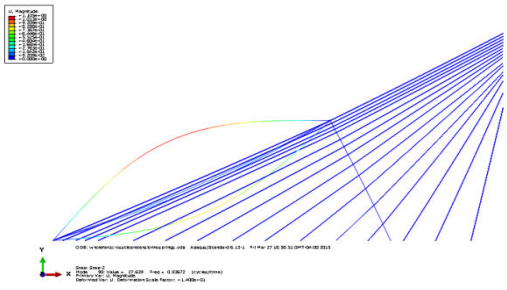

Mode 8 (f=0.83672Hz)

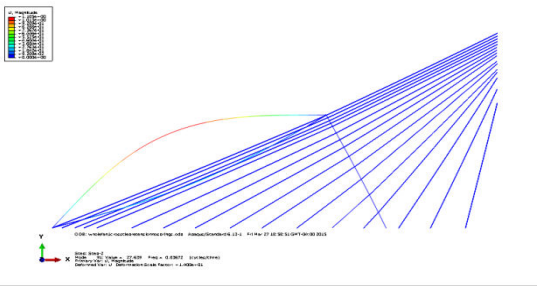

Mode 9 (f=0.83672Hz)

Figure D.1: In-plane modes 5-9 for cable network with 1 crosstie

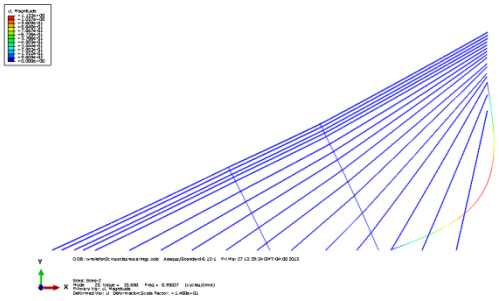

Mode 5 (f=0.95027Hz)

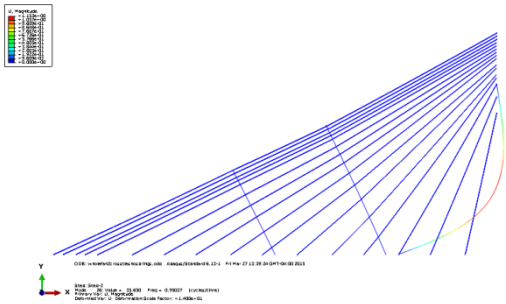

Mode 6 (f=0.95027Hz)

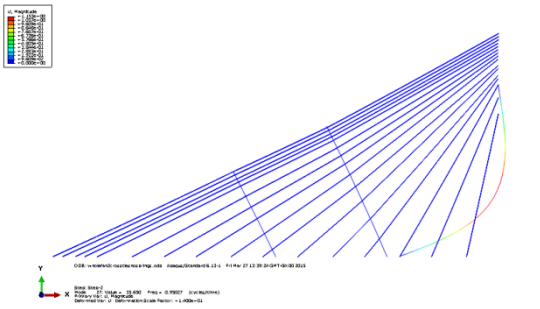

Mode 7 (f=0.95027Hz)

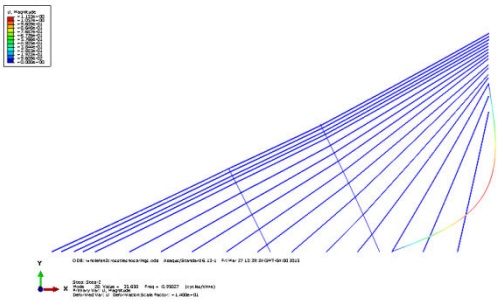

Mode 8 (f=0.95027Hz)

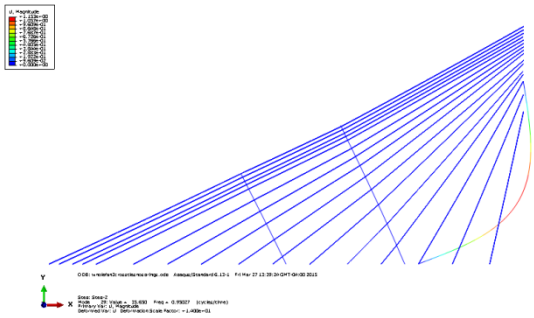

Mode 9 (f=0.95027Hz)

Figure D.2: In-plane modes 5-9 for cable network with 2 crossties

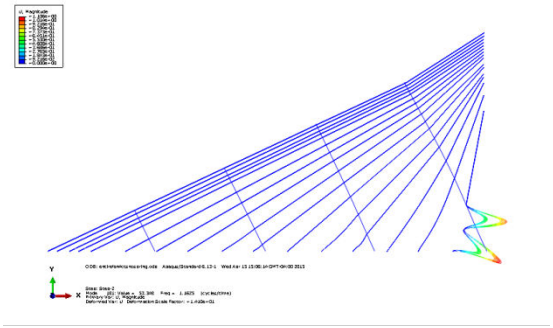

Mode 5 (f=1.1625Hz)

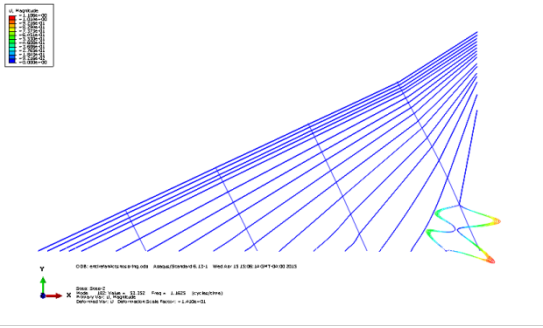

Mode 6 (f=1.1625Hz)

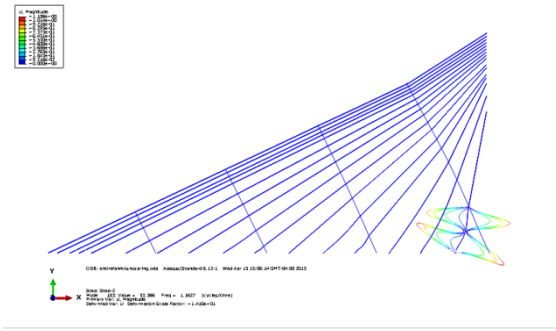

Mode 7 (f=1.1627Hz)

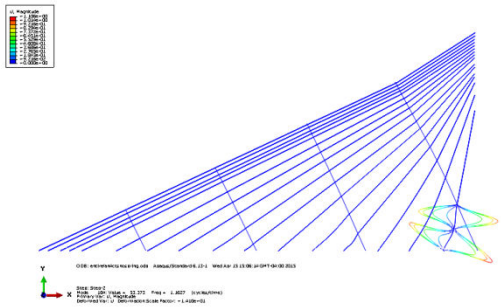

Mode 8 (f=1.1627Hz)

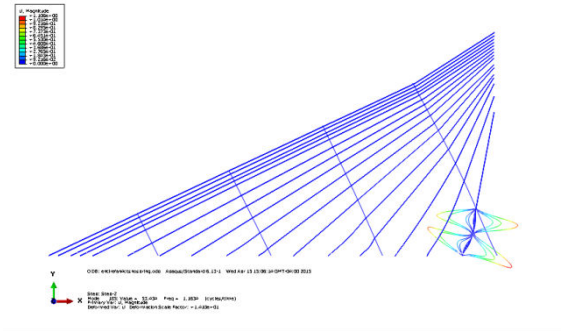

Mode 9 (f=1.1634Hz)

Figure D.3: In-plane modes 5-9 for cable network with 4 crossties

Appendix E

Additional modes of stay-cables fan modelled as multiple-strand with polymer grout

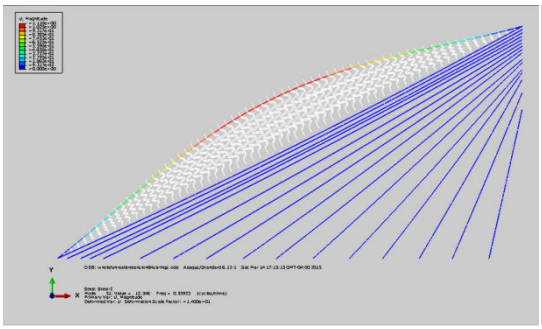

Mode 5 (f=0.55923Hz)

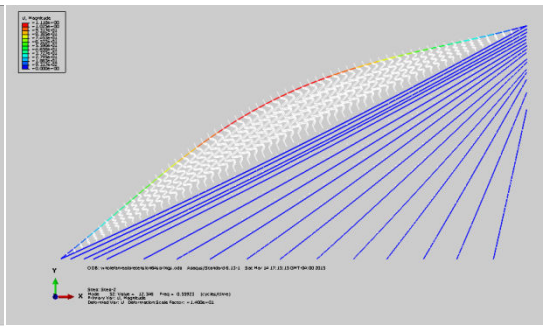

Mode 6 (f=0.55923Hz)

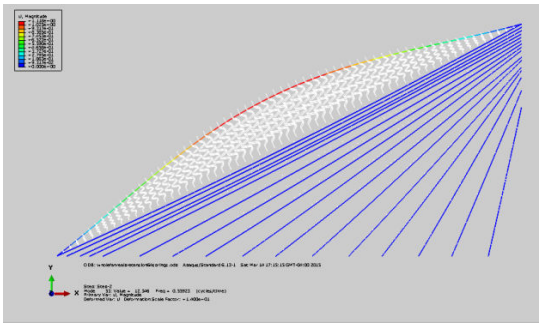

Mode 7 (f=0.55923Hz)

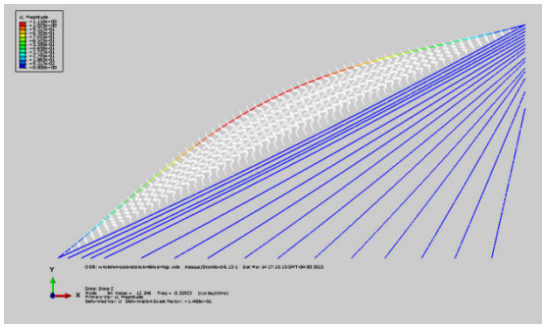

Mode 8 (f=0.55923Hz)

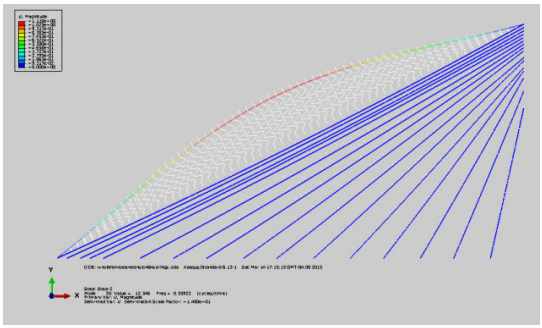

Mode 9 (f=0.55923Hz)

Figure E.1: In-plane modes 5-9 for cable network with no crosstie

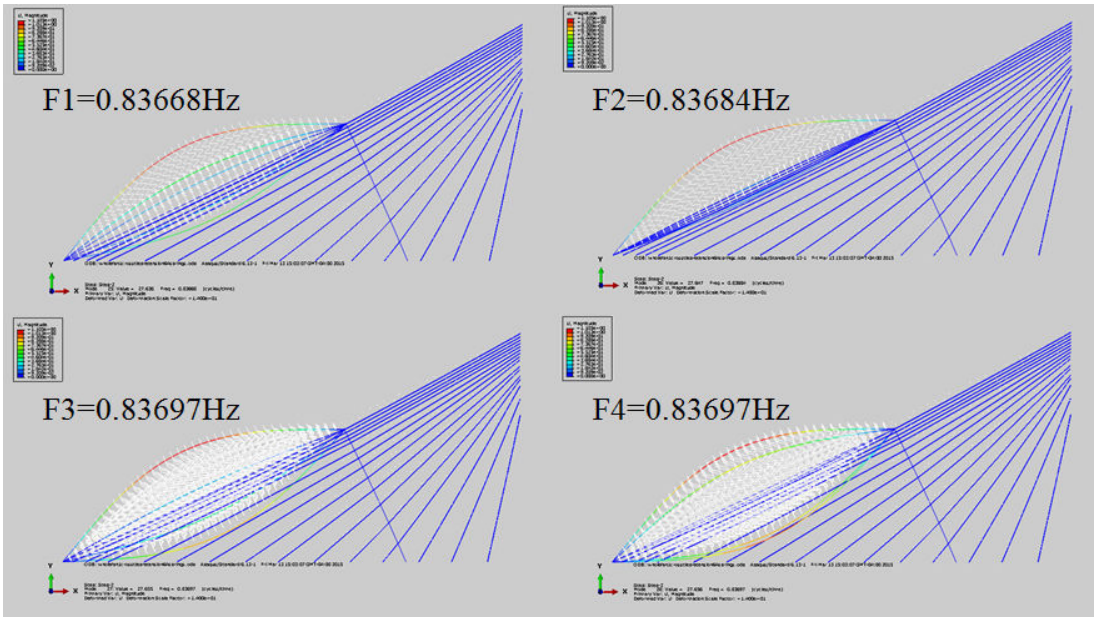

Mode 1-4

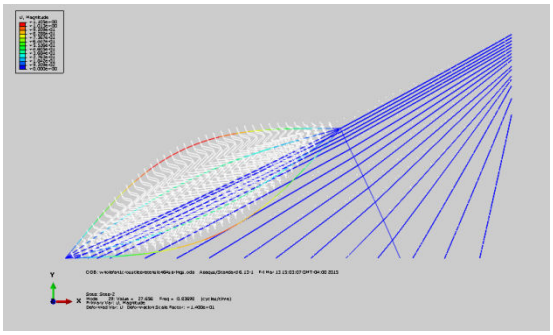

Mode 5 (f=0.83968Hz)

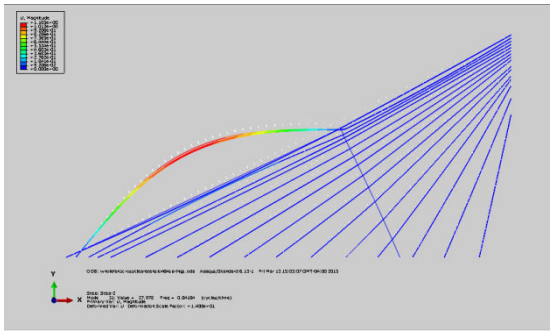

Mode 6 (f=0.84184Hz)

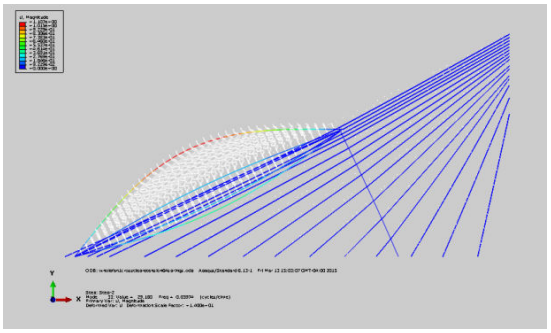

Mode 7 (f=0.85974Hz)

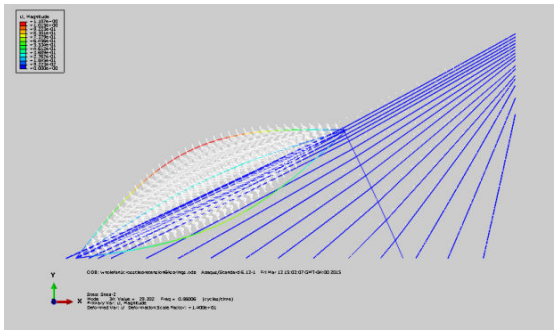

Mode 8 (f=0.86006Hz)

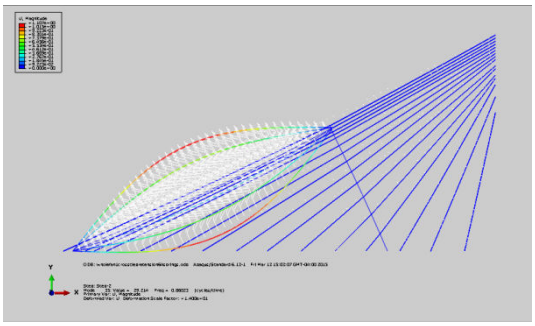

Mode 9 (f=0.86023Hz)

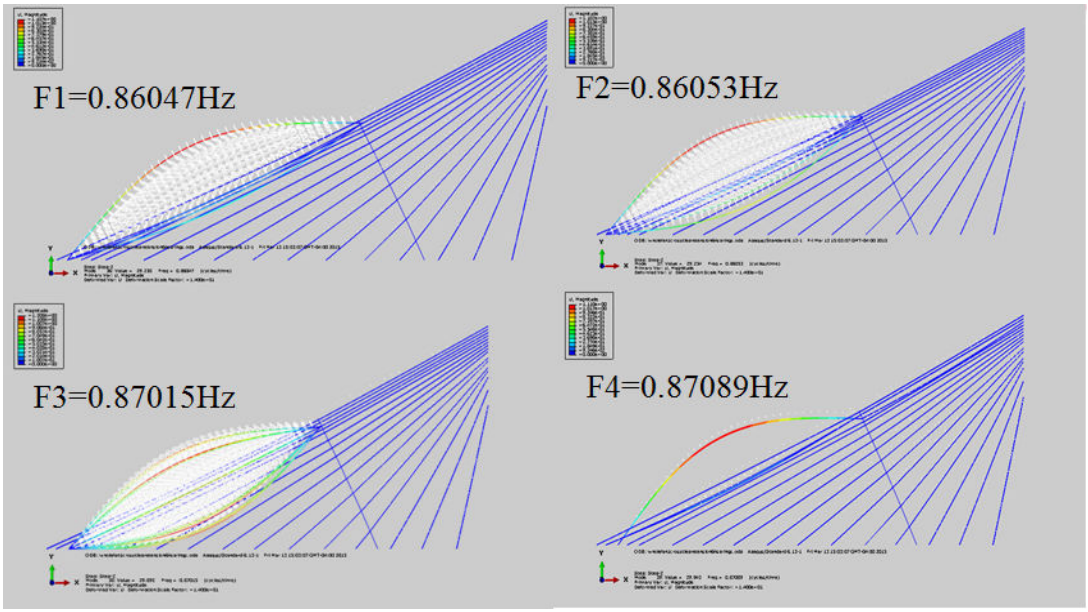

Mode 10-13

Figure E.2: In-plane modes 1-13 for cable network with 1 crosstie

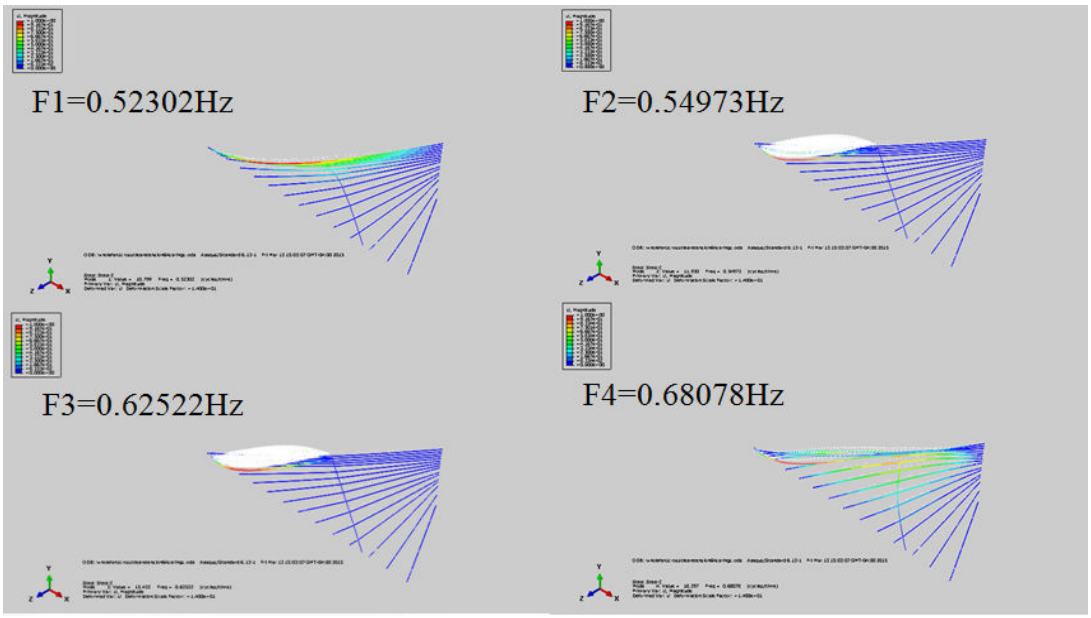

Mode 1-4

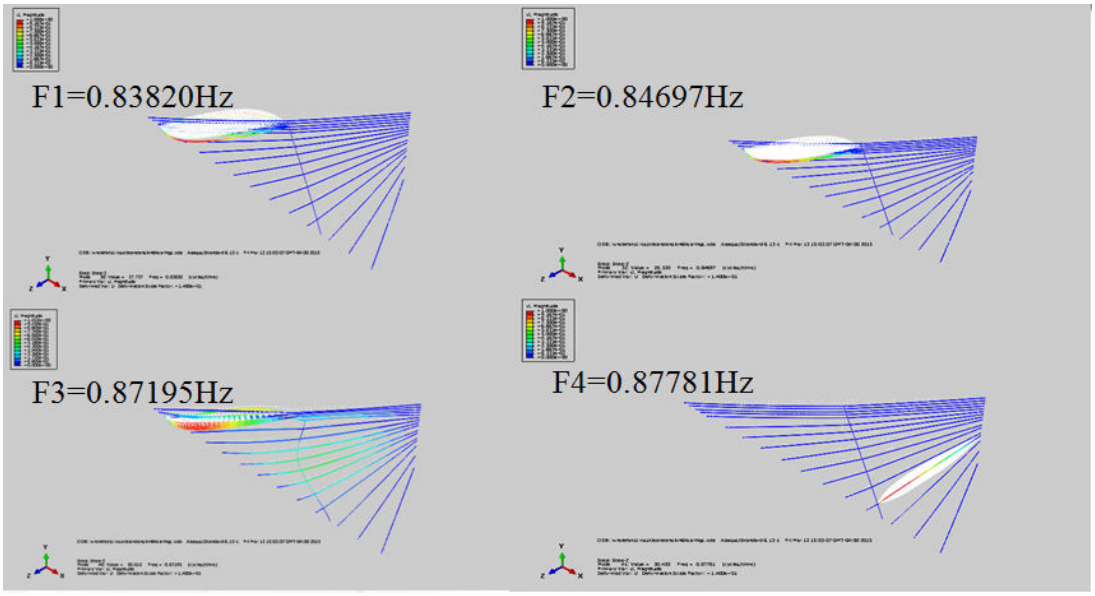

Mode 25-28

Figure E.3: Out-of-plane modes 1-4, 25-28 for cable network with 1 crosstie

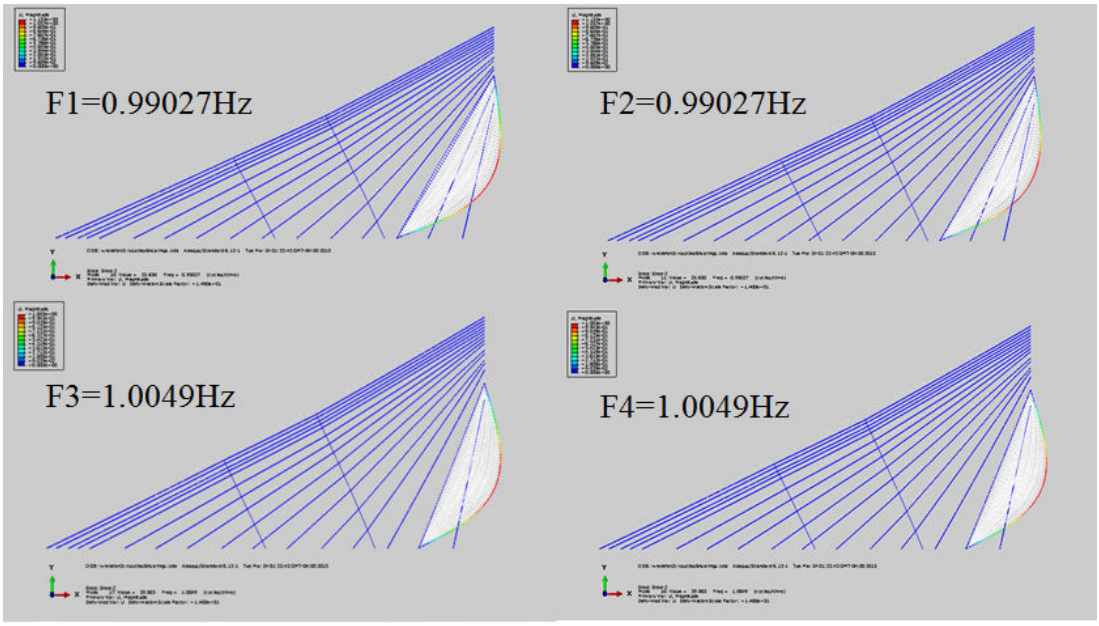

Mode 1-4

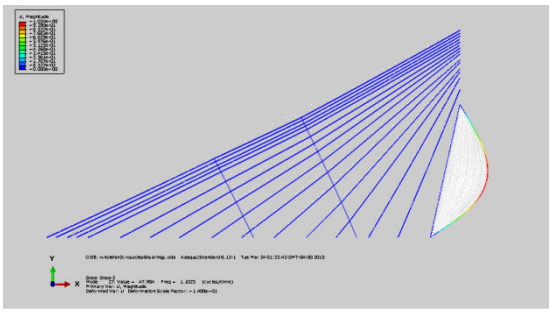

Mode 5 (f=1.1025Hz)

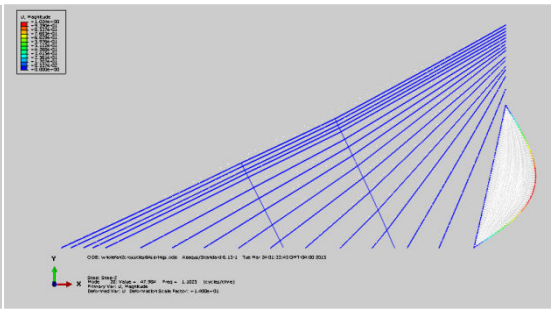

Mode 6 (f=1.1025Hz)

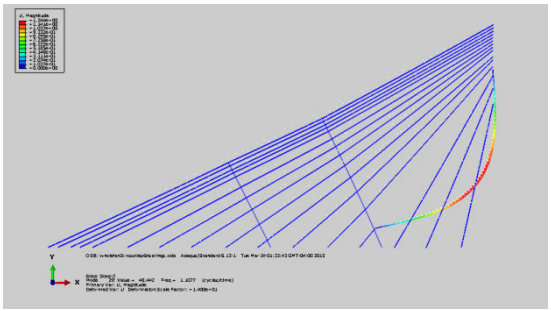

Mode 7 (f=1.1077Hz)

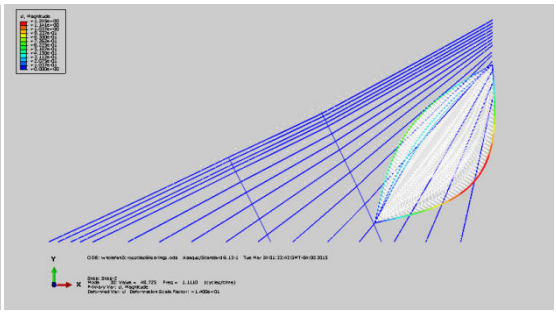

Mode 8 (f=1.111Hz)

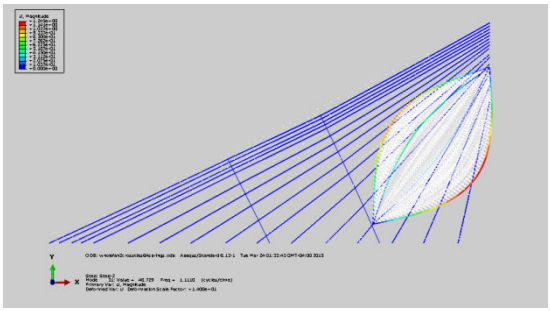

Mode 9 (f=1.111Hz)

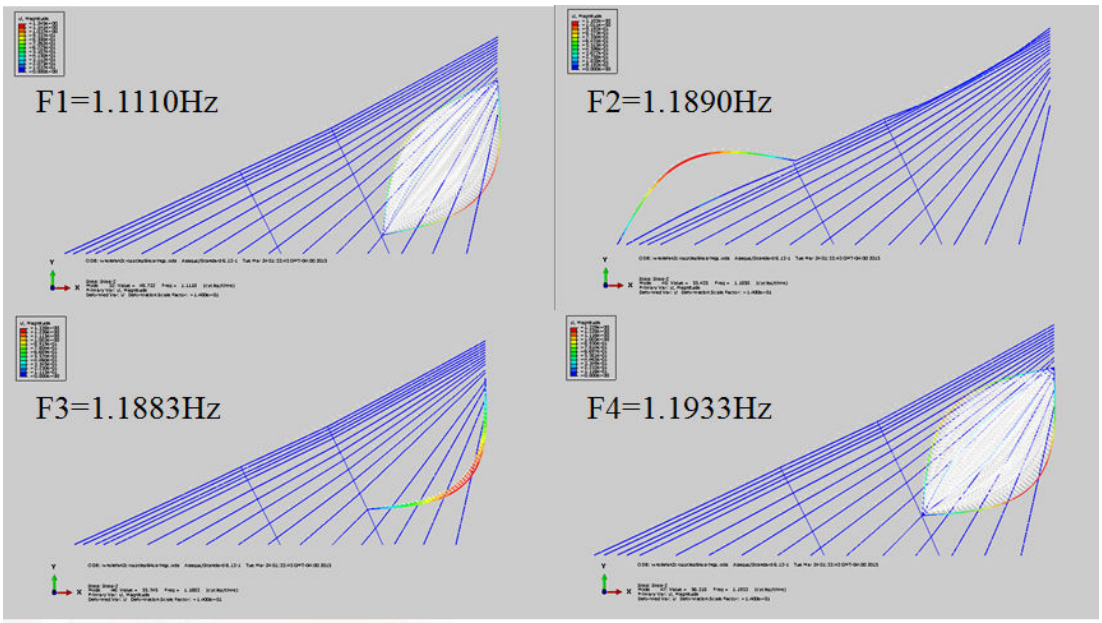

Mode 10-13

Figure E.4: In-plane modes 1-13 for cable network with 2 crossties

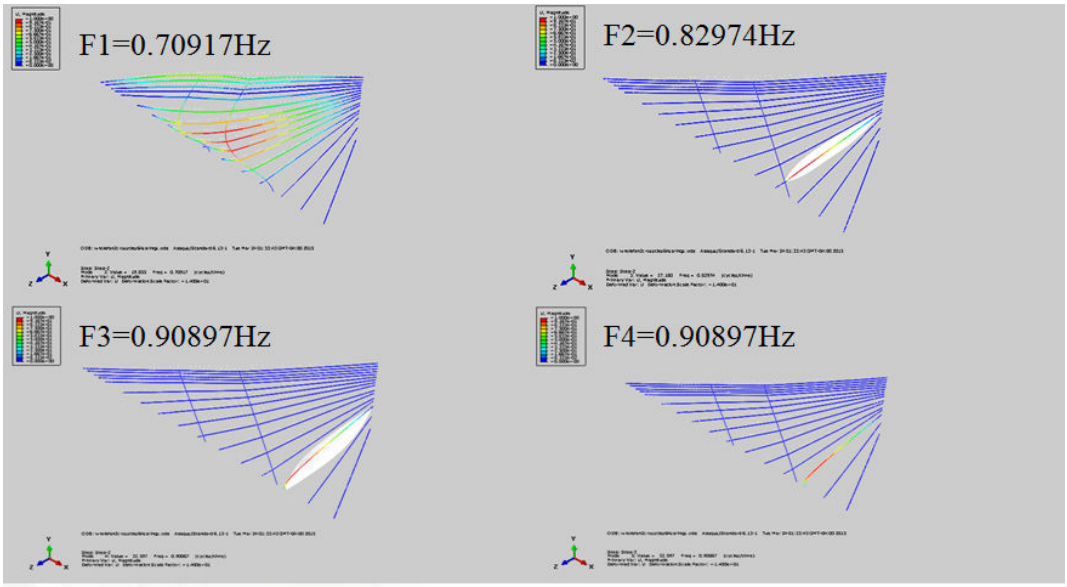

Mode 1-4

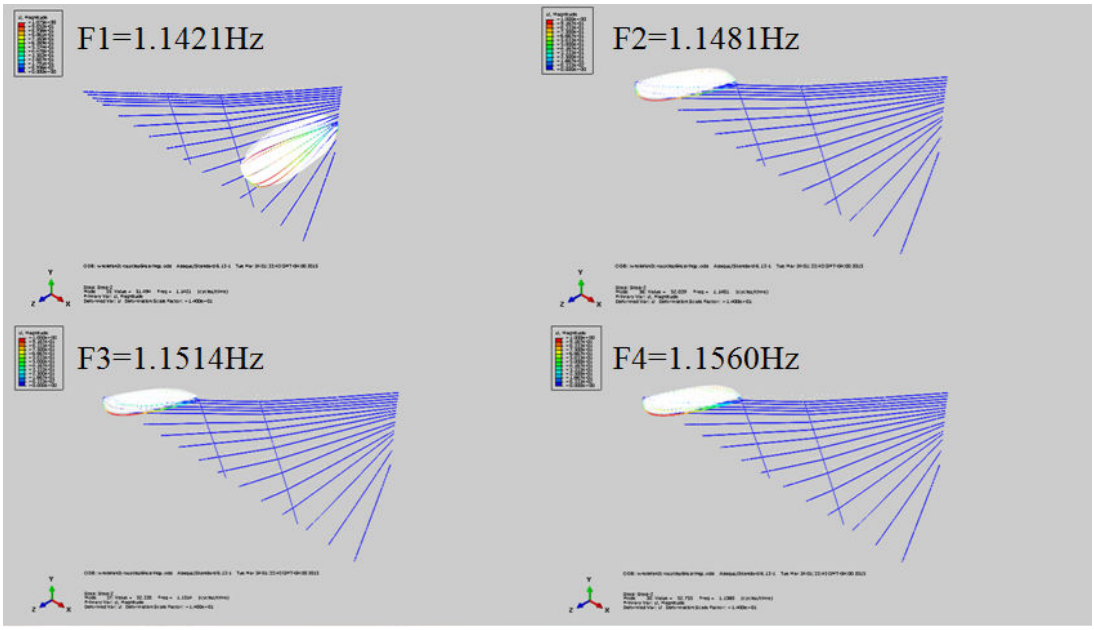

Mode 25-28

Figure E.5: Out-of-plane modes 1-4, 25-28 for cable network with 2 crossties

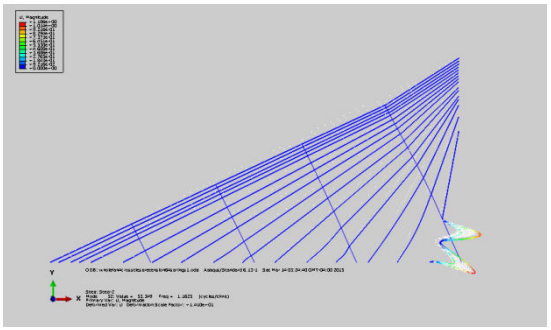

Mode 5 (f=1.1625Hz)

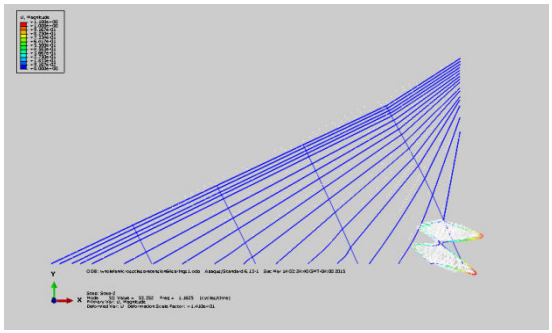

Mode 6 (f=1.1625Hz)

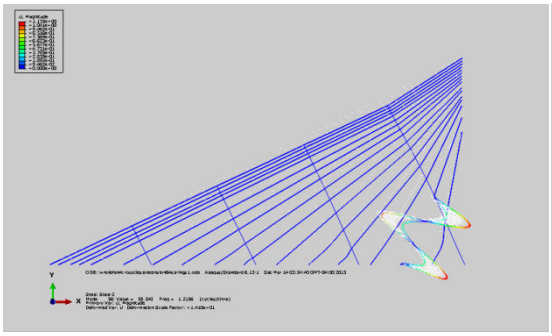

Mode 7 (f=1.2196Hz)

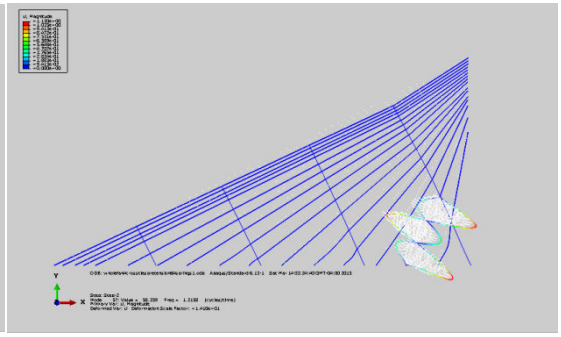

Mode 8 (f=1.2198Hz)

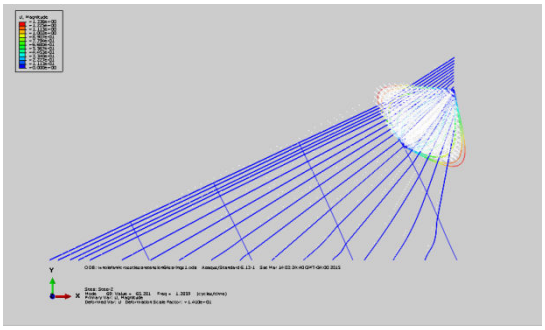

Mode 9 (f=1.2859Hz)

Figure E.6: In-plane modes 5-9 for cable network with 4 crossties

Appendix F

Additional figures of displacements at different points in the stay-cables fan

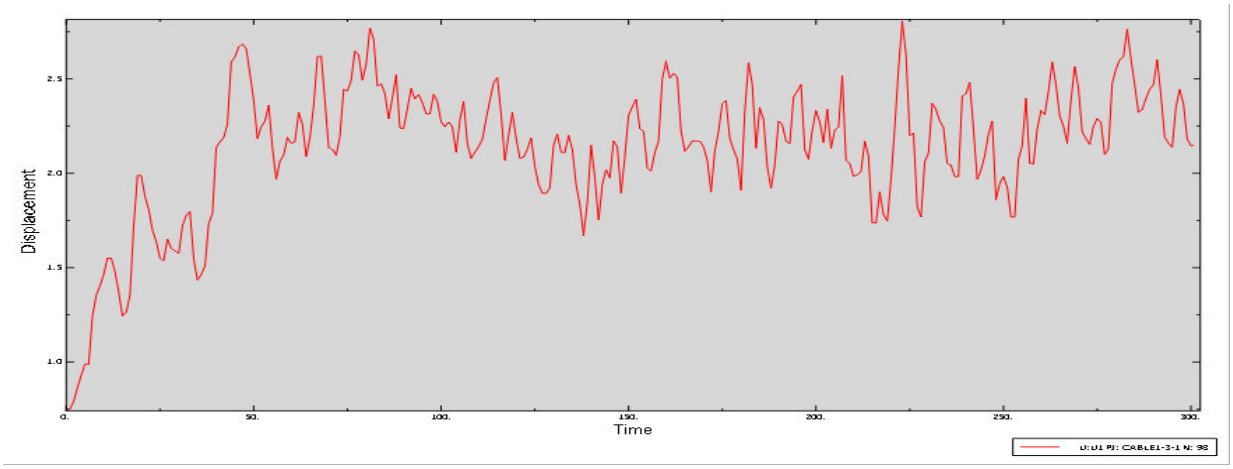

No crosstie

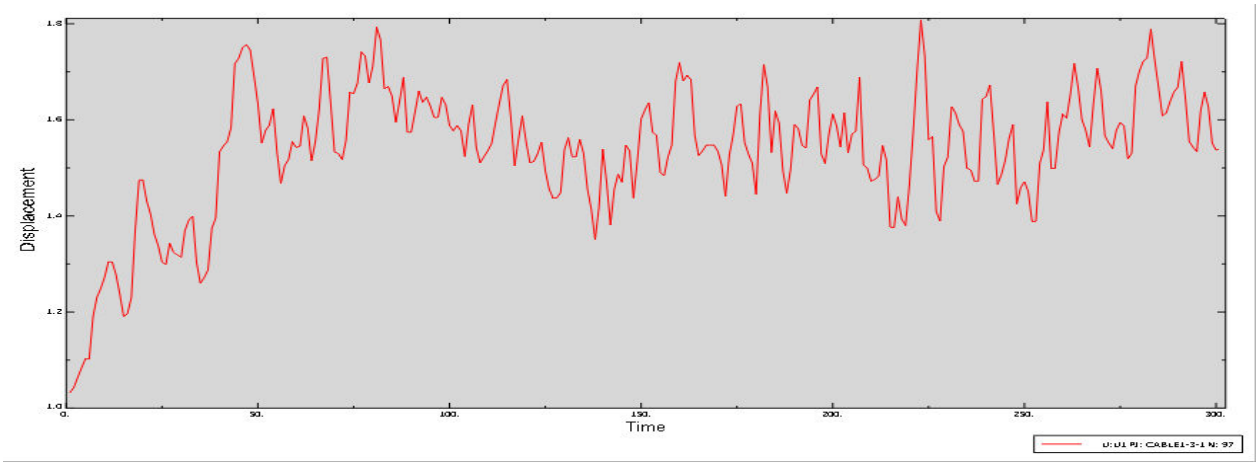

1 crosstie

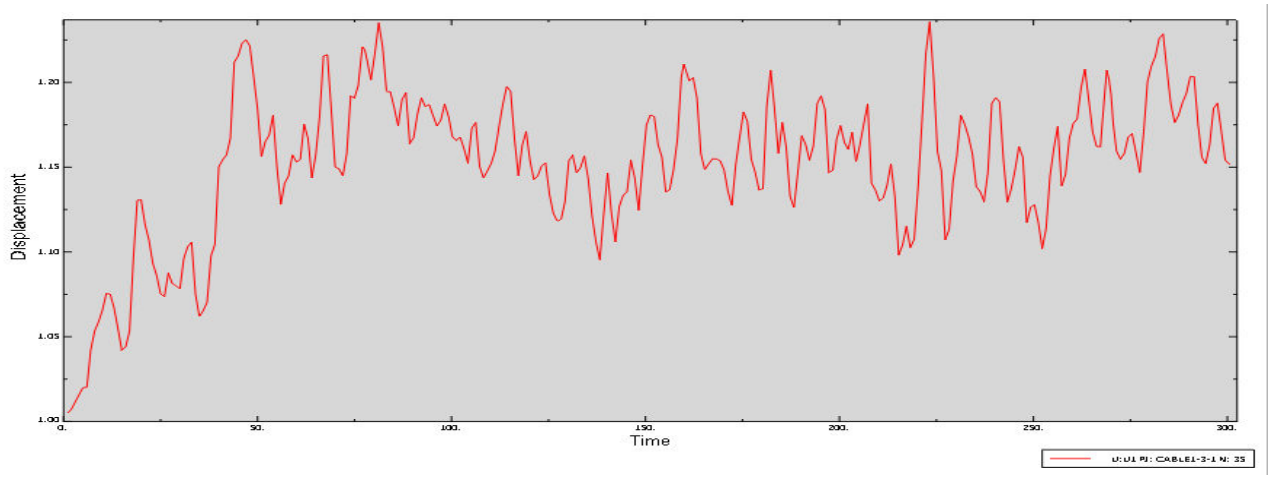

2 crossties

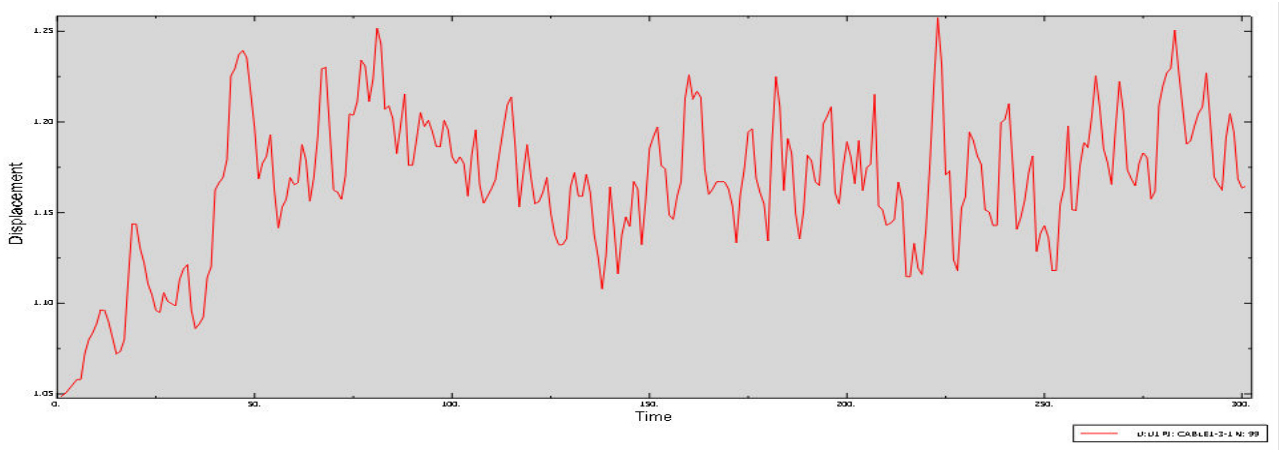

4 crossties

Figure F.1: Displacements of multiple-strand cable without grout at point A

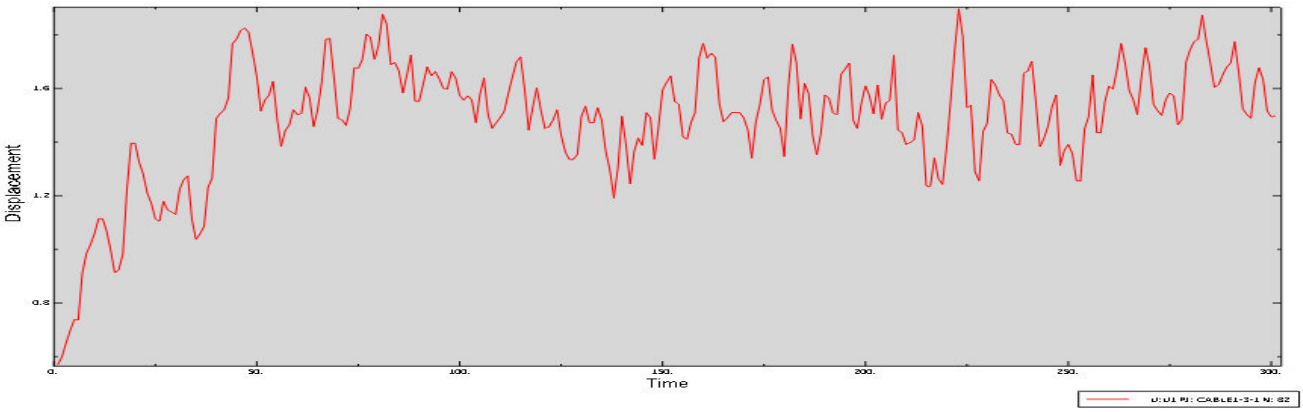

No crosstie

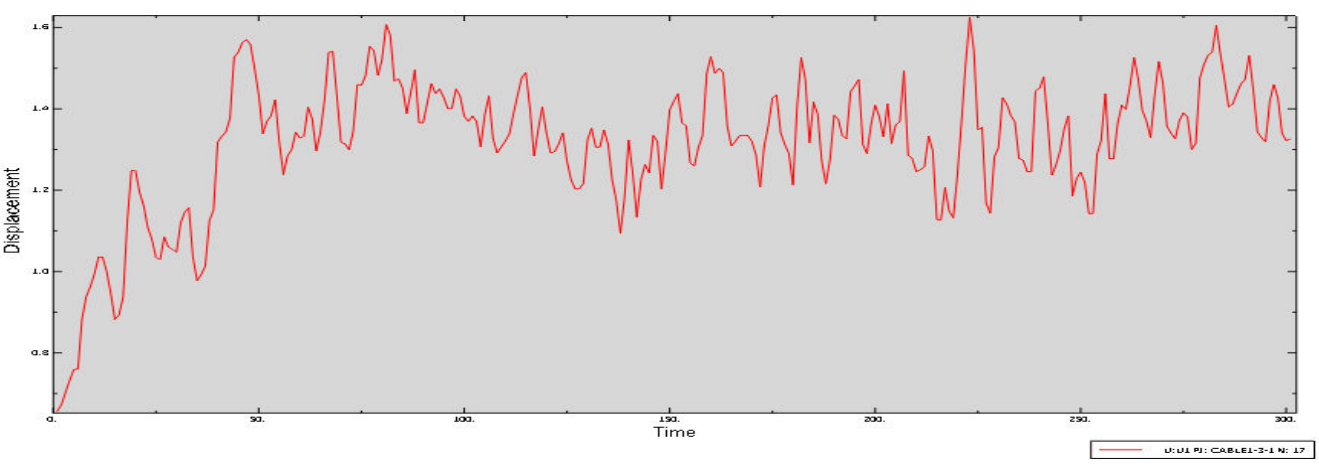

1 crosstie

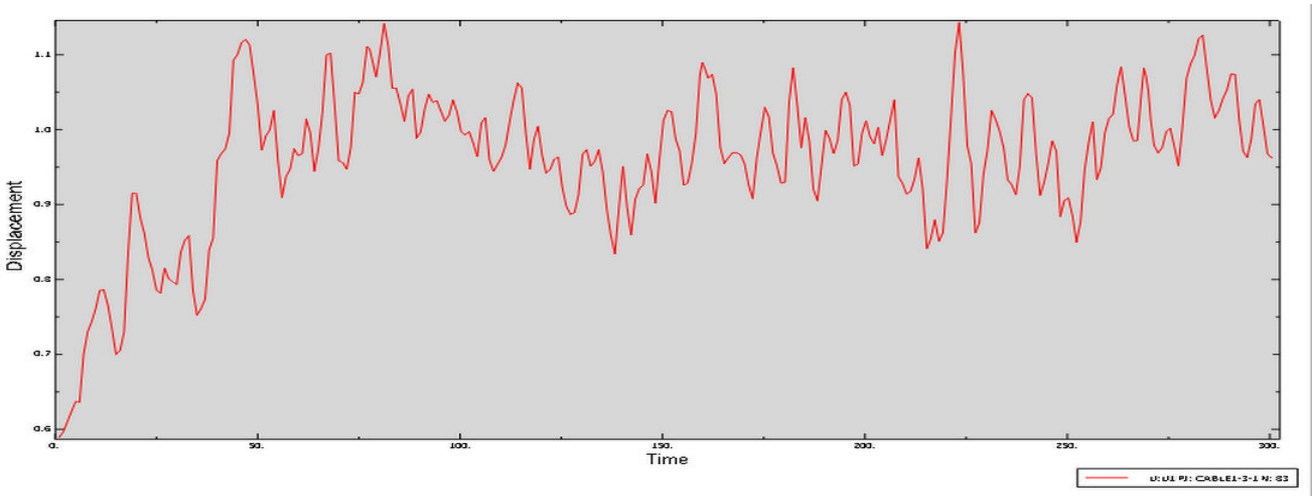

2 crossties

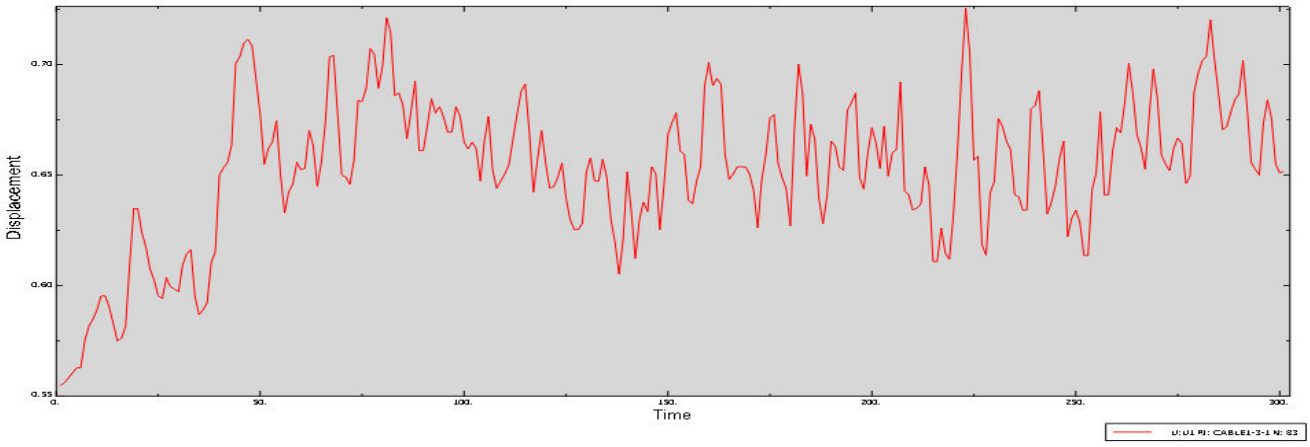

4 crossties

Figure F.2: Displacements of multiple-strand cable without grout at point B

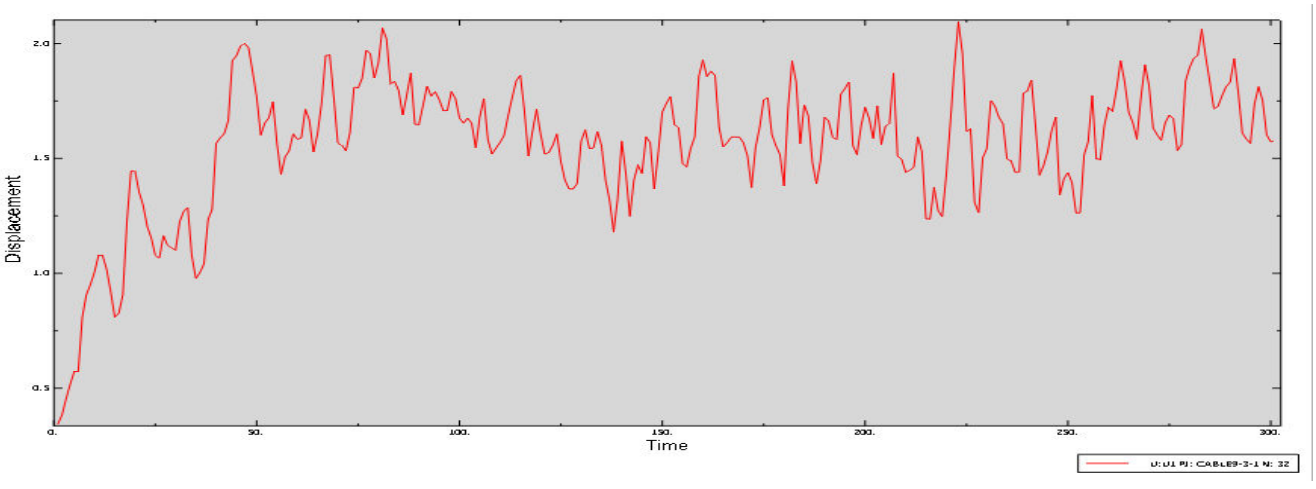

No crosstie

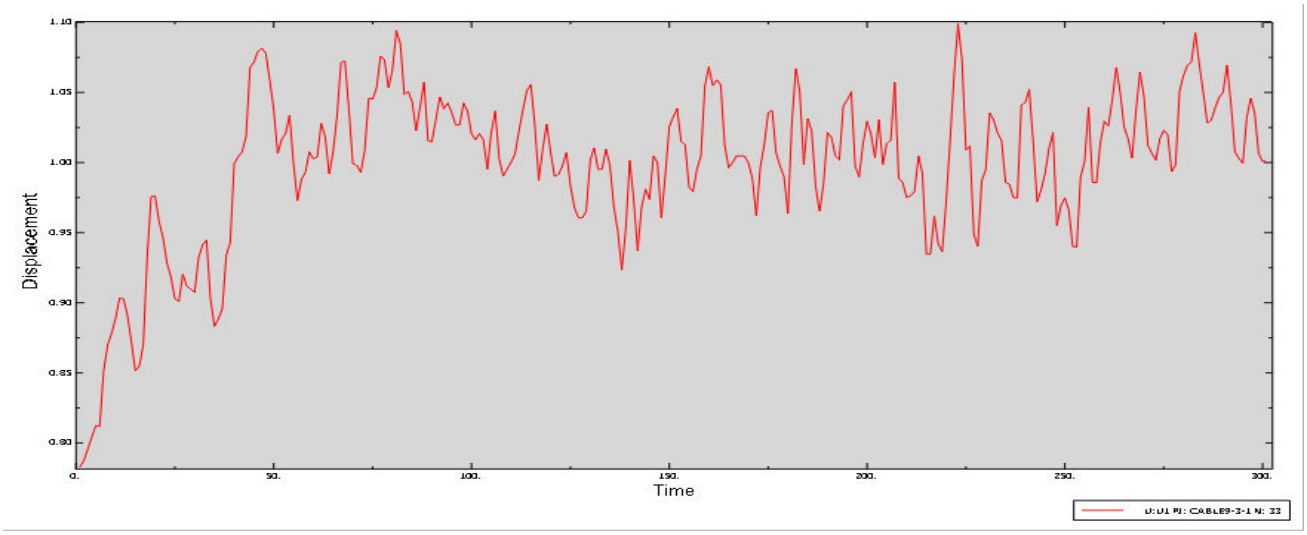

1 crosstie

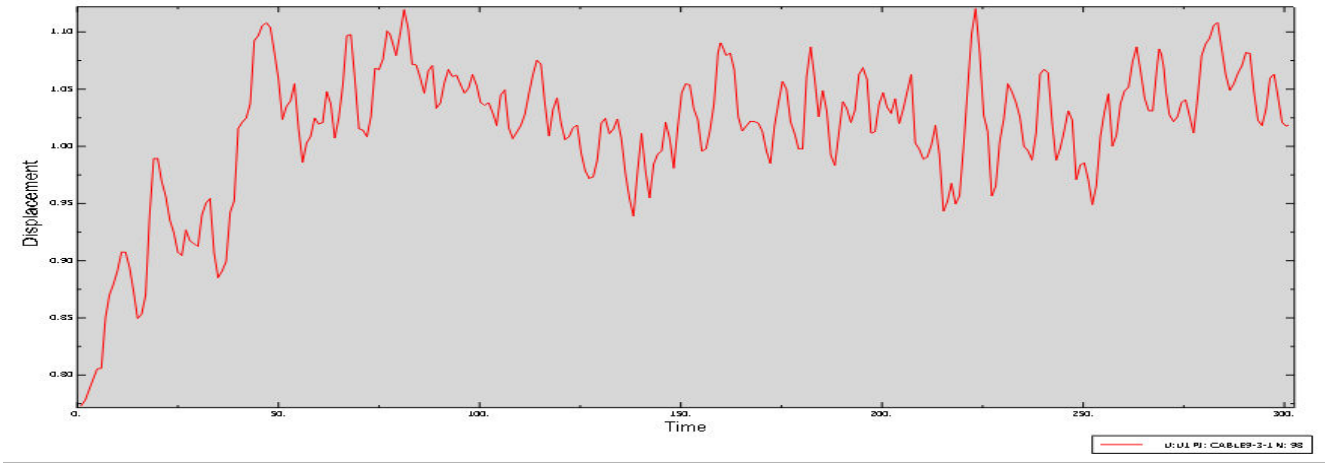

2 crossties

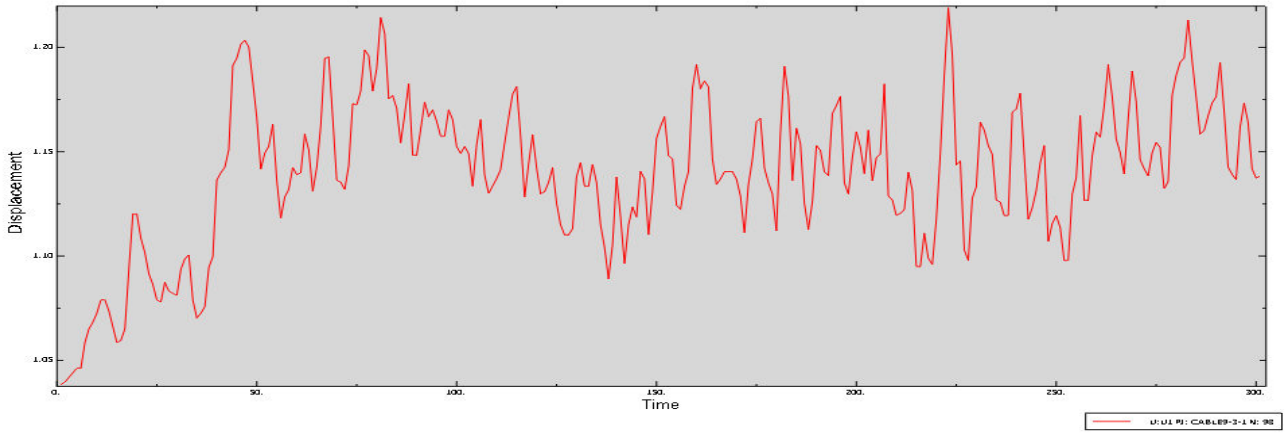

4 crossties

Figure F.3: Displacements of multiple-strand cable without grout at point C

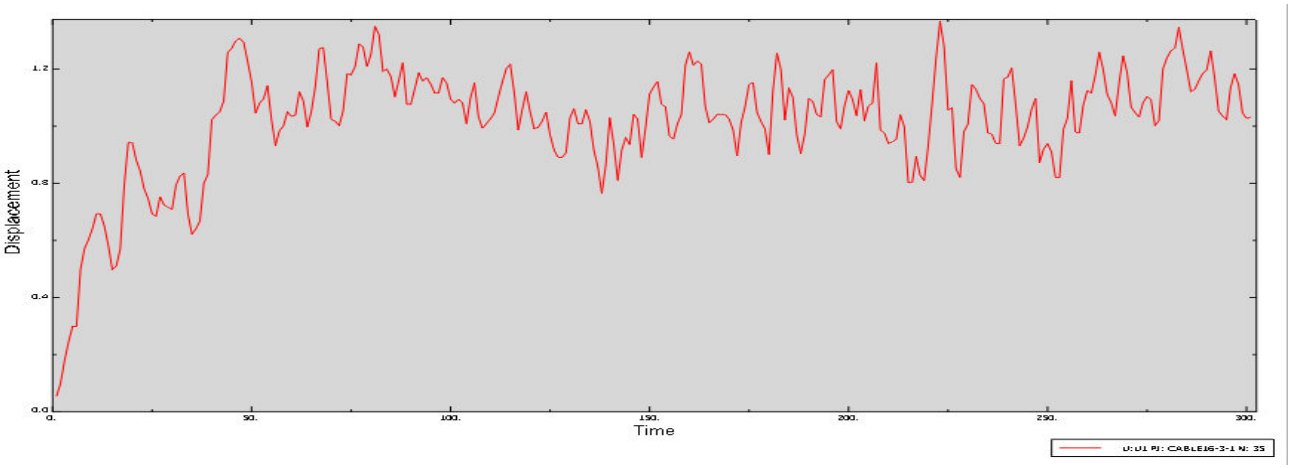

No crosstie

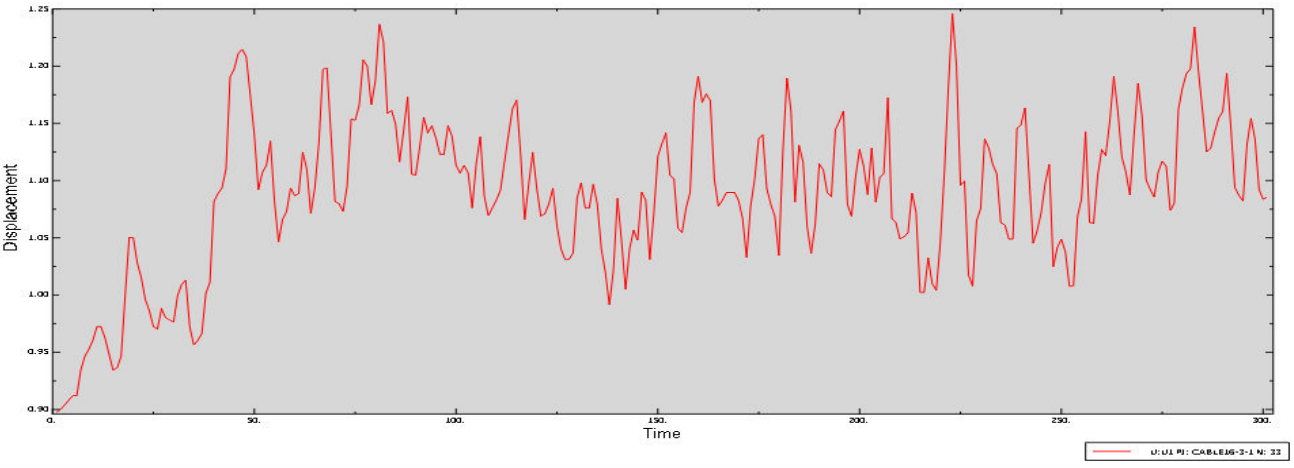

1 crosstie

Figure F.4: Displacements of multiple-strand cable without grout at point D

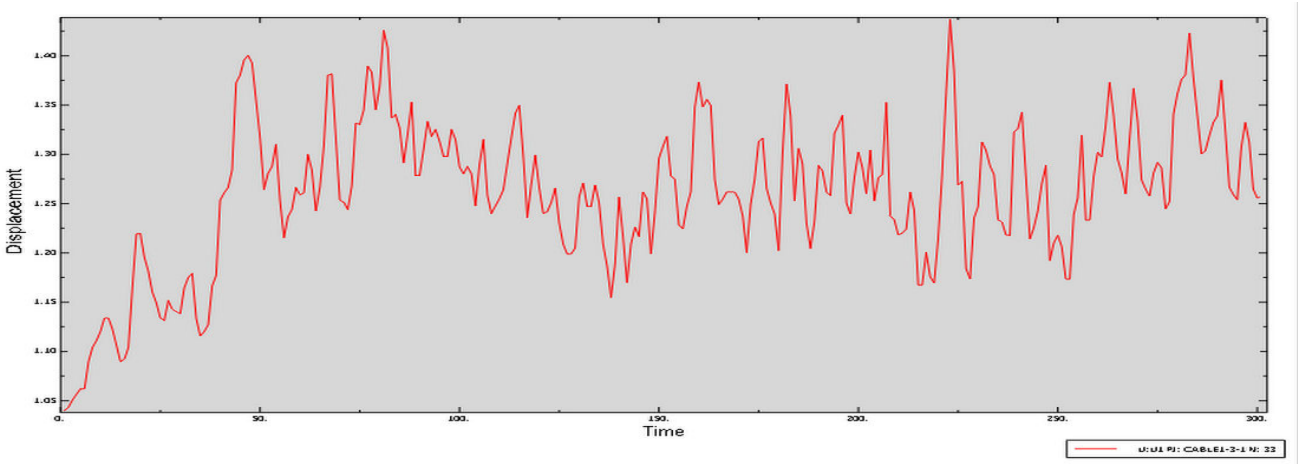

1 crosstie, A1

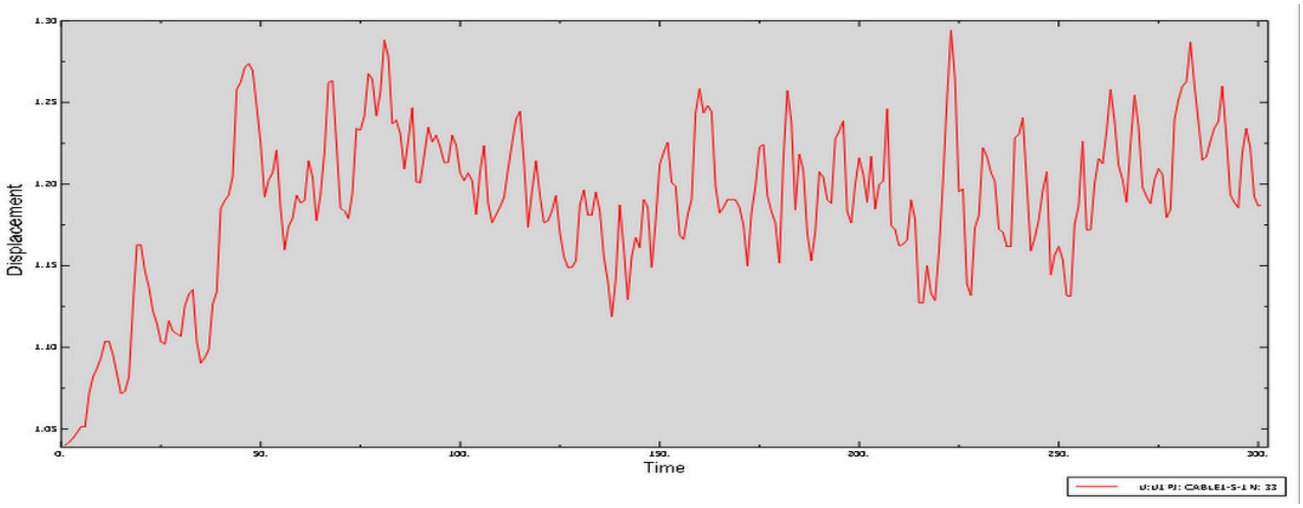

1 crosstie, A2

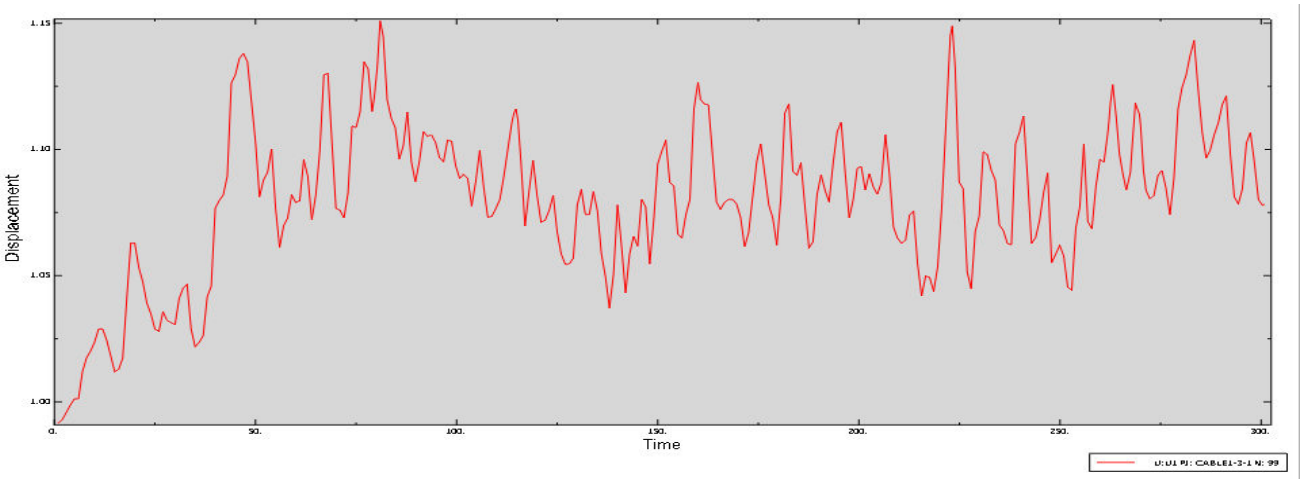

2 crossties, A1

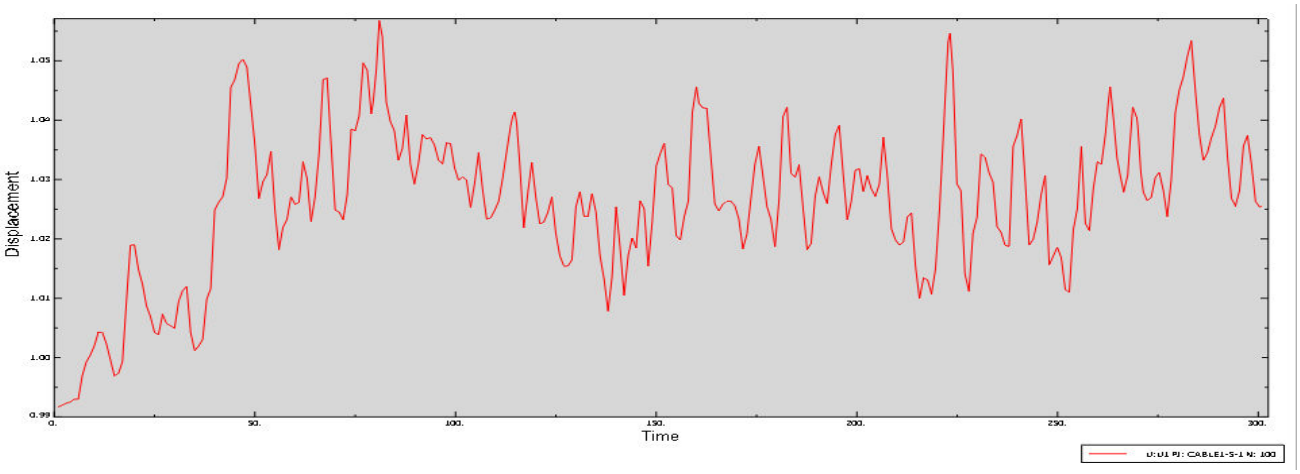

2 crossties, A2

Figure F.5: Displacements of multiple-strand cable with grout at points A1, A2

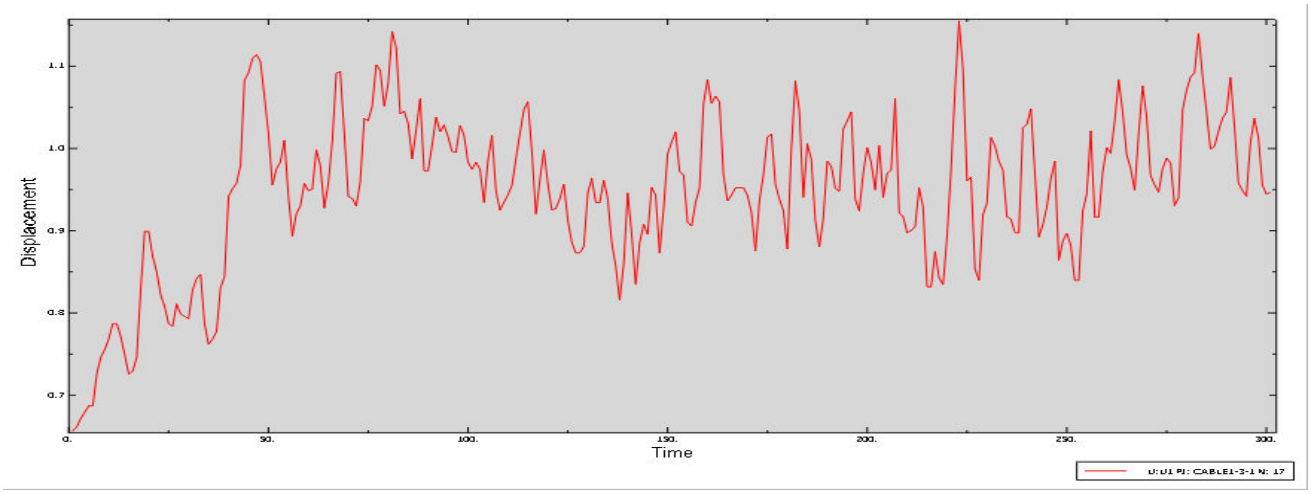

1 crosstie, B1

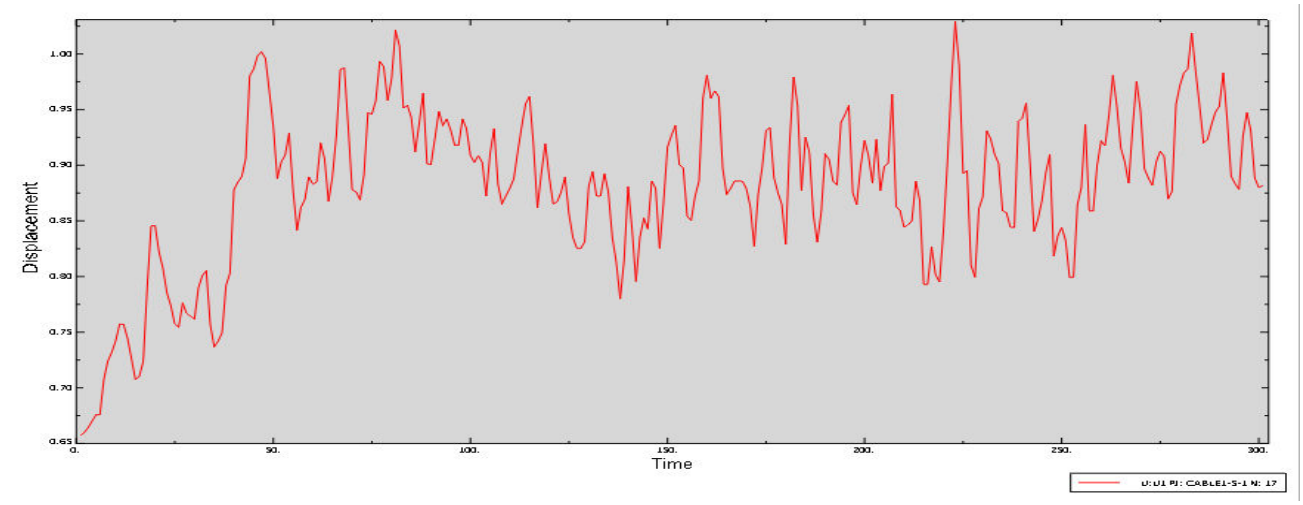

1 crosstie, B2

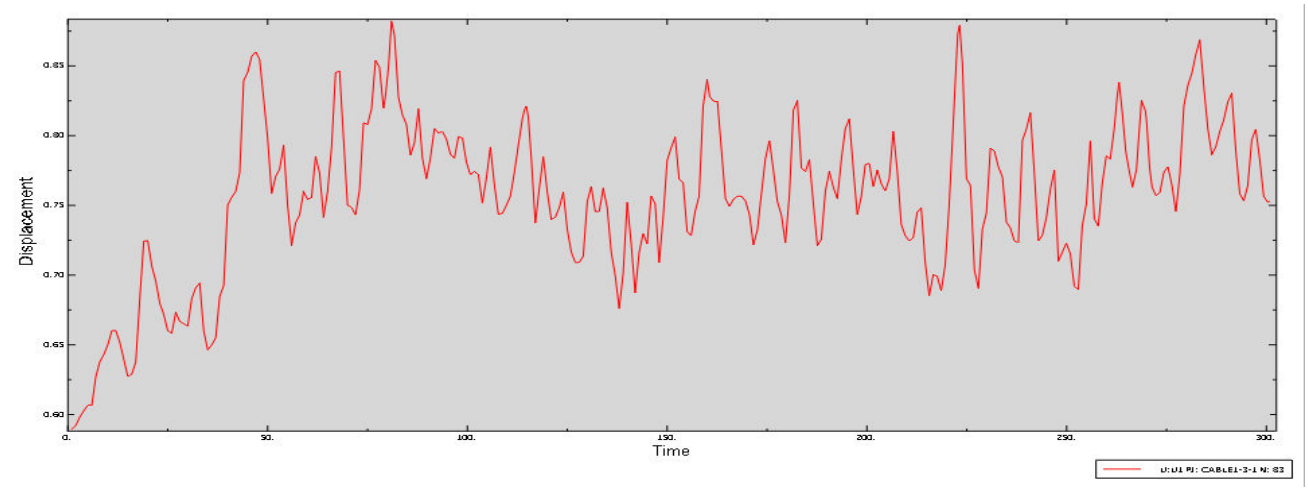

2 crossties, B1

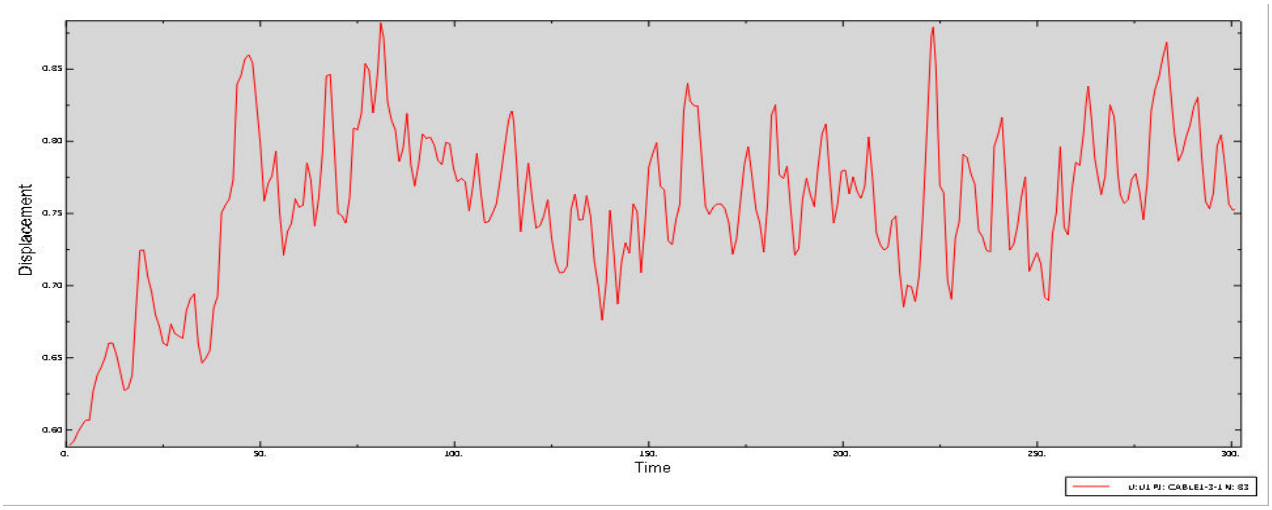

2 crossties, B2

Figure F.6: Displacements of multiple-strand cable with grout at points B1, B2

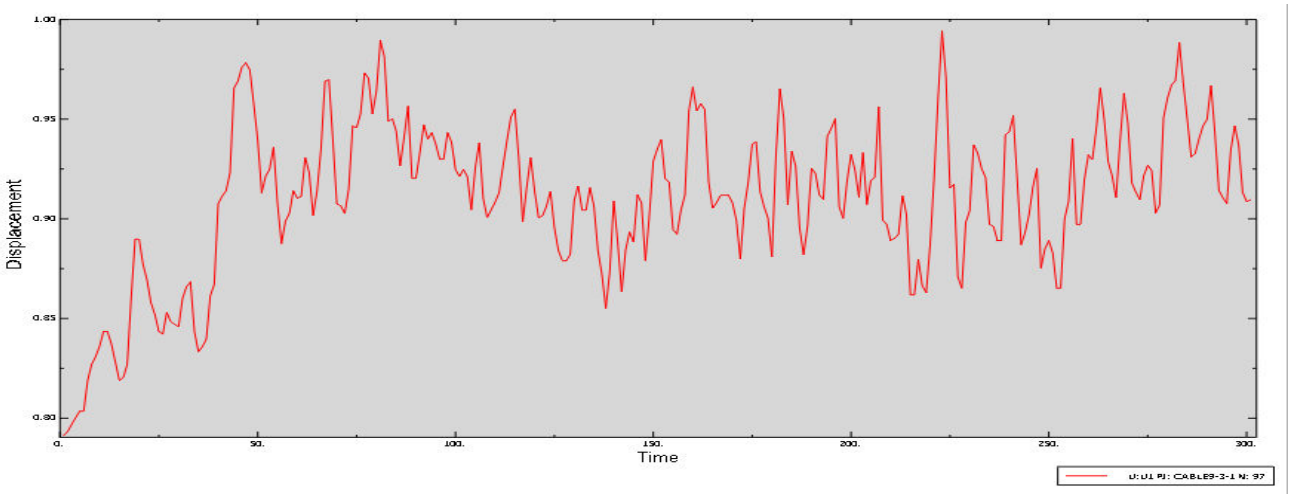

1 crosstie, C1

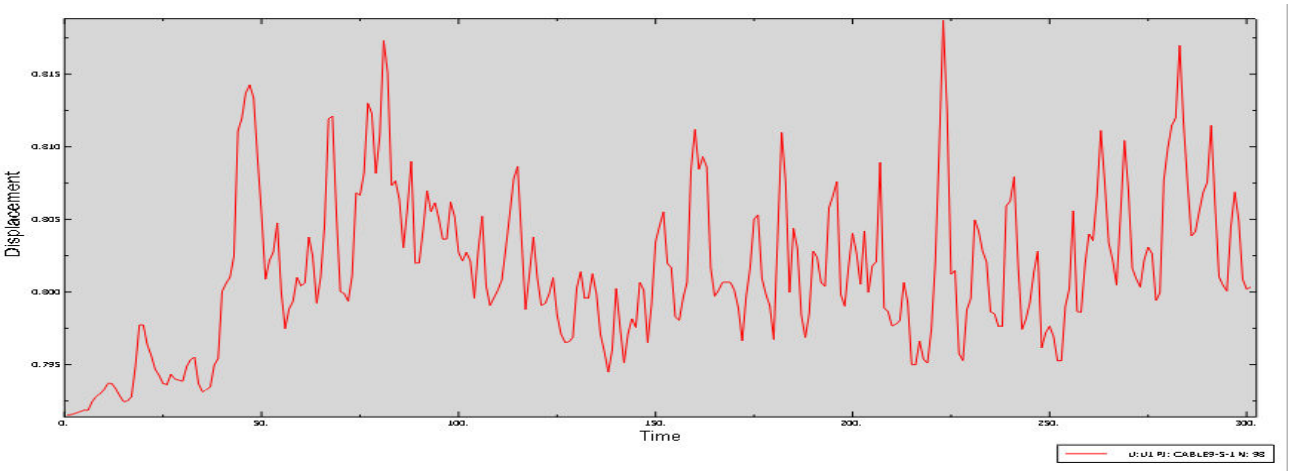

1 crosstie, C2

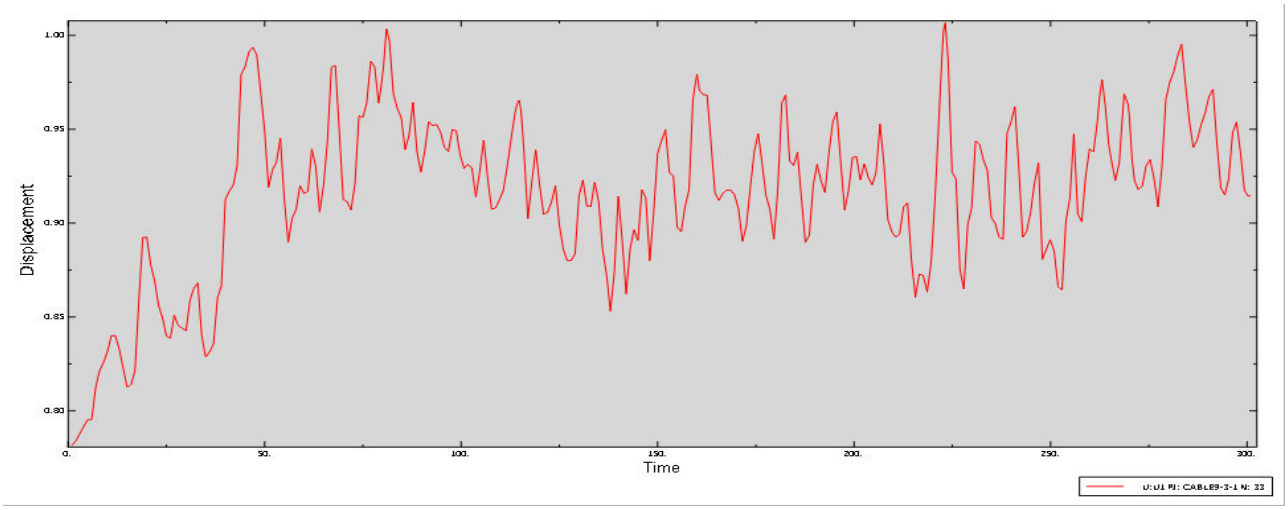

2 crossties, C1

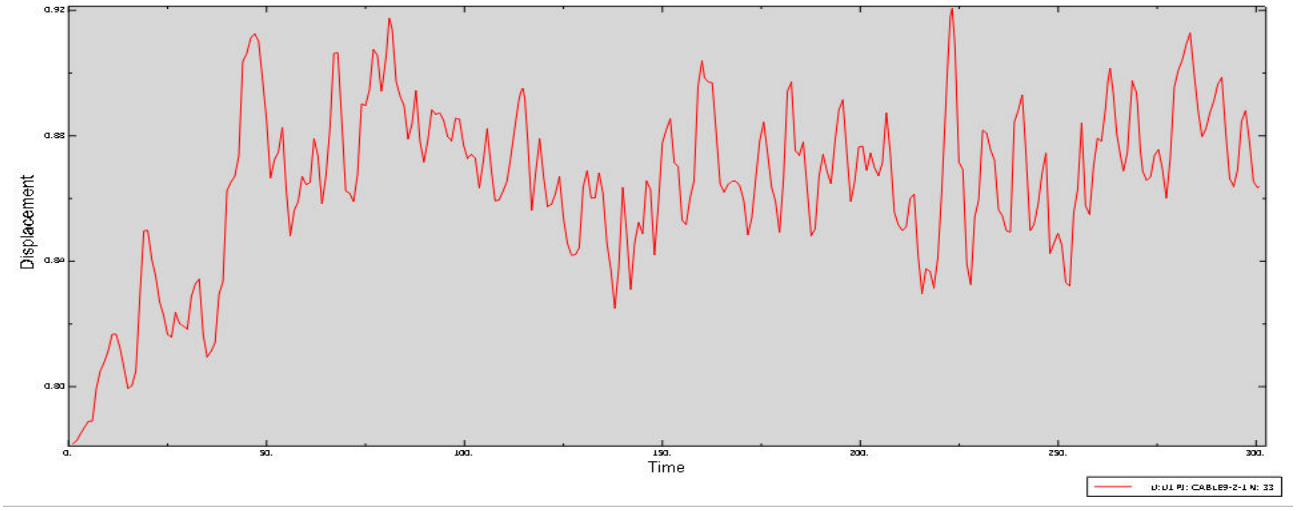

2 crossties, C2

Figure F.7: Displacements of multiple-strand cable with grout at points C1, C2